Molecular interventions to overcome the ageing of CNS stem cells

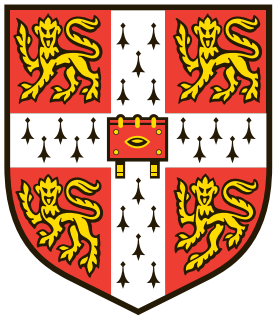

Michael Segel

Department of Clinical Neuroscience
University of Cambridge

This dissertation is submitted for the degree of
Doctor of Philosophy

Peterhouse

September 2018

Summary

Title: Molecular interventions to overcome the ageing of CNS stem cells

Name: Michael Segel

Oligodendrocyte progenitor cells (OPCs) are the dominant tissue-specific stem cell of the central nervous system (CNS). In the adult, OPCs primarily differentiate into oligodendrocytes, the cell type that wraps neurons with myelin allowing for efficient signal transduction down the axon. Increasingly, the process of adult myelination is understood as a key process in learning, memory formation, and promoting overall CNS health. With ageing, the capacity for OPCs to both self-renew and differentiate into myelinating oligodendrocytes is impaired. This loss of function is particularly detrimental for patients with demyelinating diseases such as Multiple Sclerosis. The failure of OPCs to differentiate into oligodendrocytes contributes to the progressive worsening of the symptoms with ageing. As such, there is a therapeutic imperative to better understand the ageing process of OPCs in order to find possible interventions that will overcome their age-related dysfunction. Recent advances in the generation of induced pluripotent stem cells provide proof that all cells, regardless of age, can be reconverted into embryonic pluripotent stem cells, thereby shedding all the hallmarks of the ageing process. This work provides evidence that the ageing process on a cellular level is not immutable; rather, all cells can be rejuvenated.

In each of the results chapters included in this thesis, I ask and then address four outstanding questions in the field of OPC ageing biology: 1. What governs the activity-state of adult OPCs? 2. Do OPCs irreversibly lose their plasticity during physiological ageing? 3. What causes this loss of activity in aged OPCs? 4. Are there molecular interventions that might overcome the age phenotype of aged OPCs? Addressing these questions in my thesis, I identify a vascular niche for OPCs in the adult animal and find that Wnt signaling underlies the activity-state of the quiescent adult OPC. I identify that overexpression of the reprogramming factor Myc can, alone, coax an aged quiescent OPC to behave more like a neonatal one. I describe how age-related changes in niche matrix mechanics drive the ageing-phenotype of OPCs, and how OPCs sense and respond to these changes with the mechano-transduction protein Piezo1. Finally, I have developed a novel, systemically delivered, cell-type-specific, genome engineering technique to perturb age-related genes in adult rodents.

The work presented in this thesis provides a new understanding of OPCs in homeostasis and in ageing. By identifying multiple interconnecting signalling-pathways by which adult and aged OPCs can re-activate, I have identified multiple points of therapeutic intervention. Finally, this systemically-administered but cell-type specific genome-engineering technology could be used to construct one-generation transgenic animals in an adult rodent and could have therapeutic implications for a broad-spectrum of human diseases.

Declaration

I hereby declare that except where specific reference is made to the work of others, the contents of this dissertation are original and have not been submitted in whole or in part for consideration for any other degree or qualification in this, or any other university. This dissertation is my own work and contains nothing which is the outcome of work done in collaboration with others, except as specified in the text and Acknowledgements. This dissertation contains fewer than 60,000 words including appendices, bibliography, footnotes, tables and equations and has fewer than 150 figures.

Michael Segel, September 2018

Table of contents

Acknowledgements

This work would not have been possible without the help of so many people. I would like to thank Robin Franklin for giving me the opportunity to work in his lab and for supporting everything that I have done throughout my PhD. He has given me scientific freedom coupled with complete support during my PhD. I am incredibly lucky to have worked in his group. I would also like to thank Kevin Chalut for acting as co-supervisor. He has helped to brainstorm, problem-solve, and edit manuscripts at all times of day, every day of the week. Together, Kevin and Robin have introduced me to new fields of biology, have motivated me to explore unexpected scientific avenues, and have provided scientific direction. I am very grateful.

I would also like to thank all the members of the Franklin Group who have supported me throughout my PhD. In particular, I would especially like to thank Björn Neumann from the Franklin Group; he has taught me so many new experimental methods, taught me new approaches to biology, and assisted on many rounds of manuscript revisions, regardless of his own experimental calendar. I am so grateful for his constant feedback and help. I would also like to thank Kristian Franze, Isabell Weber, and Joy Thompson for performing and analysing atomic force microscopy. I would like to thank Myfanwy Hill, Chao Zhao, and Pani Tourlomousis for helping with animal experiments, and Ruth Sims for spending many long hours imaging, and analysing light-sheet microscopy data. I would also like to thank Natalia Deja for providing data generated from her PhD. I also am grateful to Roey Baror, Beza Agley, Ginez Gonzalez, Adam Young, and Amar Sharma for helping with assorted experiments throughout my PhD.

I would like to thank Harvard University and the Harvard-Cambridge Herchel Smith fellowship for funding my PhD. This fellowship has enabled me to live, work, and research at this incredible institution. I would also like to thank the Cambridge Stem Cell Institute, BBSRC and MS Society UK for funding the work presented in this thesis.

Finally, and most importantly, I would like to thank my wife Sarah for endless support and patience throughout my PhD. It would not have been possible with you.

Statement of collaboration

Scientific research is a profoundly collaborative initiative. As such, I would like to acknowledge individuals for specific work that enabled this PhD thesis. All work not acknowledged here, I performed. All manuscript drafting, figure layout, and illustrations are my own.

Chapter 3

Chapter 3 is an equal-partner collaboration with Björn Neumann of Robin Franklin's group. With permission, I drafted the manuscript, and collated the data, but Björn and I equally shared in the design of the experiments. Natalia Murphy, a former PhD student in the Franklin group provided us with her unpublished sequencing data.

Figure 1: Ruth Sims performed the light sheet microscopy data.

Chapter 4

Much of the work in Chapter 4 would not have been possible without the help of others.

Figure 1: Björn Neumann and Myfanwy Hill assisted with the cell transplantation and brain lesion experiments. Isabell Weber of Kristian Franze's group performed the atomic force microscopy acquisition and subsequent analysis.

Figure 5: Chibeza C Agley invented and designed the hydrogels.

Figure 13: Myfanwy Hill assisted with the cell transplants.

Chapter 5

Chao Zhao, Björn Neumann, and Pani Tourlomousis assisted with the AAV tail-vein injections and the spinal cord lesioning.

Chapter 6

Chapter 6 is a collaboration with Björn Neumann of Robin Franklin's group. With permission, I drafted the manuscript, and collated the data.

Figure 3: Björn Neumann helped execute and analyse all experiments for Figure 2.

Figure 4: Björn Neumann assisted with the comet assay.

Figures 5-6: Pani Tourlomousis, Björn Neumann, and Chao Zhao assisted with the tail-vein injections and the spinal cord lesions.

Summary

Oligodendrocyte progenitor cells (OPCs) are the dominant tissue-specific stem cell of the central nervous system (CNS). In the adult, OPCs primarily differentiate into oligodendrocytes, the cell type that wraps neurons with myelin allowing for efficient signal transduction down the axon. Increasingly, the process of adult myelination is understood as a key process in learning, memory formation, and promoting overall CNS health. With ageing, the capacity for OPCs to both self-renew and differentiate into myelinating oligodendrocytes is impaired. This loss of function is particularly detrimental for patients with demyelinating diseases such as Multiple Sclerosis. The failure of OPCs to differentiate into oligodendrocytes contributes to the progressive worsening of the symptoms with ageing. As such, there is a therapeutic imperative to better understand the ageing process of OPCs in order to find possible interventions that will overcome their age-related dysfunction. Recent advances in the generation of induced pluripotent stem cells provide proof that all cells, regardless of age, can be reconverted into embryonic pluripotent stem cells, thereby shedding all the hallmarks of the ageing process. This work provides evidence that the ageing process on a cellular level is not immutable; rather, all cells can be rejuvenated.

In each of the results chapters included in this thesis, I ask and then address four outstanding questions in the field of OPC ageing biology: 1. What governs the activity-state of adult OPCs? 2. Do OPCs irreversibly lose their plasticity during physiological ageing? 3. What causes this loss of activity in aged OPCs? 4. Are there molecular interventions that might overcome the age phenotype of aged OPCs? Addressing these questions in my thesis, I identify a vascular niche for OPCs in the adult animal and find that Wnt signaling underlies the activity-state of the quiescent adult OPC. I identify that overexpression of the reprogramming factor Myc can, alone, coax an aged quiescent OPC to behave more like a neonatal one. I describe how age-related changes in niche matrix mechanics drive the ageing-phenotype of OPCs, and how OPCs sense and respond to these changes with the mechano-transduction protein Piezo1. Finally, I have developed a novel, systemically delivered, cell-type-specific,

genome engineering technique to perturb age-related genes in adult rodents.

The work presented in this thesis provides a new understanding of OPCs in homeostasis and in ageing. By identifying multiple interconnecting signaling-pathways by which adult and aged OPCs can re-activate, I have identified multiple points of therapeutic intervention. Finally, this systemically-administered but cell-type specific genome-engineering technology could be used to construct one-generation transgenic animals in an adult rodent and could have therapeutic implications for a broad-spectrum of human diseases.

Chapter 1

Introduction

Regeneration in the Kingdom Animalia

Cellular regeneration is a widespread and diverse phenomenon across the animal kingdom. Regeneration describes the process by which damaged tissue is replaced with new healthy tissue that re-establishes the appropriate tissue shape, size, and function. Fully understanding and being able to harness the cellular events that underpin regeneration has real implications for biomedical science as it would allow for therapeutic treatments that could replace diseased or damaged tissue.

To understand the processes of regeneration, it is important to appreciate the diversity of its form. There are three main methods by which adult animals regenerate following injury: cellular trans-differentiation, cellular-de-differentiation, and stem cell pool activation (Fig. 1). The earliest formal description of animal regeneration is in the cnidarian H. vulgaris or the hydra over 200 years ago (Glass, 1988). The hydra replaces damaged or lost tissue through the trans-differentiation of existing fully differentiated somatic cells into the missing cells, without proliferation (Holstein et al., 1991). Only following this complete re-patterning of the hydra, can the organism grow. This process of regeneration by trans-differentiation is echoed across the animal kingdom. In humans, following pancreatic injury or inflammation, non-endocrine cells can transdifferentiate to replace the damaged insulin-producing ß-cell (Hao et al., 2006).

Another paradigm of animal regeneration is the process by which a fully differentiated cell de-differentiates into a more developmental-like progenitor cell, proliferates, and then re-differentiates into the missing tissue. In amphibians, the axolotl or the Mexican salamander can fully regrow its limbs and tail following amputation. This is done by the de-differentiation of the var-

ious cell types (e.g. muscle, cartilage, schwann cells, skin), proliferation, and re-patterning of the lost appendage (Stocum, 1979). Again, this paradigm of regeneration is repeated in higher order animals. In the injured neonatal mouse heart, cardiomyocytes de-differentiate, proliferate, and fully regenerate the damaged heart without fibrosis or hypertrophy. This regenerative capacity, however, is lost progressively with development (Porrello et al., 2011).

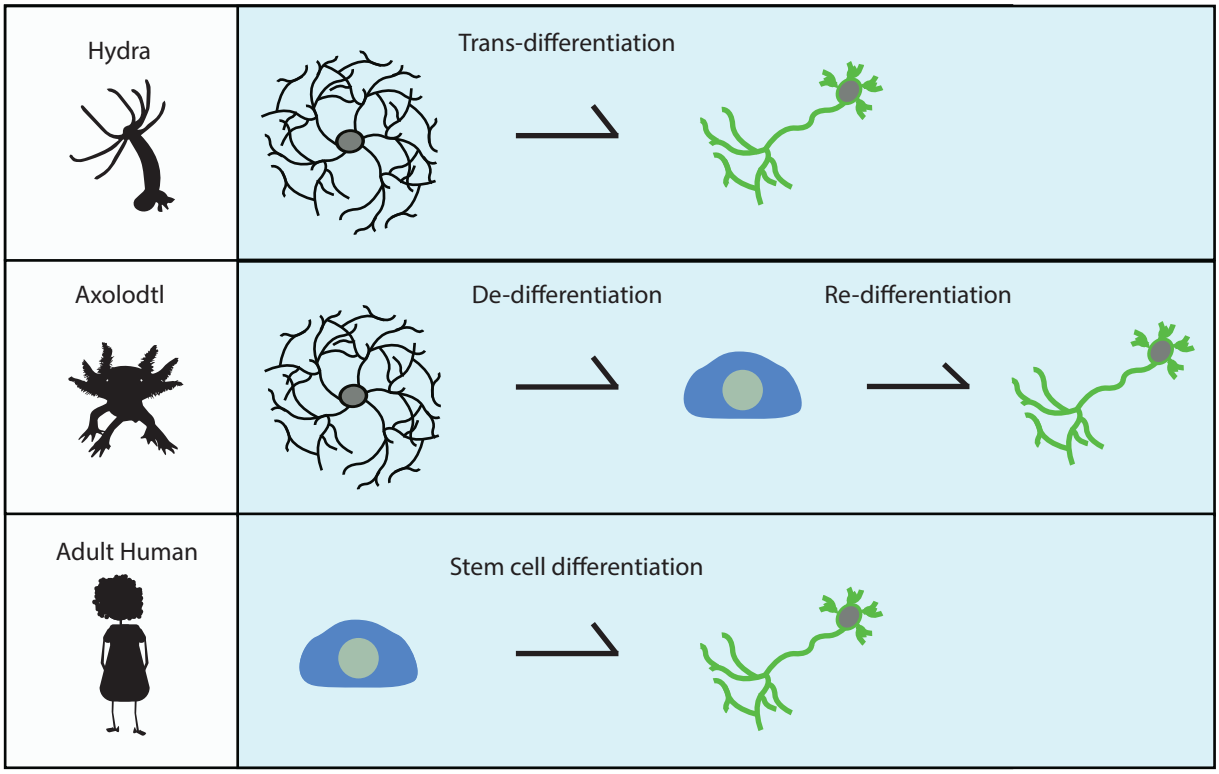

Figure 1. Models of regeneration in the animal kingdom. Illustration of the dominant methods of regeneration in the animal kingdom. To replace damaged tissue, cells can differentiate from previously committed cells, as they do in the hydra. In the axolodtl, cells first de-differentiate into a stem-like cell and then subsequently differentiate. In the adult human, the dominant method of regeneration is for specified, tissue-specific adult stem cells to activate and regenerate the damaged tissue.

The most conserved mechanism of regeneration in animals is through a reserved pool of adult stem-cells, which, upon activation, proliferate and differentiate into new tissue (Wagers and Weissman, 2004). One of the best described examples of this mode of regeneration is observed in the freshwater flatworm planaria. Planaria have a reserved pool of adult stem cells known

as neoblasts (Rossi et al., 2008). These cells are adult pluripotent stem cells, meaning they are able to differentiate into all cell types of the planaria. It has been shown that the planaria can be cut into 279 pieces, and the neoblasts can activate and fully regenerate the worms—resulting in 279 new fully reformed worms (Morgan, 1901). Conserving a pool of adult multipotent stem cells is the dominant mechanism by which adult mammals maintain both tissue homeostasis and regenerate damaged tissue in the context of disease and injury.

Dynamics of Adult Stem Cells in the Central Nervous System

In mammals, stem cells in the adult are far more restricted than the planaria in their regenerative capacity. Like planarian neoblasts, mammalian embryonic stem cells, which are derived from the inner cell mass of a blastocyst, are pluripotent, meaning they can differentiate into all the germ layers of the organism (Kleinsmith et al., 1964). Yet, throughout embryonic, fetal, and post-natal development, these embryonic stem cells differentiate into the multiple, tissue-specific cell types that comprise the adult organism. However, not all of these cells terminally differentiate with development—some remain incompletely differentiated and act as a reserved pool of tissue specific adult progenitor cells. Unlike the pluripotent embryonic stem cell, these cells are at most multipotent, meaning they can only turn into a limited number of cell types specific to their respective tissue.

Stem cells that persist for the entirety of adult life are known as adult stem cells. Some of the best understood of the adult stem cells are those of the blood, the skin, the intestine, and the muscle. To understand the biology of adult stem cells, it is important to understand the many ways they function in the adult. Long term hematopoietic stem cells, the stem cells of the blood, reside in the bone marrow and can give rise to all the cell types of the blood (Spangrude et al., 1988); however, these cells rarely divide even over the lifespan of the mouse, instead leaving most haematopoiesis to fast cycling daughter cells (Bernitz et al., 2016). Intestinal stem cells can only give rise to the cells of the intestinal villi but are perpetually active, providing a constant supply of new enterocytes, Paneth cells, goblet cells, and enteroendocrine cells (Bjerknes and Cheng, 1999). These two stem cell populations exemplify the diversity of activity-states that adult stem cells exhibit across the different tissues; each tissue-specific adult stem cell behaves in accordance with the needs of its niche.

In the central nervous system, there are three distinct adult stem cell populations: the neural stem cells of the subventricular zone; the neural stem cells of the hippocampal subgranular zone; and the oligodendrocyte progenitor cell (Fig. 2). The neural stem cell of the subventricular zone following division, migrates to the olfactory bulb and differentiates into interneurons (Doetsch et al., 1999). In rodents, these newly differentiated interneurons contribute to smell memory and other smell-linked behaviour (Lazarini and Lledo, 2011). Indeed, these neural

stem cells have been identified in the human, but their activity is negligible in the adult human brain (Sanai et al., 2004). As such, the role of these cells in normal human brain function and disease remains unclear.

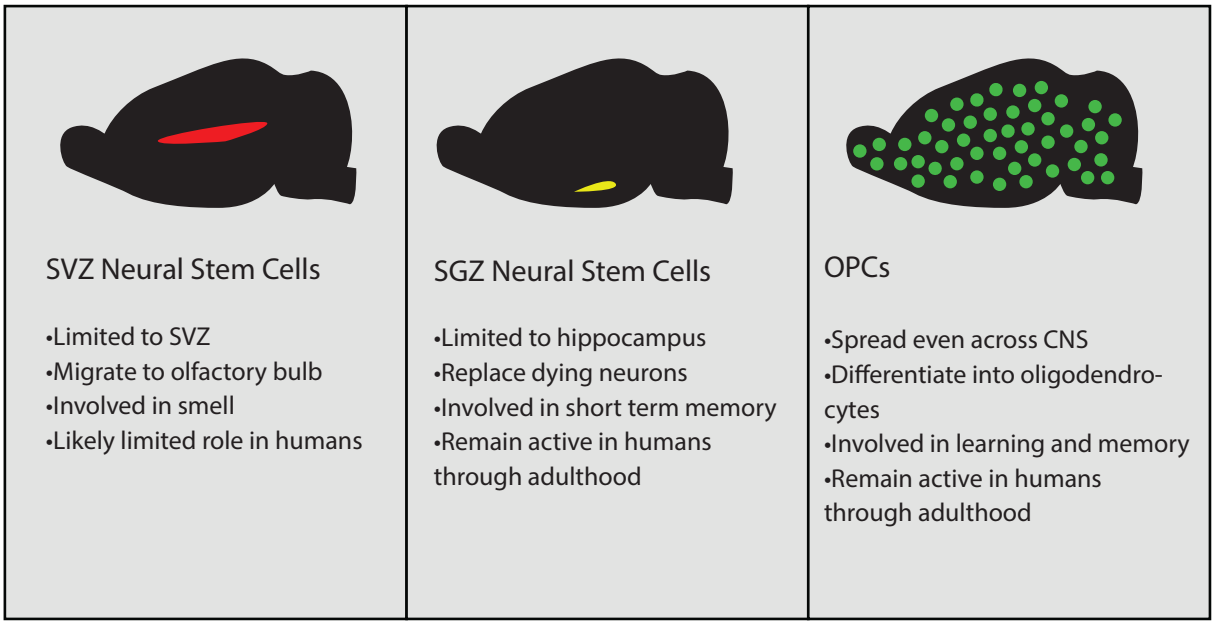

Figure 2. Stem cells of the adult rodent CNS. Illustration and brief description of CNS stem cells in a sagittal representation of the rodent CNS. The location of the stem cell population is coloured in red, yellow, and green. OPCs are the most widespread and abundant stem cell population in the adult CNS.

The neural stem cell of the subgranular zone in the hippocampus is likely more relevant for human biology. Upon differentiation into neurons, neural stem cells integrate fully into the hippocampus and are able to receive and transmit inputs from the rest of the brain (Song et al., 2002). As the hippocampus is a centre for memory processing in the brain, it is widely speculated that neural stem cell activation and differentiation is important for memory formation (Deng et al., 2010)—the theory being that new memory formation comes from the formation of a new neuron or a new set of neurons. Recent evidence using *in vivo* human radioactive carbon integration suggests that nearly a third of hippocampal neurons turn over throughout a human's postnatal life (Spalding et al., 2013). This rate of turnover, however, is age dependent and declines by fourfold in adulthood and ageing. While there are indeed high rates of turnover, this study also revealed that these neural stem cells are not adding new neurons to the hippocampus. Rather, they are simply replacing already existing ones that have been lost, and ultimately more neurons are lost than are generated in the hippocampus. It remains unclear whether these neuronal

stem cells are additive in terms of memory and cognition or simply compensatory, replacing the dying neurons of the hippocampus.

Even in rodents, the roles of the SVZ and hippocampal neural stem cells are limited, providing new neurons only in spatially-limited regions across the central nervous system. By comparison, the third type of adult stem cell, the oligodendrocyte progenitor cell, is scattered across the central nervous system, comprising 5-10% of total adult brain cells (Dawson et al., 2003). Throughout development and adulthood, the oligodendrocyte progenitor cell (OPC) gives rise to the oligodendrocyte, the cell-type that myelinates axons thereby allowing for efficient neuronal signal transduction and providing vital trophic support for neurons (Lee et al., 2012; Waxman, 1977). However, OPCs are not merely uni-potent progenitor cells; they maintain multipotent capacity and are able to self renew and differentiate both *in vitro* and *in vivo* into astrocytes and schwann cells (Zawadzka et al., 2010; Zhu et al., 2008). Taken together, these studies highlight the OPC as the most abundant and multipotent of the adult CNS stem cells. Moreover, more than any other progenitor cell population, the OPC may tell us how learning and complex thought is continued throughout adult life.

OPCs in development and the rise of the oligodendrocyte

To best understand the biology of OPCs and oligodendrocytes, it is important to understand how the oligodendrocyte lineage cells are generated in development. Following fertilisation in development, secreted signalling proteins orchestrate the differentiation of the early embryo into the multicellular organism. The key canonical signals throughout development and adulthood are Notch, Hedgehog, bone morphogenetic protein (BMP), Wnt, and fibroblast growth factor (Fgf) proteins. These signalling proteins are implicated in some way in the activation and differentiation of virtually all cell types, both embryonic and adult. This consistency of signalling pathways belies the shared evolutionary ancestry across all the stem cell niches (Brunet and King, 2017).

At mouse embryo day 7, the gastrula is formed in which all three germ layers are specified: the mesoderm, endoderm, and the ectoderm (Fig. 3). The ectoderm, the pool of cells that forms the central nervous system, is specified by supressing BMP and Nodal signalling (Dupont et al., 2005). The neural plate and the subsequent neural tube are similarly patterned, at least in part, by the modulation of BMP signalling on embryonic day 7.5 and 9.5, respectively (Wilson and Hemmati-Brivanlou, 1995). Once the neural tube is formed, the most ventral cells in the neural tube are the pool of motor neuron progenitors.

In all cells, combinations of proteins called transcription factors regulate the transcription of specific cell-type specific genes, acting as the ultimate downstream effectors of signalling molecules. This pool of motor neuron progenitor cells express the transcription factors Olig2, Pax6, Nkx6.1, and Nkx2.2 (Lu et al., 2002). Interestingly, without Olig2 at this stage in development, both motor neurons and oligodendrocytes fail to develop—revealing a common developmental dependency on the transcription factor Olig2.

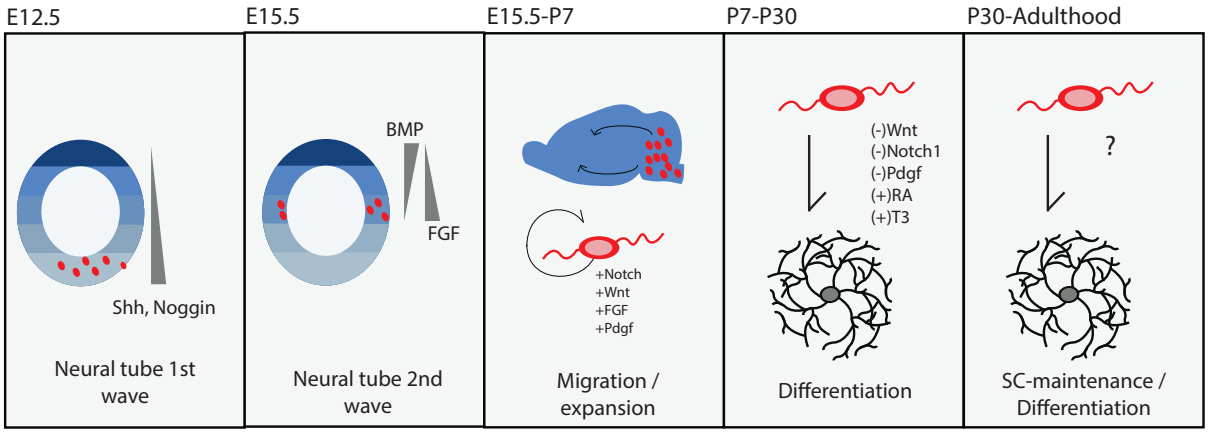

Figure 3. The development of OPCs. An illustration of the development of OPCs in the rodent. Each panel represents a timepoint in development that is crucial for the differentiation of OPCs. From E12.5 to P7 OPCs begin to proliferate across the developing CNS following exposure to Noggin, Hedgehog, Notch, Wnt, Fgf, and Pdgf signalling. Finally at p7, OPCs begin differentiating into oligodendrocytes. The nuclear hormones RA and T3 have been implicated in the differentiation of developmental oligodendrocytes. In adulthood, OPCs maintain self-renewal and differentiation capacity, though the signals that underlie both remain incompletely understood.

OPCs begin to appear following exposure to hedgehog protein and inhibiting BMP signalling at mouse embryonic day 12.5 as shown by their upregulation of the OPC-specific marker platelet-derived-growth-factor-receptor-alpha (Pdgfra) (Lu et al., 2000). Following exposure to hedgehog signalling, OPCs are specified from the motor neuron pool by the upregulation of Olig2 and Nkx2.2, and the down regulation of the neuron factors Nkx6.1 and Pax6 (Qi et al., 2003). At mouse embryonic day 15.5, a second wave of hedgehog-independent OPCs develop more dorsally along the neural tube following exposure to Fgf2, activating Olig2 using an alternative pathway (Cai et al., 2005). Using lineage tracing, the ventrally developed OPCs are dominant in the spinal cord, whereas the dorsally-developed OPCs dominate in the forebrain (Kessaris et al., 2005). Following the upregulation of Olig2 in proto-OPCs, the transcription factor binds the enhancer region of the oligodendrocyte-lineage specific region of Sox10, which in turn upregulates the expression of the OPC-specific Pdgfra (Finzsch et al., 2008; Küspert et al., 2011).

Following specification, OPCs migrate through the central nervous system along the blood vessels in the neonate (Tsai et al., 2016). Along with Fgf2, the signalling protein platelet derived growth factor alpha (Pdgfa) acts as a chemoattractant, directing OPCs across the central

nervous system in development (Bribián et al., 2006; Zhang et al., 2004). Moreover, OPCs, which uniquely express the receptor for Pdfra in the CNS, require PdgfAA for survival. By the end of development, between 20-50% of OPCs undergo apoptosis, and this survival is highly dependent on OPC exposure to PdgfAA (Barres et al., 1992; Richardson et al., 1988). As OPCs proliferate and migrate along the blood vessels, they express high levels of the receptor for the protein Wnt . At this stage in development, Wnt, along with FGF and Notch1 signalling, maintain OPCs in an undifferentiated and proliferative state (McKinnon et al., 1990; Wang et al., 1998).

Eventually, OPCs begin to differentiate into oligodendrocytes. In mice, a handful of differentiated oligodendrocytes are present at birth in the spinal cord. By post-natal day 6, a handful of cells begin to appear in the cerebellum and the brainstem. The differentiation of oligodendrocytes continues progressively into post-natal day 23, when the number of differentiated oligodendrocytes peaks (Foran and Peterson, 1992). Eventually the number of total oligodendrocytes decreases after post-natal day 23 as extra oligodendrocytes produced during development undergo apoptosis.

The exact cause of the developmental switch from migrating and proliferating progenitor cells to developmental myelination remains unknown. Moreover, it is unclear why certain white matter tracts become hyper-myelinated while grey matter regions don't. However, some molecular signals are, at present, understood. To differentiate into oligodendrocytes, many of the canonical signalling pathways mentioned (FGF, BMP, Hedgehog, Notch, Pdgf, and Wnt) must be downregulated. The nuclear receptors' retinoic acid and thyroid hormone have been shown to be positive regulators of OPC differentiation into oligodendrocytes (Barres et al., 1994). The importance of thyroid hormone regulation for OPC differentiation is highlighted by the fact that neonatal rats with hyperthyroidism and an excess of thyroid hormone have elevated levels of myelination (Marta et al., 1998).

While the initial steps of OPC differentiation remain unclear, much is known once the differentiation programme of oligodendrocytes has begun. Upon differentiation, the transcription factor Sox10 binds the promoter region of the transcription factor myelin regulatory factor (Myrf) (Hornig et al., 2013). Myrf along with Sox10 bind directly to the promoter regions of myelin component genes and upregulate their expression (Bujalka et al., 2013; Niu et al., 2012). To-

gether these genes enable the expression of myelin specific genes, the best understood of which are myelin oligodendrocyte glycoprotein (Mog), myelin-associated glycoprotein (Mag), myelin proteolipid protein (Plp1), 2',3'-Cyclic-nucleotide 3'-phosphodiesterase (CNPase), and myelin basic protein (Mbp) (Emery et al., 2009).

As mentioned previously, myelin is lipid rich membrane that wraps axons, allowing for efficient signal propagation down the axon. Oligodendrocytes wrap the axons several times to form a dense and complex membrane around the axon. Upon differentiation, OPC microfilaments polymerise and begin to form filapodia that branch out from the body of the cell (Bacon et al., 2007). Cytoplasmic channels deliver myelin proteins to the growth areas and Mbp and CNPase compact the myelin proteins in a cell-body-proximal to cell-body-distal manner (Snaidero et al., 2014). In this way, a single oligodendrocyte cell can ensheath up to 50 axons at once (Pfeiffer et al., 1993) . The amount of myelin wrapping of the axon is dictated by cell-intrinsic mTOR signalling. The wrapping occurs segmentally along the axons and the regions in between the myelin wraps are known as the nodes of Ranvier. While it is unclear why certain regions of axons are myelinated and not others, there is some evidence to suggest that region-specific cell surface markers on the axons inhibit myelination in certain areas of the CNS (Redmond et al., 2016).

The production of myelin and its wrapping of axons to promote saltatory conduction has long been established as the main function of oligodendroctyes (Waxman, 1977). By acting as the insulator on the axon membrane, oligodendrocytes increase the speed with which depolarisation events can occur down an axon by 500-5000%, thus increasing neuron signalling speed and transduction. Recent evidence has emerged that oligodendrocytes provide additional trophic support to the axon. Mouse models that were heterozygous knockouts for the Plp1 or Cnp1 gene showed only slight deficits in compact myelin wrapping, but both knockouts caused large-scale axonal degeneration (Griffiths et al., 1998; Lappe-Siefke et al., 2003). These two studies were amongst the first to highlight the possibility that oligodendrocytes perform roles in addition to the literal the wrapping of the axons.

Transporters that export pyruvate and lactate into the ensheathed neuron are embedded within the myelin wrapped sheaths (Fünfschilling et al., 2012; Lee et al., 2012). Without the transport of lactate and pyruvate into the axon, which are used in the neuronal citric acid cycle to gener-

ate cellular energy, the axon cannot sustain itself and degenerates. Finally, an even more recent and surprising study showed that oligodendrocytes deliver exosomes full of growth factors and RNA to stressed axons in order to help with their survival (Frühbeis et al., 2013).

The role of the oligodendrocyte lineage in adult CNS homeostasis

In the adult CNS, OPCs are thought to be scattered evenly throughout the CNS parenchyma (Pringle et al., 1992). They self-repulse one another and thereby maintain cell density, never invading one another's territory in the brain. If, however, an OPC is lost, the neighbouring OPC divides and the daughter cell replaces the differentiated OPC (Hughes et al., 2013). This process of OPC number maintenance must be sustained throughout adult life, as the total number of OPCs in the CNS remains constant even with ageing (Rivers et al., 2008). The outcome of adult stem cell division may be symmetric or asymmetric; after cell division, the mother cell can remain the resident stem cell while the daughter cell goes on to form the differentiated cell (Gurevich et al., 2016). Alternatively, both mother and daughter cell can divide symmetrically with both either differentiating or staying as stem cells (Snippert et al., 2010). In this way, the tissue retains the stem cell pool for future use, while also turning over old or damaged tissue. For now, the consensus is that OPCs can undergo both symmetrical and asymmetrical cell division: an OPC can divide and become two oligodendrocytes, two OPCs, or an oligodendrocyte and an OPC (Zhu et al., 2011). The signals underlying these distinct fate-decisions remain unclear.

In normal adult tissue homeostasis, OPCs primarily give rise to the oligodendrocyte. Unlike the neural stem cells of the SVZ, OPCs remain in the cell cycle throughout young adulthood (Psachoulia et al., 2009); in rodents, over a third of total brain oligodendrocytes are generated by OPCs after reaching sexual maturity (Rivers et al., 2008). Again, using radioactive carbon cell tracing, oligodendrocytes in the grey matter are found to be generated at a high rate well into the fourth decade of adult human life (Yeung et al., 2014). Once differentiated, oligodendrocytes are highly stable, with the vast majority (>90%) of oligodendrocytes born at p60 surviving for the remainder of the mouse's lifetime (Tripathi et al., 2017). These data suggest that adult myelination is not simply replacing dying oligodendrocytes; but that de novo myelination is occurring in previously unmyelinated axonal areas.

As OPCs remain active throughout adulthood, one of the most pressing issues in the field is how

and why OPCs activate and differentiate into oligodendrocytes in specific regions across the central nervous system. Some of the first work on OPCs revealed that they have the ion channels glutatmate and GABA (Barres et al., 1990). Throughout the adult brain, OPCs form synapses with both glutamatergic and GABAergic neurons (Bergles et al., 2000; Lin and Bergles, 2004). While the function of these synapses remains a mystery, *in vitro* studies have revealed that agonising AMPA receptors on OPCs with glutamate can stimulate their activation, both in terms of proliferation and differentiation. These studies suggest that OPC activation in the adult brain is tightly correlated with the activity of proximal neurons. However, the exact orientation of OPCs in the brain in relation to other cell types remains largely unknown.

In conjunction with the previous findings that OPCs form synapses with oligodendrocytes, the activation and differentiation of OPCs is context and situationally dependent. Upon activation of certain neuronal pathways, either using optogenetics or by rodent wheel running, OPCs activate and differentiate into myelinating oligodendrocytes. By genetically preventing OPC activation, in the case of the running wheel, animals were less able to learn how to run on the wheel (Gibson et al., 2014; McKenzie et al., 2014). Additionally, mice housed in isolation have behavioural problems tied to aberrant myelination in the prefrontal cortex (Makinodan et al., 2012). A recent study has shown that not only does myelination persist in middle-aged rodents, but also that myelination is enhanced in sensory rich environments (Hughes et al., 2018). Conversely, mice without whiskers, and thus sensory deprived, have a deficit in myelination in the cerebral cortex. These studies coalesce around the central hypothesis that OPCs and adult oligo-dendrogenesis are critical for adult learning and post-natal myelination.

Despite this recent interest in 'adaptive myelination' (the hypothesis that adult myelination is context and experience dependent), there is little known about the molecular mechanisms regulating adult OPC activation. The best way to understand adult stem cell activation signals is to look to other better characterised stem cell niches. Unsurprisingly, many of the same protein signals that govern embryonic development also regulate adult stem cell activation. The Notch, Hedgehog, BMP, Wnt, and Fgf proteins have been implicated in the activation and differentiation of a number of stem cell niches—each niche requires its own dose of signalling for activation from each of these signalling pathways (Kroon et al., 2008). Across tissues, high levels of Notch protein maintains adult stem cell quiescence, and losing Notch leads to the loss of the tissue stem cell pool as the stem cell pool differentiates (Bjornson et al., 2012; Chapouton et

al., 2010). In the intestinal villi, Wnt signalling protein activates the intestinal crypt progenitor cells, and the inhibition of Wnt is required for intenstinal stem cells to exit the cell cycle and terminally differentiate into Paneth cells (van Es et al., 2005). Whether these classical stem cell activation pathways play a role in homeostatic adult adaptive myelination remains to be determined.

Diseases of the myelin

As oligodendrocytes' myelin maintains axonal integrity, diseases of the myelin can be devastating. The term leukodystrophies describes any disease which causes disruption to the myelin sheath. There are a number of rare congenital leukodystrophies that cause the impromper formation of the myelin sheath. One of the best understood of the diseases that directly affects oligodendrocytes themselves is Pelizaeus–Merzbacher disease (PMD), a recessive, x-linked disease which is caused by the point-mutation or duplication of the myelin component gene Plp1. While patients with PMD appear normal at birth, the symptoms become increasingly pronounced with development. PMD varies in severity, depending on the dosage of the Plp1 gene, but at its most severe, PMD severely limits cognition, mobility, and can cause early childhood mortality (Garbern et al., 1999). Leukodystrophies such as PMD highlight the need for myelin in post-natal cognitive development: embryonic development proceeds as normal, but myelination is required for post-natal cognitive development.

As oligodendrocytes lineage cells compose ~50% of total cells of the cortex, it would follow that most diseases of the CNS involve oligodendrocytes in one way or another (Pelvig et al., 2008). Indeed, the focus of research for neurodegenerative diseases has largely been on neurons and their degeneration, but an emerging field of research is pitting the oligodendrocyte as a central player in major neurological disorders. In Alzheimer's disease, there is a marked decrease in the amount of myelinating oligodendrocytes across the human brain (Sjöbeck et al., 2005). In spinal cord injury, myelin loss is now being considered a central factor implicated in the loss of function (Papastefanaki and Matsas, 2015). While most of this work is correlative (e.g. identifying a loss of myelin in various pathologies), a surprising recent paper identified a link between schizophrenia and oligodendrocytes (Windrem et al., 2017). In this paper, the authors transplant oligodendrocyte progenitor cells from patients with schizophrenia into the CNS of shiverer mice, a congenitally hypomyelinated mouse model. They find that only with OPCs

derived from patients with schizophrenia do they observe that the mouse-human chimeric CNS is hypomyelinated and that the mice behave abnormally. This paper provides preliminary evidence in support of the hypothesis that the oligodendrocyte plays a central role in the etiology of many complex neurological diseases.

The best studied disease of myelin is multiple sclerosis (MS). In patients with multiple sclerosis, immune cells destroy the central nervous systems' oligodendrocytes. It is this death of oligodendrocytes that causes demyelination and ultimately axonal cell death (Hauser and Oksenberg, 2006). MS begins 85% of the time in patients between the ages of 20 and 30, and, for most patients, the disease is first marked by a phase of relapses and remissions as the immune system attacks and destroys the myelinating oligodendrocytes. Like many auto-immune disorders such as type I diabetes, the cause of the initial immune attack on the myelin sheath is unclear, though it is assumed to be caused by a combination of genetics and environment. Similarly, the exact cause of each subsequent relapse is unknown and can vary from person to person; however, relapse has been correlated with immune adjuvants such as the flu and other forms of infections (Andersen et al., 1993).

Following each relapse in this early phase of MS, there is a period of remission in which the clinical symptoms improve. The cause of this improvement in symptoms has been correlated with the remyelination of the demyelinated lesioned tissue (Kornek et al., 2000). Remyelination is the process by which new OPCs are recruited to the lesioned tissue site and differentiate into new myelinating oligodendrocytes to replace the immune-destroyed ones. Indeed, remyelination can occur quite efficiently in this first part of the relapse-remitting phase of the disease (Albert et al., 2007), restoring efficient signal transduction in the axon (Smith et al., 1979) However, as the disease progresses, remyelination becomes highly inefficient, leaving chronically demyelinated lesions (Compston and Coles, 2002). In the end, these chronically demylinated axons undergo Wallerian degeneration in which the demyelinated axon irreversibly deteriorates (Dziedzic et al., 2010).

Of patients with relapse-remitting multiple sclerosis, 50% ultimately develop secondary progressive MS, a phase of the disease marked by the progressive worsening of symptoms. Regardless of the variant of MS, after just 15 years following diagnosis, 75% of patients with MS are unemployed, and almost 60% of patients need help moving (Confavreux and Vukusic,

2006). Cognitive deficits as well as depression are also common amongst patients with MS.

Most available therapeutics for patients with MS seek to mitigate the effects of immune-mediated demyelination using immune-modulatory drugs. The most common classes of drugs used are interferon ß and glatiramer acetate (Ebers, 1998; Farina et al., 2005), both of which are believed to slow MS disease progression by stimulating anti-inflammatory cytokines from T cells and anti-inflammatory macrophages. A recent report showed that the two most effective approved drugs that reduce the number of relapses are Alemtuzumab and Natalizumab (Tice et al., 2016). While Alemtuzumab is a blocking antibody that binds all lymphocytes and thereby globally dampens immune funtion, Natalizumab binds and blocks the integrin that allows T cells to cross the blood brain barrier. Whilst highly effective short term, these therapeutics fall short: symptoms of most patients still worsen over time. Immune-modulation may reduce the number of immune-mediated relapses, but it does not address the primary de-myelination events, and the de-myelinated axons still undergo Wallerian degeneration (Franklin and Goldman, 2015). The lack of therapeutics able to address the central issue of demyelination in MS highlights the importance of researching the mechanisms of remyelination and the reasons for remyelination failure.

Experimental models of remyelination

To best understand advances in the field's understanding of remyelination, it is first important to review the animal models that provide the basis for these findings. A number of animal models have been developed to study the process of remyelination. Each model, naturally, has its advantages and its limitations. There are three categories of animal models that are widely used to study remyelination: immune-mediated demyelination, toxin-induced demyelination, and genetically-targeted demyelination.

Immune-mediated demyelination has been used for almost half a century (Yasuda et al., 1975). One method for causing demyelination known as experimental autoimmune encephalomyelitis (EAE) involves the co-injection of myelin component proteins such as MBP and MOG and the immune stimulant Freund's adjuvant. Together, these components cause the rodent to initiate an auto-immune attack on CNS myelin, causing widespread CNS demyelination. The immune-mediated destruction of myelin echoes the process by which patients with MS develop demyelinating lesions. While this model has led to the discovery of a number of immune-modulatory therapies to treat MS, it has largely failed to identify remyelination therapies (Ransohoff, 2012). As an uncontrolled immune-driven animal model, the lesions occur sporadically and randomly throughout limited parts of the CNS. This makes studying the molecular and cellular orchestration of remyelination difficult as the timing and speed of remyelination is hard to determine.

To study the process of remyelination itself, isolated from the variables of autoimmunity, a number of toxin induced models have been developed. Cuprizone is a copper-chelator that is specifically toxic for oligodendrocytes (Matsushima and Morell, 2001). As such, providing cuprizone in the diet of rodents causes demyelination events to appear sporadically throughout the CNS. In this model, demyelination and remyelination happen repeatedly within the lesion, which mirrors the pathology of multiple sclerosis lesions. Like the EAE model, however, the lesions develop sporadically over the course of cuprizone administration, making it difficult to characterise the state of the lesion.

The focal-demyelination toxin model escapes many of the limitations of the cuprizome model. This model involves the focal injection of a toxin such as lysophosphatidylcholine or ethidium bromide into white matter tracts (Blakemore and Franklin, 2008; Blakemore et al., 1977). The benefits of this model are that the time and location of demyelination are known. As such, the lesion site can be directly administered with cell transplants, small pharmaceutical compounds, or viral constructs, allowing for experiments that screen for factors relevant for re-myelination. As mentioned, MS is a disease of immune-mediated demyelination and OPC-mediated remyelination. In the toxin-model, the immunological element of the disease is purposefully ignored in order to focus on the biology of remyelination.

The final and most recently developed model of remyelination is the genetic ablation model. Mice were generated that carry the tamoxifen-dependent cre recombinase gene under the promoter of the myelin-specific gene Plp1 and a floxed diphtheria toxin gene (Pohl et al., 2011); in other words, following the injection of tamoxifen, Plp1 expressing oligodendrocytes across the CNS expressed the gene encoding diphtheria toxin, leading to widespread demyelination. Surprisingly, oligodendrocyte death did not lead immediately to axon death. Moreover, for unknown reasons, remyelination was highly inefficient in these mouse models. It is believed that this could be due to the expression of Plp1 in a high proportion of the progenitor cells themselves, thus depleting both the progenitor and the oligodendrocyte cell pools. While genetic ablation models hold much potential in terms of their experimental power, until the orchestration of cellular events in remyelination in the genetic ablation models is more fully established, the toxin model remains the best model for researching CNS remyelination.

Lessons from Remyelination Studies

The vast majority of new oligodendrocytes in these focal-induced demyelination studies are derived from the OPCs, though there is some evidence that neural stem cells give rise to a small proportion of oligodendrocytes (Menn et al., 2006). In one report, small numbers of labelled neural stem cells migrate from the subventricular zone following a toxin-induced lesion in the corpus callosum. It is unclear, though, the extent to which this occurs in lesions in other regions of the brain more distal to the subventricular zone. As such, the vast majority of work has gone into studying the migration, proliferation, and differentiation of OPCs.

As the toxin-lesion model provides the exact timestamp of the demyelinating insult, the orchestration of cells that contribute to remyelination in the days following the lesion is now well characterised. Almost every cell-type of the CNS plays a role in remyelination: Astrocytes surround the lesion site and secrete growth factors such as Pdgf and Fgf, regulating OPC numbers around the lesion (Woodruff et al., 2004). Semaphorins presumed to be secreted by axons stimulate the migration of the OPCs to the lesion site (Piaton et al., 2011). Pro-inflammatory microglia and peripheral macrophages phagocyte the myelin and secrete signals such as Activin-A, acting directly on OPCs to stimulate their differentiation (Kotter et al., 2006; Miron et al., 2013).

Following the activation of the astrocytes and microglia, OPCs are recruited to the lesion site where they activate and differentiate into new ensheathing oligodendrocytes. Following recruitment to the lesion site by mitogenic growth factors, OPCs begin upregulating many genes that are associated with OPC development such as their expression of Olig2, Sox2, and Nkx2.2 along the lesion border (Fancy et al., 2004). To remyelinate the lesion site, the differentiating oligodendrocytes first make contact with the denuded axon, express myelin genes, and finally wrap the axon, restoring efficient conduction down the axon. The exact molecular steps that direct this process of remyelination remain unclear. However, developmental signals such as retinoid signalling and the loss of Fgf signalling have been shown to accelerate remyelination (Armstrong et al., 2002; Huang et al., 2011).

There are some surprising differences between developmental myelination and these focal demyelination studies. The gold standard quantification for identifying and assessing the remy-

elination of the lesion is known as the g-ratio—the ratio of myelin thickness to axon diameter (Blakemore, 1974). Importantly, during the process of remyelination, axon myelin is restored but is always thinner than developmental myelin, making it easy to identify the remyelinated lesion area. The reason for this difference remains unknown.

There are some clear mechanistic differences as well that distinguish remyelination and developmental myelination; the transcription factor Olig1, while dispensable for developmental remyelination, is required for remyelination (Arnett, 2004). Conversely, the deletion of the canonical receptor Notch1 in development negatively impacts myelination, while its deletion in the adult has almost no effect on remyelination (Hu et al., 2003; Stidworthy et al., 2004). Together these results emphasize that adult remyelination echoes but does not exactly replicate developmental myelination, a fact that is likely important for developing remyelination therapies.

Ageing, regeneration, and OPCs

Like all regenerative processes, the process of remyelination becomes inefficient with ageing (Shields et al., 1999). Even in the absence of additional inflammation, remyelination efficiency is impaired, and this finding is critical for better understanding the aetiology of diseases such as multiple sclerosis. If remyelination efficiency is age-related and, at least in part, independent of the adaptive immune response, then immune-modulators cannot alone be used to treat diseases such as secondary progressive MS. To understand the reasons for the loss of remyelination efficiency with age, it is important to explore the prevailing theories of the ageing field.

Interest in the ageing field has grown in recent decades as it has become clear that ageing is the confounding factor for most adult-onset pathologies (López-Otín et al., 2013); Type ii diabetes, cardiovascular disease, neurodegenerative diseases such as Alzheimer's disease, and cancer all have increased incidence in aged populations. Moreover, developed countries are experiencing a demographic challenge with increased numbers of aged people and are investing heavily in research to mitigate the growing health care burden of age-related disease (Mahishale, 2015). As such, there is a socioeconomic imperative to better understand the ageing process.

The activity-mediated ageing hypothesis

Experimental biologists began seeking biological explanations for longevity and ageing in the early 20th century. Studies of longevity began by looking at the regulators of lifespan in drosophila and rats (Economos and Lints, 1985; Osborne et al., 1917). Quickly, these researchers identified mating and food intake as two key regulators of longevity. Female rats that were house without males lived significantly longer than rats housed with males. Drosophila that were given minimal food intake during their days of development lived significantly longer than those given excess amounts of food. This early work was continued in the 1950s with a hallmark study showing that drosophila exposed to brief bursts of high heat in early development lived longer than drosophila in normal temperature conditions (Smith, 1958). This idea that reproduction, stress, growth, and longevity were somehow linked, however, is not new: Early thinkers such as Aristotle and Galen proposed that longevity could be enhanced from sexual abstinence and minimal calorie intake (Jeune, 2013).

With the advent of modern day molecular biology, research in the ageing field began by recapitulating these early findings with the new understanding of genomics. This work began in the early 1990s with the finding that mutant C. Elegans could live twice as long as wild types (Kenyon et al., 1993). These mutant C. Elegans had a mutation in the C. Elegans *daf2* gene, the drosophila paralogue of the mammalian insulin-like growth factor (Igf1) gene. Follow up studies showed that juvenile C. Elegans that were *daf2* mutants entered prematurely into a semi-dauer state, a state of low metabolism and low reproduction (Gems et al., 1998). These studies were recapitulated again in mice with an Igf1 mutation (Holzenberger et al., 2003). Finally, when the hormone Klotho, a hormone antagonist of Igf1 signalling, was given to mice, they had an increased lifespan of up to 30% (Kurosu et al., 2005).

As Igf1 signalling is tightly linked to insulin hormone—the hormone secreted in response to elevated blood glucose levels—this trajectory of study further intensified research into the link between calorie intake, cell metabolism, and ageing. To lower insulin and insulin growth factor signalling, much work has gone into better understanding whether calorie restriction itself has an effect on ageing. Perhaps the strongest evidence to date of the importance of metabolism on longevity and health span is the decade-spanning study showing that calorie restriction in Rhesus monkeys prolongs both lifespan and healthspan (Colman et al., 2009). After 30 years, only 25% of the monkeys fed a normal diet were without disease while almost 75% of calorie restricted monkeys were without disease.

Together, these experiments coalesce around the Darwinian "disposable soma" theory of ageing (Rando, 2006). Well accepted in the ageing field, this theory suggests that the body's energy resources are optimised for growth and reproduction at the expense of somatic self-preservation. After a prolonged period of growth and activation, cells ultimately accumulate too much 'damage' to function properly. According to this theory, calorie restriction works by disrupting the flow of resources to reproductive fitness, forcing the cells into a 'self-preservation' mode at the expense of reproductive fitness. This is the prevailing theory of the ageing field whereby the stress of development into adulthood ultimately drives somatic ageing.

Intracellular age-related signalling pathways

The question of how calorie restriction via insulin signalling prolongs life and healthspan re-

mains an area of active research. Two opposing signalling pathways are important downstream targets of food intake: mTor and Ampk (Fig. 4). Under levels of high glucose, insulin signalling activates mTor signalling via PI3K and AKT. mTor in turn upregulates the ribosomal translation machinery, inhibits autophagy, and prepares the cell for cell division and growth (Russell et al., 2011). Under conditions of low glucose, AMPK signalling drives cells into the quiescent G0 phase of cell cycle, activating DNA damage repair, mitochondrial biogenesis, autophagy, and reactive oxygen species degradation (Mihaylova and Shaw, 2011). Together these two pathways counterbalance one another: mTOR promoting growth and AMPK promoting quiescence. Mouse lifespan can be increased by up to 20% *in vivo* by simply inhibiting mTor pathway with the small molecule rapamycin (Harrison et al., 2009) or by activating the AMPK pathway with the small molecule metformin (Martin-Montalvo et al., 2013).

The explanations linking mTor pathway to ageing are complicated and often times conflicting. The prevailing theory is that upon activation of mTor, cells, especially stem cells, become primed for growth. Under these growth conditions, autophagy is inhibited, DNA repair stalls, and mitochondria begin producing energy via oxidative phosphorylation. Ultimately, the downstream effects of genomic instability, the loss of autophagy, and changes in cell metabolism are seen as the main three components driving intracellular ageing. Each of these downstream underpinnings of ageing require investigation in order to create therapeutic interventions for age related disease.

Age related genomic instability

Genomic instability describes DNA damage, the loss of epigenetic marks, and three-dimensional topographical chromatin disorganization. As DNA is the underlying instruction book for cell biology, damage to the DNA itself has long been postulated as the ultimate driving factor in the ageing process (Szilard, 1959). With ageing, there is indeed an increase in the number of DNA mutations (Moskalev et al., 2013). Without functioning DNA repair master-regulator Sirt6, mice have accelerated ageing phenotypes and shortened lifespans (Mostoslavsky et al., 2006). Conversely, mice with the overexpression of Sirt6 have increased longevity (Kanfi et al., 2012).

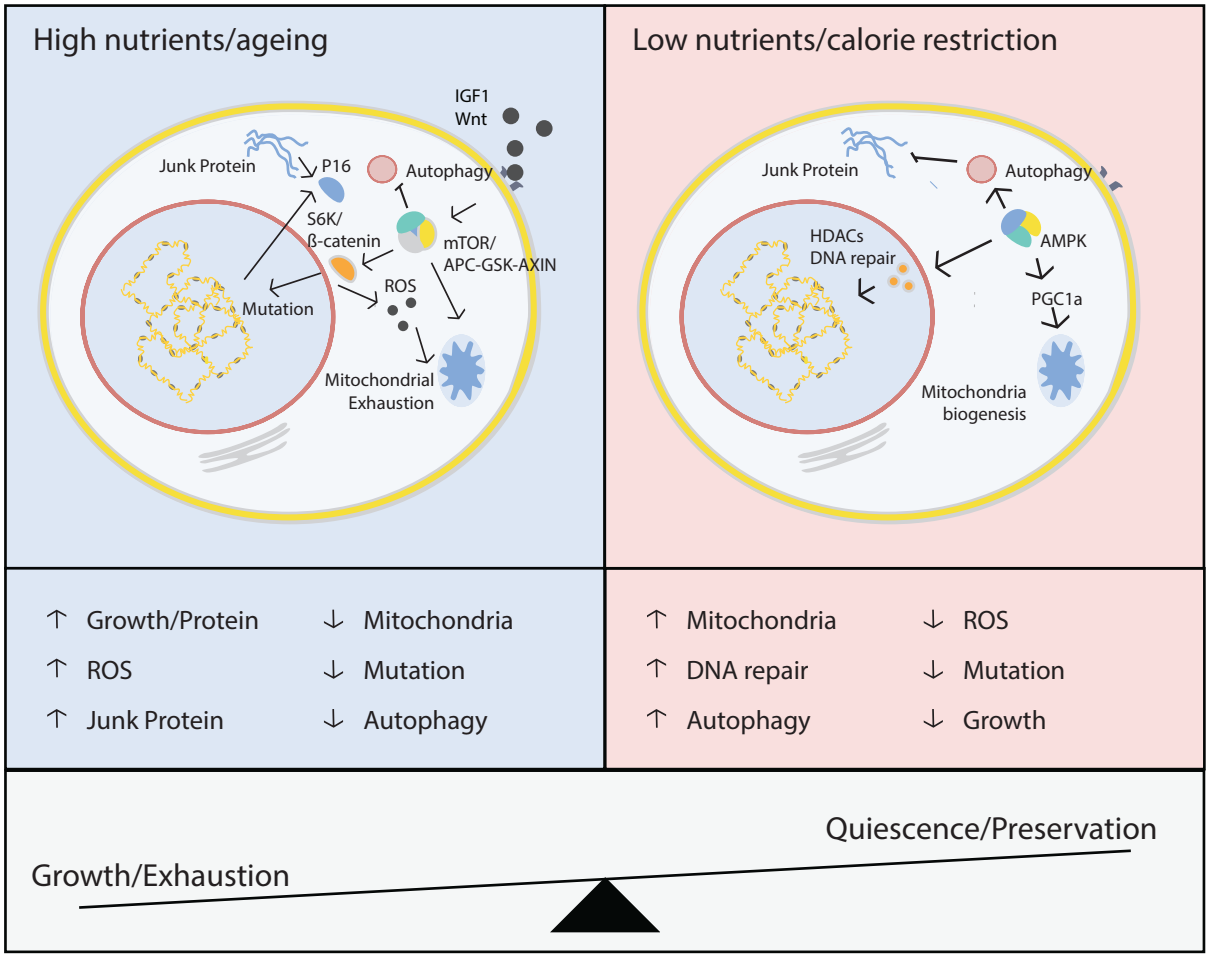

Figure 4. Growth versus cellular preservation signaling pathways. With pro-growth signaling pathways there is a hyper activation of mTOR signalling, a loss of mitochondria biogenesis, autophagy, and DNA integrity. Under low nutrient conditions, cells enter a self-preservation state; they degrade junk proteins, generate new mitochondria, and repair DNA. The ageing field largely has focused on reconciling these two cell states with the hope of promoting cellular self-preservation over cell growth and cellular ageing.

Early work in the ageing field also focused on the length of the telomeres on the ends of chromosomes. Telomeres are repeat nucleotide sequences that act as a buffer, protecting coding regions of chromosomes from damage during DNA replication. Mice without the enzyme responsible for telomere deposition—telomerase—exhibited an accelerated ageing phenotype (Rudolph et al., 1999).

Unpublished studies have shown that DNA damage in the adult alone can cause an accelerat-

ed ageing phenotype (Sinclair et al., 2016). This work, presented at a conference, described a transgenic mouse model that expresses a restriction enzyme only following exogenous dosage of doxycycline. This rare restriction enzyme was chosen only to cause double strand breaks in 100 non-coding and non-regulatory regions of the genome (Kim et al., 2016). The authors observed short-term transcriptional stability, but overtime the animals exhibited a rapidly accelerated ageing phenotype. This is perhaps the strongest work to date showing that DNA damage itself, independent of DNA mutations in coding or regulatory regions, triggers an ageing phenotype.

This reduced epigenetic stability has also been implicated in the ageing process. The epigenome generally refers to the methylation of DNA and core protein histones around which the DNA is wrapped. In ageing, both the methylation of DNA and the histone remodelling of DNA is significantly changed. DNA methylation is the tagging of DNA base pair cytosine with a methyl group and is classically associated with the silencing of DNA. With ageing, overall DNA methylation is lost in somatic cells (Wilson and Jones, 1983). While there is an overall loss in methylation with age, many promoter regions that are involved in regulating stem cell proliferation and differentiation become hyper-methylated with ageing (Day et al., 2013). In drosophila—the overexpression of Dnmt1—the methyl transferase enzyme partly responsible for DNA methylation, increases longevity (Lin et al., 2005).

The gene expression of core histones is lost progressively with ageing (Liu et al., 2013). Like DNA methylation, this loss in histone gene expression is complicated by the fact that certain kinds of chromatin remodelling actually increase with ageing. Previously considered synonymous, the histone modifications H3K27Me3 and H3K9Me3 are both histone marks that identify silenced chromatin. H3K27Me3 increases with age, a finding that corroborates the theory that quiescent aged cells have lower levels of transcription. Surprisingly, H3K9Me3 is progressively lost with ageing (Zhang et al., 2015), suggesting a divergent role for these chromatin marks. Histone deactylase enzymes classically remove acetyl groups from the core histone complexes. This causes tighter binding of the chromatin to the histones, thereby reducing transcriptional activity of the tightly-wound chromatin. With ageing, the expression of these chromatin remodelling enzymes is lost. In one study, experimental overexpression of the histone deactylase Sirt6 genes in mice increased their longevity by 15% (Kanfi et al., 2012).

Recent work has shown that the three-dimensional topographical arrangement of chromatin is crucial for proper gene expression (Dixon et al., 2012). Genes that are brought to the nuclear periphery are primed for gene expression, and clusters of genes that require co-expression are often arranged together (Peric-Hupkes et al., 2010). While no direct link has of yet been made between chromatin domain re-arrangements and ageing, there are a number of hints that changes in chromatin topography may be another driving force behind the ageing phenotype. In Hutchinson Gilford Progeroid syndrome there is a mutation of the nuclear lamina gene Lmna. Patients with this disease have an accelerated ageing phenotype and suffer from age-related diseases at a young age. The nuclear lamina describes the protein network that lines the inside of the nuclear membrane and plays a major role in shaping the chromatin into topographical domains (Guelen et al., 2008). Unsurprisingly, the cells of patients with this mutation have large amounts of chromatin disorganization (McCord et al., 2013). Similarly, in patients with another accelerated ageing disease called Werner syndrome, there are large scale topographical changes in chromatin positioning (Zhang et al., 2015). Together, these two rare diseases shed light on the importance of three-dimensional chromatin organization on the rate of ageing.

Proteostasis and ageing

Proteostasis is the process by which damaged proteins or organelles are degraded by the cell in order to preserve cellular homeostasis. There are two main mechanisms by which cells degrade proteins: autophagy and ubiquitin-mediated proteolysis. In autophagy, damaged organelles and proteins are targeted by the autophagasome and are delivered to the lysosome where they are degraded. In ubiquitin-mediated proteolysis, proteins that are typically tagged with the small protein ubiquitin are targeted by the proteasome for destruction. Both of these independent protein degradation processes are severely impaired with ageing.

In drosophila, there is a 3-4 fold increase in ubiquitinated proteins in the CNS with ageing (Simonsen et al., 2014). This suggests that proteins targeted for degradation are not being properly processed and thus accumulate within the CNS. In C. Elegans, when key components of the proteasome machinery were over-expressed, animals lived as long as those that were on calorie restriction. Conversely, when this machinery was knocked out, the animal's life was significantly shortened, even under conditions of calorie restriction (Carrano et al., 2009).

Autophagy similarly regulates the age-state of an animal. In drosophila ageing, there is a progressive loss of the autophagy genes expressed, suggesting a loss of activity of the autophagy machinery. When key components of the autophagy machinery are overexpressed, drosophila live significantly longer; without this machinery, the animals exhibit an accelerated ageing phenotype (Simonsen et al., 2014). In mice, the loss of key autophagy genes specifically in the CNS contributed to widespread neurodegeneration (Komatsu et al., 2006). Recent work has shown that hyper-activation of autophagy machinery in neural stem cells of aged animals via the autophagy regulating transcription factor TFEB rejuvenates the cells both functionally and transcriptomically (Leeman et al., 2018).

Mitochondria, cellular metabolism, and ageing

The first molecular explanation of ageing suggested that reactive oxygen species produced by mitochondria progressively impair normal cell function (Harman, 1956). In the past decades, there has been little proof validating this theory of ageing. Mitochondria, however, do lie at the heart of the ageing process. In human ageing, mitochondria morphologically become rounded and are less efficient at generating ATP via the electron transport chain (Short et al., 2005). Mice that have excessive DNA mutations in the mitochondrial DNA genome have a shortened lifespan and a severely accelerated ageing phenotype (Kujoth et al., 2005).

There are two main methods by which cells generate ATP: oxidative phosphorylation and glycolysis. Differentiating cells prefer oxidative phosphorylation over glycolysis (Cho et al., 2006). In adults, quiescent adult stem cells produce ATP using glycolysis (Folmes et al., 2012; Suda et al., 2011). Under conditions of calorie restriction, however, aged cells across multiple tissues begin increasing their number of mitochondria and increasing levels of oxidative phosphorylation (Nisoli et al., 2005). Moreover, in conditional mouse knockouts that prevent this mitochondrial biogenesis and increased oxidative phosphorylation, the effects of calorie restriction and its extension on lifespan are attenuated.

The reasons for the loss of efficient oxidative phosphorylation with ageing remain unclear. One theory is that with development and insulin-signalling there is a down regulation of AMPK signalling. AMPK via Sirtuin 1 is a master regulator of mitochondrial biogenesis transcription factor Pgc1a (Cantó et al., 2010). Without de novo mitochondrial biogenesis, mitochondria

become damaged and thereby less efficient at producing ATP via oxidative phosphorylation. By just overexpressing Sirtuin 1 or by increasing the global level of the Sirtuin 1 cofactor, NAD+, mice have increased mitochondrial longevity, oxidative phosphorylation, and increased longevity (Satoh et al., 2013; Zhang et al., 2016).

The exact reasons for increased longevity following increased ATP synthesis via oxidative phosphorylation remain unclear and wholly speculative. Intuitively, increased cellular energy would seem to suggest a more plastic and resilient cell. Another, exciting possibility is a newly identified role for ATP other than its classical role as the cell's energy source. It has been recently identified that ATP acts as a biological surfactant for proteins and prevents their aggregation (Patel et al., 2017). With increased ATP, it is possible there is a decreased aggregation of damaged cellular proteins.

Activity and Ageing: a conundrum

Across a number of tissues, the capacity of adult specific stem cells to differentiate into new tissue is significantly impaired in the context of injury (Goodell and Rando, 2015). The loss of stem cell function across a number of tissues is hypothesized to be the underlying driver of the ageing process (Oh et al., 2014). Without functional adult stem cells, tissues are unable to regenerate both in the context of disease and in homeostasis. Again, the field's consensus view for this loss of function is the underlying strain placed on the stem cell niche following postnatal development. During this period of growth there is a loss of autophagy, changes in cellular metabolism, and, most importantly, DNA damage. Despite the wealth of evidence supporting this theory, there is a growing amount of work which suggests that the ageing process is more nuanced.

Recent lessons from induced pluripotent stem cells (iPS cells) present the biggest challenge to the activity-drives-ageing hypothesis. The finding that four transcription factors, Oct4, Sox2, Klf4, and Myc, can reprogram any adult somatic cell into a pluripotent embryonic stem cell has revolutionised the field of stem cell biology (Takahashi et al., 2006). The authors showed that iPS cells, converted from adult mouse cells, could give rise to animal chimeras when injected into mouse blastocysts, differentiating into all the germ layers of development. Ultimately, these chimeric mice mature and are then able to produce viable offspring from gametes derived originally from the iPS cells (Okita et al., 2007).

A number of follow up studies confirmed that this process of reprogramming could be done in a cell from any age of donor. Surprisingly, many known age-related hallmarks disappear following reprogramming, even in iPS cells generated from aged persons. Upon reprogramming, telomere length extends, there is increased mitochondrial biogenesis, and even DNA repair mechanisms activate (Bhutani et al., 2010; Marión et al., 2009; Miller et al., 2013; Prigione et al., 2011). This process of de facto rejuvenation, however, requires this reprogramming step. One study examined fibroblasts directly converted into neurons and then compared them to fibroblasts that were first reprogrammed into iPS cells before differentiated into neurons. Directly converted neurons retained their age-state in terms of DNA methylation level and their expression of a panel of age-related genes, while the iPS cell derived neurons were rejuvenated,

losing many cellular traces of their age (Mertens et al., 2015). It is arguable that some unknown factor in the reprogramming process contains the answer to the ageing process.

If ageing is activity-driven, then the generation of highly proliferative iPS cells should only further drive an ageing phenotype, at least in the cells that are successfully reprogrammed. Recent work has considered the opposite hypothesis—that inactivity accelerates ageing. One study created a mouse in which all p16ink4a expressing senescent cells could be inducibly killed (Baker et al., 2011). Mice without senescent cells lived longer and had a lower incidence of age-related diseases.

In the most impressive study to date purporting this loss-of-activity hypothesis, the authors generated a mouse model that inducibly overexpressed the factors, Oct4, Sox2, Klf4, and Myc in transient bursts throughout the adult life of a mouse (Ocampo et al., 2016). The authors hypothesized that incomplete and 'partial' reprogramming of adult cells would reset cellular age-state but not their cellular identity. Doing so, the authors observed a 33% increase in remaining lifespan and a global loss of the cellular hallmarks of ageing. The authors of this study, however, neither examined nor considered the effects of the reprogramming factors on the ageing of OPCs.

The reasons for this activity-driven rejuvenation remain unknown. One possibility is that, as in the generation of iPS cells, a cell forced to re-enter cell cycle must fix damaged DNA and upregulate mitochondrial biogenesis pathways. Similarly, by undergoing mitosis, stem cells are able to dilute any damaged organelles in their daughter cells. One paper showed that healthy stem cells undergoing cell cycle regularly donate older mitochondria to the daughter cell (Katajisto et al., 2015). When the researchers inhibited this process of asymmetric organelle portioning, the mother stem cell lost plasticity. As such, without cell cycle, stem cells may accumulate damaged organelles and are thus unable to maintain homeostasis.

Insulin signalling and organismic growth drive DNA damage, the loss of autophagy, and impaired mitochondrial biogenesis. At the same time, activity and growth rejuvenates cells. Indeed, both theories have convincing substantiating evidence. While superficially opposing, both of these two theories could be accommodated within a new third theory: Certain types of activity are good for cell and tissue homeostasis while other types of activity are not. From

the studies examined, the types of cell states that promote healthy ageing are cell cycle and AMPK-mediated quiescence and repair. With normal ageing, however, cells get stuck in the mTOR mediated G1 phase of cell cycle growth. Whether or not this hypothesis proves true in the context of OPC ageing remains unknown.

Ageing and the Environment

To understand exactly what arrests aged stem cells in an activated G1 state is to understand the ageing process itself. The two cellular solutions to this problem of stem cell G1 arrest are: 1. To progress through cell cycle, or 2. to enter into quiescence. In aged and damaged tissue, entering into a state of self-repair and quiescence may indeed rejuvenate a stem cell, but ultimately the stem cell will need to activate and progress through the cell cycle to regenerate the aged tissue. Whether or not the aged environment is permissive to cell division in the first place is largely unknown.

Early transplant studies shed some light on this question. When healthy embryonic cells are transplanted into normal aged CNS, the cells engraft and survive but do not multiply (Hallas et al., 1980). Embryonic CNS cells transplanted into young adult animal CNS survive and do grow. These crude early studies reveal that even embryonic CNS cells at their most generative cannot progress through cell cycle in an aged environment. As such, the key to understanding the ageing process is identifying the factor that makes the aged environment so refractory to stem cell proliferation and differentiation.

Young blood and its effect on ageing

Throughout young adult development, the development of tissues is synchronised with circulating hormones until sexual maturity (Lee et al., 1975). At the end of post-natal adolescent development, pro-growth circulating hormones are gradually lost. To determine whether some unknown blood-derived hormone from young adult mice can rejuvenate an aged animal, researchers surgically linked the circulatory system of young and old mice in a process called heterochronic parabiosis. Doing so, researchers have found that a wide range of stem cells at least partially rejuvenate following exposure to a young circulatory system. Muscle stem cells repair tissue damage more efficiently, hepatocytes proliferate more, and even remyelination by

OPCs in the CNS is more efficient (Conboy et al., 2005; Ruckh et al., 2012).

Following the exposure of aged cells to young serum *in vitro*, the cells rejuvenated, further suggesting that the unknown factor is not cellular but hormonal (Conboy et al., 2005). A proteomics array showed that one circulating hormone, Gdf11, is reduced with ageing, but is increased in aged mice that have undergone the parabiosis procedure. Despite many conflicting reports, this hormone, Gdf11, has been reported to alone increase neurogenesis, cardiovascular function, and muscle regeneration (Katsimpardi et al., 2014; Loffredo et al., 2013; Sinha et al., 2014). Further studies are required to validate these reports, but the parabiosis studies emphasise the importance of non-cell autonomous factors in organismic ageing. Moreover, they suggest that the metabolic deficits implicated in cellular ageing may be symptoms, rather than causative instigators of the ageing process.

Even within a young systemic environment, however, regeneration remains limited. There have even been reports that while transient exposure to young factors transiently rejuvenates aged adults, the effect is not long-term (Shytikov et al., 2014). In mice, long term follow-up studies show that lifespan remains unchanged, as does the incidence of age-related pathologies. If young hormones alone cannot rejuvenate aged animals, then some undiscovered factor remains to explain the process of ageing.

Stem cell niche and ageing

It has long been appreciated that local environmental signals mediate the local stem cell population's activation in the case of wound healing. As previously covered, following a demyelinating insult in the CNS, neurons, astrocytes, and microglia all signal to OPCs to regenerate the damaged tissue. However, with ageing, these signalling cascades are significantly impaired. Following a demyelinating insult in the aged brain, microglia fail to exit a pro-inflammatory state and thereby do not signal to OPCs to differentiate into new oligodendrocytes (Miron et al., 2013). By promoting anti-inflammatory microglia in the CNS with the TGFB receptor agonist Activin A, OPCs can more efficiently differentiate within the lesion. Similarly, in the aged brain, astrocytes do not produce the same level of growth factors, further impairing the regenerative capacity of OPCs (Hinks and Franklin, 2000).

In addition to growth factors and intercellular signalling cascades, there are alternative mechanisms by which the niche microenvironment effects stem cell function; the stem cell niche microenvironment also includes signals from the extracellular matrix (ECM) and from the changing physical material properties of the tissue itself.

Extra cellular matrix and CNS ageing

In the central nervous system, the extracellular matrix consists of a multi-molecule structure known as the peri-neuronal net. Largely consisting of big linear Hyaluronans, di-sacharide cartilage-like molecules, and smaller chondroitin sulfate proteoglycans, the perineuronal net plays an instructive role in neural development and CNS homeostasis (Kwok et al., 2011). In early post-natal development, the perineuronal net ensheaths neuronal synapses, in an activity dependent manner (McRae et al., 2007). If the perineuronal net is degraded enzymatically, there are an increased numbers of neuronal synapses, but neurons themselves become less sensitive to the neurotransmitter glutamate (Pyka et al., 2011). As such, the perineuronal net is hypothesised to stabilise neuronal connections in development and in memory formation.

In spinal cord injury in rodents, the enzymatic degradation of the perineuronal net using chondroitinase enhances cellular and functional recovery from the injury. Following injection of chondroitinase into the injury site, axonal projections sprout across the contusion site and animals are able to regain a degree of mobility (Alilain et al., 2011; Bradbury et al., 2002). Young adult OPCs themselves become more active and are able to more completely remyelinate a demyelinating insult following treatment with a chondroitinase enzyme (Keough et al., 2016). Together, these results begin to identify the molecules underlying the regeneration-adverse conditions of the adult CNS. Moreover, these studies reveal the non-permissive role that the ECM has on cellular activity and regeneration—further complicating the reasons for OPC dysfunction in ageing.

Across the body, there is a collapse of the extracellular matrix environment homeostasis with ageing. In the hair follicle niche, there is a loss of expression of the extra cellular matrix component, Col17a1, with ageing. The authors show that following substantial hair follicle DNA damage, Col17a1 protein production stops, and the hair follicle stem cells themselves spontaneously differentiate. Without a resident stem cell population, the hair follicle ultimately dies,

and there is widespread age-related hair-loss (Matsumura et al., 2016). When the cells of the hair follicle niche over-express Col17a1, however, the hair follicle stem cells are able to maintain their stem cell identity, and the hair follicle niche does not age. A similar study in muscle finds that there is a loss of fibronectin with ageing, and that this loss underlies the loss of muscle stem cell identity and activity (Lukjanenko et al., 2016). Exogenously provided fibronectin enhances regeneration of the muscle niche following injury. These studies highlight the instructive role of the extra cellular matrix on the activity of stem cells, and that if the matrix is perturbed—as it is with ageing—then the resident tissue stem cells cannot properly function.

So far, no work has directly examined the impact of the ageing ECM on OPC function. One study found that the brain, as a whole, has a progressive accumulation of the regeneration-adverse chondroitin sulfate proteoglycan molecules (Végh et al., 2014). If these molecules underlie the lack of regeneration in the aged brain, then their compositional imbalance with ageing may well cause remyelination failure.

The exact cellular mechanism by which adult stem cells respond to changes in the extracellular matrix environment remains unclear. In the context of spinal cord injury, the protein Ptpσ has been identified as the receptor for chondroitin sulfate proteoglycans (Lang et al., 2015). If the binding of this receptor to chondroitin sulfate proteoglycans is impaired with a small molecule, axons ignore their environment and can regenerate following spinal cord injury. Whether this signalling pathway is relevant for other tissues or stem cell niches remains unknown.

Biophysics, stem cells, and CNS ageing

The relationship between tissue form and stem cell function is highly relevant to the biology of adult stem cells. In one of the first hallmark studies to explore the relationship between biophysics and adult stem cells, researchers seeded adult bone marrow-derived mesenchymal stem cells (MSCs) on synthetic hydrogels of different stiffness (Engler et al., 2006). The mammalian body is composed of tissues of varying stiffness (e.g. brain is soft and bone is stiff). As such, the authors hypothesised that adult MSCs would behave differently when put into environments of different stiffness. The authors found that on softer hydrogels, these MSCs differentiate preferentially into muscle, while on stiffer hydrogels they differentiate preferentially into bone. Modulating matrix stiffness alone changed the fate choice of the cell.

This finding that cell fate choices are impacted by extracellular matrix rigidity has implications for the field of stem cell biology. In order to expand adult muscle stem cells *in vitro*, researchers found that cells required an environment with the extra cellular matrix conditions that mimicked the *in vivo* muscle (Gilbert et al., 2010). In the intestine, a combination of extracellular matrix molecules and stiffness tuned hydrogels were required for the expansion of intestinal stem cells (Jung et al., 2011). Neonatal OPCs have been shown to exhibit increased self-renewal and differentiation capacity on soft hydrogels compared to stiff hydrogels, and have an increased propensity to differentiate into astrocytes on stiff hydrogels (Urbanski et al., 2016).

It is difficult to disentangle the effects of extracellular signalling pathways—such as the Chondroitin-Ptpσ pathway—from the effects of mechanical signalling. Matrix signalling is mediated by the composition of the extracellular matrix environment, whereas mechanical signalling is mediated by the physical stiffness of extracellular matrix proteins. Likely, both mechanical and extracellular matrix signalling are involved in parallel and interconnecting signalling pathways which communicate the exact type of environment that the stem cell is in and thus how it should behave.

Focal adhesion kinase 1 (Fak1) is one of the key proteins at this intersection of extracellular matrix signalling and mechanical signalling. When transmembrane integrins bind an extracellular matrix protein, Fak1—which is indirectly bound to the intracellular domain of the integrin via the protein paxillin—becomes activated (Mitra et al., 2005). Fak1 subsequently activates the pro-growth protein c-Jun and Erk1 which in turn activates the actin polymerising proteins Rho kinase and Myosin II. Under conditions of increased matrix stiffness, the integrins cluster together, and thereby amplify Fak signal transduction (Butcher et al., 2009). When this signalling pathway is inhibited, mesenchymal cells grown on different stiffness substrates can no longer respond to matrix stiffness and differentiate as if they were on a soft matrix (Engler et al., 2006).

Further factors mediate mechanotransduction to signal mechanical changes to the cell nucleus so that the cell can respond appropriately. Under conditions of low strain, the protein Yap1 remains bound to the intracellular domain of the transmembrane E-cadherin (Benham-Pyle et al., 2015). Under high mechanical strain, however, Yap1 is released from the cell membrane,

shuttles into the nucleus, and activates pro-growth signals. In the liver, when Yap1 is constitutively active, the liver grows by as much as 4-fold, regardless of the mechanical strains of the chest cavity environment (Camargo et al., 2007). In the CNS, neurons with re-activated Yap expression dedifferentiate and become expandable neural stem cells (Panciera et al., 2016).

The nuclear lamina are similarly part of this mechano-transduction signalling cascade. There are two main components of the nuclear lamina: nuclear lamin A/C and nuclear lamin B. With increasing tissue stiffness, there is a concurrent increase in nuclear lamin A/C (Swift et al., 2013). It is hypothesised that this increase is a protective measure, defending the nuclear DNA from shearing under high mechanical strain. Moreover, the authors show that nuclear lamin A/C acts as a tethering molecule that nucleates Yap1. Without this increase in nuclear lamin A/C, Yap1 cannot efficiently enter into the nucleus.

Despite the field's increased understanding of these mechanosensing signalling pathways, it remains difficult to wholly uncouple mechanical signaling from extracellular matrix protein signalling; all of these signalling cascades are highly dependent on both signalling mechanisms. The transmembrane gated ion channel Piezo1, however, is one of the only purely mechano-sensing proteins that has been described. Only recently discovered (Coste et al., 2010), Piezo1 and its homologues are highly conserved protein sequences that are present in the genomes of most multi-cellular organisms. No homologues have yet been discovered in bacteria. It is hypothesised that once multicellular organisms evolved, cells required a new method for sensing the 3-dimensional mechanical strain that uniquely occurs in multicellular organisms in order to coordinate growth and movement in the X, Y, and Z dimensions (Soattin et al., 2016).

The channel Piezo1 is embedded in the cell membrane, and upon mechanical strain is pulled apart to allow for an influx of ions. There, the ions act as secondary messengers communicating to the cell the mechanical strain of its environment. In developing zebrafish embryos, the loss of Piezo1 inhibits cell migration, induces cell crowding, and loses control of cell numbers (Eisenhoffer et al., 2012). In mice, the double knock-out of Piezo1 is embryonic lethal (Li et al., 2014). With a homozygous knockout of Piezo1, the blood vasculature cannot form properly as blood endothelial cells do not spread out. Instead, they grow on top of one another without self-repulsion. In mammalian adult epithelial cells, Piezo1 similarly controls cell numbers (Gudipaty et al., 2017). With epithelial wounding experiments, endothelial cells around

the wound site downregulate Piezo1. Once normal cell density is re-established, Piezo1 levels return to normal. Additional mechanistic work has found that Piezo1 mediates the influx of calcium. This increased intracellular calcium activates calpain (McHugh et al., 2010). Calpain subsequently activates integrin signalling, the phosphorylation of Fak1, and the activaction of Erk.

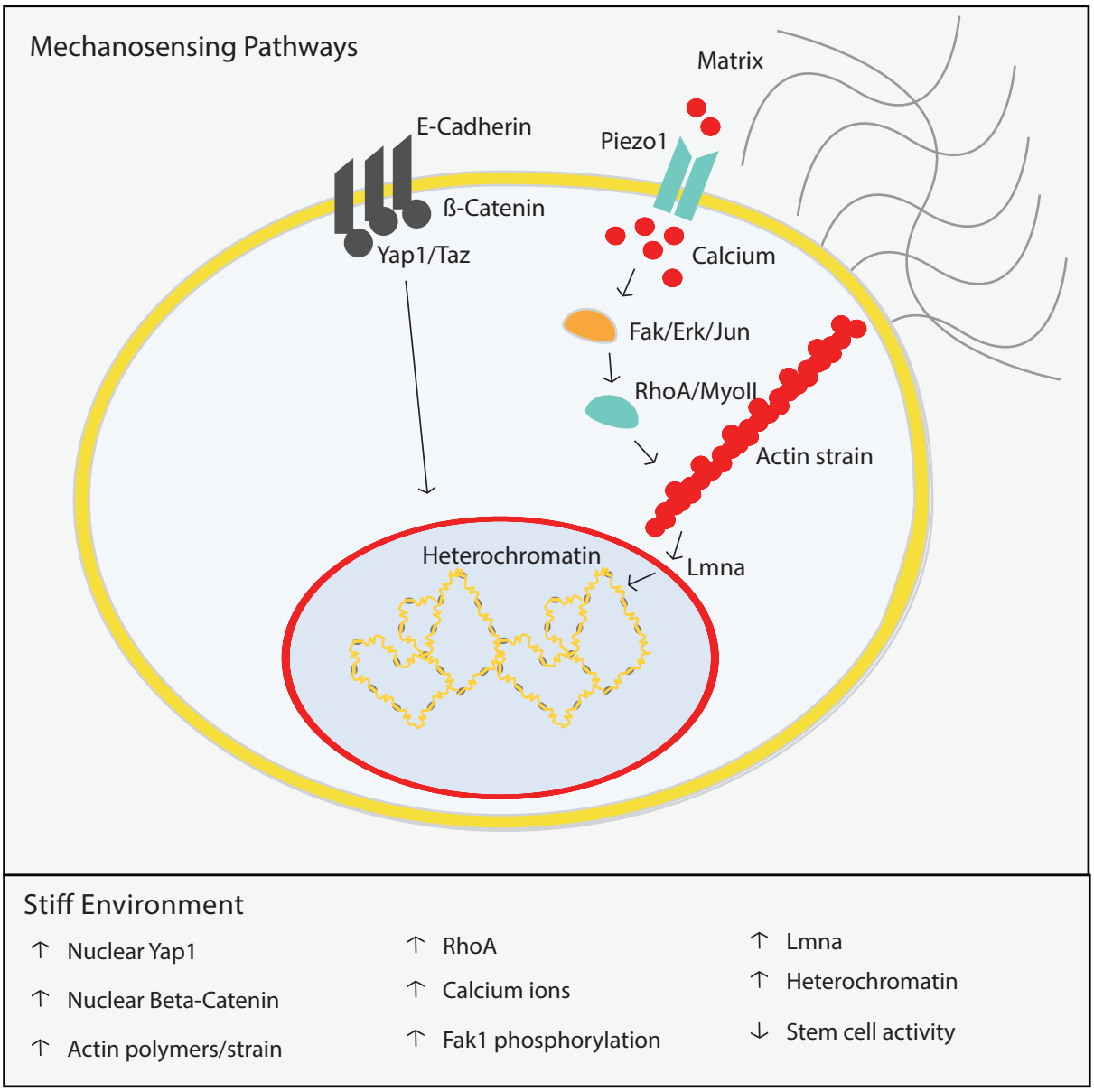

Figure 5. Canonical mechanosensing pathways. Cadherins are directly associated with Beta-catenin and Yap1. Under conditions of high strain,Yap1 and catenin are released from the nuclear membrane and enter the nucleus. Piezo1, under conditions of high strain opens, allowing for ions to enter the cytoplasm. There, they activate Fak which in turn activates Erk, Jun, and actin polymerisation. Increased actin polymerisation causes heightened strain on the nucleus, causing an increase in the protein nuclear Lmna. With increased Lmna, Yap1 enters the nucleus, there is increased heterochromatin, and ultimately a loss of stem cell plasticity.

The role of Piezo1 signalling in OPCs is unknown. Moreover, there is scant evidence that mechanics and mechano-transduction play any role in the ageing process. One recent paper shows that muscle matrix environment progressively stiffens with ageing and that aged muscle stem-cells cultured on hydrogels that mimic the stiffness of young muscle, re-activate aged stem cells (Lacraz et al., 2015). It is intuitive that matrix stiffness would change and affect stem cell function in tissues such as skin, vasculature, muscle, or gut as these tissues undergo physical mechanical strain. The CNS, however, does not undergo such obvious physiological strains throughout adult life. As such, it remains unknown what role, if any, mechanosensing and/or Piezo1 has on OPC function and regeneration.

Molecular interventions to ageing: genomic engineering in the adult

We are beginning to understand the ageing process of adult stem cells and its impact on overall organismic health. Until recently however, it has not been possible to modify the genome of an adult mammal to prolong life and healthspan. As such, most therapeutic strategies for age related-disease in humans have involved using small molecule drugs to target the relevant protein pathways. In rodents, genome engineering has allowed for the generation of transgenic animals, allowing for single specific genes to be silenced or overexpressed in a controlled manner in an adult. In order to understand whether genome engineering could ever be used as a molecular intervention for modifying the adult human, it is important to first understand the techniques that underlie the generation of transgenic animals.

Upon DNA damage, a cell repairs the damaged DNA using one of two mechanisms: homologous recombination or the error-prone non homologous end joining (NHEJ). Capitalising on this endogenous repair machinery, researchers generating transgenic animals would inject modified gene sequences flanked by tens of kilobases of site-specific homologous DNA sequences into embryonic stem cells (Capecchi, 1989). Cells with randomly damaged DNA at the exact loci of interest would undergo homologous recombination with the recombinant modified DNA fragment. This modified embryonic stem cell would then be selected for with a selection gene such as neomycin and injected into a blastocyst. If the blastocyst formed a chimera with the modified stem cells, then the postnatal mouse would have some gametes that contained the transgenes. In the second generation of mouse breeding, mice could be generated in which every cell contained the modified DNA fragment. This process of genome engineering transgenic animals, however, was highly inefficient.

The reason for this inefficiency is largely due to the fact that a cell would have to undergo spontaneous DNA damage at the exact locus being targeted for DNA repair. Moreover, in the majority of cases, and except for when the cell is progressing through S phase of mitosis, ES cells repair DNA using NHEJ, not homologous recombination. To overcome these limitations, complex genome modifying technologies, such as zinc finger nucleases and Tal-effector nucleases, were invented. Both technologies work by generating site-specific DNA breaks in order to force DNA repair at the sites. This way, cells more readily underwent homologous recombination at the exact site of interest, thereby incorporating the modified recombinant DNA fragment (Ding

et al., 2013). However, this process which is involved in generating complex sequence-specific protein fragments to target DNA breaks at the location of interest and remained inefficient; only 2% of transfected stem cells incorporated the recombinant DNA fragment at the correct loci.

The development of CRISPR (clustered regularly interspaced palindromic repeat)/Cas9 technology has allowed for the rapid and efficient manipulation of the genome (Doudna and Charpentier, 2014) . The CRISPR/Cas9 system relies on two main components: the Cas9 protein and a small ≤100 base pair (bp) guide RNA (gRNA) (Fig. 6). The gRNA sequence is designed to bind, using Watson-Crick base-pairing, to any specific 20 bp region of the genome that is followed on the 3' side of the sequence by the three base pairs XGG (AGG, TGG, CGG, or GGG) (Cong et al., 2013). The gRNA and Cas9 complex together and scan the genome until they find the complementary sequence to the gRNA target sequence. Part helicase and part nuclease, Cas9 unwinds the DNA as it scans for the gRNA target sequence and, upon binding, generates a double DNA strand break 3 base pairs upstream of the XGG site (Mali et al., 2013). Using this approach, any sequence that is followed by an XGG sequence can be specifically targeted for DNA double stranded break.

The CRISPR/Cas9 approach relies on the simple Watson-Crick base-pairing of only the 20 base pairs of the gRNA sequence, making it highly modular and easy-to-use for biologists. To generate gene knock outs, the Cas9/gRNA complex repeatedly cuts the target sequence site until the NHEJ machinery creates a gene knockout mutation. This mutagenesis technique is so efficient that, following one transfection of the Cas9/gRNA complex, almost 50% of the target gene sequences incur a gene-loss of function mutation (Ran et al., 2013). To insert a recombinant DNA sequence into a locus, the approach is similar to that of the original random integration techniques—recombinant DNA fragments are flanked by kilobases of DNA fragments that are homologous to the Cas9 targeted cut site. Upon a double stranded DNA cut by Cas9, the cell's endogenous machinery incorporates the recombinant DNA fragment. In the first uses of this technology, almost 10% of the embryonic stem cells contained the recombinant DNA fragment (Mali et al., 2013). Follow up work using a small molecule that inhibits NHEJ machinery,

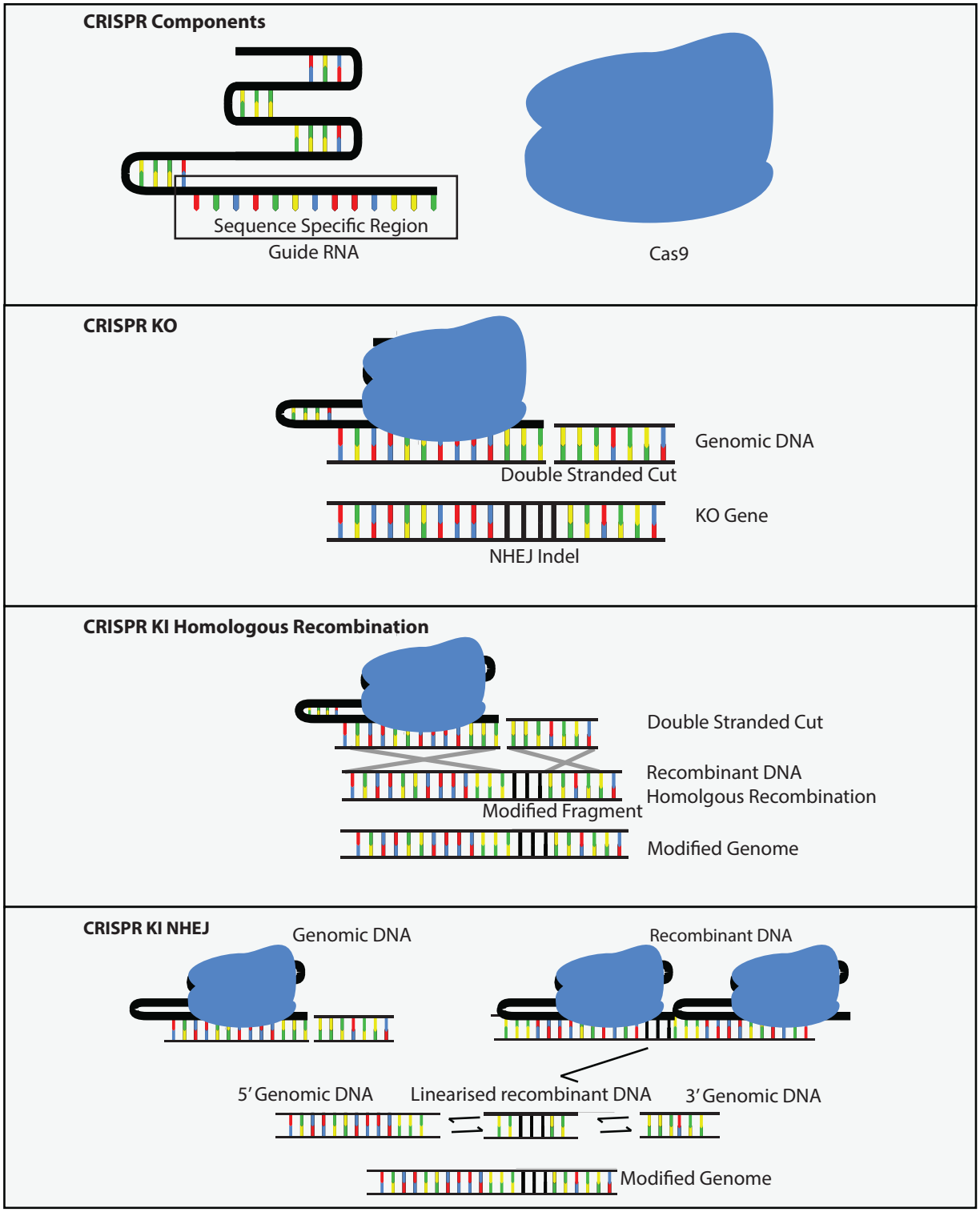

Figure 6. Methods for modifying the genome using CRISPR/Cas9. CRISPR machinery is composed of Cas9 protein and a'guide RNA'which binds to a region of interest in genomic DNA using Watson-Crick base pairing. Following binding to genomic DNA, Cas9 creates a double stranded break and the DNA can obtain insertions or deletions (Indels) following the non-homologous end joining (NHEJ) of the DNA. Harnessing cell's endogenous DNA repair machinery, researchers can insert pieces into the DNA. Genomic insertions can be performed precisely using homologous recombination or imprecisely using NHEJ.

forced cells to undergo homologous recombination, allowing for a sequence-specific, recombinant gene knock-in efficiency of ~60% (Maruyama et al., 2015).

While the CRISPR/Cas9 system has allowed for efficient genome manipulation in fast-cycling ES cells, little work has gone into editing primary cells *in vitro* or in editing adult cells *in vivo*. One recent paper systemically delivered an adeno-associated virus (AAV) containing the Cas9 gene and gRNA sequences to a mouse containing a frame-shift gene mutation in the gene dystrophin (Tabebordbar et al., 2016). This mutation, which occurs naturally in patients with Duschenne muscular dystrophy, causes widespread muscle wastage and shortened lifespan. Using two gRNA sequences that flank the mutation site, the researchers were able to excise the mutated DNA site, restoring proper protein synthesis and proper muscle physiology.

Only one paper has shown the ability to create systemic gene knock-ins in adult non-dividing cells using the CRISPR/Cas9 system (Suzuki et al., 2016). In this work, the researchers generated gRNAs targeting the neuron-specific Tubb3 gene. Simultaneously, the authors flanked a GFP gene with synthetic Tubb3 gRNA targeted sequences. At the same time that Cas9 cut the genomic Tubb3 site, Cas9 also cut either side of the GFP sequence, thus releasing the linearized GFP sequence from the supplied plasmid DNA. Then, instead of relying on homologous recombination, which occurs in actively mitotic cells, the authors relied on NHEJ, the DNA repair method used in most adult mitotic cells. Doing so, they were able to knock-in the GFP sequence into the Tubb3 sequence in non-dividing neurons. Finally, the authors packaged this system into an adeno-associated virus and injected it systemically into an animal, showing, for the first time, site-specific genome corrections and knock-ins in the adult.

Only one paper has used the CRISPR/Cas9 system in primary oligodendrocyte progenitor cells (Petersen et al., 2017). In this work, the authors use the system to partially knock down a specific gene *in vitro*. Whether or not the CRISPR/Cas9 system can be used for more complicated genomic manipulations such as knock-ins, both *in vitro* and *in vivo*, in OPCs remains unknown. Finally, whether *in vivo* CRISPR could efficiently target significant numbers of OPCs and thereby age-related pathways also remains unknown. To date, no group has proven that CRISPR can be used to target adult stem cells *in vivo*. Finally, due to the blood brain barrier, it remains unclear whether *in vivo* CRISPR of the adult/aged CNS is a feasible goal for the field of regenerative neuroscience. Such a technology would allow for the rapid dissection of genetic

pathways in the CNS, leading to the development of novel therapeutics targetting age related disease.

Aims and Objectives of this dissertation

This literature review highlights a number of gaps in our understanding of oligodendrocyte progenitor cells in the adult and aged animal: The niche of the OPC, the signals that activate the OPC in homeostasis, the biophysical properties of the aged OPC niche, and finally, the underlying cause of OPC ageing all remain unknown.

For these reasons, in this dissertation I set out to:

1. Define the niche of the adult OPC and the signaling pathways that govern OPC activation.
2. Characterize the regenerative capacity of aged OPCs following genomic reprogramming.
3. Better understand the effect of the ageing OPC niche on OPC activity and function.
4. Develop a systemically administered CRISPR/Cas9 system that specifically targets OPCs and genetically perturbs age-related pathways.

Chapter 2

Materials and methods

Animal Husbandry

Sprague Dawley rats, C57/B6 mice, and transgenic mice were bred in the Innes Building and the Stem Cell Institute Animal Facilities at the University of Cambridge. The transgenic Lgr5-CreERT2/ Td-tomato and the Confetti 2.0 mice were provided by Meritxell Huch of the Gurdon Institute (Huch et al., 2013; Livet et al., 2007). The Pdgfra-H2B animals were provided by Jenny Nichols of the Stem Cell Institute (Hamilton et al., 2003). The Sox10-Cre animals were originally provided by William Richardson lab of the University College London (Matsuoka et al., 2005). All animals were fed a standard choke diet, unless otherwise indicated, and were kept under a 12h dark 12h light cycle. All procedures were performed in accordance with the requirements and regulations of the United Kingdom Home Office.

Oligodendrocyte progenitor cell isolation protocol isolation protocol

Neonate and adult OPCs were dissected from wild-type Sprague-Dawley rats or C57/Bl6 mice and sacrificed using overdose of pentobarbital; dissected whole brains were placed immediately in Hibernate A Low Fluorescence media (HALF; prepared in-house) and placed on ice. The meninges were removed and the dissected brains were chopped using a scalpel. The HALF containing the tissue was placed into a 15mL falcon tube and spun for 2 minutes at 150g. The HALF media was aspirated, and the pelleted brain tissue was re-suspended in activated filtered dissociation media, added in equal volume to the volume of the pelleted tissue. The brains were then placed on a 55 RPM orbital shaker at 35˚ C for 30 minutes. The tissue was then centrifuged at 200g for 5 minutes, the papain was removed, and the brains were re-suspended in HALF media containing 2mM sodium pyruvate (Thermo Fisher; 11360070), and 2% B27 (Thermo Fisher; 17504-001). Using a 5mL pipette, the dissected brains were gently titurated 10 times. Using fire polished pipettes of decreasing diameter, the brains continued to be titurated until appearing as a single cell suspension. The cell suspension was then passed through

70μM filter (Corning; 352350) to remove any remaining clumps of cells. To further remove debris from the cell suspension, 1 part 90% Percoll (GE; 17-0891-01), diluted in 10x PBS was added to 3 parts cell suspension. The cell suspension was then spun at 800g for 20 minutes, re-suspended in Miltenyi washing buffer (MWB; prepared in-house), and counted. After being spun again for 7 minutes at 250g, the pelleted cells were re-suspended in 500μL MWB buffer and 2.5μL A2B5 antibody (Millipore; MAB312) per 1x107 cells. After a 30-minute incubation on a gentle rocker at 4˚ C, 5 times the volume of the cell suspension of MWB was added, and the cell suspension was spun at 250g for 7 minutes. The pelleted cells were then re-suspended in 80μL MWB and 20μL MACs beads (Miltenyi; 130-047-302). After a 30-minute incubation on a gentle rocker at 4˚ C, the cell suspension was centrifuged at 250g for 7 minutes and re-suspended in 1mL MWB. The cell suspension (max 5x108 cells) was placed in a MS column (Miltenyi; 130-042-201) on a MiniMACS Separator (Miltenyi; 130-042-102), and washed 3 times with 500μL MWB buffer, waiting each time for the liquid to pass completely through the column. In one swift move, 1mL of MWB buffer was added to the column, the column was removed from the stand and placed atop a new collection tube, and the liquid was plunged through the column. The purified population of OPCs was then diluted and counted.

Maintenance and Differentiation of OPCs

OPCs were plated at a density of 10,000 cells per 96-well (scaling linearly according to plate format) and fed on alternate days with OPC media (see media section) supplementing with 30ng/mL bFGF (Peprotech; 100-18b) and 30ng/mL PDGF (Peprotech; 100-13a). The cells were kept in an incubator at 37˚ C and 5% O2.

To differentiate the cells, media was aspirated off the cells, and replaced with OPC media supplemented with 40ng/mL Triiodo-L-Thyronine (Sigma, T2877). Media was replaced on alternate days for 7-10 days.

Media used for OPC isolation and maintenance are composed of the following:

100mL of OPC Media: 100mL of DMEM/F12 (Thermo Fisher; 11039-021), 2mL sodium pyruvate (Thermo Fisher; 11360-070), 5mg apo-transferrin (Sigma; T2036), 1.35mL 10% D(+) glucose (Sig-

ma; G8644), 1mL SATO Stock Solution (see section below on SATO), 250µL insulin (Thermo Fisher; 12585-014).

50mL of SATO Stock Solution: 50mL DMEM/F12, 33mg/mL BSA fraction V (Sigma; A4919), 4µg/mL Selenite (Sigma; S5261), 1.61 mg/mL Putrescine (Sigma; P7505), 4µg/mL Progesterone (Sigma; P0130).

5L HALF Isolation Medium: 150.1mg Glycine (Sigma; G6201), 9.8MG L-ALANINE (SIGMA; A7627), 420.7MG L-Arginine hydrochloride (Sigma; A92600), 4.12mg L-Asparagine-H2O (Sigma; A0884), 12.06mg L-Cysteine hydrochloride-H2O (Sigma; C7880), 209.6mg L-Histidine hydrochloride-H2O (Sigma; H8125), 526.1mg L-Isoleucine (Sigma; I2752), 526.1mg L-Leucine (Sigma; L8000), 583.3mg L-Lysine hydrochloride (Sigma; L5626), 149.9mg L-Methionine (Sigma; M9625), 330.4mg L-Phenylalanine (Sigma; P2126), 38.569 L-Proline (Sigma; P0380), 210mg L-Serine (Sigma; S4500), 474.8mg L-Threonine (Sigma; T8625), 79.6mg L-Tryptophan (Sigma; T0254), 360.6mg L-Tyrosine disodium salt dihydrate (Sigma; T1145), 470.6mg L-Valine (Sigma; V0500), 19.55mg Choline Chloride (Sigma; 26980), 9.53mg D-Calcium pantothenate (Sigma; C8731), 18.3mg Niacinamide (Sigma; 1462006), 20.6mg Pyridoxine hydrochloride (Sigma; P9755), 16.9mg Thiamine hydrochloride (Sigma; T4625), 36mg i-Inositol (Sigma; I5125), .5mg Ferric Nitrate (Sigma; 254223), 1997.9MG Potassium Chloride (Sigma; P3911), 369.9 Sodium Bicarbonate (Sigma; S5761), 25810mg Sodium Chloride (Sigma; S9888), 543.6mg Sodium Phosphate dibasic anhydrous (Sigma; 71640), .9633mg Zinc Sulfate (Sigma; Z4750), 22525mg D-Glucose (Sigma; g8270), 124.9 Sodium Pyruvate (Sigma; P2256), and 13465mg MOPS (Sigma M1254). Media was pH adjusted to 7.30 and filtered sterilized (Millipore; SCVPU02RE).

MWB Washing Buffer: 10x PBS (Thermo Fisher; 70011-044), 2mM Sodium Pyruvate, 2mM EDTA (Thermo Fisher; 15575-020), 10µg/mL Insulin.

Generation of varying stiffness polyacrylamide gels

Glass coverslips were washed sequentially in dH2O, 70% EtOH (Sigma; 459836), and .2M NaOH. Bottom cover slips were air-dried and pre-coated in 1.2% bind silane (Sigma; GE17-1330-01) in 95% EtOH and 5% glacial acetic acid (Fisher Scientific; 64-19-7), air dried, and subsequently polished

with lint free cloths. Top coverslips were submerged in 15% Sigmacote (Sigma; SL2-25ML) diluted in chloroform (Sigma; 288306) and incubated for 1 hour. Top coverslips were removed from the Sigmacote solution and polished with a lint free cloth. To make a soft hydrogel 7% acrylamide (Sigma; A4058), 6% bis-acrylamide (Sigma; 146072), and 48 mM 6-Acrylamidohexanoic acid were combined in dH2O. To make stiff hydrogels, 14% acrylamide and 12% bis-acrylamide were combined with 48 mM 6-Acrylamidohexanoic acid. The gels were formed by adding a final concentration of .004 g/mL TEMED (Sigma; T9281) and of .001 g/mL ammonium persulfate (Sigma; A3678) to the acrylamide solution. Acrylamide solution was rapidly pipetted onto the bottom glass coverslips and the hydrophobic top coverslip was placed on top. After 5 minutes, the top coverslip was removed with a scalpel and the bottom coverslip with the now polymerized hydrogel was washed 2 times in methanol. The hydrogels were rehydrated in PBS.

To activate the hydrogels, they were incubated in 10mM MES hydrate (Sigma; M5287) with 500mM NaCl (Sigma; S9888) in dH2O (pH 6.1) for 10 minutes. To activate the functional group in the hydrogels, the gels were incubated for 30 minutes in 480mM N-Hydroxysuccinimide (Sigma; 130672) combined with 200mM N-(3-Dimethylaminopropyl)-N′-ethylcarbodiimide hydrochloride (Sigma; E7750) added to the Mes Hydrate solution. The gels were washed 1x in 60% MeOH in PBS and then covered overnight in 50µg/mL laminin (Sigma; L2020) diluted in pH 8.2 HEPES (Sigma; H3375).

Atomic force microscopy

Rats of different ages were anesthetized with 5% isoflurane and sacrificed by intraperitoneal (i.p.) injection of a lethal dose of pentobarbitone sodium (Euthatal). The brain was dissected out and placed into cold slicing artificial cerebrospinal fluid(Koser, Moeendarbary, Hanne, Kuerten, & Franze, 2015) (s-aCSF). One half of the brain was then glued onto a vibratome platform (VT1000 S; Leica Microsystems) using superglue. 500 µm thick coronal sections of the brain were cut in cold s-aCSF bubbled with 95% O2 and 5% CO2 using one half of a Gillette 7 O' Clock double edged razor blade. The frequency was set to 75 Hz and the forward speed to ~50 µm/s. Brain sections were transferred to a Cell-Tak-coated (Corning; 354240) 35 mm glass-bottom petri dish and covered with cold measuring artificial cerebrospinal fluid (m-aCSF). Subsequently, the samples were mounted on an inverted microscope (Zeiss; Axio Observer.A1) and constantly perfused with fresh m-aCSF bubbled with 95% O2 and 5% CO2.

For blebbistatin treated AFM brains, fresh aged CNS was vibratomed as described and transferred into a 24-well plate containing m-aCSF and either DMSO or 5µM blebbistatin. The slices were then transferred into an incubator for 30 minutes and subsequently measured.

AFM indentation measurements were performed as previously described. In brief, force distance curves were recorded using a JPK Nanowizard Cellhesion 200 (JPK Instruments AG) in a raster scan (stepsize = 100-200 µm) using tipless silicon cantilevers (rat brains: Arrow-TL1, spring constant = 0.03 – 0.05 N/m; hydrogels: Sicon-TL, spring constant = 0.2-0.3 N/m; both from NanoWorld) with polystyrene beads (d = 37 µm; microParticles GmbH) glued to them. The maximum force was set to 7 nN for brain measurements and 15nN for hydrogels, and the approach speed to 10 µm/s. Images were taken using a sCMOS camera (Zyla 4.2, Andor) mounted on a Zeiss Axio Zoom.V16 on top of the AFM setup. Using a custom algorithm (Christ et al., 2010) data was analyzed for maximum indentation by fitting the force-distance curves to the Hertz model (Franze et al., 2011; Hertz, 1882; Koser et al., 2016).

$$F = \frac{4}{3}\frac{E}{1-\nu^2} r^{1/2}\delta^{3/2} = \frac{4}{3} K r^{1/2}\delta^{3/2}$$

with F = applied force, E = Young's modulus, ν = Poisson's ratio, r = radius of the probe, δ = indentation depth, and apparent elastic modulus K=E/(1-ν^2). Intact brain and decellularized brain curves were analyzed for the full indentation depth at F = 7 nN, and curves from hydrogel measurements for 0.5µm indentation depth. The shear modulus G of the polyacrylamide gels was calculated using (Moshayedi et al., 2010)

$$F = \frac{8}{3}\frac{G}{1-\nu} r^{1/2}\delta^{3/2},$$

assuming ν_PAA ~ 0.5 (Boudou et al., 2006).

Sequencing and analysis of RNA

RNA was extracted according to the Directzol RNA MicroPrep Kit (Zymo Research; R2061) with the optional DNase treatment. RNA quality was assessed with a Bioanalyzer to ensure all samples had a

RIN value of ≥ 8. DNA libraries were constructed using the SMARTer® Stranded Total RNA-Seq Kit - Pico Input Mammalian kit with multiplexed barcodes (Takara; 635005). 150 bp paired-end directional sequencing was performed on an Illumina HiSeq 4000.

Multiplexed samples were filtered, aligned to the rat UCSC rn6 assembly, normalized, and quantified using Trimmomatic, Hisat2, Stringtie, and Ballgown using a previously pubished protocol (Pertea et al., 2016). Dendrogram clustering, t-distributed stochastic neighbor embedding, gene set enrichment analysis, and heatmaps were generated in ipython notebook using the libraries pandas, matplotlib, numpy, seaborn, gseapy, and scikit-learn.

EdU incorporation assay, immunofluorescence, and imaging

For the EdU incorporation assay, 10μM EdU was added into the cell culture medium for five hours, followed by the protocol provided by the Click-iT Plus EdU Alexa Fluor 647 Imaging Kit (Thermo Fisher; C10640). Otherwise, *in vitro* tissue culture cells were fixed in 4% Paraformaldehyde (Thermo Fisher; 10131580) for 20 minutes at room temperature. The cells were then washed once in PBS (Thermo Fisher; BP3994) and then blocked in PBS with 0.1% Triton X-100 (Sigma; T8787) and 5% Donkey Serum (Sigma; D9663) for 30 minutes at room temperature.

Fixed *in vivo* tissue sections were cryo-protected overnight in 20% sucrose (Sigma; S0389), embedded in OCT (VWR; 361603E), flash frozen in dry ice and cut in 12μM sections on a cryostat. Tissue was allowed to dry on a SuperFrost Plus slide (VWR; 48311-703). Slides were either stored at – 80˚ C until use. To stain, slides were brought to room temperature and were placed in a slide chamber containing 1x Citrate buffer (Sigma; C9999). The slide chamber was brought to 100˚ C for 30 minutes for antigen retrieval. Slides were then allowed to cool to room temperature and they were washed once in PBS.

Fixed tissue for clearing was processed and stained as previously described(Susaki et al., 2015). Following perfusion and post-fixation, animal brains were sectioned using a matrix into 2mm thick sections and cleared using the CUBIC protocol. If additional immunostaining was required, tissue was stained according to the methods previously described using application-specific antibodies.

For cryosections and immunofluorescence, primary antibodies diluted appropriately (see table of antibodies) in PBS with 0.1% Triton X-100 and 5% Donkey Serum were then added to each well or

slide and they were stained overnight at 4˚ C. For most proliferation and differentiation assays, the antibodies for Olig2 and MBP were used. In cases when antibody species clashed, the Olig2-activated transcription factor Sox10 was used the identify oligodendrocyte lineage cells.

The cells or slides were then washed twice for 10 minutes in PBS with .1% Triton X-100. For one hour, cells or slides were incubated in fluorescent secondary antibodies diluted appropriately in PBS with 0.1% Triton X-100 and 5% Donkey Serum. Cells or slides were again washed twice for 10 minutes in PBS with 0.1% Triton X-100. For 10 minutes, cells were incubated with Hoechst 33342 (Thermo Fisher; H1399) diluted 1:10000 in PBS. Slides were then mounted in mounting media with DAPI (Vectashield; H-1500). Cells and slides were stored in PBS at 4˚ C.

Fixed, fluorescent cells or slides were imaged using the Zeiss Axio Observer or the Leica TCS SP5 confocal microscope. As indicated, quantifications were performed either by eye or using high-content imaging and quantification, where appropriate. To perform high content analysis, 96 well plates were imaged using the GE InCell 2000. Fluorescence intensity thresholds for each stain were set from control samples and 42 images were randomly captured from each well. To process the images, pre-set protocols from the open source software Cell Profiler were calibrated so that the software would not identify false positives. Quantifications were averaged across triplicate technical replicates. Automated quantifications were further validated and corroborated by manual quantifications of subsets of images.

Flow cytometry analysis of primary isolated OPCs was performed by fixing OPCs in suspension for 20 minutes in 4% PFA. Following fixation, cell suspension was spun at 800g for 5 minutes, and the PFA was aspirated. The cell pellet was re-suspended in 0.1% Triton X-100 and 5% donkey serum in PBS and placed for 30 minutes on ice. The suspension was spun again and incubated in primary antibody diluted 1:300 overnight at 4˚ C. The cell suspension was washed twice by spinning the cell suspension, incubating it in 0.1% Triton X-100 in PBS for 10 minutes, and spinning again. After the second wash-spin, the cell pellet was re-suspended in secondary antibodies diluted 1:500 in 0.1% Triton X-100 and 5% donkey serum diluted in PBS and incubated on ice for 2 hours. The cell suspension was wash twice again for 10 minutes each and re-suspended in PBS. Flow cytometry was performed on the Attune NxT Flow Cytometer (Thermo Fisher).

qPCR and Western Blots

Immediately following OPC isolation protocol, RNA was isolated from purified OPCs according to the Directzol RNA MicroPrep Kit (Zymo Research; R2061). RNA was stored at -80˚ C. cDNA was generated from the RNA according to the QuantiTect Reverse Transcription Kit's instructions (Qiagen; 205310). For the RT-qPCR data, pre-designed primers (see table of primers used) were used at a concentration of 400μM and an efficiency of greater than ~98% were determined for each primer pair using serial dilutions of OPC cDNA. cDNA, primers, and the Syber Green Master Mix (Qiagen; 204141) were combined according to the kit's instructions, and RT-qPCR and melting curve analysis were performed on Life Technologies' Quantstudio 6 Flex Real-Time PCR System.

Immediately following OPC isolation protocol, protein was isolated from purified OPCs using Cel-Lytic M (Sigma; C2978) protein extraction solution and a protease inhibitor (Sigma; P8340). Isolated whole protein content was measured using a BSA gradient kit (Bio-Rad; 500-0206), and gradient intensity was quantified using Tecan's Infinite 200 Pro Microplate Reader. 10μg of isolated protein was combined with 4X Bolt® LDS Sample Buffer (Thermo Fisher; B0007), brought to 95˚ C for 10 minutes and with the SeeBlue Protein Ladder (Thermo Fisher; LC5925) was run on Bolt 4-12% Bis-Tris Plus Gels (Thermo Fisher; NW04120BOX) in MES buffer (Thermo Fisher; B0002) for 35 minutes at 165 V. Protein was transferred for 90 minutes at 100 V to a PDVF membrane (Millipore; IPSN07852) in transfer buffer (Bio-Rad; 161-0732) with 20% methanol (Sigma; 322415). PDVF membranes were blocked for 30 minutes with 50% Odyssey blocking buffer (Licor; 927-40100) in TBS (Thermo Fisher; BP24711) and 0.1% TWEEN 20 (Sigma; P2287). Primary antibodies were added at the proper dilution (see table of antibodies) to the blocking buffer, and membranes were left overnight in primary antibodies and blocking buffer at 4˚ C. Membranes were washed twice in TBS with TWEEN 20 for ten minutes each wash and near infrared species-appropriate secondary antibodies were added (see table of antibodies). Membranes were stained for two hours, washed twice in TBS with 0.1% TWEEN 20, and imaged on the Licor Odyssey Fc.

Transplantation of labelled OPCs into Neonate

Neonatal and Aged OPCs were isolated in parallel using previously described MACs isolation protocol. Immediately following cell isolation, cells were labelled with Bacmam 2.0 CMV-GFP (Thermo Fisher; B10383) as per the manufacturer guidelines, and 300,000 cells were transplanted into the pre-

frontal cortex of p1-p3 neonate pups using previously published coordinates(Khazipov et al., 2015). For proliferation analysis, 75 µg/g EdU (Abcam; ab146186) was injected I.P. 14-16 hours prior to perfusion fixation.

Creating demyelinating focal lesions in vivo and delivery of small molecules

Bilateral focal demyelinating white matter lesions were created by injecting 4µL of .01% ethidium bromide into the caudal cerebral peduncles of aged female rats (≥15 months) as described previously(Woodruff & Franklin, 1999). After 7 days post lesion, 4µL of 50 U/mL chABC (Sigma; C3667), 50 U/mL of penicillinase (Sigma; P0389), or 5µM blebbistatin was injected into the lesion site using animal-specific injection-site coordinates. For proliferation analysis, 75 µg/g EdU was injected I.P. 14-16 hours prior to perfusion fixation. Dr. Myfanwy Hill performed the lesions.

For histological cryosections, animals were perfusion fixed with 4% paraformaldehyde at 21-days post lesion. For Toluidine blue stain and electron microscopy sections, animals were perfusion fixed with 4% glutaraldehyde (Sigma; 340855), and sectioned into 1.5mm thick coronal sections. The sections were post-fixed in 1% osmium tetroxide (Sigma; 201030), dehydrated in graded concentrations of ethanol, and subsequently embedded in TAAB resin. The brains were sectioned into 1µM sections using a microtome and stained with Toluidine Blue O (Sigma; T3260) according to the manufacturer's instructions.

siRNAs, modified mRNA synthesis and transfection

From cDNA, primers were generated containing the T7 promoter on the 5' end of the target transcript. Immediately downstream of the T7 promoter we inserted a Kozak sequence consisting of GCCACC followed by the start codon ATG, and performed a standard 35 cycle polymerase chain reaction according to the Phusion Polymerase kit (Thermo Fisher; F530S). Using the PCR product, we then synthesized the RNA using the synthesized DNA and HiScribe T7 ARCA mRNA Kit with Tailing (NEB; E2060S) with the addition of 5-Methylcytidine (Trilink; N-1014) and Pseudouridine (NEB; 1019). To determine fragment size of the synthesis product, we used the Quantitect Reverse Transcription Kit and ran the cDNA on a 1% Agarose gel (Thermo Fisher; 16500) at 100 volts for 30 minutes.

For a transfection of 1 well of a 96-plate-wells, each plated with 10,000 cells, .5 pmol of siRNA (GE;

D-001960-01-05) was combined with 1.5µL of Opti-MEM media (Thermo Fisher; 31985062). In a separate tube, 1.5µL of Opti-MEM media was combined with .15µL of Lipofectamine RNAiMAX reagent (Thermo Fisher; 13778030). The diluted RNAiMAX was then combined with the diluted RNA and incubated at room temperature for 20 minutes. Following the incubation, 3µL of the transfection combination was added to each well.

For the transfection of modified mRNA a transfection of 1 well of a 96-plate-well plate, each plated with 10,000 cells per well, 25 ng per well of modified RNA was combined with 1.25µL of Opti-MEM media (Thermo Fisher; 31985062). In a separate tube, 1.25µL of Opti-MEM media was combined with .0375µL of Lipofectamine Messenger Max reagent (Thermo Fisher; 13778030). The diluted lipofectamine was then combined with the diluted RNA and incubated at room temperature for 5 minutes. Following the incubation, 2.5µL of the transfection combination was added to each well.

Generation of decellularized CNS scaffold

CNS tissue of young and aged rats was dissected and immediately vibratomed in 500µM coronal sections in HALF medium on ice. Brains were decellularized using an adapted from . Sections were immediately flash frozen at -80˚ C in dH2O. Sections were rapidly thawed at 37 ˚ C. Individual sections were transferred to a 24 well plate with 4% sodium deoxycholate (Sigma; D7650) for 2 hours and placed on an orbital shaker at 105 RPM. Sections were washed in 1x PBS with 1% penstrep (Sigma; P4333) for fifteen minutes on the orbital shaker. PBS was removed and 3% Triton X-100 in PBS was added onto the sections, again shaking for 1 hour on the orbital shaker at 105 RPM. Triton X-100 was then removed and replaced with PBS. These steps of sodium deoxycholate to PBS to Triton X to PBS were repeated 3 times. Finally, the sections were transferred into a 8µM pore cell culture insert (Corning; 353097) coated in Poly-D-Lysine (Sigma; P6407) and were incubated overnight in PBS with 1% penstrep with DNAse I (Sigma; 11284932001). The following day, the sections were washed 3 times more with PBS with 1% penstrep and finally the sections were incubated in OPC media with growth factors. Freshly isolated OPCs were pipetted into the insert.

Calcium Imaging

Cells were loaded with 1µm Rhod2-am (ab142780) as per the manufacturers guidelines for 30 minutes. Cells were washed 2x in PBS, supplied with fresh media with growth factors and equilibrated in

the incubator for an additional 20 minutes. Images were acquired every 20 seconds for the duration of ten minutes of spontaneous calcium flux.

Generation and transfection of plasmids and/or minicircle vectors with Cas9, and transplantation into aged CNS

Competent minicircle bacteria strain were generated from ZYCY10P3S2T minicircle bacteria (System Biosciences; MN900A-1). For non-minicircle vectors, competent DH5 alpha cells were used (NEB; c2987). Using Phusion polymerase (Thermo Fisher; F530S), PCR fragments with 20 basepair overlaps using the primers below and the pSpCas9(BB)-2A-GFP and pAi14-GFPNLS-MC plasmids were assembled using NEBBuilder HiFi DNA Assembly (NEB; E2621S) and gel extracted (Qiagen; 28704). pSpCas9(BB)-2A-GFP (PX458) was a gift from Feng Zhang (Addgene plasmid # 48138). pAi14-GFPNLS-MC was a gift from Juan Belmonte (Addgene plasmid # 87114). AAV-CMVc-Cas9 was a gift from Juan Belmonte (Addgene plasmid # 106431). pCAG-Cre-IRES2-GFP was a gift from Anjen Chenn (Addgene plasmid # 26646). pUCmini-iCAP-PHP.eB was a gift from Viviana Gradinaru (Addgene plasmid # 103005). pHelper was a gift from CRUK. All other non-plasmid derived sequences were ordered from Integrated DNA technologies and are included in the primers table.

Minicircles were generated using previously described methods(Kay, He, & Chen, 2010) and plasmids were isolated with a Midi kit (Machery-Nagel; 740410.10). Plasmid sequences were confirmed using sanger sequencing.

Capped Cas9 mRNA with modified base pairs (TriLink; L-7206), Tubb3 targetting crRNA:tracrRNA (Dharmacon), and minicircle constructs containing reverse-strand Tubb3 target sequence were transfected into MACs sorted neonatal OPCs 24 hours after isolation using Lipofectamine LTX with plus reagent (Thermo Fisher; 15338100). To test whether vector was successfully knocked-in, a U6 forward primer along with 5' flanking Tubb3 forward primer and a 3' flanking Tubb3 reverse primer were mixed with genomic DNA isolated using QIAamp DNA Mini Kit (Qiagen; 51304) and fragments were assessed using gel electrophoresis.

OPCs were dissociated from PDL plastic 96 hours following transfection using TrypLE Express (Thermo Fisher; 12604013), re-suspended in HBSS, and 400,000 cells were slowly injected into 14 month-old females into grey matter in the prefrontal cortex using a Hamilton syringe and a stereotactic

frame. 13.5 days following transplantation, animals were injected with I.P. with 75µg/g body weight of EdU and on day 14 were perfusion fixed.

Generation of Nested CRISPR Plasmids

AAV-CMVc-Cas9 was a gift from Juan Belmonte (Addgene plasmid # 106431). pCAG-Cre-IRES2-GFP was a gift from Anjen Chenn (Addgene plasmid # 26646). pUCmini-iCAP-PHP.eB was a gift from Viviana Gradinaru (Addgene plasmid # 103005). pHelper plasmid was a gift from the Cancer Research United Kingdom viral core facility.

Using the AAV-CMVc-Cas9 plasmid backbone and AAV2 ITR sequences, we cloned in the nested CRISPR system using NEBBuilder HiFi DNA Assembly. U6, gRNA, and Ribozyme containing sequences were ordered from Integrated DNA Technologies (see Sequence table), and cloned as previously described.

Myc sequence was cloned from iPS cells (Gift of the Rowitch lab) and reverse transcribed with Protoscript II (NEB; M0368S).

Virus production protocol and in vitro, in vivo transfection, and spinal cord lesions.

AAV production and purification followed the previously described protocol(Challis et al., 2018). In brief, HEK293 cells were grown in 15mm plastic dishes and triple transfected with the pHelper plasmid, the PHP-EB capsid plasmid, and the transgene plasmid. Five days later cells were lysed and virus was isolated using Optiprep density gradient medium (Sigma; D1556) and ultra-centrifuged at 350000g. Viral layer was isolated and concentrated using Amicon Ultra-15 Centrifugal Filter Units (Sigma; Z648043-24EA). AAV titer was determined using SYBR green qPCR. For *in vitro* studies, mixed glia cells grown in 10% FBS in DMEM/F12 were infected with 100,000 viral genomes per cell per viral particle. Media was changed 24 hours later and cells were left for 96 additional hours with media changes every 48 hours. For *in vivo* administration of the virus, mice were restrained and 5E11 viral genomes per virus were injected into the tail vein of 8 week old or 18 month-old C57/Bl6 mice.

Spinal cord lesions were created by injecting 1% lysolecithin in PBS into the ventral white matter tract of the spinal cord. 21 days following tail-vein injection, mice were perfusion fixed.

For DNA/RNA extraction of CRISPR modified cells, DNA/RNA was isolated using TRIzol phase separation (Thermo Fisher; 15596026). All PCRs were performed using Phusion polymerase and Indel analysis was peformed using Tide using the default parameters(Brinkman, Chen, Amendola, & van Steensel, 2014).

Tissue Clearing, cleared staining, Light-sheet microscopy, and image analysis

Tissue clearing was performed using the CUBIC protocol, as previously described(Susaki et al., 2015). In brief, animals were perfused in 4% PFA and CNS was subsequently cut into 2 mm coronal slices using a brain matrix. Samples placed in a 48-well plate and were cleared for 3 days in the reagent 1 solution of the CUBIC tissue clearing protocol. Following the reagent 1, samples were stained in 0.5% Triton with 0.5% BSA in PBS with the laminin antibody (see antibody table) at a concentration of 1:300 for three days rotating on an orbital shaker at 37˚ C. Primary antibody was washed twice with 0.5% Triton in PBS for two hours each rotating on an orbital shaker at 37˚ C. Slices were then incubated in secondary antibody in 0.5% Triton with 0.5% BSA at a concentration of 1:300 for three days on an orbital shaker at 37˚ C. Finally, samples were again wash twice for two hours each, and placed into Reagent 2 of the CUBIC tissue clearing protocol.

Samples were placed in 50% silicone oil (Sigma; 85409) and 50% mineral oil (Sigma; M8410), and mounted on a custom-built light sheet microscope. The microscope was built by Ruth Sims at Cancer Research United Kingdom and all images were acquired using a 20x objective. Image processing was performed using OpenSPIM and Clear Volume, both open source programmes and used in FIJI.

Comet assay

For comet assays of freshly isolated OPCs approximately 5000 OPCs were resuspended in 100µl PBS and mixed with 300µl 1% low melting point agarose (37C). Cells were detached using TrypLE 1x Select (Thermo Fisher; 12563011) for 8min at 37°C. The comet assay was then performed as described31. Briefly, OPCs were centrifuged at 300g for 5 min. at room temperature and the cell pellet was resuspended with 100µl PBS and then mixed with 300µl molten low-melting point agarose (Thermo Fisher; 16520-050) pre-incubated at 37°C. The cell-agarose suspension was then applied gently onto polysine slides that were pretreated with 1% agarose and allowed to solidify at 4°C. The slides

were submersed in alkaline cell lysis buffer (0.3M NaOH, 100mM EDTA, 0.1% (w/v) N-Lauroylsarcosine (Sigma; 61745), 1.2M NaCl in ddH2O) for 16 hours at 4°C in the dark. The slides were then electrophoresed in alkaline electrophoresis buffer (0.03M NaOH, 2mM EDTA, pH > 12.3, pre-chilled at 4°C) for 25min at RT with 1V/cm, whereby the cm were measured as the distance between the electrodes. Finally, electrophoresed and propidium iodide (Thermo Fisher; P3566) stained DNA was imaged and 50-100 nuclei per animal were visually scored according to published protocols. Statistical significance was determined comparing respective damage categories between experimental groups by a two-tailed unpaired t-test. A significant result was assumed for $p<0.05$.

Animal models and Tamoxifen administration

Confetti animals were oral-gavaged for 4 days with 40 mg/day of tamoxifen (Sigma; T5648). To induce long-term labelling of Lgr5-Cre animals, food pellets were replaced with colored tamoxifen food pellets (Envigo; 130856). For pre-weaned pups, tamoxifen pellets were given to the mother and tamoxifen was given to the pups via the mothers' milk.

Table of small molecules

Small Molecule/Recombinant Protein	Concentration	Provider	Product Number
Y-27632/Rho-kinase inhibitor	10-50µM	Sigma	Y0503
Blebbistatin/ Non-muscle myosin IIa inhibitor	5uM	Sigma	B0560
CHIR99021/GSK3ß inhibitor	Range	Sigma	SML1046
Wnt 3a	50 ng/mL	Peprotech	315-20
R-Spondin-3	400 ng/mL	Peprotech	120-44
10058-F4/Myc inhibitor	27.5µM	Sigma	10058-F4

Table of antibodies

Antibody	Dilution	Provider	Product Number
Rabbit α Olig2	IHC: 1:1000	Millipore	ab9610
Rabbit α Ng2	IHC: 1:100	Millipore	MAB5384
Rat α MBP	IHC: 1:100	AbD Serotec	MCA409S
Rabbit α Lmnb1	IHC: 1:1000 WB: 1:5000	Abcam	ab16048
Goat α Lmna/c	IHC: 1:100 WB:1:7500	Santa Cruz	sc-20681
Mouse α Actin	WB: 1:20000	Sigma	556321
Mouse α CC1	IHC: 1:300	Millipore	MABC200
Goat α Sox10	IHC: 1:100	Santa Cruz	sc-17342
Rabbit α Piezo1	IHC: 1:100 WB:1:500	Proteintech	15939-1-AP
Mouse α Anti-Chondroitin Sulfate	IHC: 1:100	Sigma	C8035
Rabbit α GFP	IHC: 1:300	Abcam	ab290
Rabbit α H3K9Me3	IHC:1:500	Abcam	ab8898
Rabbit α Laminin	LSFM: 1:300	Sigma	L9393
Goat α Td-tomato	IHC: 1:300	Scigen	Ab8181
Alexa Fluor 594 Goat α Mouse IgM	IHC: 1:500	Thermo Fisher	A-21044
Alexa Fluor 488 Donkey α Rabbit	IHC: 1:500	Millpore	A21206
Alexa Fluor 594 Donkey α Rabbit	IHC: 1:400	Molecular Probes	A21207
Alexa Fluor 594 Donkey α Goat	IHC: 1:500	Thermo Fisher	A-11058
Alexa Fluor 647 Donkey α Mouse	IHC: 1:500	Thermo Fisher	A-31571
IRDye800CW D anti-Goat	WB: 1:10000	Li-Cor	926_32214
IRDye800CW D anti-Mouse	WB: 1:10000	Li-Cor	926_32212
IRDye600CW D anti-Rabbit	WB: 1:10000	Li-Cor	926_38073

Table of Primers

Gene	Forward	Reverse	Provider
Lmnb1	5'- cagattgagtatgagta-caagc – 3'	5'- agtggaagtgttcatctctg - 3'	Sigma
Lmna	5' – ctacagcaaacactaag-gaac – 3'	5'- tttttcgggatggaaacaac -3'	Sigma
Tbp	5'- catcatgagaataaga-gagcc – 3'	5' – ggattgttcttcactttgg –3'	Sigma
Lmnb1	5'-taatacgactcactatagggtaccttcggt-3'	5'-gaagatcgaccatgtcttga-caagt- 3'	Sigma
Lmna	5'- taatacgactcactatagg-gccgaggtgcgccagcgcc -3'	5'-tggcattccaaaacactttaat-gaaaagactttggcatggaggc-3'	Sigma
Gfp	5'-aagctgaccct-gaagttcatctgc -3'	5'-cttgtagttgccgtcgtccttgaa -3'	Sigma
Cas9	5'-aaacagcagattcgcctg-ga-3'	5'-tcatccgctcgatgaagctc-3'	Sigma
Minicircle Backbone	5'-ggcccgccccaactgggg-taacctttga-3'	5'-gaatcatgggaaataggccctc-cgccgagtgaagtcagcatgaggg-gcggcgcccggggagcccaa-3'	Sigma. Plasmid from addgene #87114
Myc clon-ing	5'-atgcccctcaacgt-tagct-3'	5'-ccctccgcacaagagttccg-tagc-3'	Sigma

Pdgfra gRNA	In vivo CRISPR	5'-gctccgggtatcatcttctc-gttttagagctagaaatagcaagtta-aaataaggctagtccgttatcaactt-gaaaaagtggcaccgagtcggt-gctttttt-3'	Sigma
Piezo1 gRNA	In vivo CRISPR	5'-cgattttgtagaccaccagg-gttttagagctagaaatagcaagtta-aaataaggctagtccgttatcaactt-gaaaaagtggcaccgagtcggt-gcttt-3'	
U6	5'-gagggcctatttcccatgat-tcc-3'	5'-ccggtgtttcgtcctttcc-3'	Sigma. Plasmid from addgene #48138
shPiezo1 Construct	5'-tggaaaggacgaaacaccggt-ggatgtgtgtggaagacattcaa-gagatgtcttccacacacatc-cattttttctagagggtaccggggc-ccggtcgac-3'	5'- aactagtcaataatcaatgtcg-gaactccatatatgggctatgaacta-atgaccccgtaattgattactattaata-actagtcgaccgggccccggta-3'	Sigma
shControl	5'-gtggaaaggacgaaacac-cggcaacaagatgaagag-caccaactcgagttggt-gctcttcatcttgttgtttttctagagg-gtaccggggcccggtcgac-3'	same as above	Sigma
CMV	5'-gacattgattattgactagttatta-atagtaatcaattacggggtcatt-agttca-3'	5'-ggtgaacagctcctcgcccttgct-caccatggtggcgctagcctgct-tatatagacctcccaccgtacacgc-3'	Sigma. Plasmid from addgene #48138

Table of gBlock Fragments (IDT)

Description	Sequence	Provider
U6, Pdgfra	tgtacaaaaaagcaggctttaaaggaaccaattcagtcgactggatccggtaccaaggtcgggcaggaa gagggcctatttcccatgattccttcatatttgcatatacgatacaaggctgttagagagataattagaattaatt tgactgtaaacacaaagatattagtacaaaatacgtgacgtagaaagtaataatttcttgggtagtttgcagtttt aaaattatgttttaaaatggactatcatatgcttaccgtaacttgaaagtatttcgatttcttggctttatatatcttgt ggaaaggacgaaacaccgcgatctgaactcacagtgggttttagagctagaaatagcaagttaaaataagg ctagtccgttatcaacttgaaaaagtggcaccgagtcggtgctttttttctagacccagctttcttgtacaaagt tggcgtttaaac	IDT
Ribozyme, non-Target gRNA	gcggccgcaaaggtttttctttttcctgagaaatttctcaggttttgctttttaaaaaaaaaagcaaaagacgct-ggtggctggcactcctggtttccaggacggggttcaagtccctgcggtgtctttgcttgaattcaaatc-gctgatgagtccgtgaggacgaaacgagtaagctcgtctgtattactgatattggtggggtttta-gagctagaaatagcaagttaaaataaggctagtccgttatcaacttgaaaaagtggcaccgagtcggt-gcttttgccggcatggtcccagcctcctcgctggcgccggctgggcaacatgcttcggcatggcgaatgg-gacgaataaaagatctttattttcattagatctgtgtgttggttttttgtgtgccgccactgtgagttcagatcgc	IDT
Ribozyme, Piezo1 gRNA	gcggccgcaaaggtttttctttttcctgagaaatttctcaggttttgctttttaaaaaaaaaagcaaaagacgct-ggtggctggcactcctggtttccaggacggggttcaagtccctgcggtgtctttgcttgaattcaaatc-gctgatgagtccgtgaggacgaaacgagtaagctcgtctcgattttgtagaccaccagggtttta-gagctagaaatagcaagttaaaataaggctagtccgttatcaacttgaaaaagtggcaccgagtcggt-gctttttttgccggcatggtcccagcctcctcgctggcgccggctgggcaacatgcttcggcatggcgaatg-ggacgaataaaagatctttattttcattagatctgtgtgttggttttttgtgtgccgccactgtgagttcagatcgc	IDT
Nested CRISPR System	tacaaagttggcgtttaaacccgccactgtgagttcagatcgcgaattcaaatcgctgatgagtccgt-gaggacgaaacgagtaagctcgtctcgattttgtagaccaccagggttttagagctagaaatagcaagt-taaaataaggctagtccgttatcaacttgaaaaagtggcaccgagtcggtgctttttttgccggcat-ggtcccagcctcctcgctggcgccggctgggcaacatgcttcggcatggcgaatgggacgaata-aaagatctttattttcattagatctgtgtgttggttttttgtgtgcgattttgtagaccaccaggcgg	IDT

Chapter 3

Dynamics between OPCs, niche, and progeny in the CNS

Oligodendrocyte progenitor cells (OPCs) continuously myelinate the central nervous system (CNS) throughout adulthood. Unlike other stem cells, however, the OPC in the adult has no defined niche. Moreover, the signals that underlie the OPC activation in CNS homeostasis remain unknown. Previous reports have found that in development, OPCs migrate along the blood vessels and spread out across the CNS (Tsai et al., 2016). Here, we find that OPCs remain on the blood vessels throughout adulthood, while their progeny, the oligodendrocyte, are localized to the brain parenchyma. Using single cell sequencing and lineage tracing, we have identified Lgr5 as a marker for activated OPCs whose progeny delaminate from the blood vessel and differentiate into oligodendrocytes. Finally, we have identified Wnt3a and R-spondin to activate adult OPCs *in vitro*.

Stem cells underlie homeostasis and repair in the adult. Most tissue-specific stem cells reside in a niche, an environment which protects and defines their stem cell identity (Spradling et al., 2008). It is thought that without a definite niche, stem cells would spontaneously differentiate causing widespread stem cell depletion. Upon activation, the stem cells often exit their niche, and differentiate into committed post-mitotic cells (Hsu et al., 2011). For each stem cell population, the signals for the switch from stem cell quiescence to activation are unique, but Wnt, Notch, BMP, and Hedgehog signaling make an appearance in this activation process for many tissue-specific stem cells.

In the central nervous system (CNS), there are two dominant stem cell populations: neural stem cells (NSCs) and oligodendrocyte progenitor cells (OPCs). While NSCs are spatially confined within discrete regions of the brain, OPCs are spread relatively evenly across the CNS and make up 5-10% of the total number of cells in the brain (Barres et al., 1992). OPCs differentiate into oligodendrocytes well into adult rodent and human life, albeit in an age dependent manner (Hill et al., 2018; Yeung et al., 2014). In multiple sclerosis, this loss of OPC activity with ageing may well underlie the clinical phenotype of chronically demyelinated lesions (Goldschmidt et al., 2009). Moreover, it is increasingly accepted that OPCs play a major role in normal cognitive functions and are the cell type underlying

complex psychiatric illness (McKenzie et al., 2014; Windrem et al., 2017).

Despite their clinical relevance, little is known about the OPC niche or about the factors that cause OPCs to activate and differentiate into oligodendrocytes in the homeostatic CNS. In development, OPCs migrate along the blood vessels of the CNS (Tsai et al., 2016). Endothelial cells expressing the chemokine ligand Sdf1 bind OPCs via the chemokine receptor Cxcr4 and promote their migration. In the adult, however, the precise niche of OPCs remains unknown. While NSCs are known to have a niche on the blood vessel in the adult (Shen et al., 2008), it is widely believed that OPCs are evenly scattered throughout the parenchyma of the brain (Vanlandewijck et al., 2018).

Here, using multiple lines of transgenic mice, brain clearing and light sheet microscopy, we take a macroscopic view of the CNS and find a vascular niche for OPCs across white and grey matter of the CNS. Using toxin-induced lesions and single cell sequencing, we identify the canonical stem cell marker Lgr5 to be significantly upregulated in activated adult OPCs. With lineage tracing of Lgr5 in adult mice we show that Lgr5 expressing cells live on the blood vessels while their oligodendrocyte progeny are in the parenchyma, thus establishing a spatially-defined stem cell lineage in the CNS. Finally, as Lgr5 is part of the Wnt signaling cascade, we find that Lgr5-agonist R-spondin and Wnt 3a can activate adult OPCs *in vitro*.

While NSCs have been found to have a vasculature niche, OPCs have been reported as in the CNS parenchyma. Unlike NSCs which are regionally defined and differentiate in an uni-directional manner, OPCs are spread throughout the entirety of the CNS, proliferating, differentiating, and migrating in the X, Y, and Z dimension. As such, to determine whether the OPC has a niche, we hypothesized that a macroscopic, multi-dimensional view of the CNS was required. To achieve this, we used thick 2mm tissue, the CUBIC clearing protocol, and light-sheet microscopy of aged (≥14 months) Pdgfra-H2B-GFP animals. We suspected OPCs may too have a vascular niche, so we began by optimizing the CUBIC clearing protocol using wild-type aged animals and subsequent immuno-staining blood vasculature with laminin (Fig. 1a). We used aged animals because of previous reports that the GFP-histone fusion protein lingers in newly differentiated oligodendrocytes. As aged animals have low rates of de novo myelination, we hypothesized most GFP labeling would occur in OPCs themselves.

In 2-dimensional 12.5μM cryo-sections, we observed no immediate pattern in the GFP labelled cells (Fig. 1b). However, following tissue clearing, light-sheet microscopy, and 3-dimensional reconstruc-

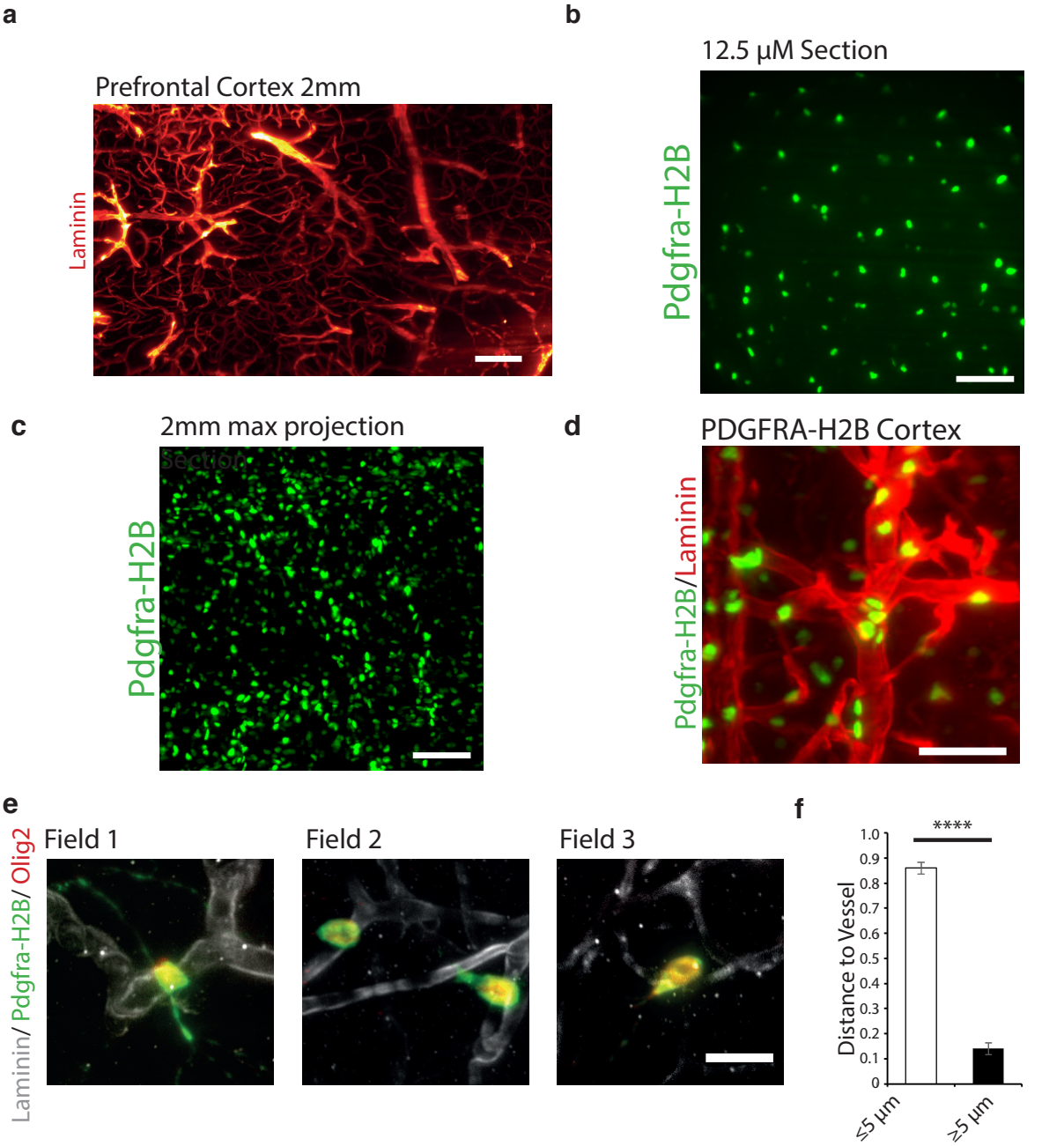

Figure 1. Adult OPCs have a vascular niche. a Tiled maximum projections across 2mm of CNS of laminin staining acquired from a custom-built light sheet microscope. Scale bar represents 50µm. b, Representative image of Pdgfra-H2B-GFP mouse cortex from a 12.5µm cryosection. Scale bar represents 100µM. c, Representative image acquired using light-sheet microscopy on Pdgfra-H2B-GFP cortex that had been cleared using the CUBIC protocol. Scale bar represents 100µM. d, Representative image acquired using light-sheet microscopy on Pdgfra-H2B-GFP cortex co-stained with laminin. Scale bar represents 50µM. e, Representative images of CUBIC cleared Pdgfra-H2B-GFP cortex that had been co-stained with Olig2 and Laminin. Scale bar represents 20µm. f, Histogram of the proportion of GFP-labelled cells within specific distances from laminin stained vasculature across multiple imaging planes. Averages represent the mean proportion of cells in given category from N = 3 biological replicates. Here, and throughout chapter, means represent quantifications of ≥200 cells quantified per replicate across ≥3 fields of view and **** indicates a one-way ANOVA significance value of ≤.001. Images were acquired by Dr. Ruth Sims of Cancer Research UK.

tion we observed GFP cells clustering around vessel like structures across the CNS (Fig. 1c). With immunostaining of laminin, we confirmed that OPCs across the CNS cluster on laminin stained blood vessels (Fig. 1d). All cells were of the oligodendrocyte lineage as confirmed by Olig2 protein co-staining (Fig 1e). More than 80% of the labelled GFP cells were within 5μM of a given blood vessel, as measured from the center of the labeled nucleus to the blood vessel (Fig. 1f). For the first time, these results show that adult Pdgfra expressing OPCs associate with the CNS vasculature.

A factor which confounds these observations is that the clearing process eliminates cells more distal to the blood vessel. To rule out this possibility, we did short term labelling (21 days post tamoxifen) of Sox10-CreER animals (Fig. 2a). Sox10 is a marker of the entire oligodendrocyte lineage, so we expected labelling of both oligodendrocytes and OPCs. Doing so, we observed bipolar, labelled OPC-like cells clustering to the blood vessel while more complex structured oligodendrocyte-like cells were distal to the blood vessel (Fig. 2b-d). Quantifying the distance of the cells to the vessel, we found that of the entire Sox10 oligodendrocyte lineage, only ~20% of cells were on the vessel (Fig. 2e). These results bolster our claim that OPCs cluster on blood vessels while the differentiated cells are away from the vessel (Fig. 2f).

We hypothesized that OPCs on the vessel upon activation in the homeostatic adult CNS would de-laminate and subsequently differentiate into the myelinating oligodendrocyte. Unlike the stem cells of the intestine and the skin, adult OPC activation in the homeostatic adult brain is a spatially and temporally rare event, making it a difficult process to study (Psachoulia et al., 2009). To understand the signaling pathways that underlie OPC activation, we re-purposed previous single cell sequencing data from our group performed by PhD student Natalia Deja. Her work, originally executed to discover the origin of Schwann cells in the CNS, experimentally activated OPCs by creating a focal area of demyelination in the adult rat caudal cerebellar peduncle using 0.1% ethidium bromide (Woodruff and Franklin, 1999). This demyelinating injury model kills all oligodendrocytes and is followed by a period of remyelination, whereby OPCs migrate to the lesion, proliferate, and differentiate into new myelinating oligodendrocytes. Ten days following the lesion, the lesion site was vibratomed from fresh CNS tissue, dissociated, and FACs sorted for the OPC marker A2B5. Cells were subsequently single-cell sequenced. Using t-distributed stochastic neighbour embedding on sequenced single cells from both lesioned and un-lesioned brain, 3 populations of OPCs emerged: homeostatic OPCs, activated cycling OPCs, and committed differentiating OPCs (Data not shown).

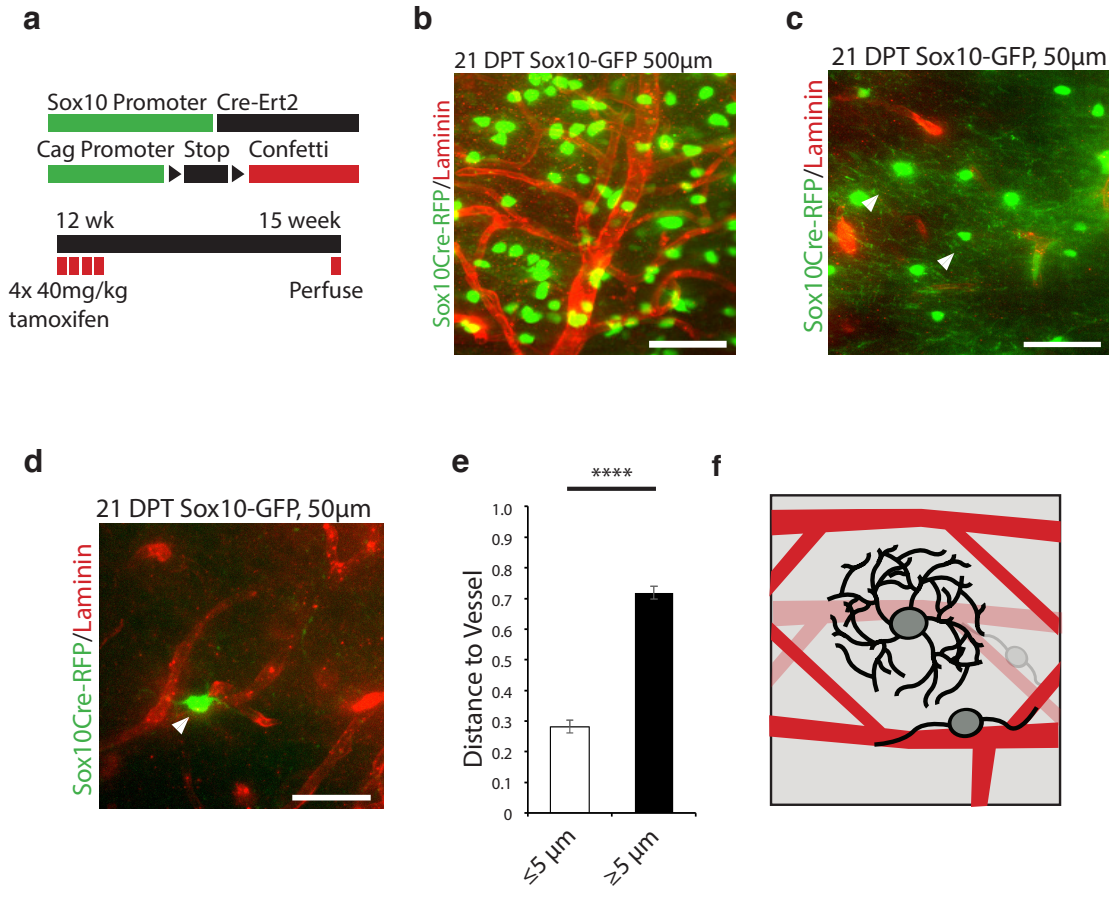

Figure 2. Adult oligodendrocytes do not have a vascular niche. a, Diagram outlining experimental strategy for labelling oligodendrocyte lineage cells in Sox10-CreErt2/Confetti adult mice. b, Maximum projection of lightsheet microscope image across 500µm of laminin and GFP labelled cells 21 days following tamoxifen induction of the Sox10 driven cre-recombinase. c, Representative image of multi-processed Sox10 labelled oligodendrocytes (indicated by arrow) and laminin. d, Representative image of bipolar Sox10 labelled OPC closely associating with laminin stained vasculature. e, Histogram of the proportion of GFP-labelled cells within specific distances from laminin stained vasculature across multiple imaging planes. Averages represent the mean proportion of cells in given category from N = 3 biological replicates. f, Cartoon diagram illustrating that undifferentiated OPCs remain closely affiliated with the vasculature while their differentiated progeny, the multi-processed oligodendrocyte, do not. Scale bars throughout the figure represent 50µm. Images were acquired by Dr. Ruth Sims of Cancer Research UK.

To determine the signalling pathways that underlie the activation of adult quiescent OPCs, we looked at the molecular signalling pathways most differentially upregulated in the activated lesion OPCs compared to the control un-lesioned tissue OPCs. Using KEGG pathway analysis, and found in Ms. Deja's work, that the modulation in ß-catenin signalling is the most upregulated pathway involved in OPC cell activation. This KEGG analysis corroborates the finding that the canonical Wnt-pathway regulating transcription factor Tcf7l2 is the most upregulated gene in the activated lesion OPC cells. As Wnt signalling is the most enriched for pathway in activated OPCs, we hypothesised that adult OPC activation is mediated by Wnt signalling, and a Wnt pathway related cell-surface receptor may initiate the Wnt signalling cascade, ultimately leading to activation. From the gene set pathway analysis, we identified the canonical stem cell activation gene Lgr5 to be amongst the most highly expressed of Wnt pathway genes in the activated lesion OPC population. The data is not shown in this thesis as the work forms the basis of Ms. Deja's own PhD thesis.

Lgr5 is a marker of stem cell activation in a number of stem cell niches, including the skin and the intestine (Buczacki et al., 2013; Jaks et al., 2008). The Lgr family of receptors regulate Wnt signalling strength by inhibiting molecular programmes that dampen Wnt signal strength (Hao et al., 2012). Previous studies in postnatal development found Lgr5 expressing neurons in the developing cerebellum, but no follow up work has looked for a role of Lgr5 in the adult CNS (Miller et al., 2014). As Wnt signalling genes and Lgr5 are enriched for in activated adult OPC populations, we hypothesised that Lgr5 would be a marker for activating OPCs in the adult. To test this, we crossed mice that expressed the Cre-ER gene under the promoter of Lgr5 with Rosa26-stop-Td-tomato mice. At 3 months of age, we dosed the animals with tamoxifen 4 times. As OPC cycling can be up to 30 days in the adult brain, we hypothesised that we would need to lineage-trace for 30 days in order to label an activated OPC expressing Lgr5 (Fig. 3a). Following 30 days, we found a significant proportion of Olig2 expressing cells that were co-labelled with Td-tomato and a smaller proportion of cells co-labelled with Td-Tomato, Olig2, and the oligodendrocyte intracellular marker CC1 (Fig. 3b-c). As such, we conclude that activated adult OPCs express Lgr5 and that oligodendrocytes generated in the adult derived from an Lgr5 expressing activated OPC. Finally, to confirm that Lgr5 expressing OPCs themselves remain on the blood vessel, we stained Lgr5 lineage traced tissue sections with laminin and found Lgr5+ OPCs to remain largely within 5µM of the blood vessel (Fig. 3d-e). Additional work is ongiong to confirm the role of Lgr5 as a marker of activated OPCs (see Discussion).

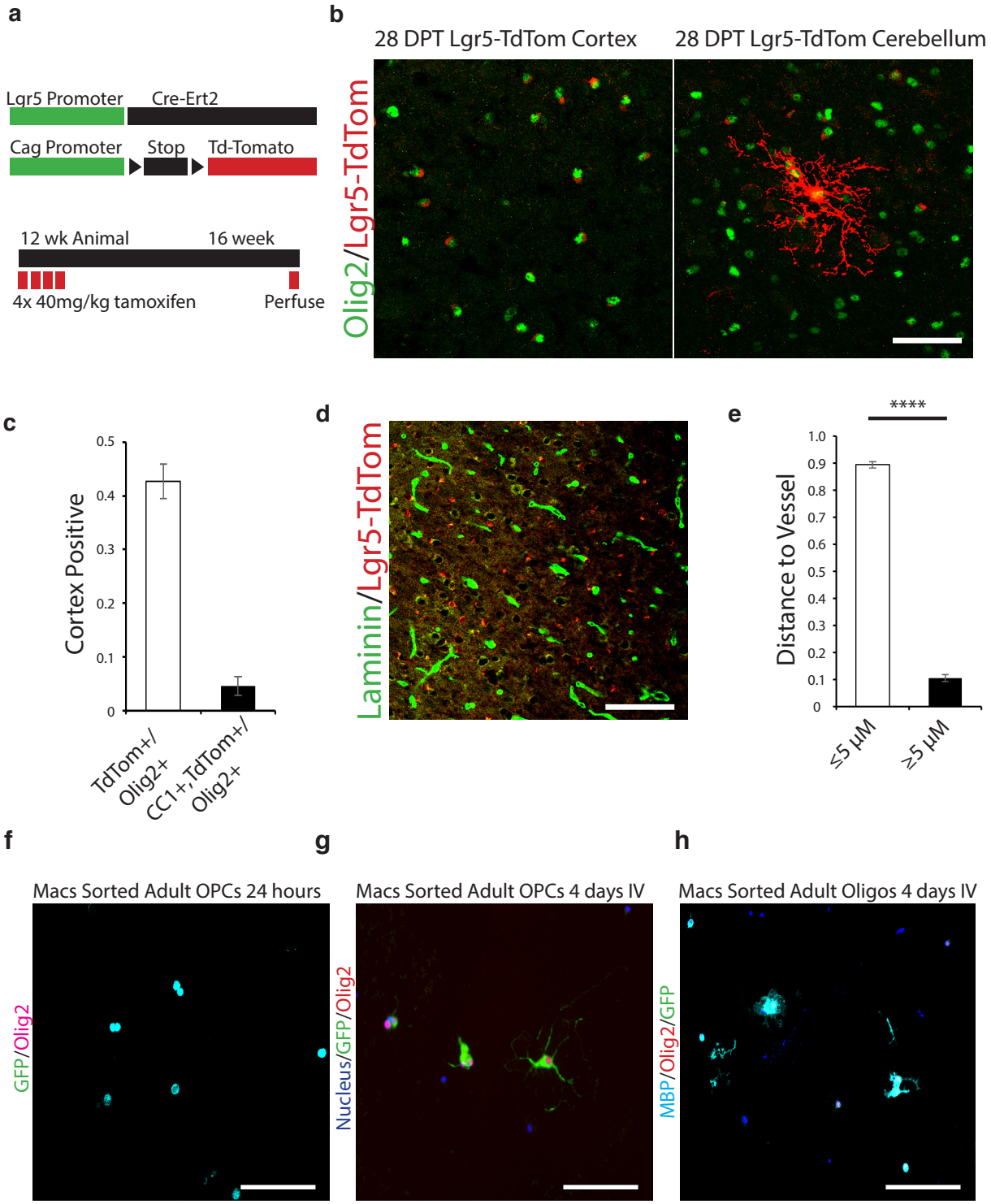
a
Lgr5 Promoter
Cre-Ert2
Cag Promoter
Stop
Td-Tomato
12 wk Animal
16 week
4x 40mg/kg tamoxifen
Perfuse
b
28 DPT Lgr5-TdTom Cortex
28 DPT Lgr5-TdTom Cerebellum
Olig2/Lgr5-TdTom
c
Cortex Positive
0.5
0.4
0.3
0.2
0.1
0
TdTom+/ Olig2+
CC1+,TdTom+/ Olig2+
d
Laminin/Lgr5-TdTom
e
****
Distance to Vessel
1.0
0.9
0.8
0.7
0.6
0.5
0.4
0.3
0.2
0.1
0
≤5 µM
≥5 µM
f
Macs Sorted Adult OPCs 24 hours
GFP/Olig2
g
Macs Sorted Adult OPCs 4 days IV
Nucleus/GFP/Olig2
h
Macs Sorted Adult Oligos 4 days IV
MBP/Olig2/GFP

Figure 3

Figure 3. Activated homeostatic OPCs in the adult CNS express Lgr5. a, Diagram outlining strategy for Lgr5 lineage tracing in the adult mouse CNS. Lgr5 Cre-recombinase animals with floxed-stop Td-tomato were oral gavaged tamoxifen 4 times at 3 months of age. 4 weeks later the animals were perfusion fixed. b-c, Representative images and quantifications of the proportion of Td-tomato, Olig2, and CC1 co-staining across the cerebellum and the cortex. Scale bars represent 50µm. d-e, Representative images and distance quantifications between Td-tomato/Olig2 cells from the laminin vasculature. Scale bars represent 100µm. f-h, *In vitro* images of MACs sorted OPCs from adult Lgr5-eGFP animals show that after 24 and 96 hours of *in vitro* in growth factors, adult OPCs express Lgr5, as indicated by the expression of GFP. Scale bars represent 100µm. All quantifications represent mean proportion from N=3 biological replicates. Animals were fed Tamoxifen by Dr. Björn Franklin of Robin Franklin's group.

If Lgr5 expression is indeed a marker of OPC activation, we hypothesised that isolated adult OPCs *in vitro* would express Lgr5 after exposure to growth factors. To test this, we sorted adult OPCs using magnetic associated cell sorting (MACs) using the marker A2B5 from adult Lgr5-eGFP transgenic animals in which all Lgr5 expressing cells also express GFP. We observed that after 24 and 96 hours *in vitro*, most of the isolated OPCs were co-labelled with GFP and Olig2 (Fig. 3f-g). However, oligodendrocytes, MACs sorted using the antibody MOG, were not GFP positive (Fig. 3h). These *in vitro* findings confirm our *in vivo* lineage tracing that Lgr5 expression is specific to activated OPCs, but not their progeny, the oligodendrocyte.

If the activity of OPCs is indeed regulated by Lgr5-mediated Wnt signal strength, then agonists of the Lgr5/Wnt signalling pathways should activate adult OPC, causing them to both proliferate, delaminate from the blood vessel, and differentiate into de novo oligodendrocytes. Using publically available single cell sequencing databases of the adult human and mouse cortex, we identified multiple Wnts and R-spondins that are expressed across the CNS (Lake et al., 2018; Zeisel et al., 2015). We found most secretors of Wnt agonists to be Rbfox3 (Neun) expressing neurons. We identified Wnt 3a and R-Spondin-3 to be the most widely expressed by neurons and oligodendrocytes across the adult CNS (Fig. 4a). R-Spondin-3 directly associates with and activates Lgr5 (de Lau et al., 2011). To understand whether these Wnt signals can modulate the activation state of OPCs, we MACs isolated 3 month-old adult mouse OPCs with the OPC specific antibody A2B5. We then treated the OPCs with various concentrations of the Wnt agonists for 5 days *in vitro* (Fig. 4b). In low levels of growth factors Pdgf and Fgf, very low levels of adult OPCs proliferated as marked by EdU incorporation or differentiated into MBP expressing oligodendrocytes (Fig. 4c-f). Following treatment with R-Spondin-3 or Wnt3a, however, >15% of cells were proliferating as marked by EdU incorporation and >20% of cells spontaneously differentiated into MBP expressing multi-processed oligodendrocytes. We thus identify the Wnt pathway and its modulation by R-Spondin-3 or Wnt3a as a significant signalling pathway underlying adult OPC re-activation, proliferation, and differentiation.

Discussion

Here we report the finding that adult OPCs live on the blood vessels across the CNS, but their progeny, the oligodendrocyte, live off the vessel. To identify the signal that underlies the activation of the adult OPC, we performed single cell sequencing 14 days following a demyelinating lesion and found Wnt

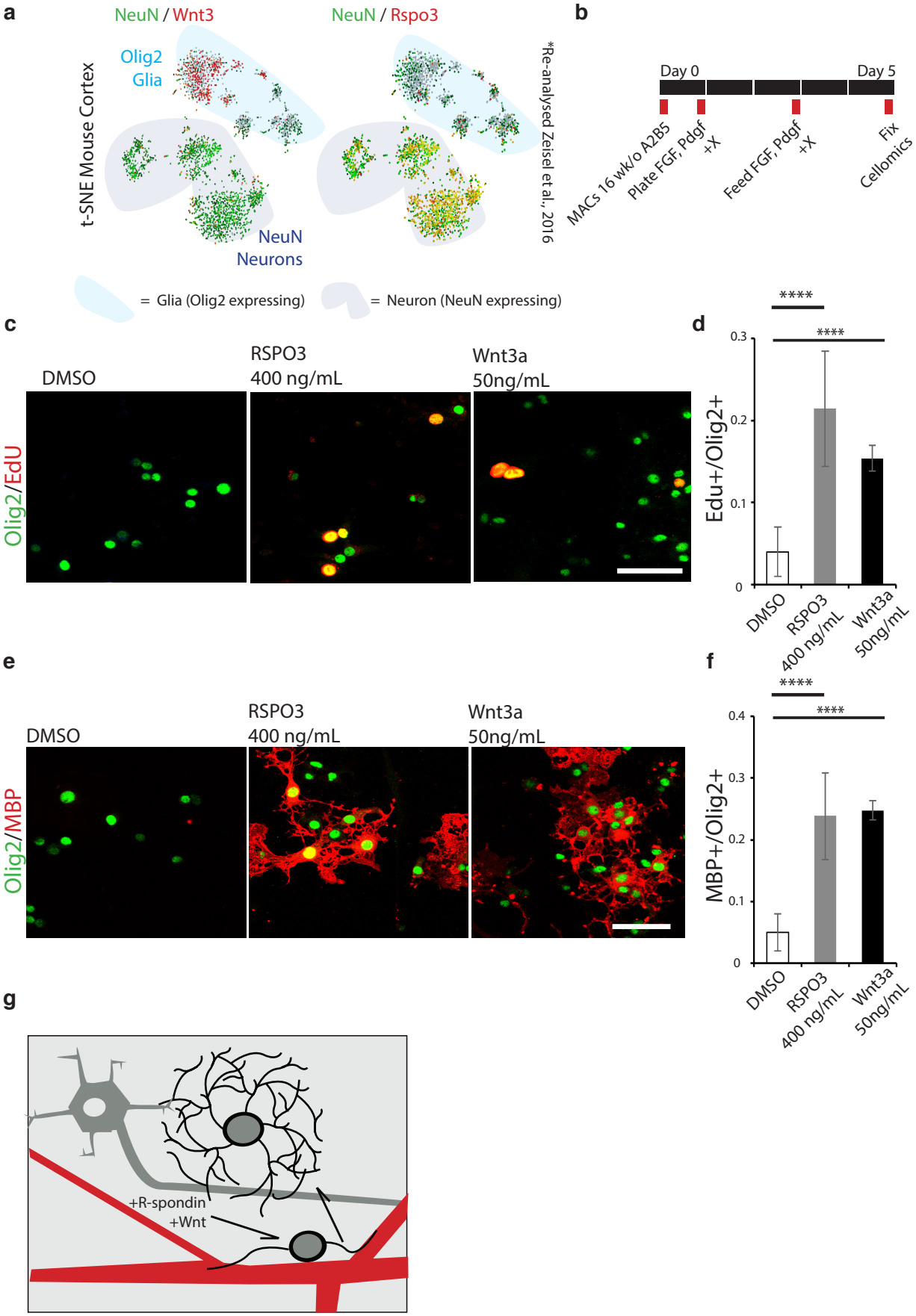
a
NeuN / Wnt3
NeuN / Rspo3
t-SNE Mouse Cortex
Olig2
Glia
NeuN
Neurons
*Re-analysed Zeisel et al., 2016
= Glia (Olig2 expressing)
= Neuron (NeuN expressing)
b
Day 0
Day 5
MACs 16 wk/o A2B5
Plate FGF, Pdgf +X
Feed FGF, Pdgf +X
Fix
Cellomics
c
DMSO
RSPO3 400 ng/mL
Wnt3a 50ng/mL
Olig2/EdU
d
****
****
Edu+/Olig2+
0.3
0.2
0.1
0
DMSO
RSPO3 400 ng/mL
Wnt3a 50ng/mL
e
DMSO
RSPO3 400 ng/mL
Wnt3a 50ng/mL
Olig2/MBP
f
****
****
MBP+/Olig2+
0.4
0.3
0.2
0.1
0
DMSO
RSPO3 400 ng/mL
Wnt3a 50ng/mL
g
+R-spondin
+Wnt

Figure 4

Figure 4. Wnt agonists activate adult OPCs. a, R-Spondins and Wnts regulate activity state of adult OPCs. a, Re-analysed tSNE plots from previously published single cell sequencing dataset from adult mouse cortex (Zeisel et al., 2015). tSNE charts show that Wnt3a and R-Spondin-3 are the dominant Wnt pathway agonists in the adult CNS. Moreover, the charts show that Rbfox3 expressing neurons are the dominant cell type secreting these proteins. b, A schematic outlining the experimental strategy for testing the effects of Wnt agonists on adult OPCs. Mouse OPCs were MACs sorted with the antibody A2B5 and plated in growth factors Fgf and Pdgf. Numerous Wnts and R-Spondins at varying concentrations were added in addition to the growth factors. c-f, Representative images and quantifications of the effects of R-Spondin-3 (RSPO3) and Wnt3a on OPC proliferation, as indicated by the labelling of EdU, and on spontaneous differentiation of oligodendrocytes as indicated by co-expression of myelin basic protein (MBP) and transcription factor Olig2. Scale bars represent 50μm and **** indicate a one-way ANOVA significance value of ≤.001. g, A schematic with the proposed model for the OPC niche in the adult brain. OPCs reside on the blood vessel. Upon activation with Wnt agonists such as R-Spondin-3 from the local niche, OPCs activate Lgr5, delaminate, and differentiate into oligodendrocytes in the parenchyma.

signalling to be the most enriched for signalling pathway amongst activating OPCs. Specifically, we found the Wnt regulating receptor Lgr5 to be enriched for within this population. Using long term *in vivo* lineage tracing of Lgr5 we found that Lgr5 marks OPCs across the CNS and that the progeny of the Lgr5 expressing OPC is the oligodendrocyte. Finally, we found that the agonist R-Spondin-3 and Wnt3, proteins expressed by cells of the neuronal lineage, are sufficient to both proliferate OPCs and cause them to spontaneously differentiate into myelin expressing oligodendrocytes (Fig. 4g). Taken together, this work describes the niche of the adult OPC and shows Lgr5-mediated Wnt signalling as the activating pathway by which adult OPCs proliferate and differentiate in the CNS.

The niche, adult stem cells, and plasticity

Previous work understanding OPC differentiation has focused largely on *in vitro* models using neonatal or embryonic-derived OPCs (Hubler et al., 2018). While these models have identified differentiation signals that underlie developmental OPC differentiation programmes, it remains unclear whether these same pathways are relevant for adult OPC differentiation. One major difference between neonatal and adult differentiation pathways is that adult OPCs must first activate, exit quiescence, and then begin the molecular programmes that underlie differentiation; *in vitro* neonatal/embryonic OPCs already are actively progressing through the cell cycle. As such, developmental OPCs require only a differentiation, not an activation signal.

We report that OPCs reside on the CNS vasculature, as they do in development (Tsai et al., 2016). Our study, however, does not identify the signal that causes OPCs to remain on the vasculature. In development, the chemokine ligand Sdf1 attracts OPCs to the endothelial cells of the brain vasculature. It remains unknown whether this mechanism for OPC homing to the vasculature remains relevant in adult OPCs. Follow up work must identify how the OPC remains on its vascular niche.

Previous work in other tissues has revealed the role of the niche for maintaining cell ‘stemness’ and stem-cell identity (Cheung and Rando, 2013; Quarta et al., 2016). Without a proper niche, stem cells undergo cell cycle and spontaneously differentiate, thereby depleting the pool of resident stem cells. With ageing, the maintenance of the niche architecture is impaired thereby leading to the depletion of the stem cell itself (Lukjanenko et al., 2016). In previous studies, preventing OPC affiliation with the vasculature in neonatal development causes an accumulation of OPCs in the CNS parenchyma (Tsai et al., 2016). Whether or not the vascular niche maintains OPC identity throughout adulthood is an

area that must be actively pursued. Moreover, whether this vasculature niche changes with ageing may explain why OPC plasticity is lost with ageing in the context of remyelination.

Here we also show that the main cell bodies of oligodendrocytes themselves are not on the blood vessel. These results suggests a oligodendrocyte lineage hierarchy wherein OPCs are on the blood vessel while oligodendrocytes themselves are in the parenchyma. However, it remains unknown how/whether the OPC delaminates from the vessel to form a myelinating oligodendrocyte. It is possible that OPCs enter into the cell cycle on the blood vessel and that the daughter cell is then positioned distal to the blood vessel. Alternatively, the OPC itself may delaminate from the vasculature, activate, and then differentiate into an oligodendrocyte.

A major limitation of our study is that we do not provide direct evidence that oligodendrocytes themselves are in the CNS parenchyma—not on the vasculature. Rather, we used a Sox10 transgenic mouse that labels all oligodendrocyte lineage cells to show that some oligodendrocyte-lineage cells are not associated with the vasculature. We then conclude, based on the evidence from the transgenic Pdgfra OPC-labelling mouse, that while OPCs are largely on the niche, many cells in the oligodendrocyte lineage are not. However, additional evidence is required to bolster the claim that oligodendrocytes themselves are not on the vasculature. Future work must use a transgenic oligodendrocyte-specific labelled mouse to that oligodendrocytes reside in the CNS parenchyma. Combined with our Pdgfra results, such a finding would confirm that these two cell types in the oligodendrocyte-lineage have spatially distinct niches.

Previous work has shown that OPCs undergo both symmetric and asymmetric division (Zhu et al., 2011). This would suggest that OPCs can either delaminate and subsequently activate or undergo mitosis, producing differentiating daughter cells that are distal to the blood vessel. The only available studies, however, examine OPCs in postnatal development and not in the homeostatic or lesioned adult brain. Moreover, these previous studies assume that all Ng2, Pdgfra expressing OPCs across the CNS, are the bona fide stem cell population. In the intestinal crypt and the hair follicle, the long-term stem cell can both symmetrically and asymmetrically divide (Hsu et al., 2011; Snippert et al., 2010). As such, OPCs likely also both symmetrically and asymmetrically divide. Current work in our group is looking at the clonal dynamics of Pdgfra expressing OPCs in the homeostatic CNS. Using Pdgfra-CreER animals crossed with animals with the Confetti 2.0 construct, we are using light sheet microscopy and laminin immunostaining to better understand the clonal dynamics of OPCs in relation

to the vascular niche.

Wnt signalling from the niche

Here we have shown that Lgr5 mediated Wnt signalling underlies the activation of OPCs in the context of the lesion, that activated OPCs express *in vivo* express Lgr5, and that certain R-Spondins and Wnt proteins drive adult OPC activation *in vitro*. Using previously published single cell sequencing databases of adult cortex, we found that Rbfox3 expressing neurons express the agonists for Lgr5 and Wnt signalling pathways. The gene expression data suggests a previously undescribed relationship between neurons and OPCs. Previous reports have documented that OPCs themselves form synapses with neurons and that glutamate at least *in vitro* can stimulate neonatal OPC activity (Bergles et al., 2000; Lin and Bergles, 2004). This work, however, does not explore any other signalling pathways that may facilitate a neuron-OPC relationship. Moreover, this work does not look at the interaction between these cell types in the adult.

It remains unclear whether Lgr5 itself is important for the functioning of OPCs or whether it is simply a marker for OPC activation. In the intestine, conditional adult knockout of Lgr5 in the crypt stem cell niche revealed no obvious phenotype (de Lau et al., 2011). This is likely due to the fact that Lgr homologues Lgr4/6 compensate for the loss of Lgr5 expression. Deletion of both Lgr4/5 in the crypt cell, however, leads to a loss of cell proliferation. In the CNS, Lgr5 has been found as a marker for gliobastoma (Nakata et al., 2013). The higher expression of Lgr5 correlates with a more adverse patient outcome. In keeping with this, we find that Lgr5 upregulated in activated OPCs; in both cases the expression of Lgr5 is correlated with proliferating glial cells. Future work will seek to determine the precise role Lgr5 plays in Wnt signal modulation and in the activation of OPCs.

A major limitation of this study is that our in vivo Lgr5 lineage tracing is short-term, based on one age-group, and largely correlative. Indeed, we show that OPCs in the CNS are the dominant cell type labelled by Lgr5, but additional lineage tracing experiments are required to bolster our claim that Lgr5 is an activation marker specifically for adult OPCs. A major question is whether Lgr5 is an important marker for activating OPCs in post-natal development. To test this, we have recently begun an experiment in which neonatal transgenic mice have been given tamoxifen for 30 days. If Lgr5 is a marker for active OPCs in development, then we would expect all oligodendrocytes to stem from Lgr5 expressing OPCs. If we do not observe widespread oligodendrocyte labelling with RFP, then we

would have found a novel marker distinguishing active adult OPCs from active neonatal developmental myelination.

In this chapter, I claim that OPCs but not differentiated oligodendrocytes express Lgr5 in the adult CNS. To show this, I co-stained sections from the Lgr5-Cre transgenic animal Olig2 and CC1. I found that the dominant cell type labelled with RFP are Olig2+ but CC1- OPCs. With lineage tracing, I found a small subset of differentiated oligodendrocytes labelled with RFP. I claim that these differentiated oligodendrocytes must stem from a Lgr5 expressing OPC. However, I provide no evidence that these differentiated oligodendrocytes no longer express Lgr5. A necessary future experiment will be to use the Lgr5-eGFP-Cre mouse in which all Lgr5 expressing cells express GFP and RFP while the progeny of Lgr5 expressing cells only express RFP. With our working hypothesis, this mouse model would show that active OPCs themselves are both GFP and RFP, meaning that they are at the moment expressing Lgr5, while oligodendrocytes themselves are only RFP expressing, meaning that oligodendrocytes stem from an Lgr5 expressing OPC, but themselves no longer express Lgr5. Such experiments are required to confirm the claim that Lgr5 specifically label active OPCs, not oligodendrocytes, in the adult CNS.

Throughout the chapter, I claim that Lgr5 labels active OPCs. However, I do not provide evidence showing that all active OPCs, rather than a subset, express Lgr5. To show that active adult OPCs express Lgr5 in the adult, experiments are currently ongoing in which we crossed Lgr5-Cre-ER mice with Sox10-flox-DTA animals. This way, all cells that are Lgr5, Sox10 co-expressing will be ablated with the diphtheria toxin (DTA) when the animal is fed tamoxifen. In these adult transgenic mice, we created an area of focal demyelination in adult mice and fed the mice tamoxifen. If our hypothesis is correct, then active Lgr5/Sox10 expressing OPCs in the lesion area will be ablated and remyelination will fail to occur. If this is the case, then we can confirm that all active OPCs express Lgr5 and that without this population of cells, adult myelination/remyelination cannot occur.

In the intestine, the Paneth cells are one of the major cell types of the epithelium. Paneth cells secrete Wnt and R-spondin and thereby signal to the intestinal Lgr5-expressing crypt stem cell to self-renew and differentiate into new intestinal epithelium (Sato et al., 2011). By secreting Wnt agonising proteins, the Paneth cell regulates the numbers and activation state of the resident stem cell population. It is therefore conceivable that the neuron in the CNS plays a similar role to the Paneth cell in the

intestine. As neurons require myelination for efficient signal transduction and for trophic support, it follows that the neuron itself contains the secretory proteins that signal for additional myelination. As such, the neuron secrete these Wnt agonising proteins, stimulating local vasculature associated OPCs to activate and differentiate into novel myelinating oligodendrocytes. Future work must determine the distribution of the various cells within the CNS; only by fully understanding the spatial distribution of adult CNS cells can we fully define the niche of the OPC and thereby understand the inter-cellular milieu of signals that may underlie the activation of adult OPCs.

With the growing belief that adaptive myelination is a mode by which learning and memory occur in the adult CNS, it is now important to understand the exact signals by which this process takes place. Following on from this work, we hope to inhibit the secretion of Wnt agonists by the neuron in the adult. Doing so, we will be able to determine whether adult de novo myelination will be able to occur even in the absence of neuron-derived Wnt signalling. Conversely, we would hyper-activate neuron-driven Wnt signalling by knocking down Wnt signalling antagonist Gsk3ß and determine whether adult OPCs hyper-activate, proliferating at higher numbers and hyper-myelinating the CNS.

With this work, we have begun to elucidate the stem cell niche and activating factors that cause OPC activation in tissue homeostasis and in injury. We position the OPC as a bona fide stem cell population in its niche. Looking forward, we hope to investigate the mechanisms of other, better-characterised stem cell niches and apply them to the oligodendrocyte lineage. Doing so, we hope to better understand the adult OPC in its niche with the goal of developing new therapies to promote myelination/re-myelination in the adult CNS.

Chapter 4

Tissue stiffness contributes to the ageing of central nervous system progenitor cells

Ageing causes a decline in tissue regeneration due to a loss of function in adult stem and progenitor cell populations (Goodell and Rando, 2015). An important example is the deterioration of the regenerative capacity of the widespread and abundant population of central nervous system (CNS) multipotent stem cells known as oligodendrocyte progenitor cells (OPCs) (Sim et al., 2002). A relatively overlooked potential source for this loss of function is the stem cell niche, a source of cell-extrinsic cues including chemical and mechanical signalling (Gopinath and Rando, 2008; Swift et al., 2013). In this study, we show that the progenitor microenvironment stiffens with age, and that its stiffening is sufficient to cause the age-related loss of OPC function. We use biological and novel synthetic scaffolds to mimic the stiffness of young brain and find that isolated aged OPCs cultured on these scaffolds are functionally and molecularly rejuvenated. When we disrupt mechanotransduction, OPC proliferation and differentiation rates were increased *in vitro* and remyelination accelerated *in vivo*. We identify the mechanoresponsive ion channel Piezo1 as a primary mediator of OPC mechanical signalling. Inhibition of Piezo1 overrides environmental mechanical signals *in vivo* and allows OPCs to maintain activity in an aged CNS. We demonstrate that tissue stiffness is a primary regulator of aging in OPCs, and provide new insights into how adult stem and progenitor cell function changes with age.

The ageing of adult stem and progenitor cells lies at the heart of the ageing process. In the aged CNS, efforts to reverse progenitor cell ageing have involved restoring genomic stability by overexpressing telomerase or promoting histone deacetylation to increase neuro- and glio-genesis (Jaskelioff et al., 2011; Shen et al., 2008). Cell-extrinsic factors such as exercise can stimulate aged CNS progenitor cell proliferation and differentiation *in vivo* (Yau et al., 2012), while exposure to blood borne factors and cells from young adult circulation can enhance progenitor

differentiation and CNS remyelination *in vivo* (Ruckh et al., 2012). Despite these advances, the mechanisms of OPC ageing, including the bridge between cell extrinsic and cell intrinsic factors, remain elusive.

A prevailing theory is that a loss of growth factor exposure underlies progenitor cell quiescence in ageing (Hinks and Franklin, 2000). To test this theory, we magnetic bead-purified neonatal (≤P7) and aged (≥20 months) primary rat OPCs of over 88% purity using the OPC specific marker A2B5 (Fig. 1a) and cultured them in conditions known to enable self-renewal of isolated neonatal progenitor cells on poly d-lysine (PDL) coated tissue culture plastic (Tang et al., 2001). Only 5% of aged OPCs proliferated even after 5 and 14 days of *in vitro* culture, as labeled by EdU incorporation (Fig. 1b). In the same conditions after 5 days *in vitro*, over 35% of neonatal OPCs proliferated under the same conditions (Fig. 1c).

In order to first determine whether this apparent loss of proliferation in aged OPCs is reversible, we labelled aged OPCs (≥20 months) with GFP using a baculovirus, a virus which can infect cells in a matter of hours. This property of the virus allowed for cells to be isolated, infected, and re-transplanted in the same day. The cells were then transplanted into the prefrontal cortex of postnatal day 1 neonatal rats and 9 days later identified proliferating cells by EdU injection (Fig. 1d). After 10 days *in vivo*, transplanted aged OPCs regained their capacity to both proliferate, as labelled by EdU incorporation, and differentiate, as labelled by coexpression with the oligodendrocyte differentiation marker CC1 (Fig. 1e-h). Transplanted aged OPCs proliferated and differentiated at rates comparable to transplanted age-matched neonate controls. Both aged and neonatal OPCs remained of the oligodendrocyte lineage as determined by lineage marker Olig2. By comparison, there were no proliferating progenitors in the CNS of the aged animal litter-mates (Fig. 1i), and as shown later in the chapter, neonatal OPCs transplanted into aged brains lose their self-renewal capacity. Therefore, aged OPCs can become activated in the neonatal niche but not in their native niche or *in vitro* even with high concentrations of FGF and PDGF, the growth factors sufficient for young adult OPC proliferation.

The cell niche, the microenvironment in which OPCs reside, is a key factor in the regulation of OPC ageing (Gopinath and Rando, 2008; Keough et al., 2016). Given that aged OPCs regain

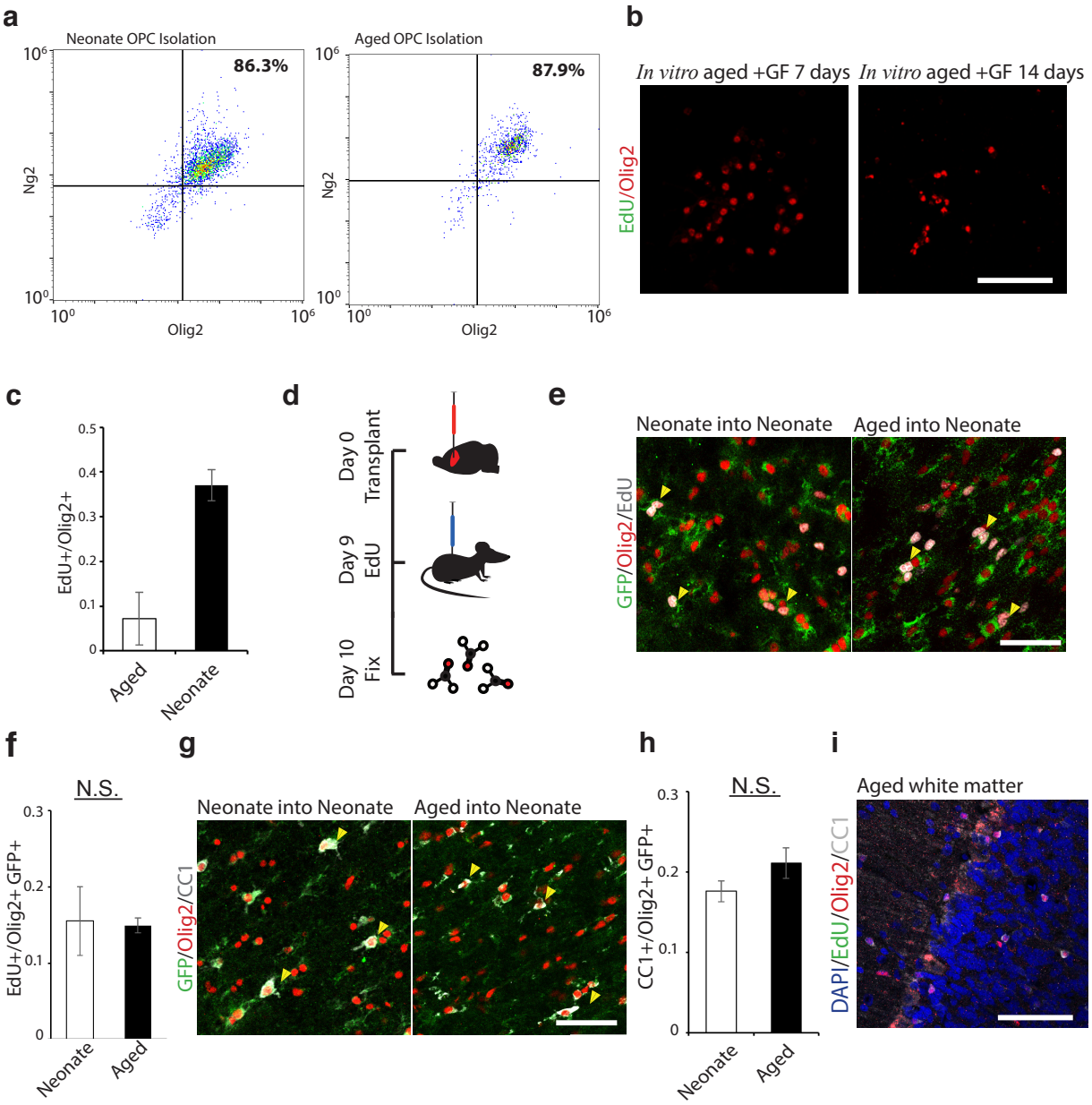
a
Neonate OPC Isolation
86.3%
Ng2
Olig2
Aged OPC Isolation
87.9%
b
In vitro aged +GF 7 days
In vitro aged +GF 14 days
EdU/Olig2
c
EdU+/Olig2+
Aged
Neonate
d
Day 0 Transplant
Day 9 EdU
Day 10 Fix
e
Neonate into Neonate
Aged into Neonate
GFP/Olig2/EdU
f
N.S.
EdU+/Olig2+ GFP+
Neonate
Aged
g
Neonate into Neonate
Aged into Neonate
GFP/Olig2/CC1
h
N.S.
CC1+/Olig2+ GFP+
Neonate
Aged
i
Aged white matter
DAPI/EdU/Olig2/CC1

Figure 1

Figure 1. Dynamics of OPC activation, *in vitro* and *in vivo*. a, Flow cytometry analysis on MACs purified OPCs confirm that we are able to isolate a pure population of Olig2+/Ng2+ OPCs from both neonate and aged brains. b, EdU labelling of OPCs after 1 and 2 weeks *in vitro*. c, Quantifications of N=3 replicates of neonatal and aged OPCs in proliferation conditions on PDL coated tissue culture plastic after 5 days. d, Schematic of transplantation. e-h, Representative images and quantifications of the proliferation and differentiation rates of transplanted neonatal and aged OPCs in the prefrontal cortex 14 days following transplantation. Unless otherwise indicated, throughout the text proliferating cells are quantified as the proportion of EdU+ out of total Olig2+/GFP+ transplanted OPCs, and differentiated cells are quantified as a proportion given in the figure, in this case the proportion of CC1+ out of total GFP+/Olig2+ cells. Arrows highlight example positive cells. Averages represent N = 4 biological replicates, error bars represent standard deviation throughout the text. i, Representative image of 16 month old female white matter and grey matter with triple labelling of Olig2, EdU, and CC1. Throughout figure, scale bars represents 50μM. Here and in all points in the text and figures, P-value significance is calculated by one-way ANOVA and indicated by ***, **, and * representing < 0.001, < 0.01, and < 0.05, respectively. Here and throughout chapter, ≥200 cells were counted per biological replicate.

their proliferation and differentiation capacity in the neonatal niche, we next asked if changes in the tissue microenvironment underlie the observed differences in OPC activation state. To address this question, we generated decellularized brain scaffolds of neonatal and aged rat brains with a protocol using freshly vibratomed brain slices (Fig. 2a-b)(De Waele et al., 2015). Immunostaining of this decellularized brain ECM confirmed significant changes in chondroitin sulfate proteoglycan (CSPG) with age (Végh et al., 2014) (Fig. 2c). We then seeded aged OPCs on both neonatal and aged decellularized brain ECM (Fig. 2d). Aged OPCs seeded on neonate decellularized brain ECM showed a more than 10-fold increase in their proliferation rate compared to aged OPCs seeded on aged ECM (Fig. 2e-f). When placed in differentiation conditions with T3, aged OPCs seeded on neonate decellularized brain ECM also had a greater than 10-fold increase in their differentiation rate compared to that of aged OPCs seeded on aged decellularized brain ECM (Fig. 2g-h). Neonatal OPCs lost their proliferative capacity when seeded on aged ECM but not on neonate ECM (Fig. 2i-j).

As the ageing ECM negatively effects the activity-state of OPCs, even in the presence of growth factors, we hypothesized that digesting the ECM of the aged CNS would activate aged OPCs. Previous work has shown that the glycosaminoglycan degrading enzyme chondroitinase ABC (chABC) efficiently digests this dominant CNS ECM molecule (Keough et al., 2016). To assess whether disrupting ECM mechanics with chABC in the aged CNS enhances OPC regeneration, we generated focal areas of demyelination in aged (≥18 months) rats using a well-established lesion model (Fig. 3a-b). Following injection of chABC directly into the area of demyelination at day 7 there was a ~3 fold increase in both EdU+ OPCs and in Olig2+/CC1+ differentiated oligodendrocytes at 14 days post lesion (Fig. 3c-f). These results showed that the ECM itself has an inhibitory role in the function of ageing OPCs.

Alterations in chondroitin sulfate levels in frog brain tissue cause changes in its mechanical properties *in vivo* (Koser et al., 2016), suggesting that brain mechanics may change during ageing. In agreement with this hypothesis, brain tissue stiffens progressively as rats develop from neonates into adults (Elkin et al., 2010). We therefore asked if the CNS continues to stiffen with ageing. To address this, we determined the apparent elastic moduli of fresh brain sections of rats of different ages using atomic force microscopy (AFM) (Fig. 4a) and found that, in the prefrontal cortex, both white and grey matter progressively and significantly stiffened by a factor of ~2.5 with ageing (Fig. 4b-f, decellularized ECM in Fig. 4g). This increase in ECM stiffness

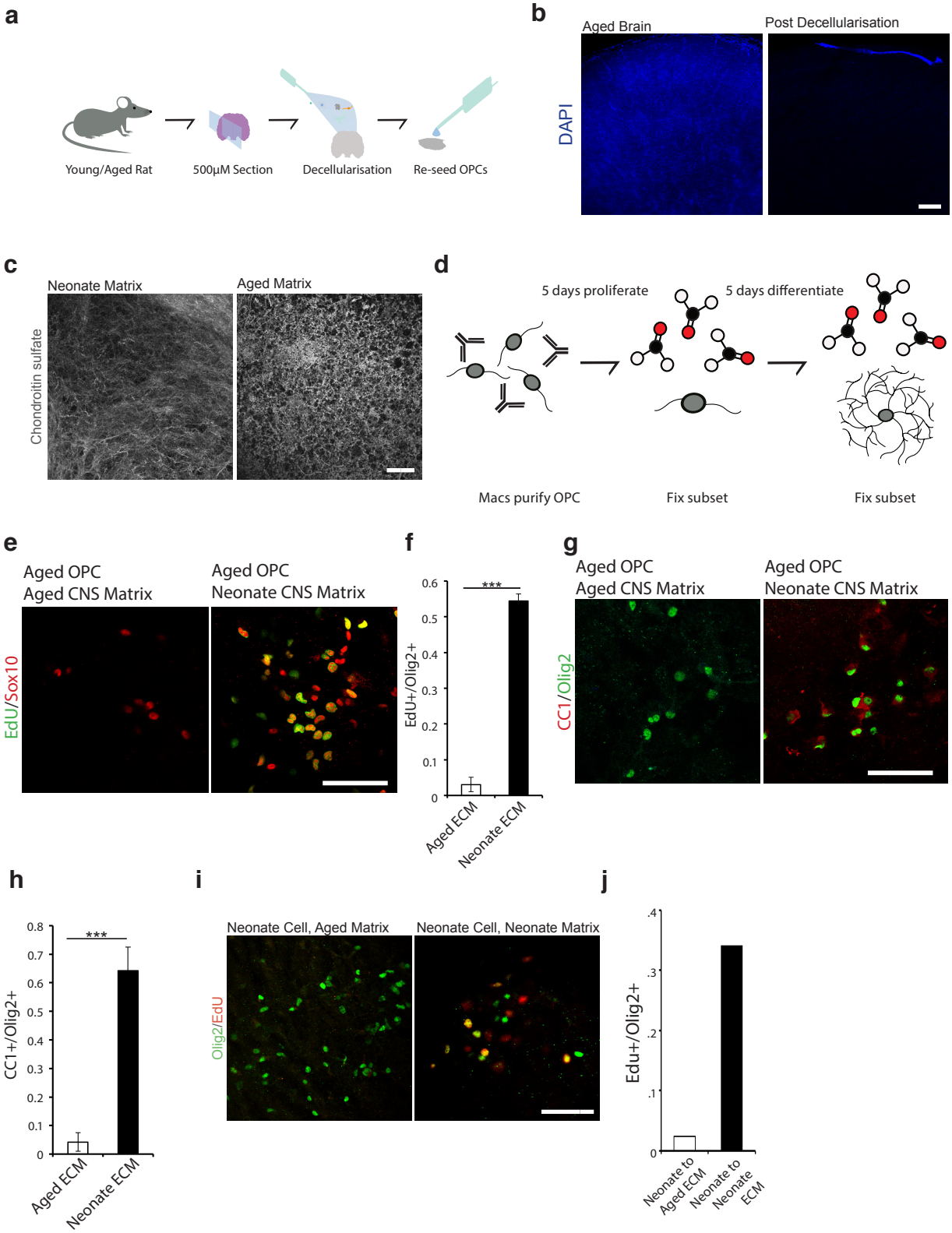
a
Young/Aged Rat
500µM Section
Decellularisation
Re-seed OPCs
b
Aged Brain
Post Decellularisation
DAPI
c
Neonate Matrix
Aged Matrix
Chondroitin sulfate
d
5 days proliferate
5 days differentiate
Macs purify OPC
Fix subset
Fix subset
e
Aged OPC
Aged CNS Matrix
Aged OPC
Neonate CNS Matrix
EdU/Sox10
f
EdU+/Olig2+
***
Aged ECM
Neonate ECM
g
Aged OPC
Aged CNS Matrix
Aged OPC
Neonate CNS Matrix
CC1/Olig2
h
CC1+/Olig2+
***
Aged ECM
Neonate ECM
i
Neonate Cell, Aged Matrix
Neonate Cell, Neonate Matrix
Olig2/EdU
j
Edu+/Olig2+
Neonate to Aged ECM
Neonate to Neonate ECM

Figure 2

Figure 2. The neonatal CNS matrix restores the function of aged OPC. a, A schematic overview of the decellularization protocol. b, A DAPI staining following the decellularization protocol shows no remaining nuclear DNA, indicating complete cell removal. Scale bar represents 200μM. c, Rat brains of different ages were decellularized, fixed, and stained for chondroitin sulfate proteoglycans (CSPGs) show that extracellular matrix remains intact following the decellularization protocol. Scale bar represents 20μM. d, A schematic of the re-cellularization protocol. OPCs are MACs purified using the OPC surface marker A2B5, cultured for 5 days in proliferation conditions. A subset of these brain ECM are fixed with PFA and the remaining brain ECM are placed into differentiation conditions for 5 days. e-j, Representative images and quantifications of the proliferation and differentiation rates of aged and neonatal OPCs seeded onto both neonate and aged (≥18 months) decellularized ECM. Scale bars represent 50μm. Averages represent means from N=3 biological replicates.

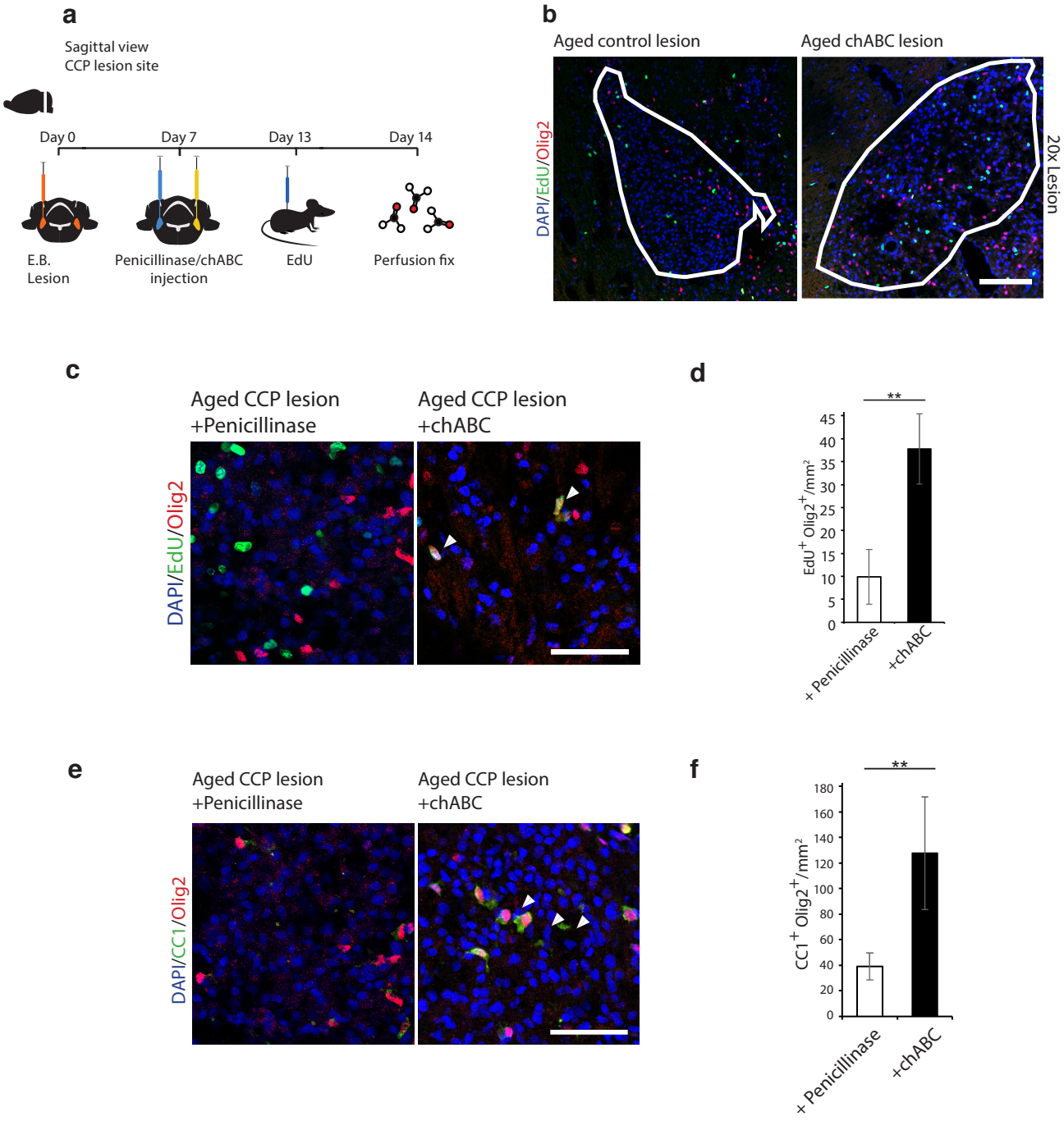

Figure. 3. Chondroitinase chABC enhances activation of OPCs in aged lesions. a, A schematic overview of the lesioning and subsequent injection of small molecules into the lesion site. b, Representative traces of CCP lesions. Scale bar represents 100µM. c-f, Representative images of proliferating and differentiating cells per mm2 of CCP lesion cores 14 days post lesion and 7 days post direct injection of penicillinase/chABC into N=4 aged females (≥ 18 months). Scale bar represents 100µM. Here and through chapter, lesion experiments were performed by Dr. Myfanwy Hill of Robin Franklin's group.

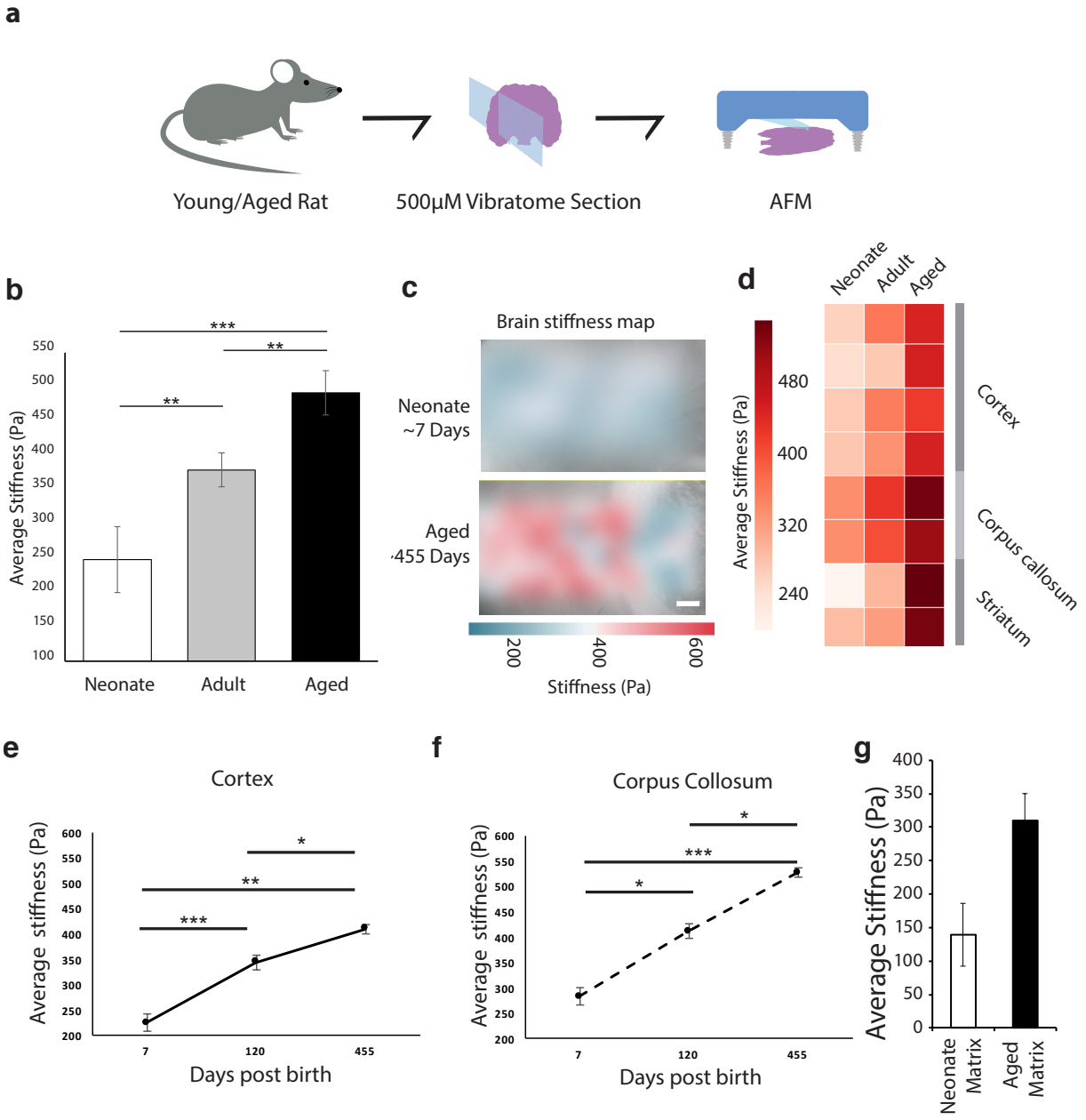

Figure 4. Rat brain tissue stiffens with ageing. a, A schematic of the preparation of brains for AFM. b, Global apparent elastic moduli K (Pa) of brains at different ages determined by AFM indentation measurements. Shown are means of 3 sections from 3 animals each. c, Representative stiffness maps of a neonate (~7 days post natum) and an aged brain (~455 days post natum). Scale bar represents 50µm. d, Regional mean stiffness values calculated by mapping AFM measurements to brain slice. e-f, Both grey and white matter stiffen progressively with ageing. Mean apparent elastic modului K are reported across N=3 brain slices across N=3 animals. g, Atomic force microscopy mean stiffness values of N=2 neonate and N=2 aged decellularized brain ECM confirm that decellularized brain ECM, too, stiffens with ageing.

with ageing mirrors the increase in genes associated with the cytoskeleton that occurs in adult OPCs compared to neonatal OPCs (Moyon et al., 2015).

Changing the stiffness of the cell niche is known to lead to alterations in the levels of pro-differentiation signals in some stem cell systems(Swift et al., 2013), and the mechanical properties of the environment are known to modulate neonatal OPC function *in vitro* (Jagielska et al., 2012). These results led us to hypothesize that the observed increase in brain stiffness alone might be sufficient to cause the reduced proliferation and differentiation rates of aged CNS progenitor cells.

To test our hypothesis, we developed synthetic polyacrylamide hydrogels to mimic the stiffening of the ECM with age. These hydrogels were specifically designed to present the same ECM composition and density to the cells independent of stiffness, enabling the investigation of cellular changes due to mechanical signals alone. Only ~5% of aged OPCs plated on stiff hydrogels proliferated (Fig. 5a-c); however, ~55% of aged OPCs plated on soft hydrogels underwent proliferation. Moreover, under differentiation conditions, only ~5% of aged OPCs differentiated into myelin basic protein (MBP) expressing cells on stiff gels, while more than 50% of aged OPCs on soft hydrogels differentiated into MBP expressing oligodendrocytes (Fig. 5c-e). In contrast, neonatal OPCs, similar to aged OPCs, lost their capacity to proliferate and differentiate on stiff substrates (Fig. 5f-i).

The loss of proliferation was surprising given that neonatal OPCs can proliferate on poly d-lysine (PDL)-coated tissue culture plastic. However, we observed that the long-term activity of neonatal OPCs on PDL-coated plastic was isolated to spheres that detached from the substrate, suggesting that PDL-coated plastic itself may not be sufficient for maintenance of OPC activity but relies on the instability of ECM attachment (Fig. 5j). The hydrogels, on the other hand, have covalently bound ECM and are therefore stable long-term, with no floating spheres observed.

The stiffness-mediated activation of aged progenitor cells was independent of seeding density, and the high levels of proliferation were lost with the progressive stiffening of the hydrogels (Fig. 6a-b). Moreover, no significant changes in cell survival were detected on the soft or stiff hydrogels (Fig. 6c-d). These results suggested that the ‘activation state’ of OPCs is predominantly regulated not by the age of the cell or ECM chemistry, but by ECM stiffness.

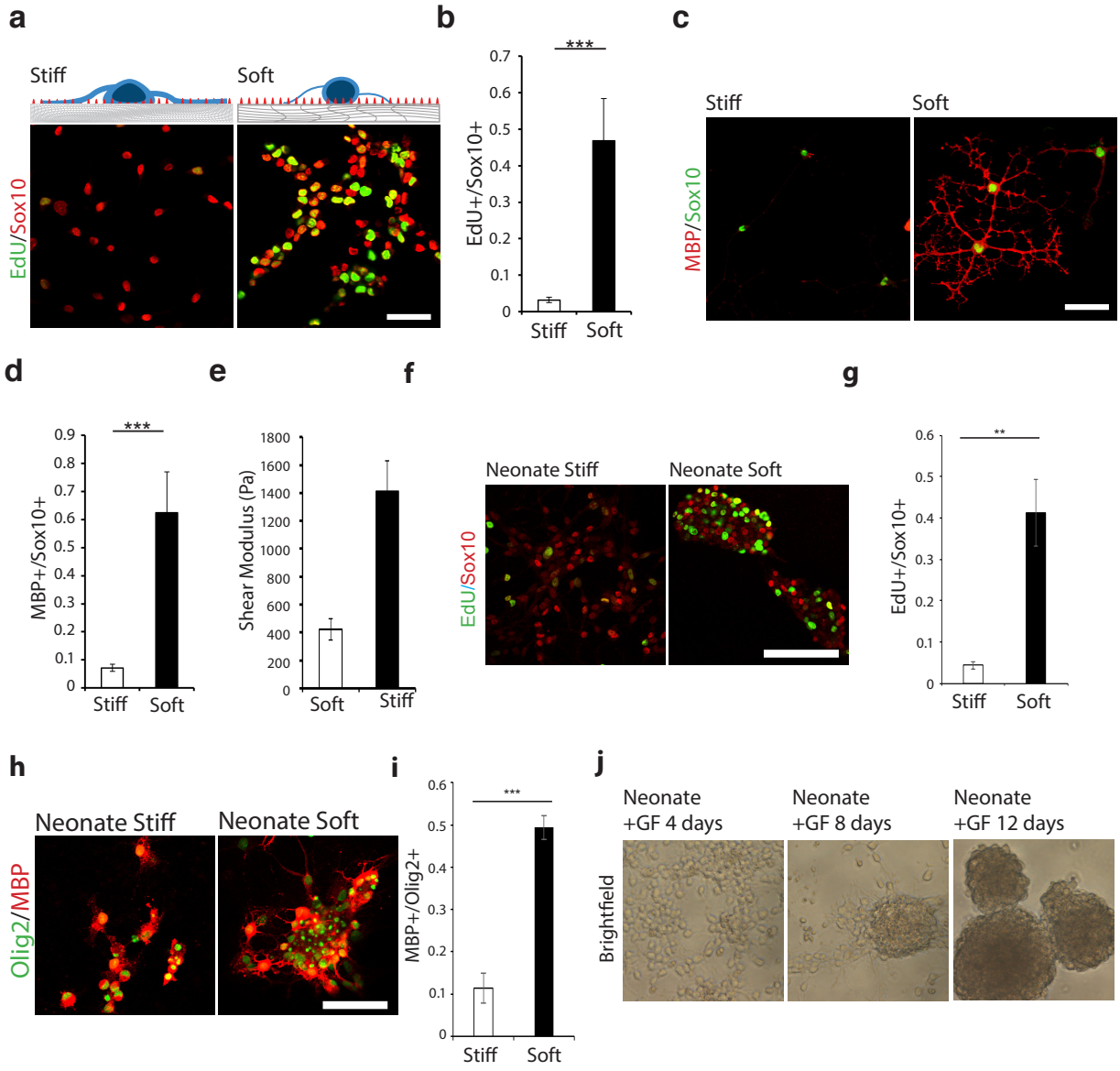

Figure 5. A soft environment mimicking the stiffness of neonatal CNS tissue alone can restore the function of aged OPCs. a, (Top) Schematic represents OPCs cultured on top of stiffness tuned hydrogels. (Bottom) Representative images of aged OPCs seeded on the substrates with b, quantification of proliferation rates. c,d, Representatative images and quantifications of differentiation rates of aged OPCs seeded on soft and stiff substrates. e, Mean shear moduli determined by AFM of our fabricated 'soft' and 'stiff' hydrogels. a-d, Scale bars represent 40µm. f-g, MACs purified neonatal OPCs cultured on stiff hydrogels lose their ability to proliferate following 5 days in proliferation conditions. Neonatal OPCs cultured on soft hydrogels, however, continue to proliferate. h-i, Similarly, neonatal OPCs cultured on stiff hydrogels inefficiently differentiate into oligodendrocytes following 5 days in differentiation conditions. Conversely, neonatal OPCs differentiated on soft hydrogels efficiently differentiate into oligodendrocytes. f-i, Scale bars represent 100µm. j, Representative brightfield images of neonatal OPCs over-time *in vitro* on PDL tissue culture plastic cultured with growth factors. Throughout figure, means represent quantifications from N=3 biological replicates or in the case of the AFM, from N=3 independent hydrogel fabrications.

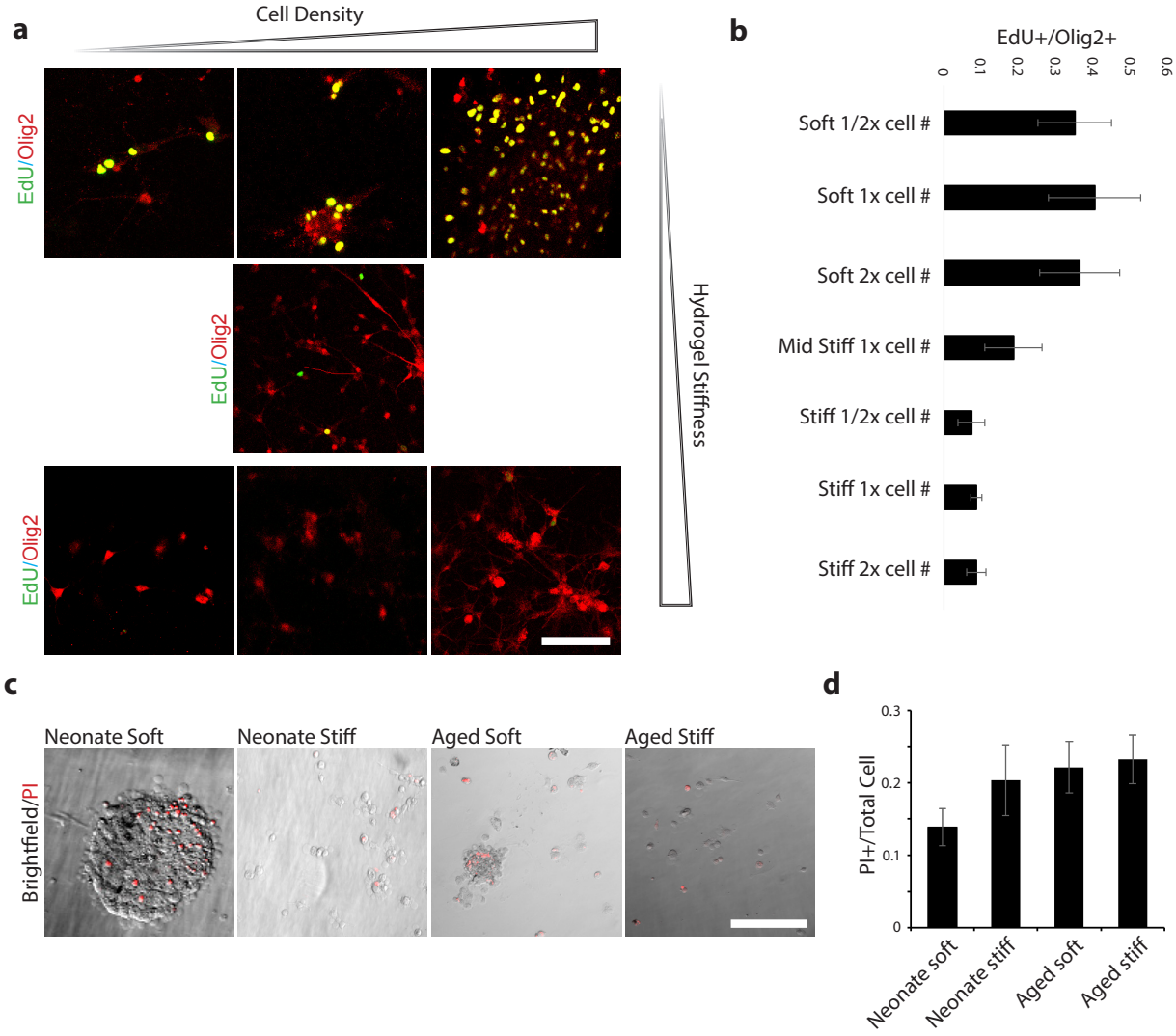

Figure 6. Cell density and cell death do not significantly confound observed effects of mechanical environment. a-b, Representative images and quantifications of N=3 replicates of EdU labelled OPCs seeded at .5x, 1x, and 2x cell seeding densities on increasingly stiff hydrogels after 120 hours in culture show cell-density independent, stiffness-dependent OPC activation. c-d, Labelling and quantifications of N=3 assays of OPC viability of both neonatal and aged progenitor cells on soft and stiff hydrogels after 48 hours in culture with propidium iodide (PI). Throughout figure, scale bas represent 100μM

To further investigate if the soft environment pushes the identity of aged OPCs closer to that of neonatal OPCs, we performed RNA sequencing on acutely isolated aged and neonatal OPCs and compared them to both cell types seeded on stiff and soft hydrogels *in vitro*. We found using principal component analysis and hierarchical clustering that OPCs isolated from both neonatal and aged rats and cultured on soft hydrogels transcriptomically resembled freshly isolated neonatal OPCs more closely than aged and neonatal OPCs cultured on stiff hydrogels (Fig. 7a-b). However, OPCs cultured on stiff hydrogels did not cluster closely with acutely isolated aged OPCs, revealing both the effect of growth factors and *in vitro* conditions on OPC gene expression profile and the inability of the stiff niche environment to fully recapitulate the ageing process. From the transcriptomics analysis, softness is *the* variable that allows aged OPCs to more closely resemble neonatal OPCs; to understand the reasons for this, we next looked at the differential gene expression data between aged OPCs cultured on stiff and on soft hydrogels. Over 1300 genes were significantly (p-value $\leq$.05) differentially expressed between OPCs cultured on soft and cultured on stiff hydrogels and 21% of these upregulated genes were similarly upregulated in neonatal OPCs compared to aged OPCs (Fig. 7c-d). Matrix related genes such as Dab1, Acan, and Plxnd1 were upregulated in aged OPCs cultured on stiff hydrogels while cell-cycle and DNA repair genes such as Cdk1na and Sirt7, OPC activation genes such as Etv1, and hippo pathway genes such as Rassf2 were amongst the most upregulated genes in aged OPCs cultured on soft hydrogels.

Next we asked if enriched pathways overlap with pathways known to be involved in ageing such as metabolism, cell cycle, inflammation, and DNA stability (Goodell and Rando, 2015). Using gene set enrichment analysis, we found that the gene sets most significantly increased in expression in OPCs seeded on soft over stiff hydrogels were involved in the same age-related pathways such as proteostasis, metabolism, DNA replication, and DNA repair (Fig. 7e). Finally, expression of genes associated with many of these enriched gene sets such as Pdgfra, Ascl1, and Lmnb1 were also increased in expression in both neonatal OPCs and in OPCs grown on soft hydrogels (Fig. 7f). These results indicate that a soft environment holistically reinstates transcriptional programs associated with the reversal of the ageing process. Together with the increase in proliferation and differentiation on soft hydrogels, our results suggested that a soft environment rejuvenates aged OPCs.

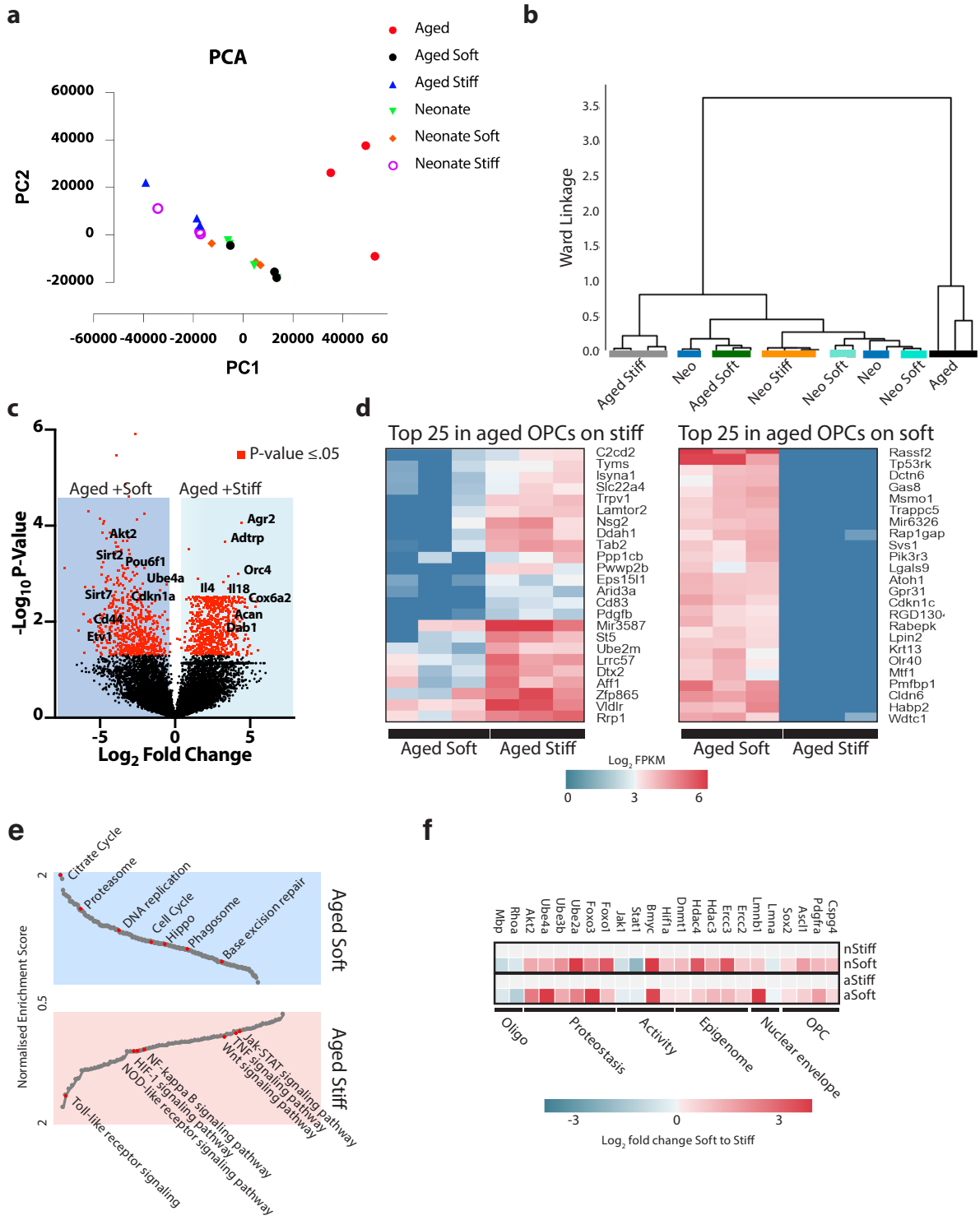
a
PCA
Aged
Aged Soft
Aged Stiff
Neonate
Neonate Soft
Neonate Stiff
PC2
PC1
b
Ward Linkage
Aged Stiff
Neo
Aged Soft
Neo Stiff
Neo Soft
Neo
Neo Soft
Aged
c
P-value ≤.05
Aged +Soft
Aged +Stiff
-Log10 P-Value
Log2 Fold Change
d
Top 25 in aged OPCs on stiff
Top 25 in aged OPCs on soft
Aged Soft
Aged Stiff
Log2 FPKM
e
Normalised Enrichment Score
Aged Soft
Aged Stiff
f
nStiff
nSoft
aStiff
aSoft
Oligo
Proteostasis
Activity
Epigenome
Nuclear envelope
OPC
Log2 fold change Soft to Stiff

Figure 7

Figure 7. A soft environment mimicking the stiffness of neonatal CNS tissue transcriptomically rejuvenates aged OPCs. a, Principal component analysis (PCA) and included legend on RNA sequencing differential gene expression analysis. The PCA was performed on the FPKM values for each of the six biological conditions. Legend is provided b, Hierarchical clustering with Pearson correlation and Ward's linkage shows that aged OPCs on soft hydrogels more closely resemble neonatal OPCs than do OPCs on stiff hydrogels. c, Volcano plot of differential expressed genes between aged OPCs cultured on soft versus stiff hydrogels. Red dots show significantly upregulated expressed genes ($p < .05$). d, Heatmap showing the log2 FPKM expression of the 25 genes with highest fold increase in expression between aged OPCs cultured on stiff versus soft hydrogels and the top 25 genes with the highest fold increase in expression between aged OPCs cultured on soft versus stiff hydrogels. All genes shown are significantly differentially expressed with a p-value of $\leq .05$. e, Gene set enrichment analysis reveals a number of pathways differentially expressed in aged OPCs grown on soft hydrogels versus aged OPCs grown on stiff hydrogels. f, Enrichment analysis for genes involved in OPC and stem cell activation, proteostasis, and genetic and epigenetic stability as shown by mean FKPM $\log_2$ fold change of individual genes.

In order to gain a better understanding of the mechanism by which a soft microenvironment rejuvenates aged OPCs, we probed specific potential factors known to be involved in the transduction of mechanical signals into an intracellular response. We first investigated mechanotransduction via actin contractility by asking if small molecule inhibitors of actin contractility could phenocopy the effects of a soft environment. To do this, we treated aged OPCs on stiff substrates with blebbistatin, a non-muscle myosin II inhibitor, which is known to affect neonatal OPC function (Baer et al., 2009; Wang et al., 2012). We found that the inhibitor increased the proliferation and differentiation rates by 5 fold when applied to aged OPCs on stiff substrates (Fig. 8a-d). There was no corresponding increase in proliferation of aged OPCs on soft substrates treated with blebbistatin, indicating that the increase in proliferation is specific to the inhibition of mechanotransduction upon actomyosin relaxation (Fig. 8e-f).

To determine the effect of actin contractility on the adult CNS *in vivo*, we first injected blebbistatin into un-lesioned grey matter of N=3 14 month old female rats. In the homeostatic aged CNS, there are almost no cells proliferating 10 days following a control delivery of DMSO, while in the blebbistatin injected brain, a small but significant proportion of cells were labelled with EdU (Fig. 8g-h). To determine the effect of blebbistatin in a lesion context, we injected 5µM blebbistatin into the lesion to perturb OPC contractility (Fig. 8i). At 14 days post-lesion, we observed more than 3 times the number of Olig2+, CC1+ differentiated oligodendrocytes in lesions treated with blebbistatin than in controls in each aged animal (n=4) (Fig. 8j-k). We confirmed these results by analysing the extent of remyelination detectable on sections of resin-embedded lesions counter stained with toluidine blue. By blind lesion-ranking analysis, we found significantly improved remyelination in blebbistatin-injected lesions compared to the DMSO controls (Fig. 8l-m). Taken together with the *in vitro* data of blebbistatin-treated OPCs, these data suggest that inhibiting actomyosin contractility-mediated mechanotransduction has a positive effect on the activation and subsequent differentiation of aged OPCs.

Having established actomyosin contractility as a major contributor to ageing in OPCs, we next sought more specific factors that may play a role in the mechanically-induced ageing response. First, we probed the mechanotransduction factor Lamin A/C, a ‘mechanostat’ that is known to mediate actin contractility (Swift et al., 2013). Our sequencing data showed an age-correlated increase in expression of the nuclear lamina component Lmna with ageing as well in OPCs cultured on stiff hydrogels. As such we confirmed the sequencing results with qPCR, Western

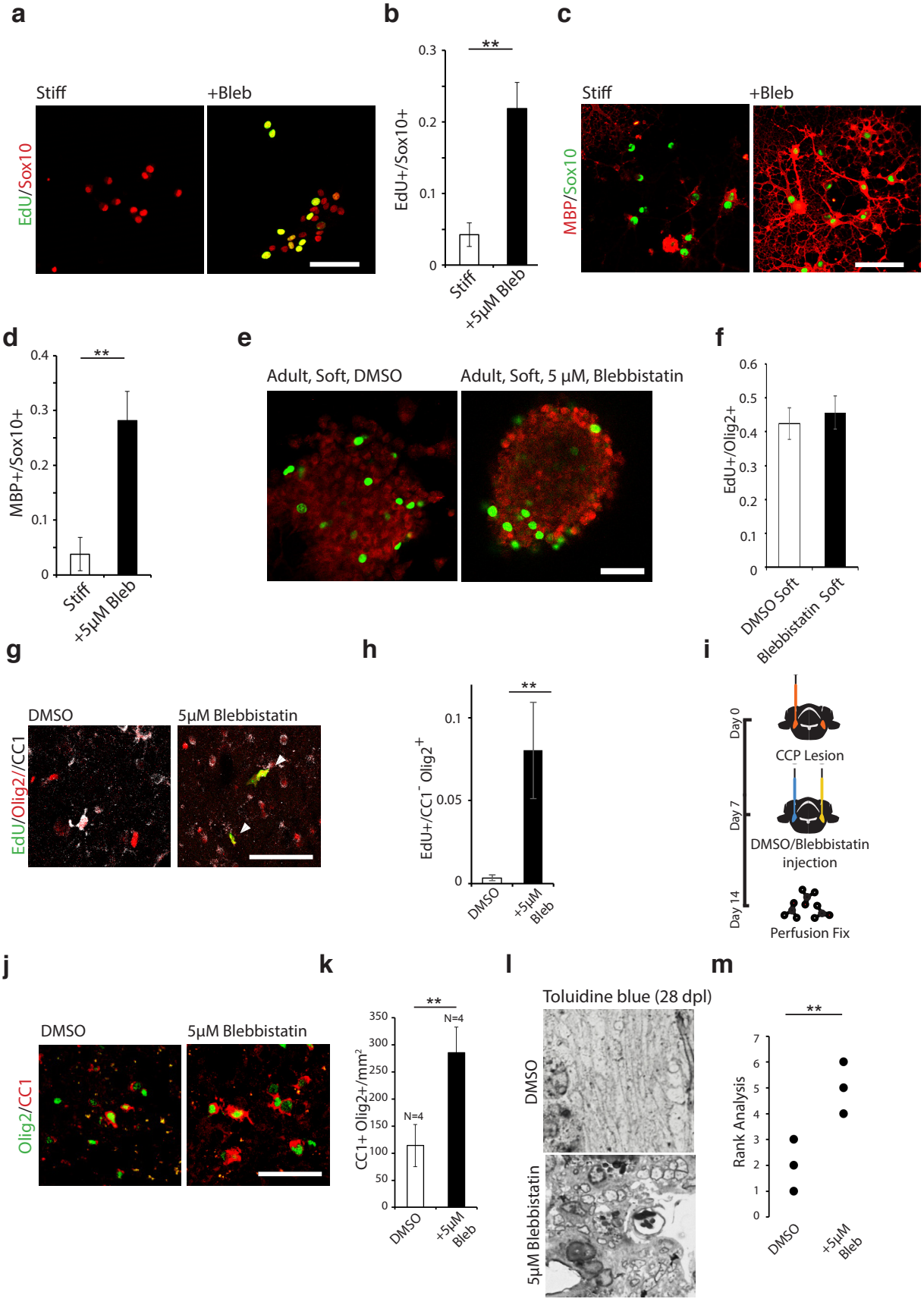
a
Stiff
+Bleb
EdU/Sox10
b
**
EdU+/Sox10+
0.3
0.2
0.1
0
Stiff
+5μM Bleb
c
Stiff
+Bleb
MBP/Sox10
d
**
MBP+/Sox10+
0.4
0.3
0.2
0.1
0
Stiff
+5μM Bleb
e
Adult, Soft, DMSO
Adult, Soft, 5 μM, Blebbistatin
f
EdU+/Olig2+
0.6
0.5
0.4
0.3
0.2
0.1
0
DMSO Soft
Blebbistatin Soft
g
DMSO
5μM Blebbistatin
EdU/Olig2//CC1
h
**
EdU+/CC1- Olig2+
0.1
0.05
0
DMSO
+5μM Bleb
i
Day 0
CCP Lesion
Day 7
DMSO/Blebbistatin injection
Day 14
Perfusion Fix
j
DMSO
5μM Blebbistatin
Olig2/CC1
k
**
N=4
N=4
CC1+ Olig2+/mm2
350
300
250
200
150
100
50
0
DMSO
+5μM Bleb
l
Toluidine blue (28 dpl)
DMSO
5μM Blebbistatin
m
**
Rank Analysis
7
6
5
4
3
2
1
0
DMSO
+5μM Bleb

Figure 8

Figure 8. Targeting mechanical signalling factors to overcome environmental stiffness. a-d, Representative images and quantifications of the effects of Blebbistatin targeting actomyosin activity on the proliferation and differentiation rates of aged OPCs *in vitro*. e-f, Representative images and quantifications of N=3 adult OPCs on soft hydrogels treated with Blebbistatin or DMSO show no change in rates of proliferation. Scale bar represents 50μM. g-h, Representative images and quantifications of EdU labelled Olig2+CC1- OPCs 7 days following the injection of 5μM blebbistatin into the grey matter of N=3 14 month-old females. i-k, Schematic, representative images, and quantifications of the differentiation rates of aged OPCs following the injection of 5μM of blebbistatin at 14 days post lesion in *in vivo*-toxin-induced lesions. The data represents N=4 15 month-old age male rats. Differentiated oligodendrocytes are quantified as the proportion of CC1+ Olig2+ co-positive cells per mm2 of lesioned area. Scale bars represent 50μM. l-m, Toluidine blue staining on transverse sections of lesions of N=3 16 month old female rats show that remyelination at 28 days post lesion is accelerated. Blind rank analysis is based on average ranking for N=3 images per lesion with a higher ranking indicating better remyelination. Dr. Myfanwy Hill performed the lesion experiments in this figure.

Blots, and immunohistochemistry (Fig. 9a-g).

As nuclear Lmna increases with ageing and with stiffness, we hypothesised that its increase underlies the *in vitro* ageing phenotype. We knocked down Lmna in aged OPCs on stiff hydrogels, which had no statistically significant effect on the activation state of aged progenitor cells (Fig. 10a-d). However, mRNA overexpression of Lamin C, the dominant Lmna splice variant in OPCs, in neonatal OPCs on soft hydrogels led to a significant loss of OPC activation (Fig. 10e-i), suggesting that Lamin A/C plays at least some role in mediating mechanically induced ageing in OPCs.

Other potential mechanotransducers include mechanosensitive ion channels such as Piezo1. Piezo1 regulates cell density and stem cell activation by responding directly to external mechanical signals such as substrate stiffness by tuning the influx of the second messenger calcium (Eisenhoffer et al., 2012; He et al., 2018; Li et al., 2014). Our sequencing data, verified by Western blot, showed that Piezo1 is one of the most highly expressed proteins potentially involved in mechanical signalling in OPCs (Fig 11a-d). Reanalysing previous single cell sequencing databases in both human and mouse, we identified Piezo1 to be uniquely specifically expressed in Sox10 positive, Cspg4 positive, but MBP negative cells (Fig. 11e-h) (Lake et al., 2018; Zeisel et al., 2015). Finally, using immunohistochemistry on rat brains of various ages, we found Piezo1 to be both peri-nuclear and in the processes of Olig2+, but CC1- labelled OPCs in the adult and aged rat grey matter (Fig. 11i-j).

To test the role of Piezo1, we transfected a Piezo1 siRNA into aged OPCs cultured on stiff hydrogels. Following knockdown, we observed that aged progenitor cells proliferated and differentiated 3 to 5 fold more than the non-targeting siRNA control on stiff hydrogels (Fig. 12a-d). Piezo1 knock-down on soft hydrogels showed no additive effect on proliferation (Fig. 12e-f). As Piezo1 is a non-selective cation channel that gives rise to calcium transients, we next used calcium imaging to investigate if substrate mechanics impacted intracellular calcium dynamics. Aged OPCs regularly demonstrated calcium transients on stiff hydrogels with ~20% of cells fluxing calcium over a 10 minute period of time. OPCs on soft hydrogels had virtually no calcium fluxes; moreover, transfection with Piezo1 siRNA abolished these calcium transients in aged OPCs on stiff hydrogels (Fig. 12g-i). Given the central role of calcium in controlling integrin signalling via Calpain 1 (McHugh et al., 2010), we hypothesised that stably knocking

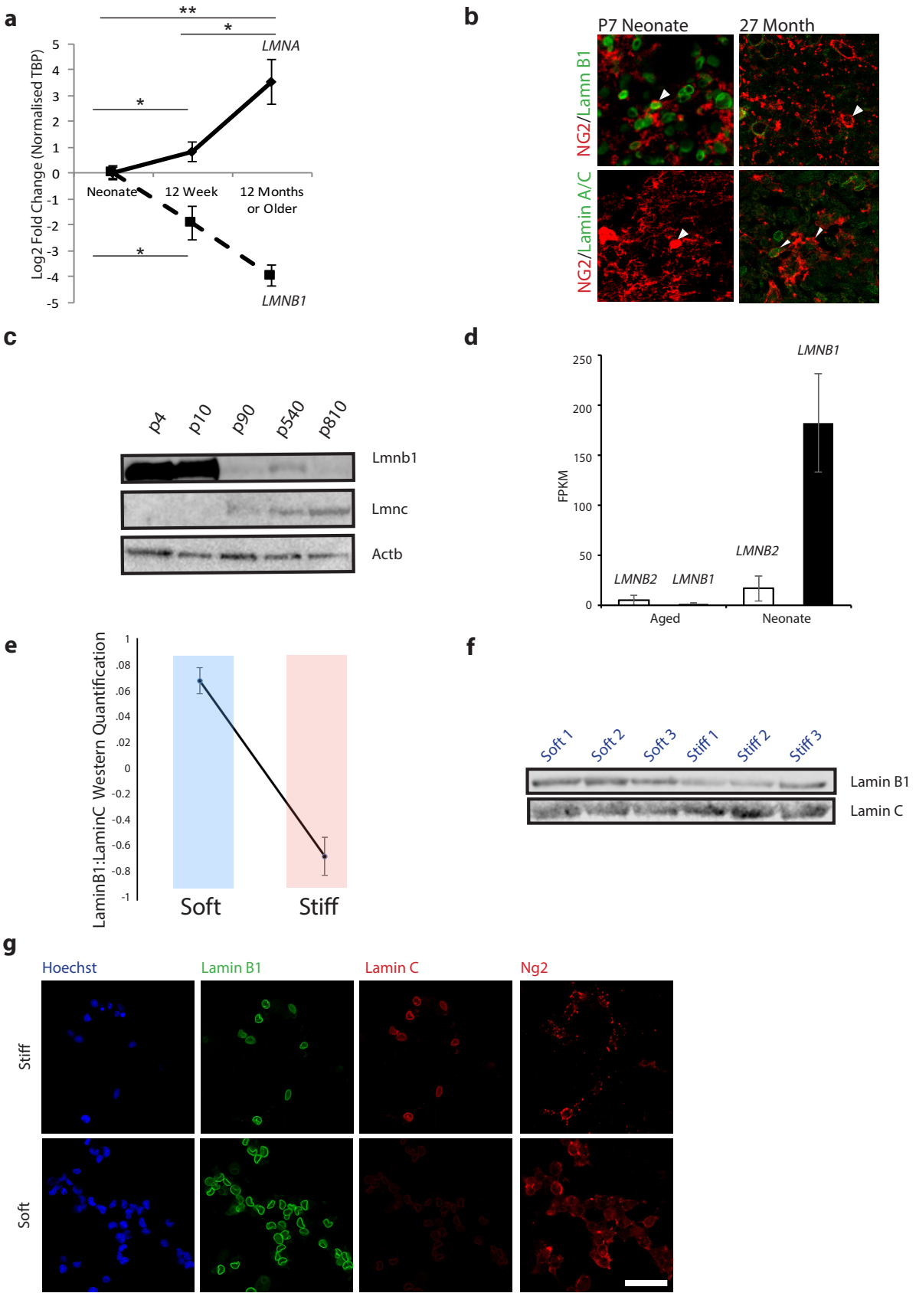
a
**
*
*
*
LMNA
LMNB1
Log2 Fold Change (Normalised TBP)
5
4
3
2
1
0
-1
-2
-3
-4
-5
Neonate
12 Week
12 Months or Older
b
P7 Neonate
27 Month
NG2/Lamn B1
NG2/Lamin A/C
c
p4
p10
p90
p540
p810
Lmnb1
Lmnc
Actb
d
LMNB1
250
200
150
100
50
0
FPKM
LMNB2
LMNB2
LMNB1
Aged
Neonate
e
LaminB1:LaminC Western Quantification
1
.08
.06
.04
.02
0
-0.2
-0.4
-0.6
-0.8
-1
Soft
Stiff
f
Soft 1
Soft 2
Soft 3
Stiff 1
Stiff 2
Stiff 3
Lamin B1
Lamin C
g
Hoechst
Lamin B1
Lamin C
Ng2
Stiff
Soft

Figure 9

Figure 9. The nuclear lamina composition of OPCs changes both with ageing and in response to niche stiffness. a, qPCR on OPCs reveal a loss of Lmnb1 and gain of Lmna with ageing. Values represent averages of OPCs from N=3 animals for each time point and are the Log2 ΔΔCT values normalized to Tbp. b, Representative images of *in vivo* cerebellar grey matter cryo-sections confirm nuclear lamina changes that occur withageing. Scale bar represents 50μm. c, Western blot of Lamin B1 and Lamin C from freshly isolated OPCs of different ages confirms qPCR data. d, RNA-sequencing data of nuclear Lmnb2 in neonatal and aged OPCs show low levels of expression in both age groups. e-f, Western blot quantifications of aged OPCs grown on soft and stiff hydrogels. g, Representative images of nuclear lamina changes in OPCs on different stiffness hydrogels. Scale bar represents 50μM.

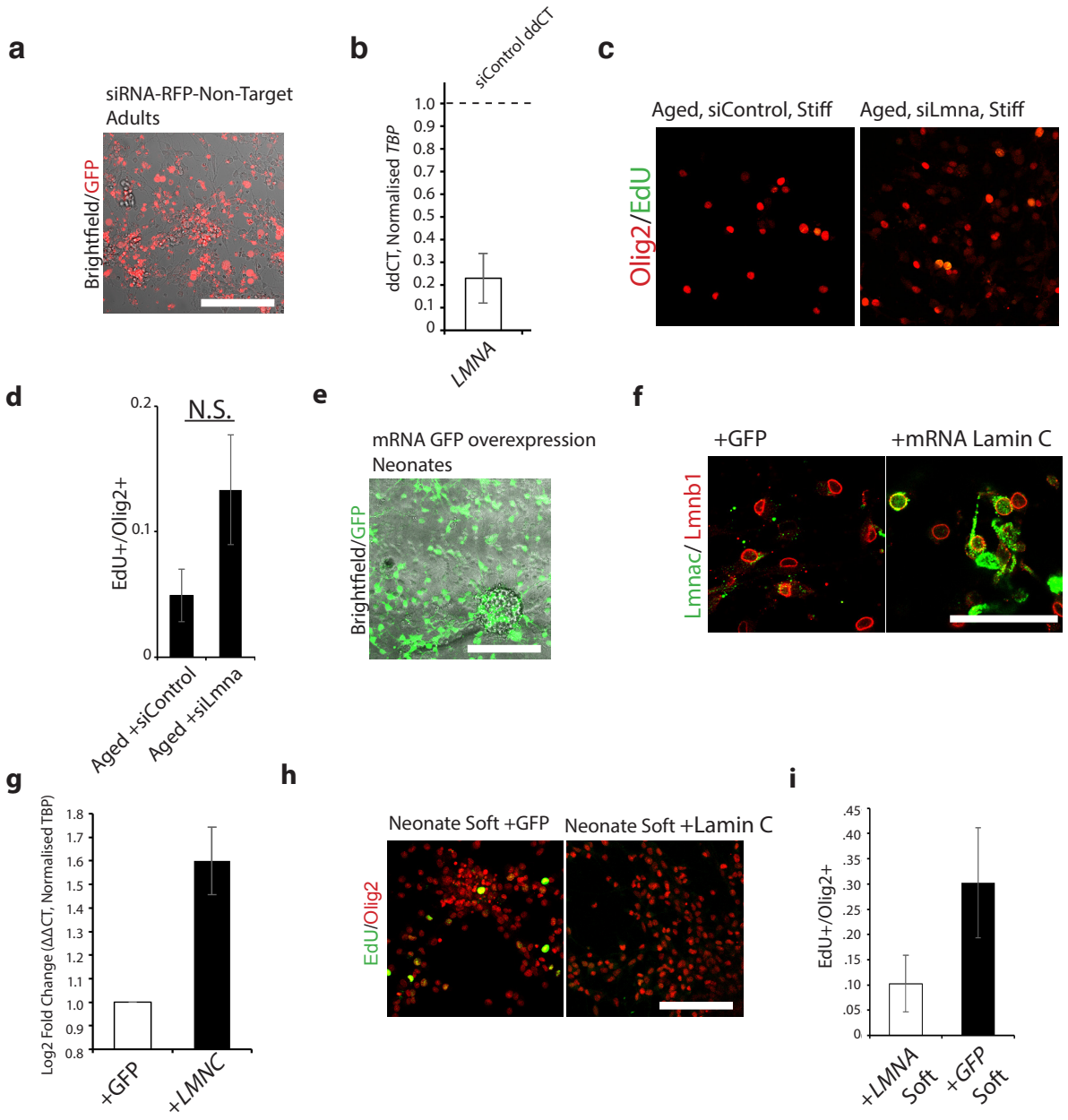

Figure 10. Role of nuclear Lmna in OPC self-renewal. a, Representative image of RFP-conjugated non-targeting siRNA shows high efficiency siRNA transfection. Bright-field shows high proportion of transfected to untransfected cells. b, qPCR on adult OPCs 48 hours following transfection with siRNAs. Values represent averages of OPCs from N=3 animals and are the Log2 ΔΔCT values normalized to Tbp. c-d, Representative images and quantifications of the proliferation of N=3 aged OPCs in growth factors on stiff hydrogels following transfection with siRNAs. Scale bar represents 50µm. e, Representative image of GFP encoding mRNA in neonatal OPCs shows high efficiency transfection. Scale bar represents 100µM. f, Representative images showing efficient transfection, high translation, and proper protein localization of Lamin C in aged OPCS. Scale bar represents 25µM. g, qPCR data 5 days post-transfection from RNA isolated from transfected OPCs. Means represent log ΔΔCT means across N=3 technical replicates from N=2 biological replicates. h-i, Representative images and quantifications of N=3 replicates in neonatal OPCs on soft hydrogels show loss of proliferative capacity 120 hours following Lmnc mRNA overexpression. Scale bar represents 100µM.

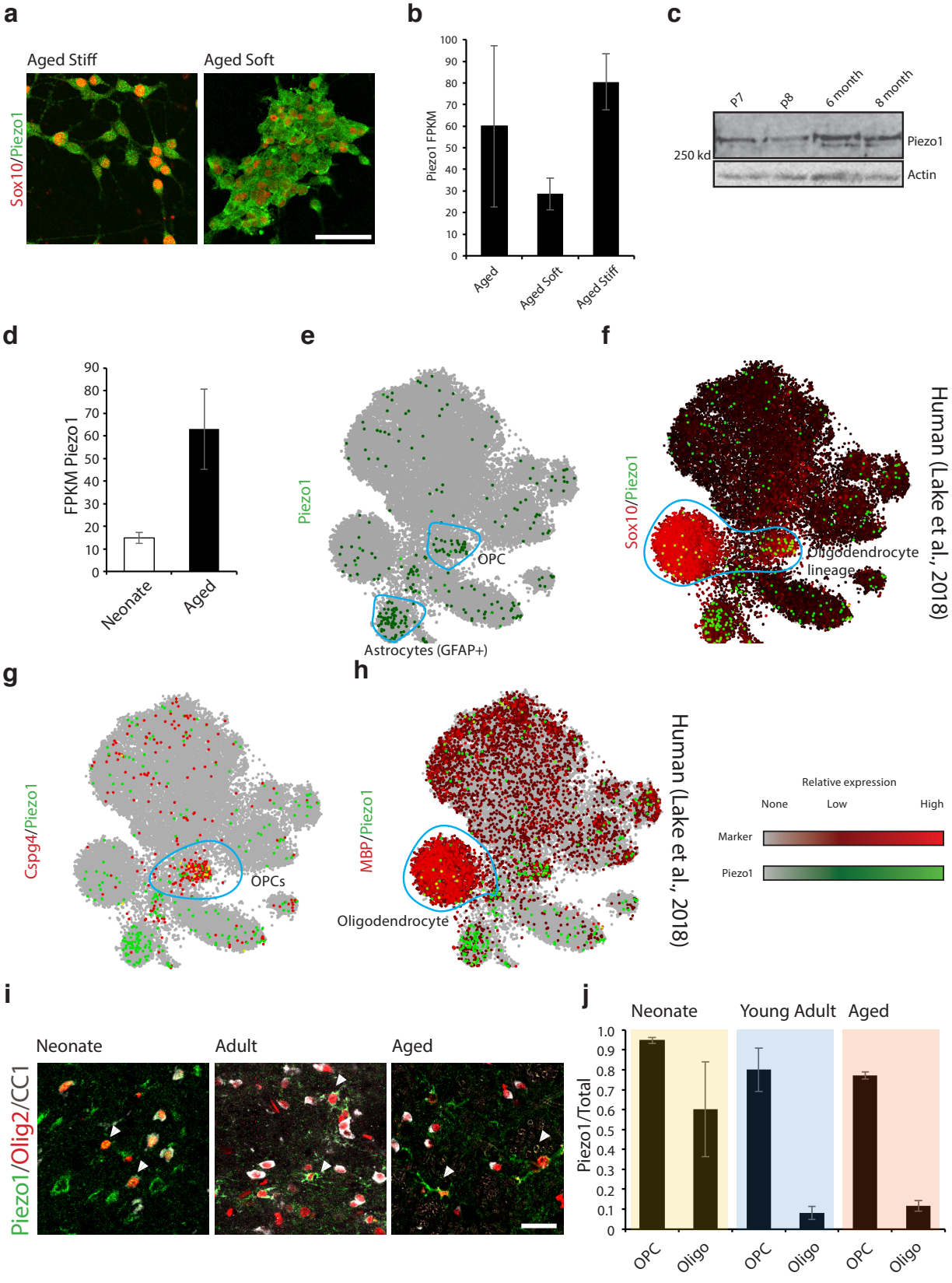
a
Aged Stiff
Aged Soft
Sox10/Piezo1
b
Piezo1 FPKM
Aged
Aged Soft
Aged Stiff
c
P7
p8
6 month
8 month
250 kd
Piezo1
Actin
d
FPKM Piezo1
Neonate
Aged
e
Piezo1
OPC
Astrocytes (GFAP+)
f
Sox10/Piezo1
Oligodendrocyte lineage
Human (Lake et al., 2018)
g
Cspg4/Piezo1
OPCs
h
MBP/Piezo1
Oligodendrocyte
Human (Lake et al., 2018)
Relative expression
None
Low
High
Marker
Piezo1
i
Neonate
Adult
Aged
Piezo1/Olig2/CC1
j
Neonate
Young Adult
Aged
Piezo1/Total
OPC
Oligo
OPC
Oligo
OPC
Oligo

Figure 11

Figure 11. Piezo1 is widely expressed by OPCs. a, Representative images and sequencing data of aged progenitor cells on soft and stiff hydrogels and sequencing data of Piezo1. Scale bar represents 100µm. c, Western blot for Piezo1 in acutely isolated OPCs show modest increase in protein expression from neonates to adults. d, Mean FPKM values across 3 biological replicates of Piezo1 in neonatal and aged acutely isolated OPCs. e-h tSNE plots of human single cell-sequencing studies showing Piezo1 (green) cells co-expressing Sox10 and Cspg4 (red) in adult grey matter. Cells expressing both Piezo1 and the respective lineage-specific marker appear as yellow. Relevant cell populations, based on their marker expression, are labeled with a light blue circle. Expression legend is provided. i-j, Representative images and quantifications of the proportion of Piezo expressing OPCs (as labelled by Olig2+CC1-) and oligodendrocytes (as labelled by Olig2+CC1-) in the CNS grey matter in the rat of N=3 P7, N=3 3 month-olds, and N=3 14-month old animal. Scale bars represent 25µm.

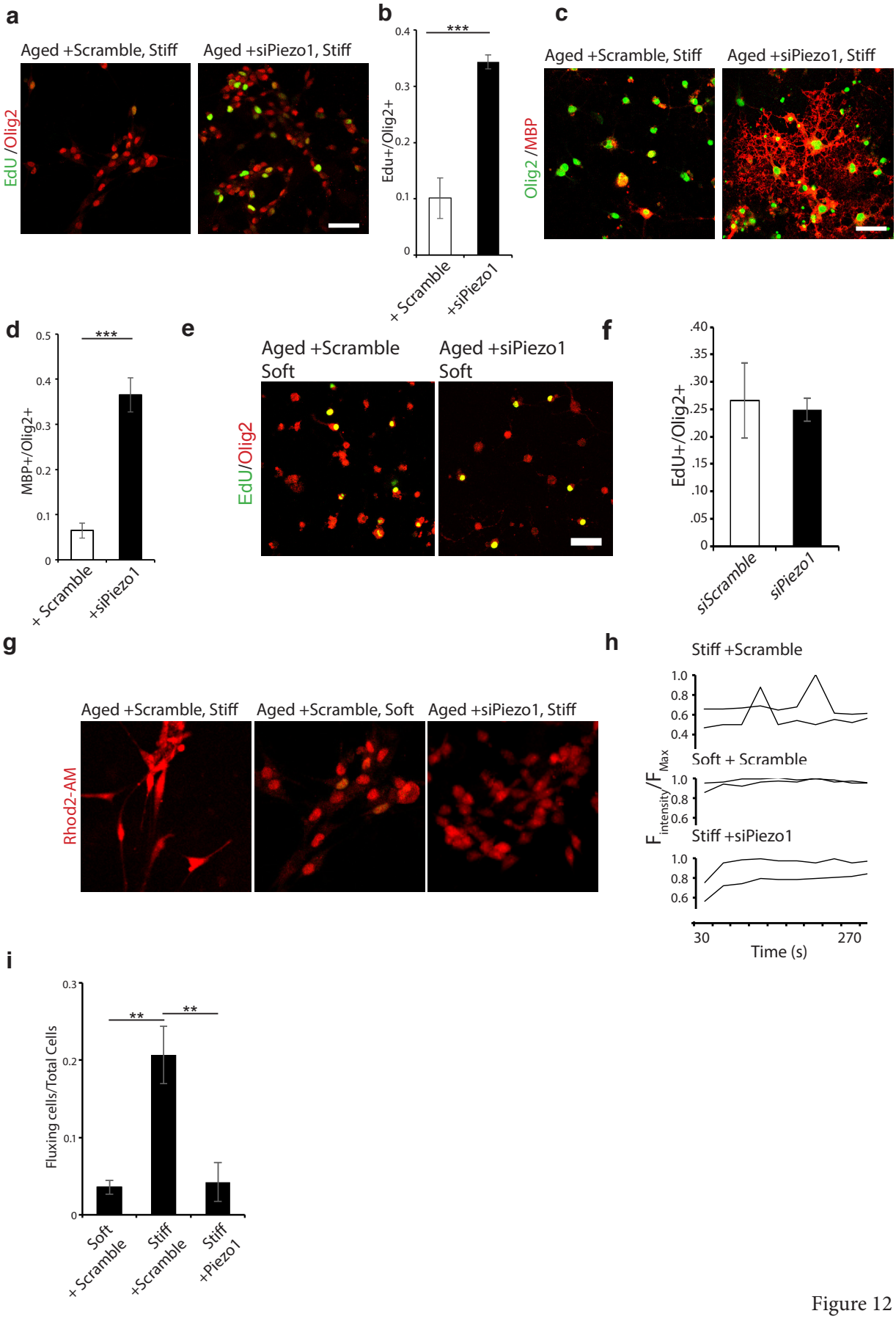
a
Aged +Scramble, Stiff
Aged +siPiezo1, Stiff
EdU /Olig2
b
***
Edu+/Olig2+
0.4
0.3
0.2
0.1
0
+ Scramble
+siPiezo1
c
Aged +Scramble, Stiff
Aged +siPiezo1, Stiff
Olig2 /MBP
d
***
MBP+/Olig2+
0.5
0.4
0.3
0.2
0.1
0
+ Scramble
+siPiezo1
e
Aged +Scramble
Soft
Aged +siPiezo1
Soft
EdU/Olig2
f
EdU+/Olig2+
.40
.35
.30
.25
.20
.15
.10
.05
0
siScramble
siPiezo1
g
Aged +Scramble, Stiff
Aged +Scramble, Soft
Aged +siPiezo1, Stiff
Rhod2-AM
h
Stiff +Scramble
Soft + Scramble
Stiff +siPiezo1
F intensity /F Max
1.0
0.8
0.6
0.4
30
270
Time (s)
i
**
**
Fluxing cells/Total Cells
0.3
0.2
0.1
0
Soft
+ Scramble
Stiff
+Scramble
Stiff
+Piezo1

Figure 12

Figure 12. Piezo1 knockdown activates adult and aged OPCs. a-d, Representative images and quantifications of the proliferation and differentiation rates of N=3 biological replicates aged OPCs cultured on stiff hydrogels transfected with siScramble or siPiezo1. Scale bar represents 25μm. e-f Representative images and quantifications of N=3 biological replicates of aged OPCs transfected with a control siRNA or with a Piezo1 siRNA on soft hydrogels. Scale bar represents 50μm. g, Representative Rhod-2am-stained live cell images of aged progenitor cells on soft and stiff hydrogels transfected with siScramble or siPiezo1. h, Example traces of individual cells fluxing with calcium (ΔF) over 270 seconds. Fluorescence was normalized to the maximum fluorescence intensity per cell over the acquisition time. i, Quantifications of the proportion of cells that fluxed calcium ≥1 time throughout the 540 second image acquisition period from N=3 biological replicates.

down Piezo1 would allow OPCs to maintain self-renewal capacity, even in an aged stiff environment.

To test this hypothesis, we first needed to develop a means to stably silence Piezo1 in neonatal OPCs. There are numerous technical difficulties in transfecting and genetically perturbing primary OPCs. OPCs are primary cells that cannot grow clonally, are slowly dividing, do not readily undergo homologous recombination (data not shown), and have a small cytoplasm to nucleus ratio, making them hard to transfect; as such, common-use genetic and viral approaches are inefficient in OPCs. Therefore, we generated a system using Cas9 mRNA, transcribed gRNAs, and HITI-mediated minicircle vectors to efficiently knock in a Piezo1 shRNA-GFP overexpression cassette into the unused Tubb3 locus (Fig. 13a)(Suzuki et al., 2016). This Cas9-mediated knock-in of shRNA-GFP has the benefit of having a characterizable monotonic knock-down across the pool of cells expressing the GFP. Neonatal OPCs transfected with this construct showed high transfection efficiency and a knock down of Piezo1 by ~80% (Fig. 13b-e). When this construct was knocked-into aged OPCs on stiff hydrogels, the aged OPCs demonstrated a nearly tenfold increase in proliferation (Fig. 13f-g).

We next transfected Piezo1-targeting and non-targeting control constructs into neonatal OPCs, and transplanted them into the aged prefrontal cortex (Fig. 13h). Fourteen days after transplantation, both control and Piezo1 knock-down cells engrafted. Piezo1 knock-down cells did not migrate, remaining as proliferating cells at the transplantation site, whereas control cells extended processes, and were distributed across the grey matter. Almost none of the control neonatal OPCs proliferated in the aged cortex, losing their proliferative capacity (Fig. 13i-j). However, OPCs expressing the knockdown of Piezo1 continued to proliferate, with ~20% of neonatal OPCs remaining Edu positive, indicating a high level of maintained OPC activity despite the adverse aged microenvironment. This result represents the first time, to our knowledge, that neonatal OPCs have been injected into undamaged aged CNS and maintained their ability to proliferate, and it clearly demonstrates the importance of mechanical signalling in the age-related loss of function in OPCs.

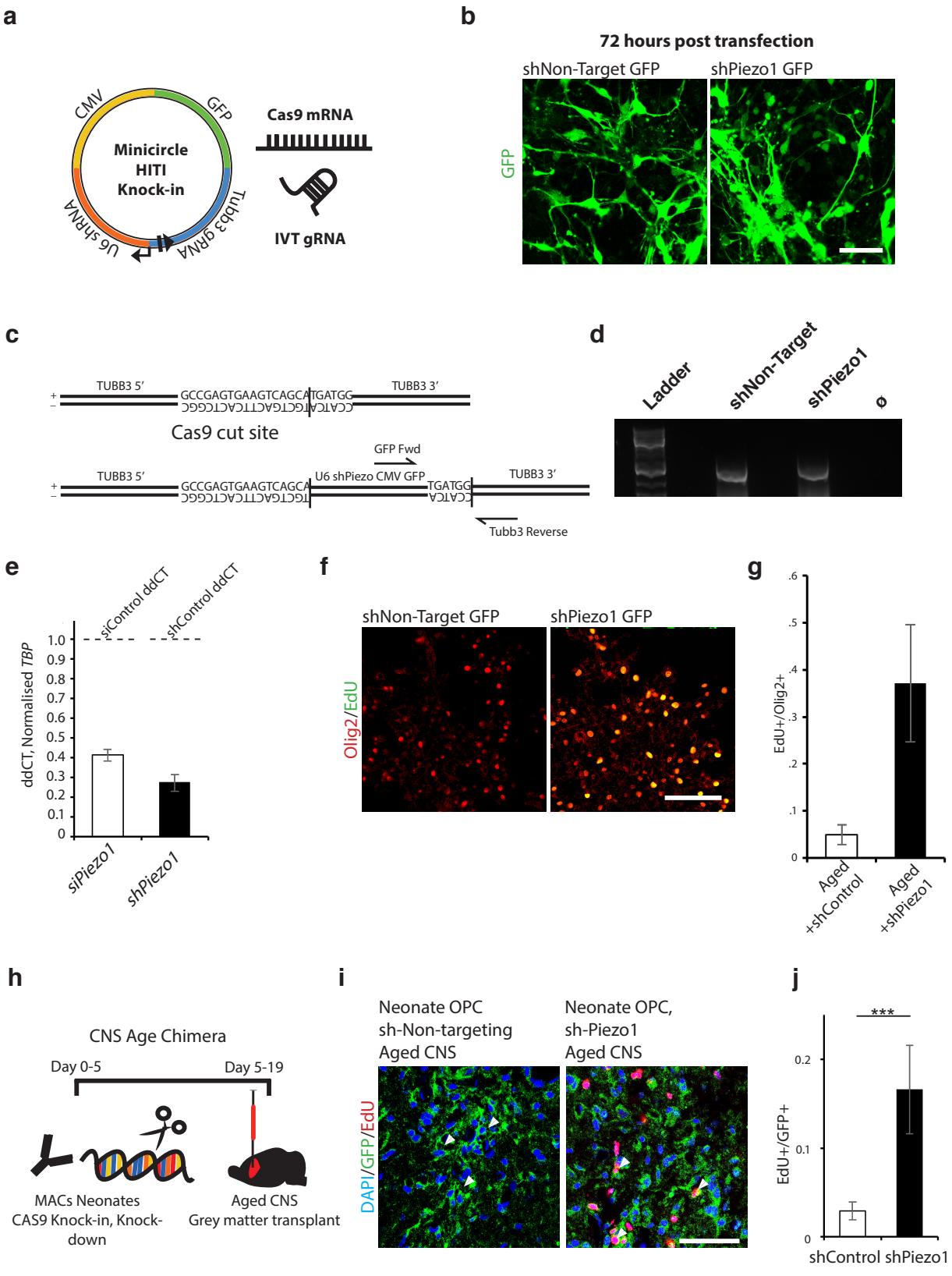
a
CMV
GFP
Minicircle
HITI
Knock-in
Tubb3 gRNA
U6 shRNA
Cas9 mRNA
IVT gRNA
b
72 hours post transfection
shNon-Target GFP
shPiezo1 GFP
GFP
c
TUBB3 5′
GCCGAGTGAAGTCAGCATGATGG
TUBB3 3′
Cas9 cut site
GFP Fwd
U6 shPiezo CMV GFP
Tubb3 Reverse
d
Ladder
shNon-Target
shPiezo1
ø
e
siControl ddCT
shControl ddCT
ddCT, Normalised TBP
siPiezo1
shPiezo1
f
shNon-Target GFP
shPiezo1 GFP
Olig2/EdU
g
EdU+/Olig2+
Aged +shControl
Aged +shPiezo1
h
CNS Age Chimera
Day 0-5
Day 5-19
MACs Neonates
CAS9 Knock-in, Knock-down
Aged CNS
Grey matter transplant
i
Neonate OPC
sh-Non-targeting
Aged CNS
Neonate OPC,
sh-Piezo1
Aged CNS
DAPI/GFP/EdU
j
***
EdU+/GFP+
shControl shPiezo1

Figure 13

Figure 13. Piezo1 mitigates the cell response to the stiffening CNS niche. a Schematic for Cas9-mediated genomic manipulation using *in vitro* transcribed (IVT) gRNA, Cas9 mRNA, and in-house-made minicircle vectors overexpressing Piezo1-targetting shRNAs. b, Representative images show high rates of co-transfection of minicircle with Cas9 mRNA and IVT gRNA. Scale bar represents 25μM. c-d PCR design and appropriate fragment length of correctly knocked-in Minicircle fragment construct. e, qPCR data 48 hours post-transfection of adult OPCs with Piezo1 siRNA and Piezo1 shRNA construct from RNA isolated from transfected OPCs. Means represent log ΔΔCT means from N=3 biological replicates. f-g, Representative images and quantifications show Cas9 knock-in of shPiezo1 fragments in aged OPCs on stiff hydrogels phenocopies the effect of the siRNA Piezo1 in aged OPCs. Scale bars represent 100μM. h, Neonatal OPCs were transfected with Cas9-mediated knock-in shRNA construct 24 hours following MACs sorting. i-j, Representative images and quantifications of GFP-expressing, EdU labelled cells in the grey matter of N=4 14 month old female rats. Quantifications are presented as a proportion of EdU+ out of total GFP+ cells. Arrows represent example quantified cells. Scale bar represents 50μM. Dr. Myfanwy Hill performed the cell transplantations shown in this figure.

Discussion

In this study, we showed that adult CNS progenitor cells do not undergo intrinsic irreversible changes with ageing. Instead, they acquire properties that reflect the age of their environment, specifically its mechanical features. As the CNS stiffens with age, OPCs respond by becoming less efficient at proliferating and differentiating both *in vitro* and *in vivo*. We found that reducing actomyosin contractility attenuated the age-related loss of OPC function, and identified the mechanosensitive ion channel Piezo1 as a key player in the mechanical regulation of the ageing response (Fig. 14). Other canonical ageing pathways such as genomic and epigenetic instabilities, should now be considered in the context of how they are responding to the mechanical microenvironment. Furthermore, we conclude that ECM mechanics are an important determinant of the success of stem cell-based therapeutics that aim to treat age-related diseases. We found that young progenitors transplanted into aged lesion environments lose optimal regenerative properties; however, we point to a means to mitigate that response. We can attenuate the negative reaction to the aged microenvironment by decreasing the ability of the CNS progenitor cells to respond to mechanical signals from the CNS niche. Our findings open up the important possibility that niche stiffness is a general factor driving ageing in the adult CNS.

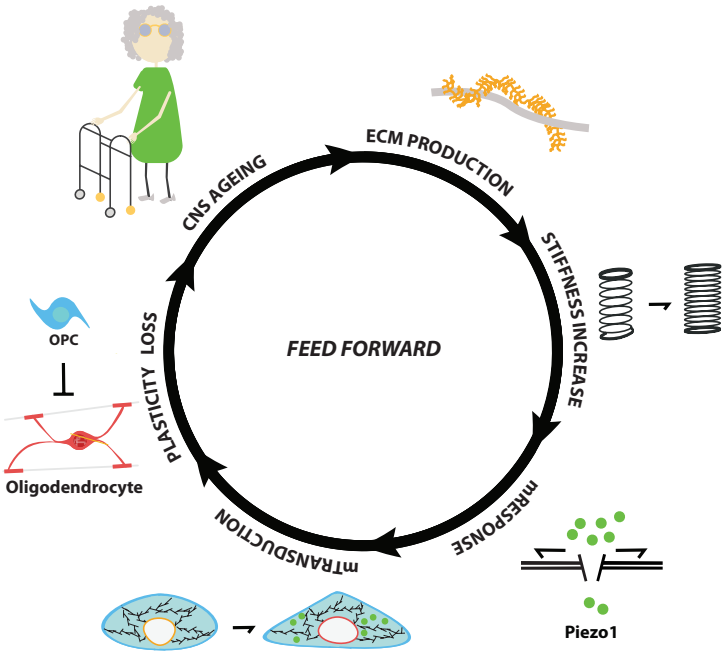

Figure 14. Working model of stiffness-mediated ageing hypothesis. With ageing, memory formation and normal cognitive development is associated with the deposition of ECM. The ECM in turn accumulates stiffening the tissue. This stiffening results in the Piezo1-mediated loss of activity of the CNS resident progenitor cell population the oligodendrocyte progenitor cell. The proposed model is that this comprises a feed forward loop which ultimately leads to prolonged OPC inactivity, and ultimately, CNS ageing.

Cell non-autonomous ageing of OPCs

Since previous work identified somatic cell nuclear transfer (SCNT) as a method for reprogramming the age state of an adult cell into an embryonic cell, it has been known that the genetic material of cells, even from an adult or aged mammal, retains the capacity to de-differentiate, form an embryo, and give rise to a viable, sexually competent adult clone (Wilmut et al., 1997). As such, even aged somatic cells must retain the intrinsic capacity to rejuvenate. Many groups have examined the capacity for adult cells to be reprogrammed into embryonic ones (Mertens et al., 2015) and have looked at cell intrinsic mechanisms to rejuvenate aged stem cells within their lineage. Here, we have uncoupled stem cell intrinsic ageing from environmental niche ageing. We have found that aged OPCs, when transplanted into a neonatal, brain environment, maintain the capacity to proliferate and differentiate into myelinating oligodendrocytes.

One previous paper similarly looked at the capacity for adult human OPCs to myelinate the neonatal mouse brain and found that adult OPCs retain the capacity to efficiently differentiate into myelinating oligodendrocytes (Windrem et al., 2004). This study used adult human OPCs, however, and did not examine the effects of ageing on OPCs. Our results further this previous work by showing that OPCs maintain their generative capacity throughout ageing. However, in aged CNS lesions, OPCs fail to differentiate into new myelinating oligodendrocytes (Kuhlmann et al., 2008). As aged OPCs can indeed efficiently proliferate and differentiate as shown by the work presented here, remyelination failure is thus likely the failure of the niche to sufficiently activate aged cells.

A major limitation of the transplantation study shown in Figure 1 of this chapter is our use of the baculovirus to label neonatal and aged OPCs. Baculovirus, a non-integrating DNA virus, labels cells only for the first few rounds of cell replication, after which the GFP transgene and GFP protein is diluted and disappears. This property of the baculovirus limited our transplantation study in so far as we were only able to follow aged cells in the neonatal environment for a short period (10 days). Whether or not these aged OPCs in the neonatal environment would continue to proliferate and contribute to normal development myelination is unknown. An important follow up experiment will be to repeat the transplantation assay, but with transgenic, constitutively expressing fluorescent mice or rats. This would have the advantage that the transplanted cells

would constitutively express the fluorophore, allowing for long term tracing of transplanted cell activity. Follow up studies must include both long term functional proliferation analysis and semi-thin resin sections to determine whether aged OPCs myelinate in the same manner as neonatal OPCs. Until then, it is unclear whether the observed phenotype of aged OPCs in the neonatal environment is stable or whether they stop proliferating after periods longer than 10 days.

This set of hetero-chronic allografts has sparked further questions regarding the environmental effect on the age state of cells. If the aged environment underlies the aged state of OPCs, then we would hypothesise that a neonatal OPC serially transplanted into a neonate would not age—without ever being exposed to an aged environment, a stem cell would proliferate ad infinitum. A similar question actively being pursued is whether a human neonatal OPC transplanted into a neonate rodent would adopt the age-state of the rodent. After ~14 months, remyelination of the rodent CNS becomes inefficient. In its native environment, a 14 month old human OPC would still be just an infant, and as regenerative as a neonatal mouse. Would, however, a 14 month old human OPC in the environment of the mouse brain assume an aged-cell like identity, contributing to inefficient remyelination? If environment alone determines age state, then the genomic expression and epi-genomic landscape of the transplanted human OPCs should resemble that of an aged mouse OPC. Such experiments are crucial to understanding cell intrinsic versus cell extrinsic factors which underlie ageing.

The CNS, OPCs, and stiffness

The local and systemic environment of the neonatal CNS is dramatically different from that of the aged CNS. Systemic factors found in the blood, such as hormones, as well as local niche factors, such as locally secreting Wnts and Pdgf, likely underlie, at least in part, the re-activation of aged OPCs that are transplanted into the neonatal CNS. However, even in the presence of growth factors, aged OPCs *in vitro* cannot efficiently enter into cell cycle or differentiate into oligodendrocytes. Thus, some unknown factor must underlie their re-activation.

To better understand the changing niche of the CNS, we performed atomic force microscopy on the brain and found that the brain progressively stiffens with ageing. This stiffening is partially due to the accumulation of matrix proteins. Additional work we have done—though not

presented here—shows that the degradation of matrix CSPGs with chABC can soften the aged CNS by nearly 1/3rd. These results indicate that the deposition of matrix in the postnatal CNS contributes to the stiffening of the adult brain.

Matrix proteins in the brain are believed to be deposited as neuronal and glial scaffolding, holding together the synapses in the adult brain to preserve neural networks (Kwok et al., 2011). These matrix proteins are secreted in response to sensory experience—mice deprived of light do not deposit such proteins in the occipital lobe (McRae et al., 2007). As such, with experience, there is more matrix, and likely an increase in tissue stiffness and a subsequent loss of OPC activity. Future work must determine the exact changes in CNS matrix with ageing, their effects on stiffness, and on OPC function. Moreover, this proposed axis linking the development of the adult mammalian CNS and the loss of OPC plasticity must be explored.

When we place aged OPCs on soft neonate-brain-like hydrogels in the presence of high concentrations of growth factors, we see that aged OPCs reactivate and are able to both proliferate and differentiate into oligodendrocytes whereas aged OPCs on stiff hydrogels cannot. From this work, we show that niche bio-mechanics are an important factor for OPC activation. A number of studies in muscle and intestine similarly found that soft matrix environments promote self-renewal conditions *in vitro* (Gilbert et al., 2010; Jung et al., 2011). One paper found significant improvement in iPS cell generation when the cells were reprogrammed in very soft matrices (Caiazzo et al., 2016). Together with our results, it is becoming increasingly evident that many stem cells, both embryonic and adult, are more stem-like in soft environments.

Despite this observation that aged OPCs on soft hydrogels functionally rejuvenate and transcriptomically resemble neonatal OPCs, it is also clear that growth factors and the in vitro environment play a major role in determining the age state of OPCs. From the PCA data and the hierarchical clustering, aged OPCs cultured on stiff hydrogels cluster more similarly to neonatal OPCs than they do acutely isolated aged OPCs. Clearly, exposure of growth factors has a ‘rejuvenating’ effect on aged OPCs in vitro and that niche stiffness alone does not fully recapitulate the effects of OPC ageing. However, aged OPCs cultured on stiff hydrogels do not cluster as closely to neonatal OPCs as do aged OPCs cultured on soft hydrogels. These results show that the niche mechanics further rejuvenates cells but alone is likely insufficient to drive rejuvenation. While we show that mechanics plays a dominant role in OPC activity, we do not

disentangle *in vitro* these confounding effects of growth factors and mechanical environment. Future work must examine the role of mechanics in the absence of exogenous growth factors and whether even then, a soft mechanical environment can transcriptomically rejuvenate aged OPCs.

The evolutionary underpinnings for the effects of a soft niche remain unexplored. One possibility is that stem cell activation requires the physical space for the cell to undergo division and differentiation. Softness may act as a proxy, signalling to the stem cell that there is the physical space to activate. There is biological precedent for this hypothesis in the planaria and hydra (Florea, 2017; Watanabe et al., 2009). Before the mother organism is too damaged/aged, a new organism buds off, forming a new organism. Rather than repair the damaged tissue, the stem cell buds off, finds new space and creates an effective clone of the mother organism. Similarly, recent work trying to generate iPS cells in the adult rodent *in vivo* found that the cells largely become senescent and cannot gain pluripotency in the *in vivo* environment (Mosteiro et al., 2016). Like the hydra and planaria, immortality of humans—the capacity of the human cell to self-propagate ad infinitum—requires the reprogrammed cell to be removed from the endogenous niche environment. Perhaps again this highlights the stem cell's need for space and the absence of matrix protein. Future work will aim to examine this relationship between physical space and stem cell activity in order to better understand the role of space on stem cell function.

Piezo1 and OPCs

We identify that OPCs probe the mechanics of their environment using the mechanosensor Piezo1. From single cell sequencing data and immunohistochemistry of the cortex, we find that Piezo1 expression is limited to the astrocytes and OPC population within the brain. We also show that without Piezo1 protein, OPCs both *in vitro* and *in vivo* retain the capacity to proliferate, even in a mechanically stiff/aged environment.

In this chapter, I show that transplanting neonatal OPCs that have a knockdown of Piezo1 maintain their proliferative capacity, even in an aged CNS. This experiment, however, does not address the role of Piezo1 in the homeostatic undamaged aged brain. The transplantation assay effectively creates a micro-injury in the brain at the transplantation site. While control OPCs transplanted lost their proliferative capacity, the fact that Piezo1 knock-down OPCs maintain at

least some of their proliferation capacity does not mean that Piezo1 alone dictates cellular activation state. Rather, it is an equally likely possibility that signals from the local injury site from the transplantation in conjunction with lost Piezo1 expression allow cells to proliferate, even in the aged CNS. In order to conclusively determine the role of Piezo1 in OPCs, future work must use Piezo1 conditional knockout mice to study the role of Piezo1 in OPCs throughout CNS development, in homeostasis, and in the context of a demyelinating insult.

Piezo1 is a transmembrane ion channel protein. Under conditions of high strain, the Piezo1 channel opens, allowing for the flow of ions into the cell (Coste et al., 2010). These ions act as secondary messengers to convey to cytoplasmic proteins that the cell is in a stiff environment. Yet, the evolutionary underpinnings of why OPCs uniquely express Piezo1 remain unclear as the brain is not an obviously mechanically strained organ. One hypothesis is that Piezo1 itself senses cell density. In homeostatic skin epithelium, Piezo1 is expressed within the processes of cells (Gudipaty et al., 2017). In cases of injury, however, Piezo1 dissociates from the cell cytoplasm, becoming perinuclear. Once the epithelium re-establishes normal cell density, Piezo1 re-localises to the cytoplasm. Upon knocking down Piezo1, the epithelium over proliferates, creating blebs of hyper-proliferating cells. These findings complicate the previously established hypothesis that Piezo1 is a pure-mechanostat. The authors argue, instead, that Piezo1 is a monitor of normal homeostatic cell density.

In work shown in this paper, we have found Piezo1 to be perinuclear in neonatal OPCs and within the OPC processes during adulthood. Additionally, in unpresented work we have found Piezo1 to be perinuclear in OPCs when in a young adult lesion and within the processes in aged lesions when OPCs appear stuck at the periphery of the lesion. This bolsters the previous publication's claim that Piezo1 is a counter of normal cell density rather than a pure mechanostat. Within the lesion OPCs re-localise Piezo1 to be peri-nuclear as the cells undergo mitosis and differentiate. These findings complicate our work's overarching claim that OPC age state is described by mechanics alone. Perhaps cross-linking density of matrix protein would be a more appropriate description of this phenomena. It is possible that a soft hydrogel environment mimics the environment of a low density matrix environment thus tricking the OPC to re-enter cell cycle and differentiate into an oligodendrocyte.

With these revelations, we now hypothesise that OPC ageing begins at the end of overall brain

growth. Once the brain reaches maximal size, matrix, and cell density, OPCs via Piezo1 cannot activate as there is contact-inhibition that negatively regulates cell-cycle. Piezo1 is the protein within the cell that senses overall organ growth termination and signals to the OPC to slow cell cycle. Once this occurs, OPCs enter a prolonged phase of G1, thus intrinsically ageing in the manner described in the introduction. If OPC ageing begins once the CNS stops growing, then the true underlying cause of CNS ageing is the overall regulator of organ size.

Recent work suggests that overall brain size and development is tethered to bone growth (Oury et al., 2013). As bones grow they secrete the circulatory hormone osteocalcin. This hormone has a direct effect on the growth and development of the CNS (Obri et al., 2018). When development finishes, however, the bones stop its secretion. If the termination of organ growth coincides with the beginning of physiological ageing, then identifying the biological parameters that govern overall organismic and organ size is the key to understanding the ageing of stem cells. Future work must determine what these organismic size determinants are to truly understand the basis for physiological ageing.

Chapter 5

Cell-type specific, systemically administered Nested CRISPR in wild type aged mice reveals a role for Piezo1 in the stem cells of the CNS

In chapter 4, I show that Piezo1 activity has a major role in modulating the activity state of oligodendrocyte progenitor cells (OPCs), the dominant stem cell population in the adult central nervous system (CNS). To rapidly dissect the role of Piezo1 in the OPCs of the adult and aged CNS in both homeostasis and in regeneration, we have built a dual adeno-associated virus (AAV) nested CRISPR/sp. Cas9 system which efficiently genome engineers OPCs of the adult CNS following a single intravenous injection of AAV particles. We have combined multiple genome engineering strategies, including synthetic CNS-targeting AAVs, non-homologous-end-joining (NHEJ) mediated knock-ins, and RNA-triple helix structures and ribozymes to efficiently manipulate the gene Piezo1, specifically in OPCs. Doing so in the aged CNS, we have observed an increase in OPC self-renewal in homeostasis and accelerated regeneration following CNS injury. Finally, using a modified nested CRISPR technique, we have generated an OPC-specific, Piezo1 reporter-animal and show that OPCs across the CNS express Piezo1. These findings highlight the importance of Piezo1 in OPC activity and provides a new experimental approach to rapidly hypothesis-test the role of specific genes on individual cell populations in the adult and aged animal.

As discussed briefly in the previous chapter, the mechano-sensing gated ion channel Piezo1 was first identified as a gene upregulated in the glia of Alzheimer human brains and as a negative regulator of Ras signalling (McHugh et al., 2010). Since then, Piezo1 has also been identified as a regulator of cell number in development and in epithelial wound healing (Eisenhoffer et al., 2012; Gudipaty et al., 2017). In drosophila, gut stem cells activate in response to increased food load via Piezo1. Finally, Piezo1 knockout mice die embryonically partially as a result of the failure of the vasculature to develop normally (Li et al., 2014). In the previous chapter, we identified Piezo1 as fundamental to the activation of OPCs in the adult and aged CNS. Under conditions of mechanical stress, Piezo1 inhibits OPC self-renewal and differentiation, and its knockdown allows cells to self-renew both in vitro and

in vivo, even in an aged environment. We hypothesize that Piezo1 negatively regulates OPC activation once the brain attains maximal size and cell density.

Generating an inducible, OPC-specific Piezo1 knockout animal in aged mice is a laborious and time-intensive process using traditional transgenic animal models—transgenic animals must breed for multiple generations and ultimately the animals must age for over a year. To circumnavigate this process, we combined three genome engineering strategies to create an OPC specific Piezo1 knockout in wild type C57/Bl6 adult and aged mice. Recent work has shown that a dual AAV system delivered systemically can knock-in genes into precise genomic locations of adult post-mitotic cells (Suzuki et al., 2016). One AAV delivers a Cas9 gene under a CMV promoter while the other AAV delivers the sequence-specific gRNA under a U6 promoter and knock-in fragment flanked by gRNA cut sites, encoded in the reverse compliment orientation. Advances in the creation of synthetic AAV capsids has allowed for the generation of a CNS-specific and highly-efficient integrase-deficient AAV which targets >80% of all neurons >60% of glia in the adult mouse CNS (Challis et al., 2018). Finally, recent advances in synthetic biology have harnessed RNA-triple helical structures and self-cleaving ribozymes to drive the polycistronic expression of fluorescence proteins and gRNAs under RNA polymerase II promtoers (Nissim et al., 2014; Yoshioka et al., 2015).

We have harnessed all three of these technologies in synthetic biology to create a widespread, *in vivo*, CNS-targeting AAV that efficiently deletes Piezo1, specifically in OPCs in an adult and aged mouse. Doing so, we observe that OPCs have an increased rate of self-renewal in the homeostatic aged brain and increased regeneration in a focal toxin model of demyelination. Finally, we have generated a novel multilevel nested CRISPR system which effectively acts as an *in vivo*, OPC specific, Piezo1 reporter, revealing widespread Piezo1 expression across the adult CNS. These results demonstrate widespread targeted cell-type specific genome modifications in the adult mammal and emphasise the importance of Piezo1 for regeneration and repair of the damaged CNS.

OPCs lack a cell type described promoter sequence that could drive the expression of a transgene specifically in OPCs. Moreover, there are not many genes uniquely expressed by OPCs. In transgenic animals, the endogenous Pdgfra gene has been targeted to drive a Cre-recombinase to activate OPC-specific transgene expression (Rivers et al., 2008; Zawadzka et al., 2010). As such, we targeted Pdgfra to drive OPC specific transgene expression. First, we generated an PHP-EB AAV expressing Cas9 under a CMV promoter (Fig. 1). To target specifically OPCs, we generated a second PHP-EB

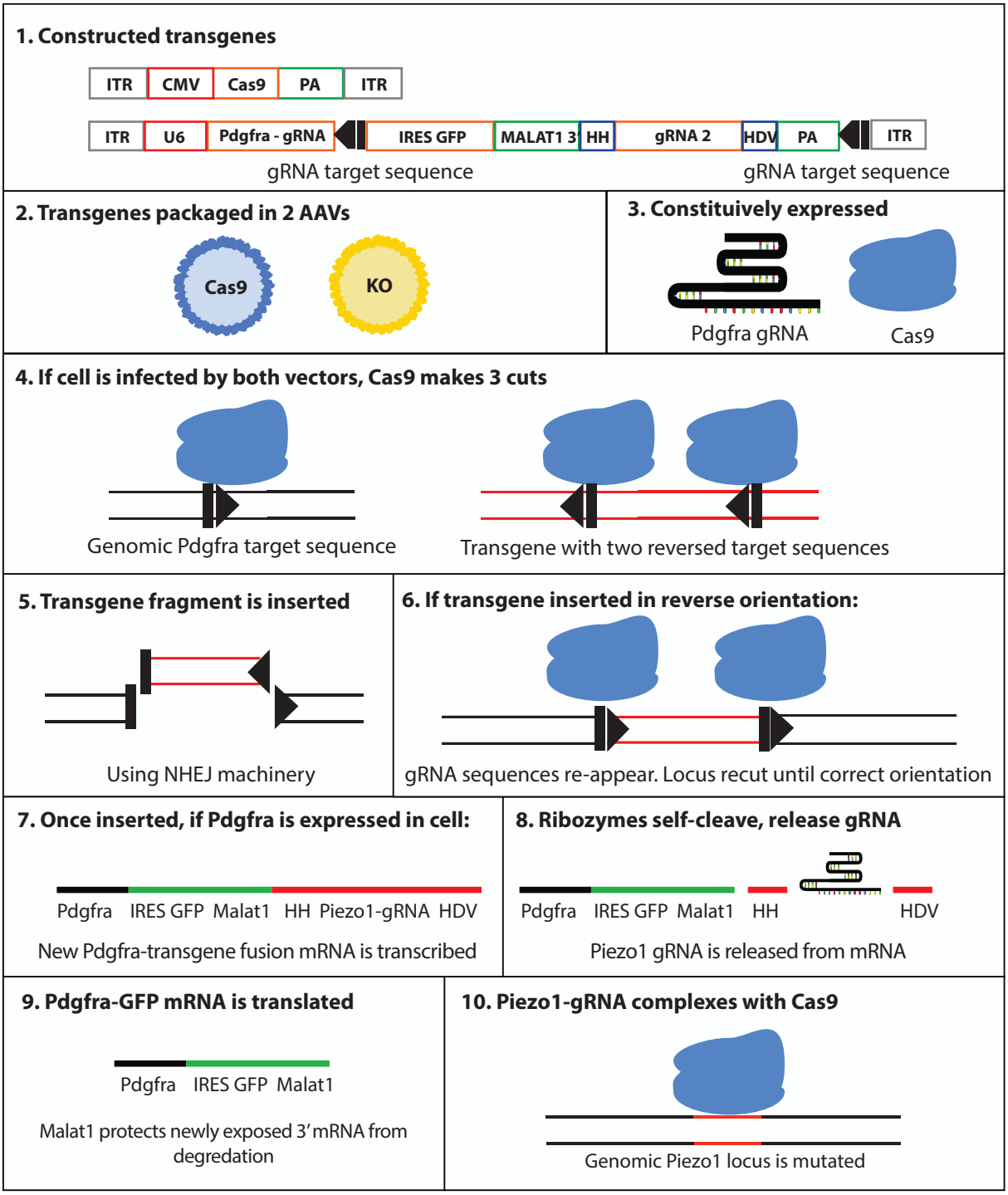

Figure 1. A nested CRISPR system for cell-type specific gene knock outs. A schematic outlining the approach. A non-homologous end-joining mediated knock-in of a construct is inserted into a gene specific to a given cell type. This construct contains a ribozyme flanked second gRNA, targeting Cas9-mediated gene knockdown to a second locus. HH is an abbreviation for Hammerhead ribozyme, HDV for hepatitis delta virus ribozyme, PA for poly-adenylation sequence, and ITR for an internal terminal repeat sequence. Square and triangle represent gRNA target sequence.

AAV vector expressing a 3' UTR targeting Pdgfra gRNA under the RNA polymerase III U6 promoter. Adjacent to the polymerase III termination sequence of repeat thymines, we inserted a Pdgfra gRNA cut sequence, antisense to the endogenous gRNA target sequence. Downstream of the cut sequence we placed an IRES-GFP followed by the 3' end of the Malat1 gene, a PolyA replacement sequence that stabilises mRNA by forming a RNA triple helix (Wilusz et al., 2012). Downstream of the helix we placed synthetic ribozyme-flanked gRNA targeting either Piezo1 or a non-targeting control gRNA. Finally, adjacent to the final PolyA signal, we inserted another antisense Pdgfra gRNA cut sequence. As described previously (Suzuki et al., 2016), when the Pdgfra gRNA sequence is expressed from the U6 promoter, both the endogenous genomic locus and the transgene is cut. The excised GFP-gRNA fusion gene is then inserted with NHEJ machinery into the endogenous Pdgfra cut locus. Once inserted, the GFP-gRNA transgene is expressed only when Pdgfra is also expressed. With the transcription of the fusion GFP-ribozyme-flanked-gRNA transcript, the ribozymes self-cleave, releasing the Piezo1 targeting gRNA. Moreover, the newly exposed 3' UTR of the GFP mRNA is protected from degradation due to the 3' UTR of the Malat1 gene. As such, when Pdgfra gene is expressed, GFP and a secondary gRNA sequence targeting the Piezo1 gene locus are also expressed. This technique theoretically makes it possible to mutate the Piezo1 locus only in Pdgfra expressing cells, creating an effective OPC specific Piezo1 animal knock out.

While the PHP-EB vector efficiently infects the adult CNS, it has yet to be determined whether the vector can efficiently infect OPCs. To determine the efficacy of our vector in knocking in the transgene construct with the PHP-EB AAV, we dissociated p1 neonatal mouse pup brains and infected them overnight with both the Cas9 AAV and our knock-in cassette. As a control we created a transgene that encodes for GFP and a non-targetting gRNA. Five days after infection, we found that PHP-EB has the capacity to infect OPCs and that our knock-in construct is specifically expressed in Olig2 expressing OPCs in vitro (Fig. 2a-c). PCR of the knock-in fragment showed that the fragment is inserted into the correct locus (Fig. 2d). We confirmed using sanger sequencing and TIDE analysis that the Piezo1 locus contains gene mutations 5 days following infection specifically in mixed brain cells infected with a Piezo1 knock-out virus (Fig. 2e). However, with a Western blot we observed minimal reduction in Piezo1 protein in the mixed glia cells 5 days following infection with the knock-out virus (Fig. 2f); this is likely due to the low proportion of OPCs within the mixed glia population. Future work will be to determine whether Piezo1 protein levels are reduced with the Nested CRISPR system in a purified population of OPCs.

As the Nested CRISPR construct works in vitro, we next determined whether this construct would

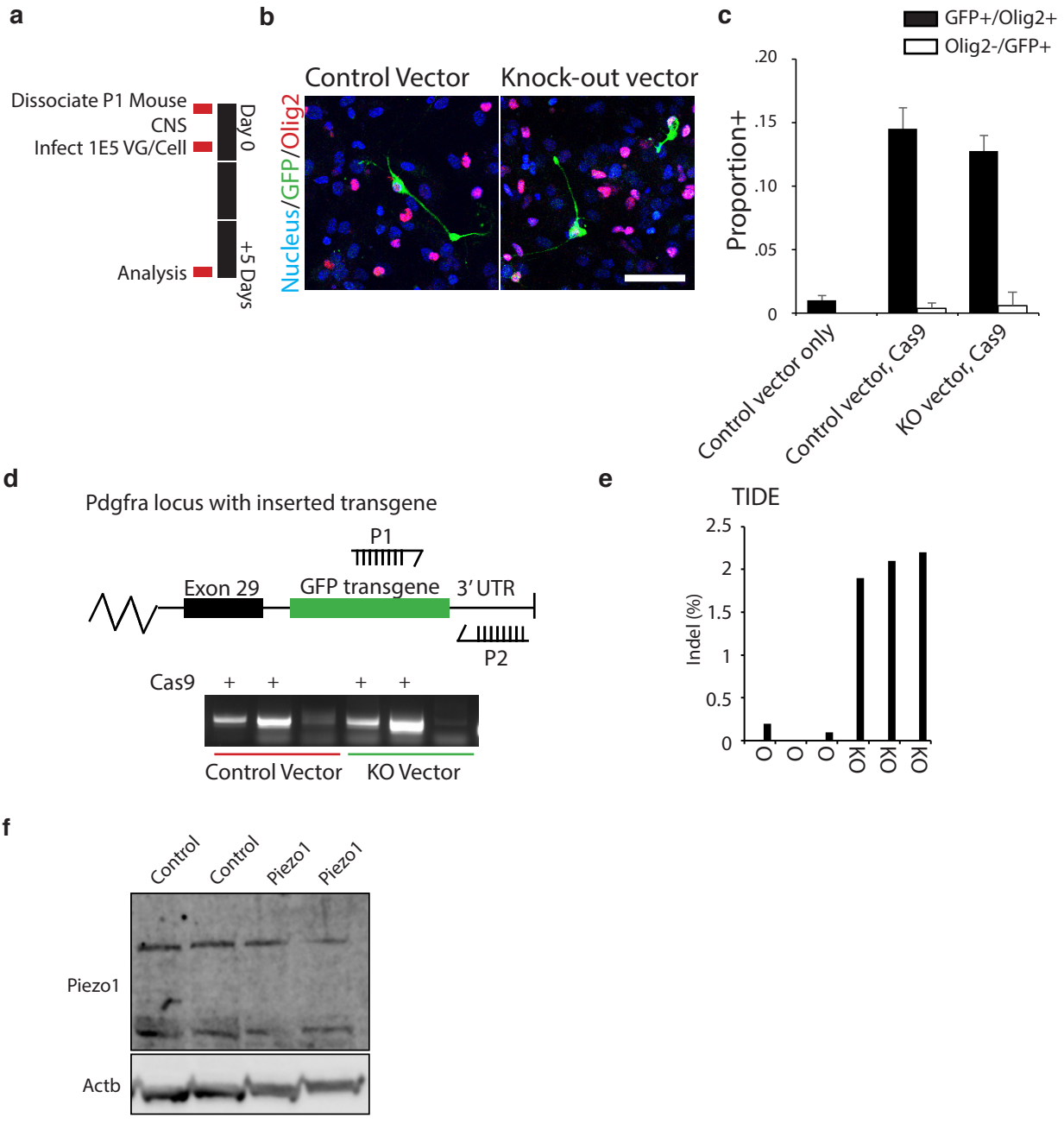

Figure 2. Validating nested CRISPR system *in vitro* for the Piezo1 locus. a-c, Representative images and quantifications of infected mixed glia cells with construct. Quantifications represent positive proportion of either GFP+ cells out of total Olig2 expressing cells or proportion of Olig2 expressing cells out of total GFP expressing cells. Averages represent means N=3 biological replicates and error bars represent standard deviation. Scale bars show 50µm. d, A schematic and a DNA gel of the Pdgfra locus following CRISPR/Cas9-mediated knock-in confirms construct knock-in in the correct position. P1 signifies forward primer while P2 represents the reverse primer used for the PCR. e, Indel detection of the Piezo1 locus confirmed by Sanger sequencing and TIDE analysis. f, Western blot shows minimal reduction in Piezo1 protein 5 days following infection. Here and throughout chapter, ≥200 cells were counted per biological replicate.

work in vivo. To test the efficacy of the vector, we tail vein injected 5 x 10^{11} of each of the knock-in vector and the Cas9 vector in 12 week-old mice (Fig. 3a). After 21 days, we perfusion fixed the animals. In both the control, non-targeting gRNA and the Piezo1 targeting knockout vector, we found GFP expressing cells across the CNS, including the cortical grey matter, the striatum, the corpus callosum, the cerebellum, and the spinal cord (Fig. 3b-d). We found that nearly 30% of Olig2 expressing oligodendroglia lineage expressing cells expressed GFP within the cerebellum and the cortical grey matter. In the corpus callosum we found nearly 50% of all Olig2 expressing cells also expressed GFP. Olig2 labels all cells of the lineage, both the OPC and its progeny, the oligodendrocyte, but the proportion of Olig2 expressing cells that express GFP reflects the ratio of OPCs to oligodendrocytes. This suggests that the vast majority of OPCs in the CNS successfully received the transgene. Moreover, across the CNS, very few GFP labelled cells were Olig2 negative, suggesting the expression of the knock-in cassette in the Pdgfra locus is highly selective for the OPC population. To confirm correct integration of the transgene within the Pdgfra locus, we isolated DNA from fresh CNS tissue of infected animals and performed a PCR (see Fig. 2d). Similar to *in vitro*, we found correct transgene integration in animals infected with both the Cas9 and non-targetting or Cas9 and Piezo1 KO vectors, but not in animals infected with the GFP vector only (Fig. 3e). As the construct correctly integrates into significant numbers of adult CNS, we next determined whether the Pdgfra driven Piezo1 gRNA was sufficient to create insertion-deletion mutations (indels) in the Piezo1 locus in vivo. To test this, we homogenised adult cortex, PCR amplified the Piezo1 locus, Sanger sequenced the fragment, and performed TIDE analysis on the loci (Brinkman et al., 2014). We found that ~2-3% of the Piezo1 loci contained indels (Fig. 3f-g). In control non-targeting gRNA knock-in animals, we observed no significant indels at the Piezo1 locus. As we homogenised whole brain tissue, the exact proportion of OPCs with mutated Piezo1 cannot be determined with this approach. As referenced in the discussion, the rate of Piezo1 indels remains a main focus of future studies. However, together with the immunohistochemistry, we can confirm that GFP is expressed uniquely in the oligodendrocyte lineage.

As Piezo1 regulates proliferation rates *in vitro* as shown in chapter 4, we next looked at whether Piezo1 enhances OPC proliferation and differentiation in the context of CNS regeneration/remyelination. To test this, we tail vein injected 18 month-old aged animals with the vector pools. After 1 week, we demyelinated ventral spinal cord white matter by direct injection of 1% lysolecithin (Fig. 4a). At 13 days post lesion, we injected EdU, and one day after that, we perfusion fixed the animals. We found that in the GFP-only AAV infected animals, there were a high proportion of GFP expressing cells on the periphery of the lesion (Fig. 4b-f). These Olig2 expressing cells had a low rate of proliferation as

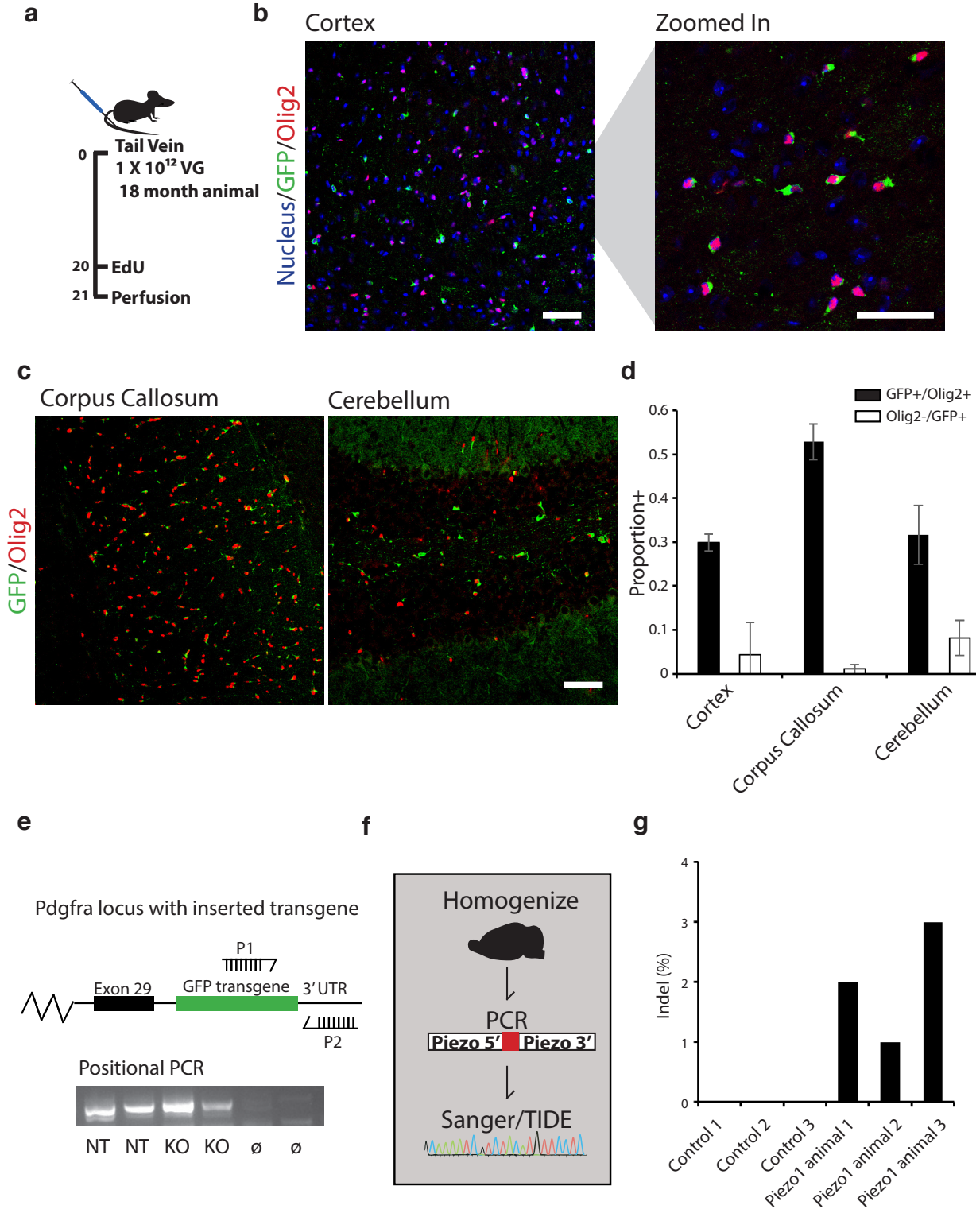
a
Tail Vein
1 X 10^12 VG
18 month animal
0
20
EdU
21
Perfusion
b
Cortex
Zoomed In
Nucleus/GFP/Olig2
c
Corpus Callosum
Cerebellum
GFP/Olig2
d
GFP+/Olig2+
Olig2-/GFP+
Proportion+
0.6
0.5
0.4
0.3
0.2
0.1
0
Cortex
Corpus Callosum
Cerebellum
e
Pdgfra locus with inserted transgene
P1
Exon 29
GFP transgene
3' UTR
P2
Positional PCR
NT NT KO KO ø ø
f
Homogenize
PCR
Piezo 5'
Piezo 3'
Sanger/TIDE
g
Indel (%)
4
3
2
1
0
Control 1
Control 2
Control 3
Piezo1 animal 1
Piezo1 animal 2
Piezo1 animal 3

Figure 3

Figure 3. Widespread and targeted Nested CRISPR in the adult CNS. a, A schematic outlining the experimental strategy. Animals were tail-vein injected with $5x10^{11}$ of both the knock-out and Cas9 AAV. The animals were perfusion fixed 21 days later or tissue was taken for DNA analysis. b-d, Representative images and quantifications of GFP/Olig2 co-expressing cells across multiple regions of the CNS. Data taken from N=3 control knock-out animals. Scale bars represent 50µm. e, Schematic of modified genomic locus and PCR confirms correct genomic integration of knock-in fragment from N=2 biological replicates of the non-targeting control vector (NT), the Piezo1 knock-out vector (KO), or a non-infected animal (ø). f, Schematic determining Piezo1 knockout efficiency following AAV injection. DNA was isolated from the homogenized brains of tail-vein injected animals, the Piezo1 locus was Sanger sequenced, and analyzed using TIDE. g, TIDE results show INDEL efficiency following Piezo1 gene targeting using the nested CRISPR system.

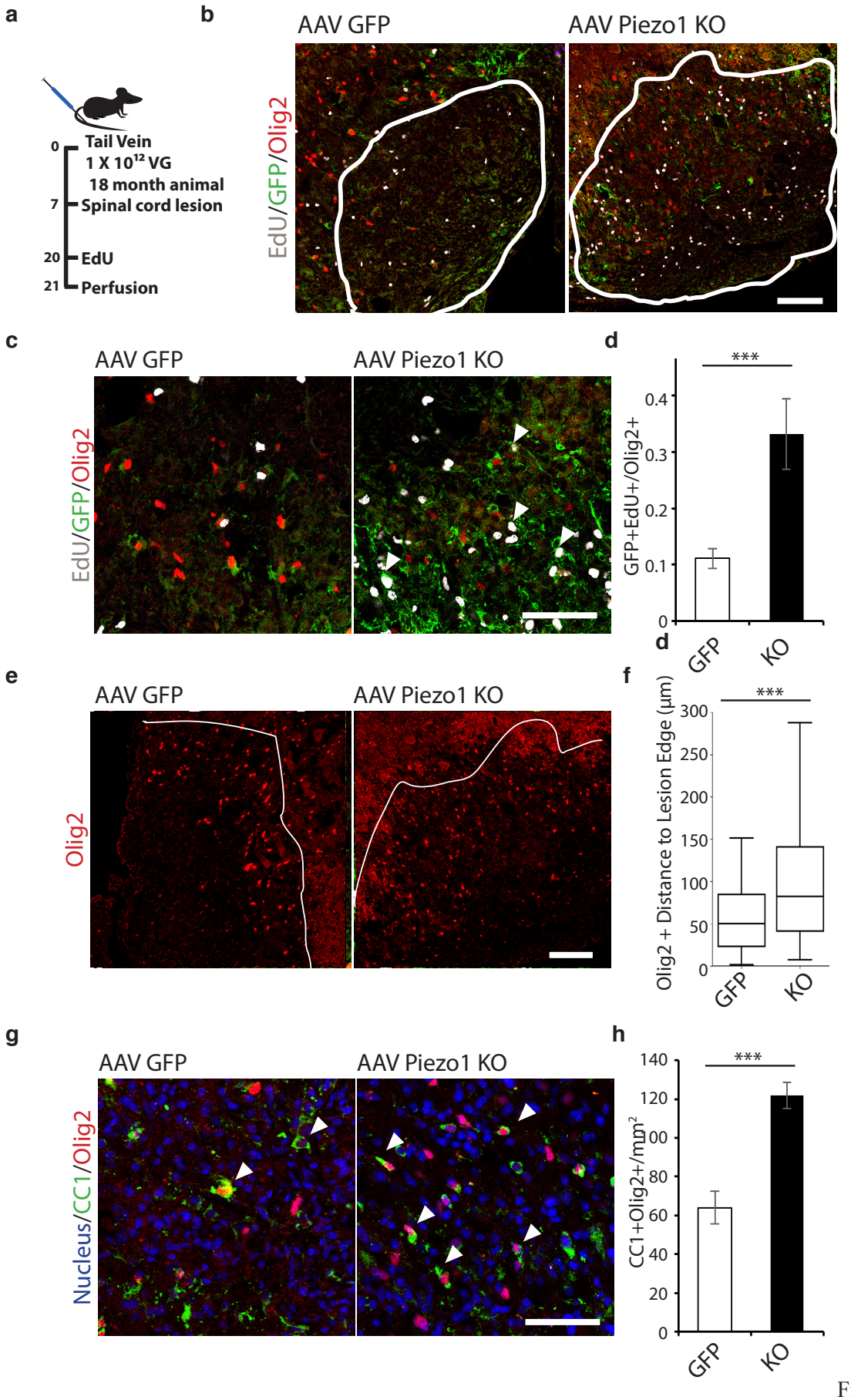
a
b
AAV GFP
AAV Piezo1 KO
EdU/GFP/Olig2
0
Tail Vein
1 X 10^12 VG
18 month animal
7
Spinal cord lesion
20
EdU
21
Perfusion
c
AAV GFP
AAV Piezo1 KO
EdU/GFP/Olig2
d
***
GFP+EdU+/Olig2+
0.4
0.3
0.2
0.1
0
GFP
KO
e
AAV GFP
AAV Piezo1 KO
Olig2
f
***
Olig2 + Distance to Lesion Edge (µm)
300
250
200
150
100
50
0
GFP
KO
g
AAV GFP
AAV Piezo1 KO
Nucleus/CC1/Olig2
h
***
CC1+Olig2+/mm2
140
120
100
80
60
40
20
0
GFP
KO

Figure 4

Figure 4. Piezo1 knockout using nested CRISPR system promotes regeneration in the aged CNS. a, Schematic of spinal lesioning following tail-vein injection of CRISPR system. b, Representative images of white matter lesion with white line indicating the lesion area. Scale bar represents 100μm. c-d, Representative images and quantifications from N=3 mice of EdU incorporation into Olig2/GFP expressing cells in the lesion core. e-f, Representative images and box whisker plot quantification of white matter lesion stained only for Olig2 show increased OPC infiltration into the lesion site following Piezo1 knockout. Lesion site indicated by white line. Scale bar represents 100μm. g-h, Representative images and quantifications of the number of CC1+/Olig2+ per mm2 of lesion area in N=3 control or Piezo1 knockout animals. Throughout figure, *** represents p-value significance of ≤.01 as determined by a one-way ANOVA. Here and throughout chapter, lesions were performed by Dr. Chao Zhao, affiliated with Robin Franklin's group.

indicated by incorporation of EdU. In the Piezo1 KO infected animals, however, Olig2 expressing cells migrated deep within the lesion core and had ~3.5 fold higher rates of proliferation compared to the control. As previously reported, remyelination occurs inefficiently in the aged adult (Sim et al., 2002). In the control GFP aged lesion, we found the large majority of CC1+/Olig2+ oligodendrocytes at the periphery of the lesion, with few differentiated cells within the core of the lesion. In the aged Piezo1 KO animal, however, we found a two fold increase of differentiated oligodendrocytes within the lesion, many of them within the lesion core (Fig. 4g-h). Together, these results show that Piezo1 regulates the activity-state of aged OPCs; by knocking it out, specifically in OPCs, we improve the proliferation and differentiation capacity of OPCs in an aged lesion.

We next made small modifications to the AAV system to see if it would be possible to knock-in GFP into the Piezo1 locus, only in cells expressing Pdgfra, effectively creating an OPC-specific Piezo1 reporter construct. To do so, we repositioned the ribozyme flanked Piezo1 gRNA such that all Pdgfra expressing cells express the Piezo1 gRNA (Fig. 5a). As such, all cells expressing Pdgfra would also express the Piezo1 gRNA. Immediately downstream of Piezo1 gRNA sequence, we put a second round of reverse complement Piezo1 gRNA cut sequences flanking an IRES-GFP sequence. This way, in Pdgfra expressing OPCs, the Piezo1 gRNA would be expressed, the IRES-GFP sequence would be excised and inserted into the Piezo1 locus via NHEJ. This way, all Pdgfra- Piezo1- co-expressing OPCs would be labelled with GFP.

To confirm that this system works in vitro, we again over-night infected dissociated p1 mouse neonates with either a combination of Cas9 and the knock-in vector or with the Cas9 vector alone. We found significant proportions of Olig2 expressing cells expressing GFP, showing an exclusive knock-in into the oligodendroglial lineage (Fig. 5b). To confirm whether this system works *in vivo*, we infected N=3 12 week old animals with 5×10^{11} of each of the viral particles (Fig. 5c). At 3 weeks post tail-vein injection we again observed a high proportion of Olig2 expressing cells co-expressing GFP (Fig. 5d). In the corpus callosum there were significant numbers of Olig2/GFP co-expressing cells. Moreover, GFP expression was limited to Olig2 expressing cells, again confirming that the system is specific to OPCs. Future work must determine the extent of GFP labeling present across the CNS. Finally, to show the correct integration of the transgene *in vivo*, we performed a PCR of homogenised cortex and found proper integration of GFP into the Piezo1 locus, only in the animals that received the multiplexed nested CRISPR construct (Fig. 5e). In this way, we effectively created a cell-type specific, gene-specific reporter in the adult CNS 21 days following a single intravenous injection of AAV particles.

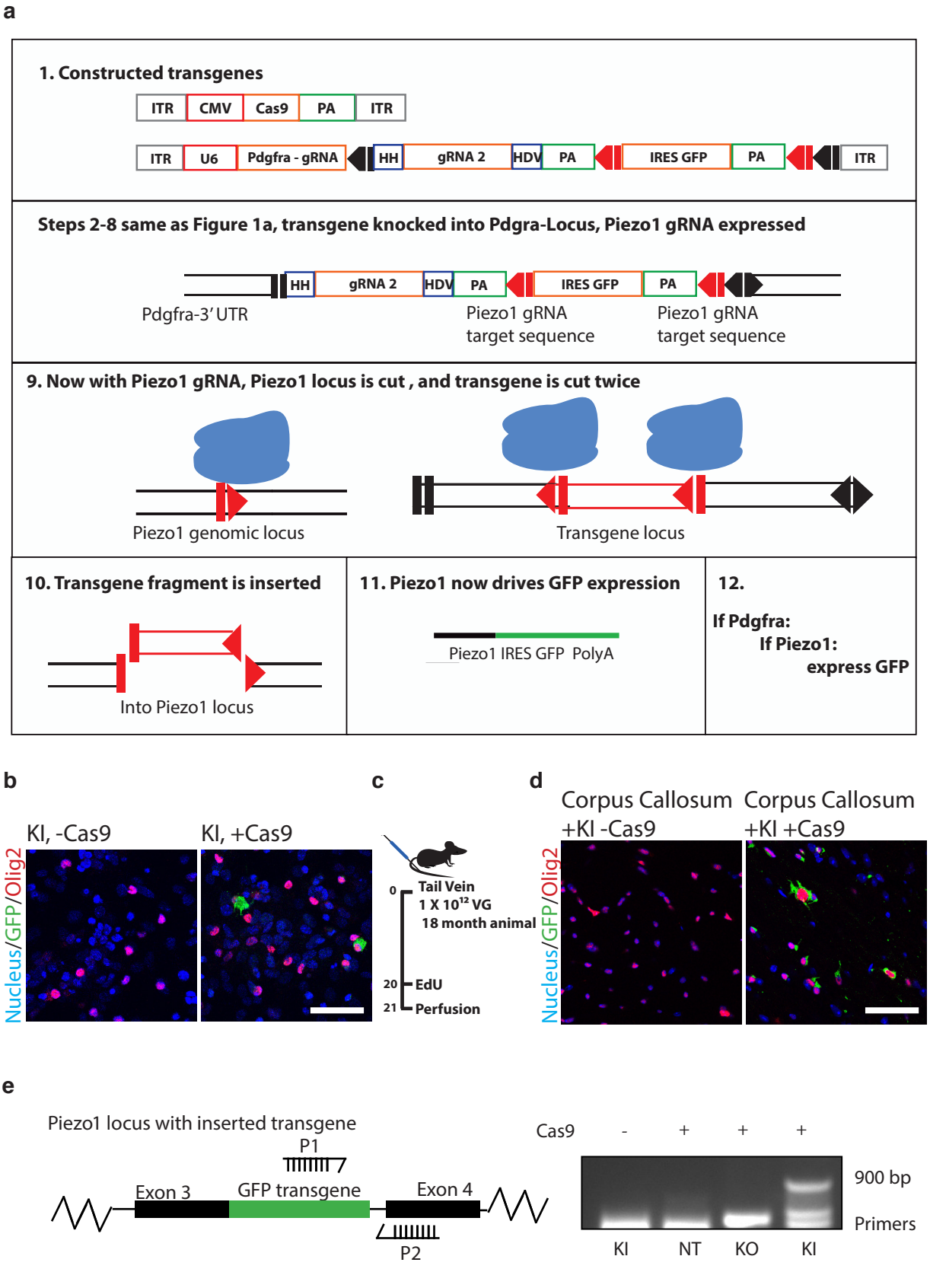
a
1. Constructed transgenes
ITR
CMV
Cas9
PA
ITR
ITR
U6
Pdgfra - gRNA
HH
gRNA 2
HDV
PA
IRES GFP
PA
ITR
Steps 2-8 same as Figure 1a, transgene knocked into Pdgra-Locus, Piezo1 gRNA expressed
HH
gRNA 2
HDV
PA
IRES GFP
PA
Pdgfra-3' UTR
Piezo1 gRNA target sequence
Piezo1 gRNA target sequence
9. Now with Piezo1 gRNA, Piezo1 locus is cut , and transgene is cut twice
Piezo1 genomic locus
Transgene locus
10. Transgene fragment is inserted
Into Piezo1 locus
11. Piezo1 now drives GFP expression
Piezo1 IRES GFP PolyA
12.
If Pdgfra:
If Piezo1:
express GFP
b
KI, -Cas9
KI, +Cas9
Nucleus/GFP/Olig2
c
0
Tail Vein
1 X 10^12 VG
18 month animal
20
EdU
21
Perfusion
d
Corpus Callosum +KI -Cas9
Corpus Callosum +KI +Cas9
Nucleus/GFP/Olig2
e
Piezo1 locus with inserted transgene
P1
Exon 3
GFP transgene
Exon 4
P2
Cas9 - + + +
900 bp
Primers
KI NT KO KI

Figure 5

Figure 5. Multiplexed Nested CRISPR shows Piezo1 is expressed by Pdgfra+ OPCs. a, Schematic overview of the Nested CRISPR system. If a cell expresses Pdgfra, a Piezo1 gRNA is expressed and an IRES GFP DNA fragment is inserted into the Piezo1 locus. b, Mixed glia cells infected with AAV overnight and left for 5 days confirm that there is GFP expression and that the GFP expression is specific for OPCs. c-d, Schematic and representative images of young adult (12 week) mouse cortex 21 days following a tail vein-injection of the knock-in cassette with Cas9 or the knock-in cassette on its own. Images show widespread GFP/Olig2 co-localization. e, Schematic and DNA gel showing correct genomic integration of the IRES-GFP cassette into the Piezo1 gene locus in not in the non-targeting gRNA vector (NT) or in the previously reported knock out vector (KO). P1 represents the forward primer for the 'positional PCR' and P2 shows the reverse primer. Across figure, scale bars represent 50μm.

Discussion

Here, we have shown the role of the mechano-sensor Piezo1 in tissue homeostasis and in CNS regeneration. To elucidate its role, we have developed a dual AAV-system using the synthetic serotype PHP-EB. We have shown the capacity for this system to efficiently engineer the nervous system's dominant stem cell population, the OPC. Using synthetic biology techniques, we have created a Nested CRISPR system, in which the CRISPR-mediated knock-in of a secondary gRNA downstream of a cell-type specific promoter enables a cell-type specific gene knock-out. Specifically, we have applied this system to understanding Piezo1, and have shown that in the context of an aged demyelinating lesion, the knockout of Piezo1 allows for enhanced OPC proliferation and differentiation within the lesion environment. Finally, to better understand the expression of Piezo1 across the CNS, we generated a multi-levelled Nested CRISPR system. This system allows us to engineer an OPC-specific Piezo1 GFP reporter in an adult mouse. The implications for these findings are manifold: we have identified a major role for Piezo1 in remyelination, and emphasise the importance of biophysical pathways for regenerating the aged CNS. Additionally, we have created an in vivo CRISPR-mediated genome engineering system in which specific cells of the adult can be targeted and subsequently genome engineered. This system is highly modular and these findings could have implications for the broader biological community.

Limitations of the Nested CRISPR System

The synthetic PHP-EB AAV serotype delivered intravenously can deliver genetic information to ~80% of cells in the CNS (Challis et al., 2018). This makes the PHP-EB AAV vector one of the most powerful tools for the neuroscience community. AAVs, however, have their limitations. AAVs have a maximum gene carrying capacity of ~5 kb, including the ~300 base pairs required for transgene packaging into the AAV. This size constraint limits the ability to deliver large or poly-cistronic transgenes.

A major challenge in gene therapy is delivering transgenes to specific cells within the body. This would minimize the off-target effects of the therapeutic and provide a competitive advantage over currently available broad-spectrum untargeted pharmaceuticals. Using cell-type specific promoter sequences, the authors in the original publication demonstrate that they are able to deliver fluorescent genes to specific-cells within the CNS. Fluorescent proteins are relatively short ~750 bp, and the cell-type specific promoter sequences they use are pre-characterized, short (~500 bp), and efficiently expressed. Other cell types such as the OPC have undefined cell-type specific promoter sequences while

oligodendrocytes have much larger >1000bp promoter sequences (Challis et al., 2018).

Even if a small promoter sequence has been previously described, the capacity for AAVs to deliver transgenes is limited. For one thing, many genes are larger than the 5000bp AAV size constraint. Here, we show the importance of Piezo1 on the activity of adult OPCs. However, gain of function experiments, wherein Piezo1 is overexpressed, would not be feasible with the AAV system as the Piezo1 transgene itself is >7500 bp. This size constraint is a limitation for therapeutics as well. Duchenne muscular dystrophy is caused by a mutation in the gene dystrophin (>11000)(Tabebordbar et al., 2016), and, due to its size, delivery of the corrected transgene is not feasible with AAVs.

These limitations pose major hurdles for CRISPR mediated gene editing. The CRISPR gene Cas9 is itself large (>4000 bp). As such, combining Cas9 with a tissue-specific promoter, such as MBP, is not feasible. Moreover, OPC-specific targeting of Cas9 expression is not feasible due to OPCs lack of a defined cell-type specific promoter sequence. Finally, even with a short promoter sequence and a synthetic short poly-adenylation sequence, a Cas9 AAV vector is already at maximal size capacity. This means that multiplexing the Cas9 gene with a sequence specific gRNA already surpasses the size limitations of the AAV vector.

In this chapter, I combine three different technologies to create a cell-type specific gene knock-out in an adult mouse brain. As referenced previously, all 3 technologies were independently developed and published. However, the work in this chapter is largely preliminary and a number of aspects of the Nested CRISPR system remain unknown. Throughout the text, I show that GFP protein expression co-localises largely with Olig2 expressing oligodendrocyte lineage cells and that, with PCR, the genomic fragment integrates in the right locus. However, future work must confirm that the IRES-GFP-gRNA transgene is uniquely integrated in the correct Pdgfra locus. This problem of the specificity of transgene integration is compounded by the fact that we are introducing genomic fragments into aged animals. As shown in Chapter 6 of this thesis, there is increased DNA damage in OPCs with ageing. This increase in DNA damage and presumably double stranded DNA breaks means that the NHEJ machinery may insert the GFP-gRNA transgene into alternative loci in the genome, not just the locus cut by the Cas9 enzyme. Moreover, as the transgene is preceded by the IRES sequence, if the transgene is inserted into a transcribed region of the genome, GFP will be translated, regardless of its site of genomic integration; this would significantly undermine the OPC specificity of the system as cells that transcribe these other loci would target Piezo1 for degredation. One way to test the precision of the system would be to FACs sort GFP expressing cells from an infected aged brain and perform deep

DNA sequencing. Doing so, we would be able to calculate the frequency with which the transgene appears at the correct loci. Only then could we confirm whether the Nested CRISPR is specific enough to be used in the aged CNS.

Even if the system does specifically introduce the GFP-gRNA transgene to the Pdgfra locus, it remains unclear whether the secondary Piezo1 targeting transgene is efficient at creating insertion-deletions in the Piezo1 locus. In this chapter, we homogenised whole mouse brain cortex and found low rates of mutations at the Piezo1 locus both in vitro and in vivo. As OPCs are only 5% of the total cells within the CNS and if this Nested CRISPR system is truly cell-type specific, then we would expect the mutation rate at the Piezo1 locus to be at most 5%. To truly understand the rate of Piezo1 knockout *in vivo* in OPCs, Pdgfra expressing OPCs must be FACs sorted from the brain and analysed in a similar method as described in this chapter. While the TIDE analysis provides a simple tool for understanding the total number of insertion-deletions in a population of cells, the only method for understanding the per-cell mutation rate across both Piezo1 alleles is to perform single-cell amplicon sequencing; this approach would determine the proportion of cells with either a heterozygous or a homozygous loss of function of mutation at the Piezo1 locus, as described previously (Suzuki et al., 2016). Both approaches for determining the in vivo Piezo1 mutation rate are ongoing as such analysis is *required* to prove the efficacy of the Nested CRISPR system.

Overcoming AAV limitations

To evade these size and promoter limitations, previous work has shown that Cas9 can be divided up into two fragments of ~2000 bp packaged into two separate AAVs and subsequently injected into animals (Yang et al., 2016). There, the two Cas9 fragments are transcribed separately but the protein fragments complex with one another once translated. In this way, the authors are able to multiplex Cas9 with a fluorescent protein and a sequence specific gRNA. With this approach, it would be possible to target oligodendrocyte-specific gene promoter MBP with Cas9, a fluorophore, and a sequence-specific gRNA, allowing for oligodendrocyte-specific genome modifications.

Many cells, however, lack a defined cell-type specific promoter sequence. As such, targeted, cell-type specific transgene delivery for cell-types such as OPCs remains undescribed in the literature. To overcome these limitations, we used a dual CRISPR AAV system, as previously described (Suzuki et al., 2016). In this work the authors infect the muscle following the delivery of two AAV particles: one

encoding Cas9 and the other a gRNA sequence, and a knock-in cassette flanked by gRNA cut sites. If a cell is infected with both particles, Cas9 will complex with the gRNA, cutting the genome and releasing the knock-in cassette from the transgene construct. The knock-in cassette is then inserted into the genome using non-homologous end-joining. Doing so, the authors are able to express GFP from an endogenous promoter sequence. We combined this technique with a previously described synthetic biology technique in which gRNAs can be expressed from cell-type specific promoters using self-cleaving ribozymes (Nissim et al., 2014). Together, we knock-in a gRNA into a cell-type specific promoter, and thereby make genome modifications specifically in the OPC in the CNS.

This system is highly modular, capable of driving multiple-levels of genome manipulation from any gene expressed in a given cell type. However, a simple all-in-one AAV would likely increase the efficiency and simplicity of the system. With our system, this is not feasible due to size constraints of the well-characterized Cas9 derived from the bacterial species Streptococcus pyogenes. Recent work has identified Cas9 orthologues across a number of bacterial species (Kleinstiver et al., 2015). The smallest orthologue is Cas9 derived from the bacterial species Campylobacter jejuni (cj Cas9). Due to its size of ~2900 bp, cjCas9 has generated excitement in the field of in vivo gene editing and has already been used to successfully genome edit in vivo using an AAV (Kim et al., 2017). cjCas9 is ~1100 bp smaller than the originally described Cas9 and provides 1100 bp extra for transgene delivery. Using this extra space for transgene delivery, we hope to combine our ribozyme-mediated cell-type specific CRISPR technology with the cjCas9 to create an all-in-one nested CRISPR system.

A gene-specific promoter database for all coding genes would diminish the advance of this nested CRISPR system. If the Pdgfra locus were to have a well-established and short promoter sequence, then we could drive Cas9 and/or gRNA expression using this promoter; doing so, we could drive OPC-specific gene editing. This would circumnavigate the need to first knock-in a ribozyme-flanked gRNA into the Pdgfra locus, likely making the entire cell-type specific CRISPR system more efficient. Publically available epigenetic databases open up our capacity to readily identify the promoter regions of specific genes (Rosenbloom et al., 2012). Open chromatin domain sequencing (DNAse-seq and ATAC-seq) of fetal human brain reveals distinct open chromatin domains 500-2500 bp upstream of the Pdgfra locus. Future work will be to dissect the components of these open-chromatin domains, identifying the minimal promoter components that drive Pdgfra expression in OPCs with the hopes of one day driving the CRISPR/Cas9 system from a minimal Pdgfra promoter sequence. By driving the CRISPR machinery from a cell-type specific promoter, I hope to circumnavigate many of the discussed limitations of the

Nested CRISPR system.

Improving on the system

Here, we report on our ability to create multi-level CRISPR knock-ins, in which the expression of a single gene can drive the knock-in of a second gene at a separate locus. The design of this system is not without its limitations. Recently, Cas9 cutting has been shown to have a multitude of off target effects, including large scale insertions and deletions (Kosicki et al., 2018). However, this paper used the PiggyBac transposase system combined with Cas9 to introduce genome modifications. This is an unusual approach for introducing the CRISPR technology into cells and the combinatorial effect of Cas9 with transposase remains unknown. Similarly, it remains unknown whether other methods for the introduction of CRISPSR machinery would have such widespread off-target effects.

Despite the limitations of this previous study, it is highly plausible that long-term expression of Cas9 would have adverse effects on genome integrity. As such, a 'closed loop' nested CRISPR system would help mitigate any potential off target effects. One could imagine a system in which the CRISPR machinery itself is shut off following indel-creating/fragment knock-in. Our multi-leveled system relies on two sequence-specific gRNAs to direct the Cas9 first to the Pdgfra locus and then to the Piezo1 locus. The Pdgfra gRNA is expressed using the constitutively active U6 promoter. Previous work in vitro created synthetic programmable CRISPR networks in which the expression of one gRNA shut off the expression of another gRNA (Nissim et al., 2014). The authors multiplexed the first gRNA using self-cleaving ribozymes with an additional sequence that was antisense to the second gRNA; doing so, the authors created a gRNA mop. When the first gRNA was expressed, the mop was also expressed and thereby inactivated the second gRNA. With only a few modifications, we could similarly include a mop sequence such that once the Piezo1 gRNA is integrated into the Pdgfra locus, the Pdgfra gRNA is mopped up and inactivated. Finally, one could imagine a system in which once the GFP fragment is knocked into the Piezo1 locus, a ribozyme flanked Cas9 targeting gRNA is also expressed; once nested gene-editing is completed, Cas9 protein would target the Cas9 transgene itself, thereby turning off the system. Future work will be to tinker with these modifications to create a closed loop CRISPR system, improving upon the efficacy of the system and avoiding any off-target effects.

This multiplexed nested CRISPR system is highly modular and can be used to better understand the role of individual genes in specific cell-types. Here, we employed the system to better understand the

role of Piezo1 in Pdgfra expressing OPCs in the aged 18-month-old CNS. Using the nested CRISPR system, we were able to do this rapidly and cost-effectively. The virus took 2-3 weeks to construct, synthesize, and validate in vitro and an additional 3 weeks following tail-vein injection. After just 6 weeks, we had a 19-month-old aged transgenic animal, a process that previously would have taken years and with high-experimental risk. Moreover, the construction of these viruses is scalable, allowing us to create multiple gene-targeting vectors in the time it would take to make just one. In the future, we will use this technology as a platform to better understand the role of individual genes on adult and aged OPC activation and differentiation in vivo. We will be able to do so quickly and for multiple genes, allowing for rapid-hypothesis testing in animal models. Despite the power of this system to rapidly generate animal models, the potential off target effects of Cas9 and the imprecise nature of DNA repair via NHEJ means that the Nested CRISPR approach will unlikely be used as a cell-type specific gene knock out strategy for CRISPR-based human therapeutics.

Piezo1 and OPCs

In chapters 4 and 5 of this thesis, we look at the effect of Piezo1 on OPCs *in vitro* and *in vivo* in the context of remyelination. However, it remains unknown whether Piezo1 has a role in OPCs in post-natal development or in steady-state adult brain homeostasis. To test this, we are currently conducting experiments in which an *in vivo* AAV CRISPR system was injected into the tail vein of P1 mice pups. After 6 weeks, we will look to see if OPCs without Piezo1 have phenotypic differences in total cell number or in the total numbers of oligodendrocytes. As I hypothesise in Chapter 4, Piezo1 may be a regulator of total OPC number in the CNS and prevents cellular crowding. I expect that without Piezo1, there will be an increase in total OPC cell number and an increase in the proportion of proliferating OPCs. Finally, while the Nested CRISPR system allows for the rapid hypothesis testing of individual genes in OPCs, the effects of AAV-mediated CRISPR are heterogeneous—with each cell infected containing different rates of mutation depending on the region of the CNS. As such, there is still a role for traditional animal models that rely on the Cre recombinase technology. The most robust method for determining the role of Piezo1 in development, homeostasis, and in remyelination is still to breed Piezo1-floxed animals with animals that contain an OPC-specific Cre Recombinase transgene. Perhaps, with continuing advances in vectors that target specific tissues and the develop-

ment of technologies with increased genome engineering efficiency eventually traditional transgenic mouse models could be replaced all together. Until then, a transgenic mouse-model would allow for an inducible, widespread, and uniform Piezo1 knockout in OPCs and would likely more fully address the role Piezo1 in the CNS.

Chapter 6

Activity-state via the oncogene Myc describes the age state of CNS progenitor cells

Like many adult stem cell populations, the capacity of oligodendrocyte progenitor cells to proliferate and differentiate is significantly impaired with ageing. Previous *in vivo* work has shown that tissue-wide transient expression of the reprogramming factors Oct4, Sox2, Klf4, and Myc extends lifespan and enhances somatic cell function. Here we show that just one of these reprogramming factors, Myc, is required to rejuvenate aged OPCs as determined both by *in vitro* assays and by transcriptome profiling. Neonates that are treated with an inhibitor for Myc lose their capacity to both proliferate and differentiate *in vitro*. Finally, re-purposing the CRISPR technology described in chapter 5 of this thesis, we show that OPCs that have increased Myc expression *in vivo* both proliferate and differentiate more efficiently in an aged lesion environment. Together, these results directly link Myc activity to cell age-state and thereby provide further insights into the biology of ageing.

In normal development, mammalian embryonic stem cells uni-directionally differentiate into adult somatic cells. During this process, cells progressively commit to the various lineages of the adult organism. In the adult, a reserve pool of tissue-specific adult stem cells, however, do not terminally differentiate; rather, they remain undifferentiated, differentiating into tissue-specific cell-types as needed to maintain homeostasis or repair damaged tissue. In the CNS, the most widespread and abundant cell population is the OPC (Dawson et al., 2003). In adulthood, OPCs self-renew and give rise primarily to new myelinating oligodendrocytes. OPCs remain actively cycling and differentiating well into adulthood (Hill et al., 2018; Yeung et al., 2014). However, with ageing, the capacity for OPCs to both self-renew and differentiate into myelinating oligodendrocytes is significantly impaired (Psachoulia et al., 2009). In toxin-induced lesion models of white matter remyelination, the OPCs fail to remyelinate the damaged tissue (Sim et al., 2002). This loss of function is likely relevant for patients with demyelinating diseases such as multiple sclerosis.

In the past decade, our understanding of the ageing process has changed dramatically. With the discovery of pluripotent stem cells and subsequent work, it is now clear that cells do not undergo im-

mutable changes with ageing. Rather, with the reprogramming factors Oct4, Sox2, Klf4, and Myc, aged cells, regardless of their physiological age, can be reset to their embryonic form, thereby erasing all the cellular hallmarks of ageing (Mertens et al., 2015; Takahashi et al., 2007). In the most impressive study to date, the authors hypothesized that while long term exposure to the reprogramming factors reset cellular age-state entirely, short transient bursts of the reprogramming factors would only partially reprogram the cell to a younger more rejuvenated version (Ocampo et al., 2016). Doing so, the authors observed that transient bursts of expression of these four reprogramming factors extends the lifespan and the regenerative capacity of aged animals.

Much work has gone into restoring the regenerative capacity of aged OPCs (Shen et al., 2008). Aged OPC function can be enhanced by overexpressing histone deacetylases. In parabiosis studies, the aged OPCs can more efficiently remyelinate aged lesioned tissue when they are exposed to systemic factors from the young circulatory system (Ruckh et al., 2012). Both studies show that the function of the aged OPC can, at least in part, be restored. Despite these original findings, little is known about the molecular processes underlying the ageing of OPCs. Moreover, it remains unknown what role, if any, the reprogramming factors have on the ageing of progenitor cells.

Here, we use the principals of iPS cells and partial reprogramming to identify whether any of the individual or combinations of reprogramming factors have the capacity to rejuvenate aged progenitor cells. Using mRNA overexpressing vectors on primary isolated aged OPCs, we identify the reprogramming factor and oncogene Myc alone as sufficient to reverse the hallmarks of OPCs ageing. Conversely, inhibiting the function of Myc in neonatal OPCs using a small molecule, we inhibit the *in vitro* generative capacity of the cells. Using transcriptomics and *in vitro* assays to detect genetic and epigenetic stability we find that OPC age-state can be modulated by the presence or absence of Myc activity. Finally, using the novel technology of systemically administered AAVs and *in vivo* CRISPR we have found that Myc overexpression in OPCs promotes their self-renewal and differentiation capacity, even in aged animals.

While systemic, transient overexpression of the OSKM reprogramming factors have been shown to extend lifespan and regenerative capacity in aged mice, the role that each of the reprogramming factors play in the observed effects of partial reprogramming remains unknown (Fig. 1a). Moreover, it is unclear whether all or just some of the reprogramming factors have a role in rejuvenation. We hypothesized that the reprogramming factors with the largest role in regenerating aged progenitor cells would

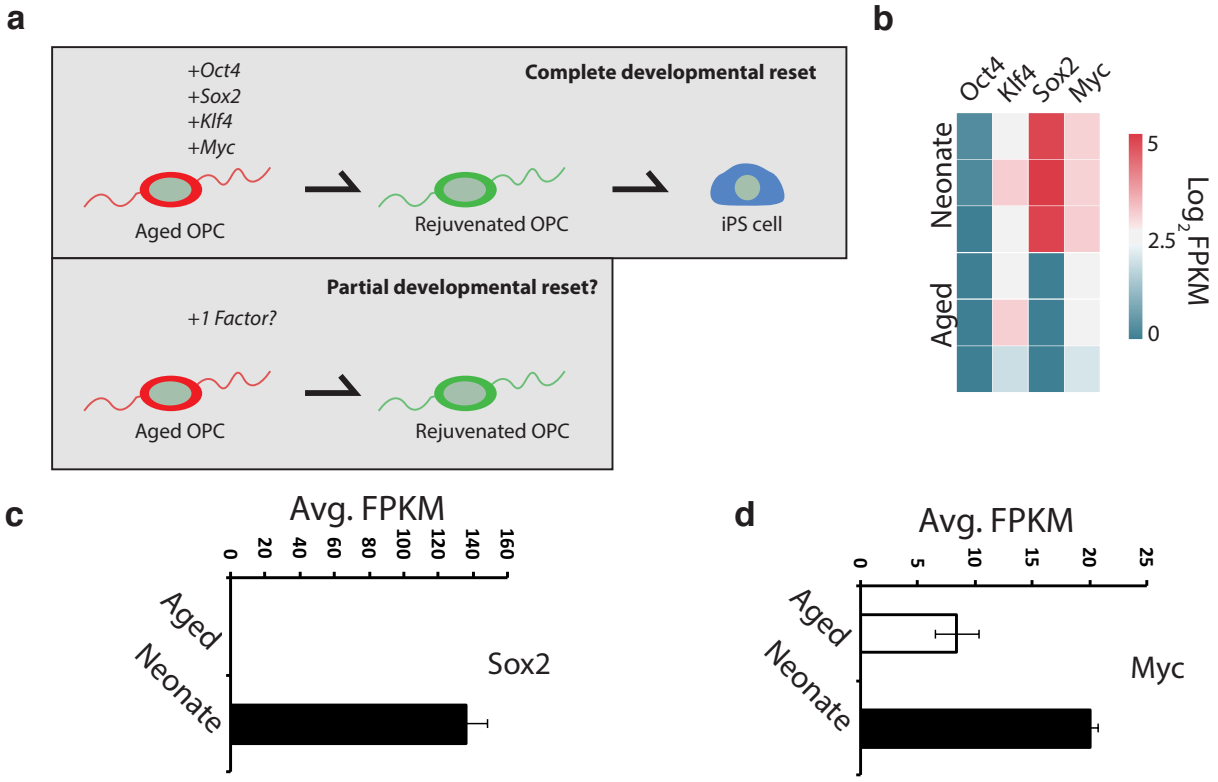

Figure 1. Reprogramming factors are expressed by primary neonatal but not aged OPCs. a, Cartoon diagram illustrating the underlying principle of partial reprogramming for rejuvenating aged OPCs. b, A heatmap of the log2 fold change FPKM values of the reprogramming factors Oct4, Sox2, Kl4, and Myc in neonatal versus aged rat OPCs. c-d, Mean FPKM values for Sox2 and Myc in neonatal and aged OPCs. Throughout figure, bar charts represent mean from N=3 biological replicates and error bars represent standard deviation.

be the factors that are expressed in neonatal OPCs, when OPCs are at their most generative. Using sequencing data from primary aged (≥14 months) and neonatal (≤p7) rat OPCs isolated using magnetic associated cell sorting (MACs) based on the OPC marker A2B5, we observed the transcription factors Sox2 and Myc to be expressed in neonatal OPCs but not in aged OPCs (Fig. 1b-d). The other factors Klf4 and Oct4 are not expressed at any age-point in the OPC lifecycle.

As Sox2 and Myc are the only two transcription factors ever expressed by neonatal OPCs, we hypothesized that over-expression of the factors individually could partially re-program primary aged OPCs *in vitro*. To accomplish this, we MACs sorted aged OPCs and plated them in high concentrations of growth factors. From previous work, we have found that the standard neonatal *in vitro* conditions of OPCs with the factors Pdgf and Fgf alone are insufficient to drive the proliferation of aged progenitor cells. One day following plating, we transfected the aged cells with synthetic modified mRNAs encoding eGFP, Sox2, Myc, or a combination of Sox2 and Myc. Transfection of eGFP encoding mRNA into aged OPCs is highly efficient, with over 80% of OPCs expressing the gene after 48 hours (Fig. 2a-b). We found high levels of proliferation of aged OPCs in the Sox2, Myc transfected conditions but a much less pronounced effect when Sox2 was transfected alone (Fig. 2c-d). However, we found that Myc overexpression alone recapitulated the phenotype of the combination Sox2, Myc treatment; 4 days after 1 round of transfection of Myc, 19 month old OPCs had a ~9 fold increase in their rates of proliferation as labeled by EdU incorporation and co-localization with the oligodendrocyte lineage marker Olig2 (Fig. 2e-f). When the cells were put into differentiation condition media with the pro-differentiation signal T3 for five days, aged OPCs transfected with GFP had low rates of differentiation ≤5% while those transfected with Myc efficiently differentiated into oligodendrocytes as defined by their co-expression of Olig2 and myelin basic protein (MBP) (Fig. 2g-i). The overexpression of the oncogene Myc not only increased aged OPC proliferation but also their differentiation.

As Myc alone is sufficient to promote both the proliferation and differentiation of aged OPCs *in vitro*, we hypothesized that Myc activity is necessary for the self-renewal and differentiation capacity of neonatal OPCs. To test this, we used the low molecular weight compound 10058-F4 (Myci), which inhibits both Myc and n-Myc activity by blocking the dimerization of Myc and Max (Zirath et al., 2013). As such, it is a well-established small molecule for selectively studying the role of Myc in neonatal OPCs (Scognamiglio et al., 2016). In this work, the authors found that ES cells treated with Myci become dormant, losing their proliferative capacity. Upon restoration of Myc activity, however, ES cells re-enter cell cycle. To see if Myc modulation with Myci similarly effects neonatal OPC

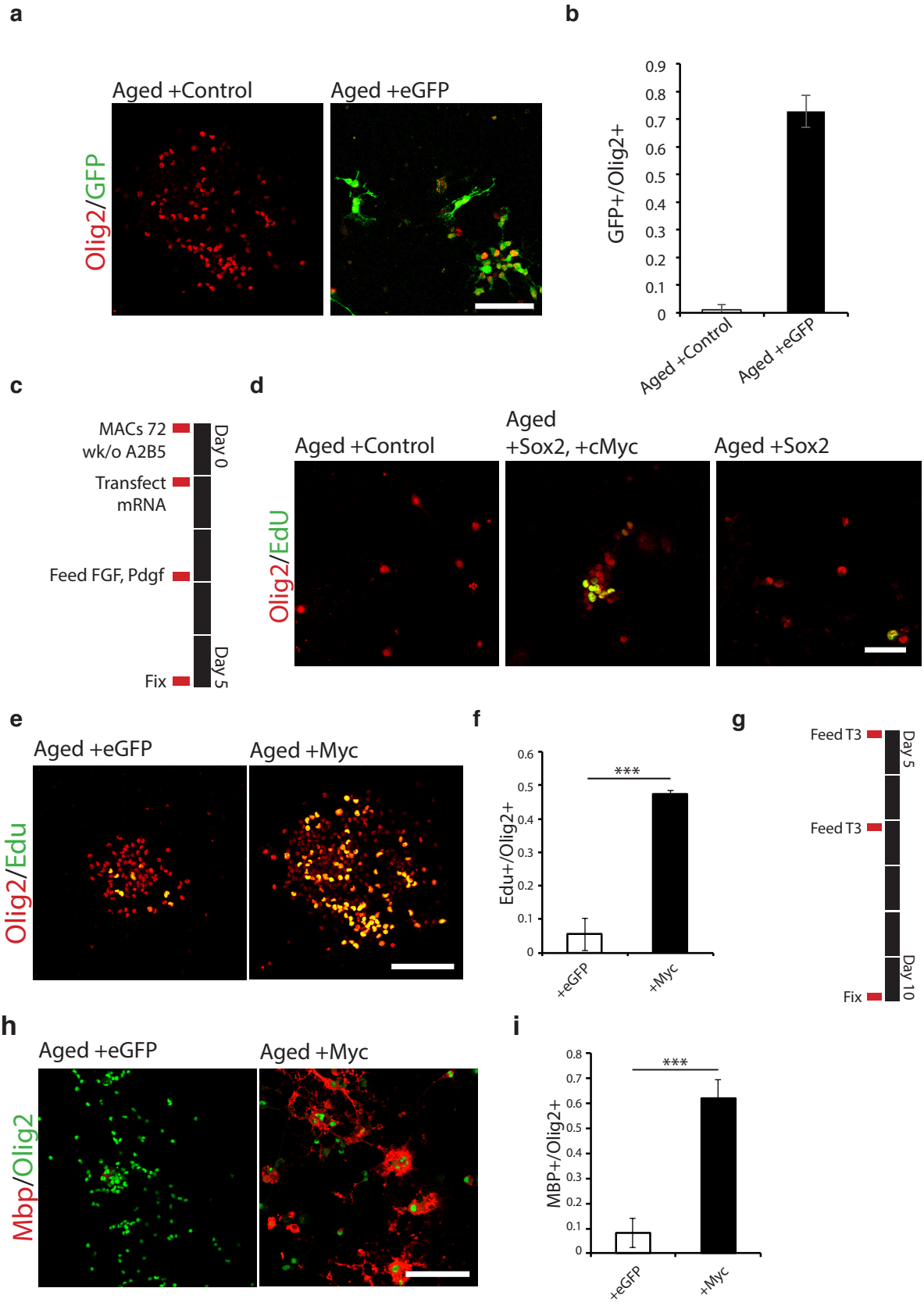
a
Aged +Control
Aged +eGFP
Olig2/GFP
b
GFP+/Olig2+
0.9
0.8
0.7
0.6
0.5
0.4
0.3
0.2
0.1
0
Aged +Control
Aged +eGFP
c
MACs 72 wk/o A2B5
Transfect mRNA
Feed FGF, Pdgf
Fix
Day 0
Day 5
d
Aged +Control
Aged +Sox2, +cMyc
Aged +Sox2
Olig2/EdU
e
Aged +eGFP
Aged +Myc
Olig2/Edu
f
Edu+/Olig2+
***
0.6
0.5
0.4
0.3
0.2
0.1
0
+eGFP
+Myc
g
Feed T3
Feed T3
Fix
Day 5
Day 10
h
Aged +eGFP
Aged +Myc
Mbp/Olig2
i
MBP+/Olig2+
***
0.8
0.7
0.6
0.5
0.4
0.3
0.2
0.1
0
+eGFP
+Myc

Figure 2

Figure 2. Myc alone reactivates aged OPCs. a-b, Representative images and quantifications of the transfection efficiency of modified mRNA in aged OPCs. Control transfections were transfected with lipofectamine without mRNA encoding GFP. Scale bars represent 100μm. c, Schematic overviewing *in vitro* gene over-expression assay for aged OPC activation. d, Representative images of -1 experiment showing the combinatorial effect of Sox2/Myc overexpression in aged OPCs. Scale bar represents 50μm. e-f, Representative images and quantifications of EdU incorporation in Olig2 stained aged OPCs transfected with either GFP or Myc modified mRNA. g, Schematic overview of *in vitro* gene over-expression assay for aged OPC differentiation. h-i, Representative images and quantifications of aged OPCs transfected with either GFP or Myc modified mRNA and placed into differentiation media conditions. e-i, Scale bars represent 200μm. Throughout figure averages represent means from N=3 biological replicates and *** signifies a one way ANOVA P-value of ≤.01. Here and throughout chapter, ≥200 cells were quantified per biological replicate.

activity state, we first found the maximum non-lethal dose of the compound. We found that 16-28μM results in minimal cell death after culturing neonatal OPCs for 48 hours in growth factors. At 16μM after 5 days culturing *in vitro* with Fgf and Pdgf, neonatal OPCs lost virtually all of their proliferative capacity, while neonatal OPCs cultured in DMSO maintained their self-renewal capacity as shown by EdU incorporation (Fig. 3a-c).

If cells were exiting cell cycle by the inhibition of Myc, then it is possible that the cells were just differentiating into post-mitotic oligodendrocytes, not just transitioning to a slowly-cycling adult OPC. Moreover, if the neonatal OPCs were simply out of cell cycle but equally as regenerative, then withdrawing Myci and placing them into differentiation conditions with T3 should efficiently differentiate the OPCs into MBP expressing oligodendrocytes; this would suggest that the OPCs were simply quiescent. To test these potentially confounding hypotheses, neonatal OPCs were either pre-treated with Myci prior to differentiation or treated with Myci during differentiation (Fig. 3d). Neonatal OPCs placed in differentiation conditions for 5 days following 2 days treatment with 16μM Myci in growth factors remain Olig2 expressing but fail to form MBP expressing oligodendrocytes. Whereas, control DMSO treated OPCs maintain their differentiation capacity (Fig. 3e-f). Similarly, neonatal OPCs treated with Myci in differentiation conditions also fail to differentiate into MBP expressing differentiated oligodendrocytes. These results show that Myci treatment does not drive terminal differentiation into Oligodendrocytes or Olig2 negative astrocytes; rather, inhibition of Myc drives neonatal OPCs towards a quiescent state such that, at least over the course of 5 days, OPCs fail to re-activate and differentiate— even in the absence of Myci.

If Myc activity alone describes the age state of an OPC, we hypothesized that the modulation of Myc activity would affect age-related pathways. To test this, we sequenced acutely isolated neonatal and aged OPCs, neonatal OPCs treated with Myci, and aged OPCs transfected with Myc. We found that aged and neonatal OPCs clustered separately as shown by hierarchical clustering and principal component analysis (PCA) (Fig. 4a-b). Neonatal OPCs that were treated with Myci clustered separately from both aged OPCs and neonatal OPCs while OPCs treated with only DMSO were similar to acutely isolated neonatal OPCs. Aged OPCs transfected with Myc mRNA clustered more closely with acutely isolated neonatal OPCs, while aged OPCs transfected with GFP mRNA clustered less closely with neonatal OPCs. PCA analysis shows that while Myc overexpression *in vitro* drives aged OPCs to a more neonatal-like transcriptional state, neonatal OPCs treated with Myci do not resemble aged OPCs; rather, neonatal OPCs treated with Myci enter an undefined cell-state that must be further examined.

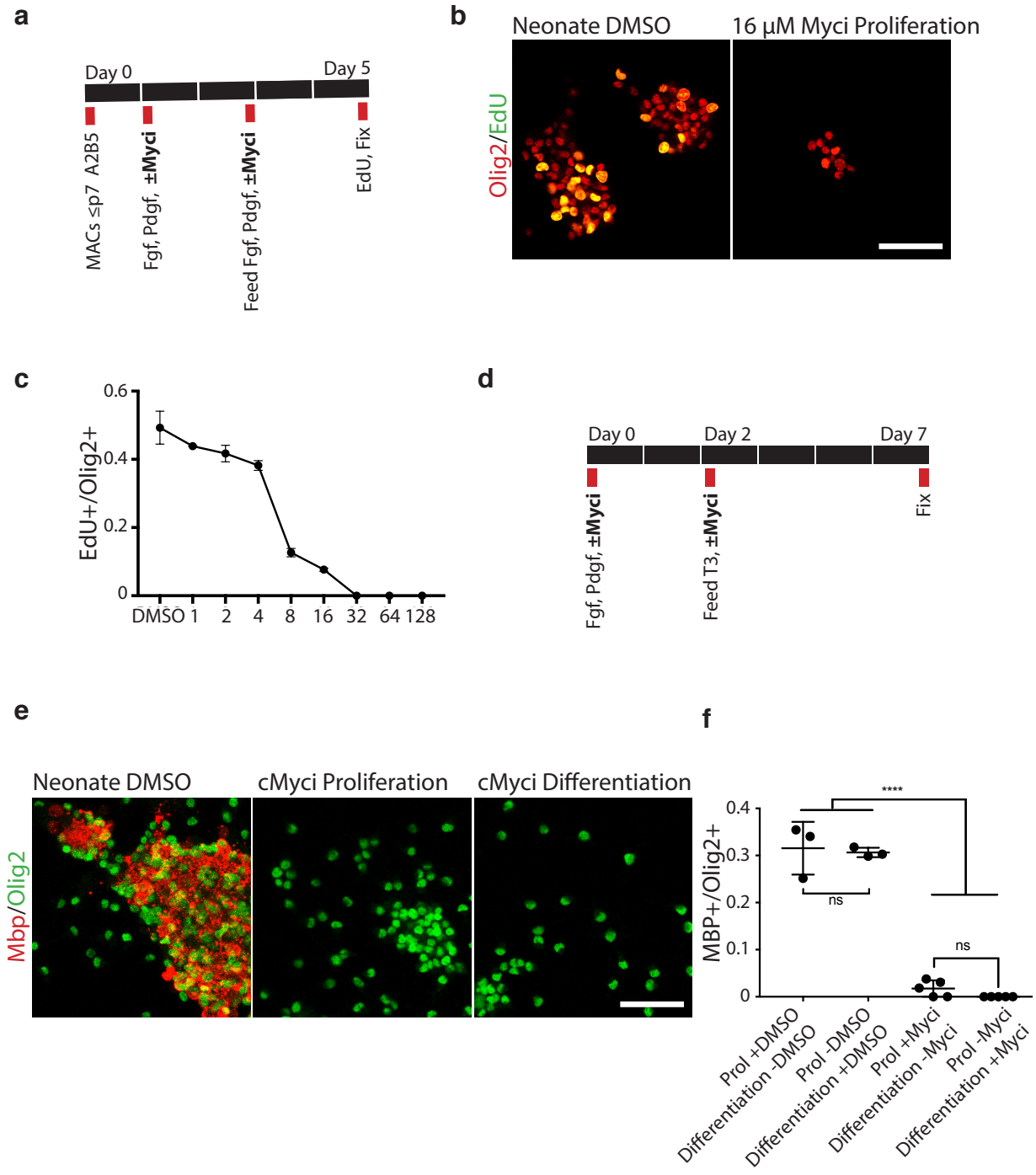

Figure 3. Neonatal OPC loss of proliferative and differentiation capacity following inhibition of Myc. a, Schematic outlining experimental strategy for Myci treatment and neonatal OPCs. b-c, Representative images and quantifications of EdU incorporation from N=3 biological replicates showing the effects of varying concentrations of Myci on Olig2+ ≤P7 neonatal OPCs. d, Schematic outlining strategy for understanding the effects of Myci on neonatal OPC differentiation. e-f, Representative images and quantifications of N=3 biological replicates of the effects of Myci on the differentiation of Olig2+ neonatal OPCs into MBP+ oligodendrocytes. OPCs were either treated with Myci in proliferation conditions (Prol) or in differentiation conditions. Scale bars represent 50µm and **** signifies a Tukey's multiple comparisons test after One way ANOVA. In this figure, quantification and experimental design was assisted by Dr. Björn Neumann of Robin Franklin's group.

To better understand the process by which Myc allows aged OPCs to more closley resemble neonatal OPCs in terms of their transcriptome, we looked at individual genes and gene sets that changed between aged OPCs transfected with GFP and those transfected with Myc. Amongst the most significantly up-regulated genes in Myc transfected aged OPCs were proliferation-related genes such as Gas6 and the DNA replication and RNA transcription components Med13 and Noc3l, while aged OPCs transfected with GFP had high levels of cytoskeletal genes such as Hax1 and pro-inflammatory genes such as Il1rn (Fig. 4c-d). These specific genes highlight the types of pathways enriched for in gene set enrichment analysis. We found that in aged OPCs transfected with Myc, there was enrichment for genesets involved in oxidative phosphorylation, cell cycle, and ribosome biogenesis. The enrichment of these specific gene sets emphasizes the importance of Myc activity on overall cell activity (Fig. 4e). Finally, in aged OPCs transfected with Myc, specific OPC activation genes such as Sox2 and Nkx2.2, and oligodendrocyte lineage genes such as Mbp and Mog, all increased in their expression (Fig. 4f). This would suggest that as OPCs activate with the increase of Myc, they upregulate the genes required for their differentiation.

Aged OPCs transfected with Myc had an increase in expression of a large number of DNA repair genes such as the Ercc1 and Rad50. To determine the DNA integrity following Myc activity modulation, we performed the comet assay under alkaline conditions, a technique developed to detect all forms of DNA damage. Neonatal OPCs *in vitro* treated with DMSO, retained their DNA integrity, with only ~15% of OPCs having DNA damage as indicated by the proportion of tailed 'comets'. Conversely, in aged OPCs transfected with only GFP, ~60% of all OPCs had DNA damage (Fig. 4g-h). Only 30% of comets of aged OPCs transfected with Myc had tailed comets, indicating at least half as much DNA damage following Myc transfection. Neonatal OPCs treated with Myci retained their DNA integrity, as indicated by a low proportion of tailed comets. It is likely that 5 days *in vitro* is insufficient time to cause high levels of DNA damage, even in conditions of low Myc activity. Together, these results show that the re-introduction of Myc *in vitro* can increase the transcript expression levels of DNA repair machinery and ultimately repair damaged DNA in aged OPCs.

We next sought to determine the effect of Myc activity in regeneration in the aged lesion environment. Using a similar approach to the one explained in Chapter 5 of this thesis, we re-purposed the systemically administered AAV (PHP-EB) (Challis et al., 2018). In conjunction with the AAV, we used the CRISPR technique developed in Chapter 5 to direct the sequence-specific integration of genomic

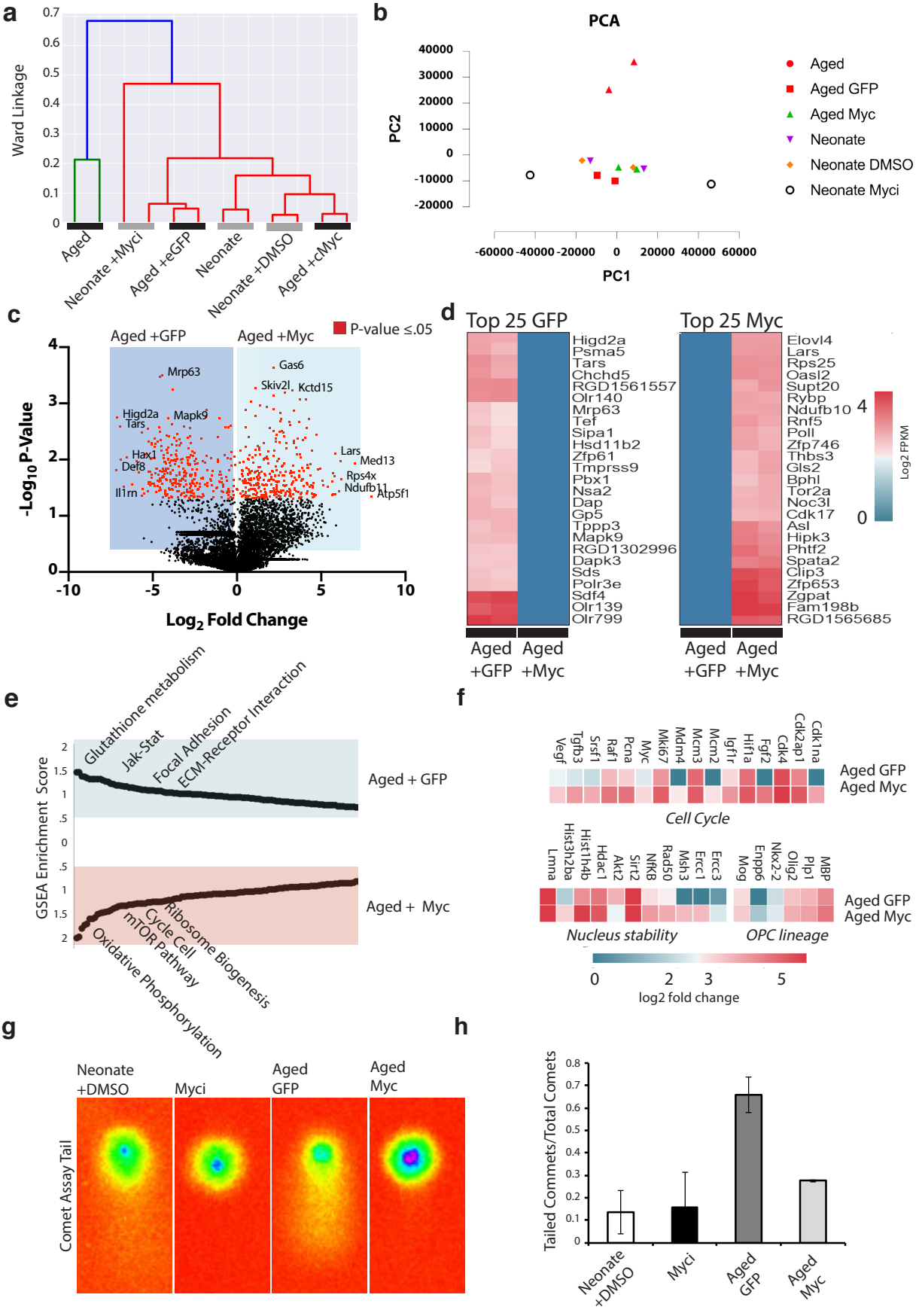
a
Ward Linkage
Aged
Neonate +Myci
Aged +eGFP
Neonate
Neonate +DMSO
Aged +cMyc
b
PCA
PC2
PC1
Aged
Aged GFP
Aged Myc
Neonate
Neonate DMSO
Neonate Myci
c
Aged +GFP
Aged +Myc
P-value ≤.05
-Log10 P-Value
Log2 Fold Change
Mrp63
Gas6
Skiv2l
Kctd15
Higd2a
Tars
Mapk9
Hax1
Def8
Il1rn
Lars
Med13
Rps4x
Ndufb11
Atp5f1
d
Top 25 GFP
Top 25 Myc
Higd2a
Psma5
Tars
Chchd5
RGD1561557
Olr140
Mrp63
Tef
Sipa1
Hsd11b2
Zfp61
Tmprss9
Pbx1
Nsa2
Dap
Gp5
Tppp3
Mapk9
RGD1302996
Dapk3
Sds
Polr3e
Sdf4
Olr139
Olr799
Elovl4
Lars
Rps25
Oasl2
Supt20
Rybp
Ndufb10
Rnf5
Poll
Zfp746
Thbs3
Gls2
Bphl
Tor2a
Noc3l
Cdk17
Asl
Hipk3
Phtf2
Spata2
Clip3
Zfp653
Zgpat
Fam198b
RGD1565685
Log2 FPKM
Aged +GFP
Aged +Myc
e
GSEA Enrichment Score
Glutathione metabolism
Jak-Stat
Focal Adhesion
ECM-Receptor Interaction
Aged + GFP
Aged + Myc
Ribosome Biogenesis
Cycle Cell
mTOR Pathway
Oxidative Phosphorylation
f
Vegf
Tgfb3
Srsf1
Raf1
Pcna
Myc
Mki67
Mdm4
Mcm3
Mcm2
Igf1r
Hif1a
Fgf2
Cdk4
Cdk2ap1
Cdk1na
Aged GFP
Aged Myc
Cell Cycle
Lmna
Hist3h2ba
Hist1h4b
Hdac1
Akt2
Sirt2
NRKB
Rad50
Msh3
Ercc1
Ercc3
Enpp6
Mog
Nkx2-2
Olig2
Plp1
MBP
Aged GFP
Aged Myc
Nucleus stability
OPC lineage
log2 fold change
g
Neonate +DMSO
Myci
Aged GFP
Aged Myc
Comet Assay Tail
h
Tailed Commets/Total Comets
Neonate +DMSO
Myci
Aged GFP
Aged Myc

Figure 4

Figure 4. Transcriptomic modulation of OPC age state with Myc activity a, Hierarchical clustering with Ward linkage of acutely isolated aged OPCs, neonatal OPCs, aged OPCs transfected *in vitro* with Myc or GFP, and neonatal OPCs treated with provided legend. with Myci or with DMSO. b, Principal component analysis of each replicate with legend provided. c, Volcano plot of differentially expressed genes between aged OPCs transfected with GFP and those transfected with Myc. Red dots indicate genes that have statistically significant difference (P-value ≤.05) in fold-change expression. d, Heatmap showing the log2 FPKM expression of the 25 genes with highest fold increase in expression between aged OPCs transfected with GFP versus Myc transfected OPCs and the top 25 genes with the highest fold increase in expression between aged OPCs transfected with Myc versus GFP. All genes shown are significantly differentially expressed with a p-value of ≤.05. e, Gene set enrichment analysis of aged OPCs transfected with either GFP or Myc. Highlighted gene sets are age-related pathways enriched for in the compared groups. f, Selected genes from various genesets show a number of differentially expressed genes between Myc and control transfected aged cells. g-h, Representative images and quantifications of the comet assay for DNA damage. Quantifications represent the mean for each labelled cell group from N=3 biological replicates. For each replicate 50-100 nuclei were quantified.

fragments into slowly-dividing/post-mitotic cells (Suzuki et al., 2016). With these two technologies, we developed a dual AAV system. One virus delivers the sp. Cas9 gene under the CMV promoter, while the other delivers a construct which contains both an overexpression sequence for 3'UTR-targetting Pdgfra gRNA and a knock-in cassette containing IRES-Myc-T2A-GFP, flanked by reversed gRNA target sequences (Fig. 5a). This system allows for GFP and Myc to be expressed in all Pdgfra expressing OPCs of the CNS following a single intravenous injection of the dual-AAV system. Similar to the approach taken in Chapter 5, we targeted the 3' UTR for transgene integration to avoid perturbing the gene expression of Pdgfra itself. Finally, this provides for the controlled expression of Myc as only OPCs express Myc; once the OPC differentiates into an oligodendrocyte and downregulates Pdgfra, Myc expression is also lost.

To confirm that this CRISPR AAV system works, we infected dissociated p1 neonate mouse pup CNS with the vectors. As a mixed cell population, GFP should only be expressed in cells also expressing the oligodendroglia lineage marker Olig2. Indeed, five days following infection, we found significant populations of Olig2 expressing cells also expressing GFP (Fig. 5b). After confirming that the system works *in vitro*, we tail vein injected both AAVs into aged 18 month old mice and then perfused the animals 3 weeks after that (Fig. 5c). Three weeks following the initial tail vein injection, DNA PCR on the homogenized cortex revealed the correct genomic integration of the control, GFP-only vector and of the GFP-Myc vector (Fig. 5d). qPCR on the RNA from homogenized brain revealed a 4 fold upregulation of Myc transcript in the animals that received the Myc-GFP AAV compared to animals that received the GFP only vector (Fig. 5e). Cryo-sections of un-lesioned grey and white matter in the spinal cord showed over 35% of Olig2 expressing cells staining positive for GFP and <10% of total GFP cells staining negative for Olig2 (Fig. 5f-g). These results show that the CRISPR knock-in efficiently targets the CNS and that the expression locus is highly specific for OPCs.

After confirming the knock-in efficacy of the Myc over-expression system, we tail vein injected the AAVs into mice, lesioned the mice one week later, and perfused the animals two weeks after that (Fig. 6a). To determine the rate of proliferation in Myc-AAV infected animals, mice received an intraperitoneal injection of EdU 24 hours prior to perfusion fixation. In the lesion of the control GFP infected animal, we observed ~10% EdU labeled, Olig2 stained OPCs; moreover, most of these proliferating cells were at the periphery of the lesion site (Fig. 6b-d). In the Myc vector infected animal, however, ~40% of the Olig2 stained cells in the lesion were labeled with EdU. Similarly, in the control GFP infected animals, there were few Olig2+, CC1+ oligodendrocytes within the core of the lesion (Fig.

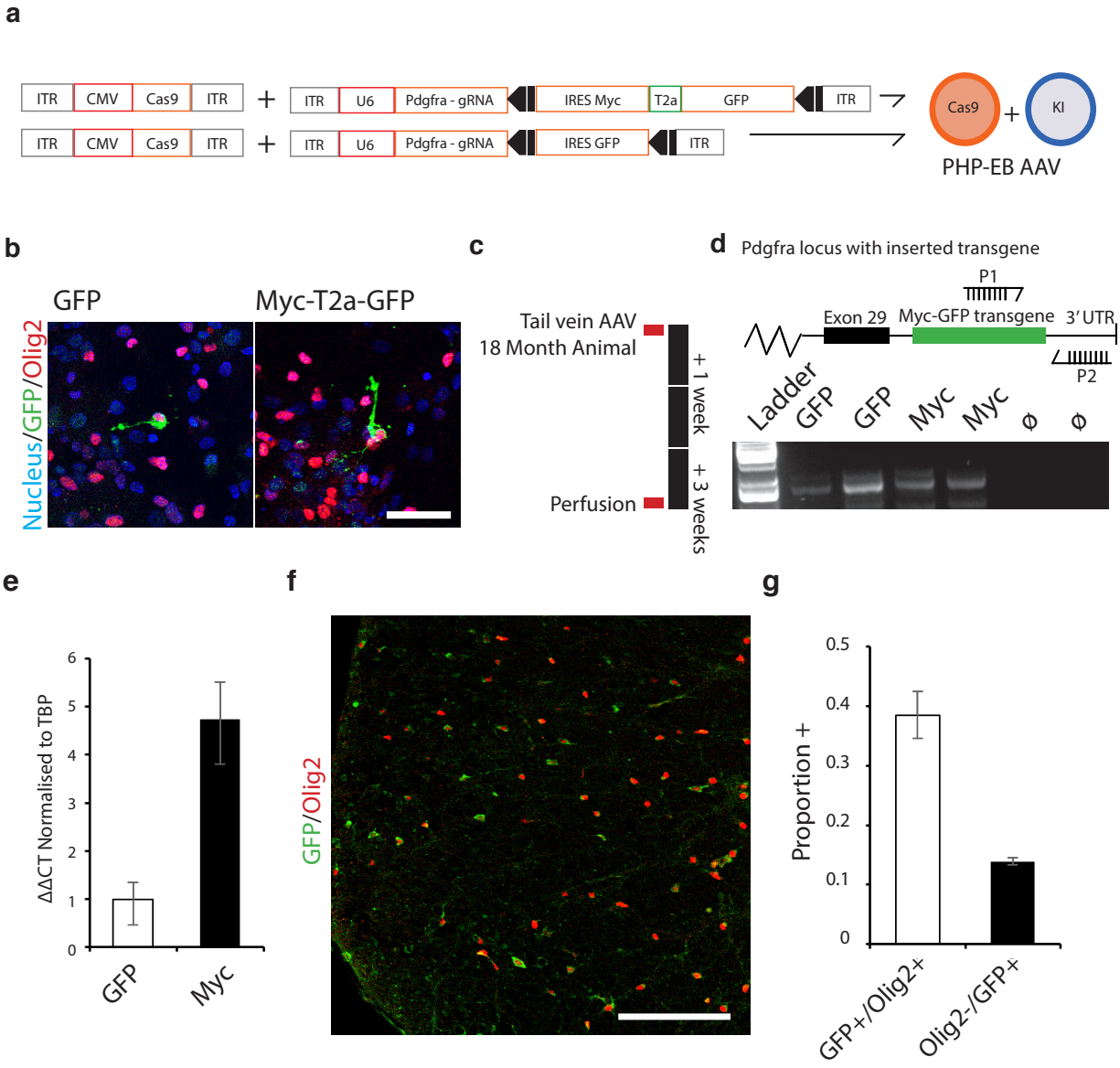

Figure 5. Systemic, cell-type specific, *in vivo* CRISPR knock in of Myc is specific for OPCs. a, Schematic outlining the control and Myc overexpressing AAV vectors. For the general mechanism of action refer to Figure 1a in Chapter 5 of the thesis. b, Representative images of *in vitro* infection of CRISPR AAV in dissociated P2 mouse brain reveals transgene GFP expression is limited to Olig2 expressing OPCs. c, Schematic overview of *in vivo* CRISPR experiment. d, Schematic of the integration site of transgene in 3' UTR of Pdgfra and PCR of homogenized mouse cortex in N=2 aged animals per treatment category shows gene fragment knock-in in correct genomic loci three weeks post tail vein injection of AAV. P1 represents forward primer within transgene and P2 represents reverse primer in 3' UTR of Pdgfra gene locus. e, qPCR for Myc from N=3 homogenized aged mouse cortex 3 weeks post AAV tail vein injection of either GFP or Myc overexpression vector. ΔΔCT normalised to housekeeping gene Tbp. f-g, Representative image and quantifications of un-lesioned white/grey matter of the spinal cord reveal the efficiency of our *in vivo* CRISPR system and of the expression specificity of Pdgfra for Olig2 expressing OPCs—only ~10% of GFP positive cells are not Olig2+. Averages represent mean from N=3 animals and scale bar represents 100µm.

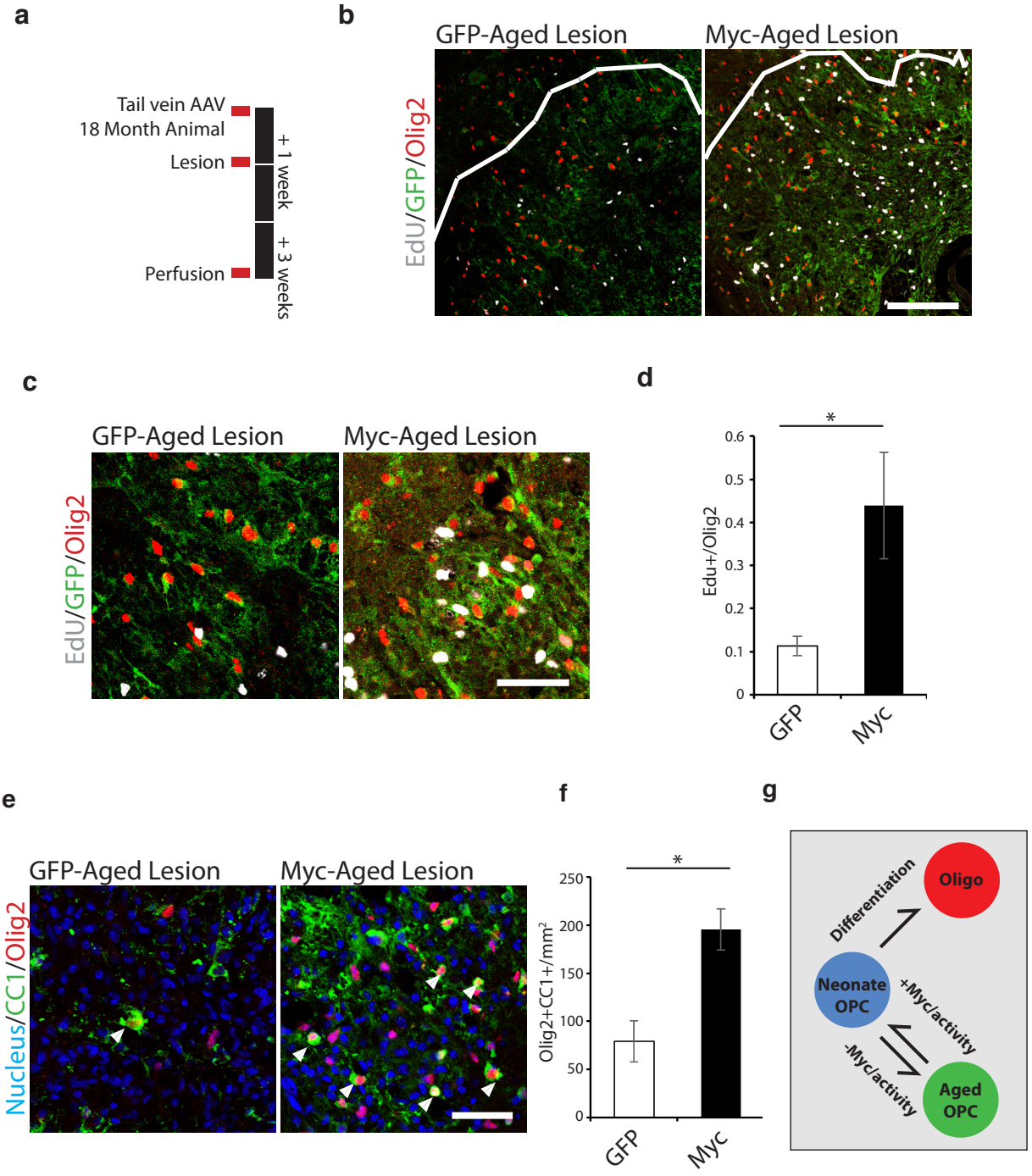

Figure 6. Myc overexpression enhances regeneration *in vivo*. a, Schematic overview of the AAV and lesion timeline. b, Representative images of EdU labelled, Olig2,GFP co-stained lesioned aged spinal cord 3 weeks following tail vein injection of AAV. Lesion border outlined with white line and scale bar represents 100µm. c-d, High power representative images and quantifications of EdU incorporation in GFP/Olig2 stained aged lesion cores. e-f, Representative images and quantifications of CC1/Olig2 co-labelling per mm2 in aged lesion cores. Throughout figure means represent averages from N=3 animals, scale bars, unless otherwise indicated, show 50µm, and * represents a 1 way ANOVA value of <.01. g, Schematic overviewing the role of Myc in determining the age state of OPCs. Dr. Chao Zhao of Robin Franklin's group performed the animal lesions.

6e-f). In the Myc infected animal, however, there was an almost 4-fold increase in the number of labeled CC1+ and Olig2+ oligodendrocytes within the lesion core. Together, these results reveal that the controlled-expression of Myc can functionally re-activate aged OPCs within the context of a demyelinating lesion; Myc does not just cause the proliferation of aged OPCs into the lesion area, but also their differentiation into oligodendrocytes.

Discussion

Here we present our findings that partial reprogramming of aged OPCs does not require all four of the reprogramming factors: Oct4, Sox2, KLf4, and Myc. Rather, the transient overexpression of Myc in aged OPCs *in vitro* can reactivate OPCs, allowing for high levels of OPC proliferation and differentiation (Fig. 6g). Conversely, we have shown that the treatment of Myci on neonatal OPCs removes cells from the cell cycle and, even upon Myci's withdrawal, neonatal OPCs are unable to differentiate into MBP expressing oligodendrocytes. Using transcriptomics and assessing DNA damage, we have also shown that, regardless of the physiological age of the cell, OPCs age-state can be re-written through the manipulation of Myc activity. Finally, using an *in vivo* CRISPR, dual-AAV system, we have shown that the OPC-specific overexpression of Myc can dramatically increase the rate of OPC activation and differentiation, even in the context of an aged lesion environment. Together, this work highlights the importance of Myc in enabling aged stem cell populations to activate and subsequently regenerate damaged tissue.

Reprogramming factors and partial reprogramming

Previous reports have identified that the transient tissue-wide overexpression of all four original reprogramming factors can attenuate the hallmarks of ageing and prolong lifespan (Ocampo et al., 2016b). They argue that the brief overexpression of these factors drives cells to reprogramme—not to pluripotency—but to a younger more rejuvenated cell type. Despite this, the authors neither seek to understand the role of each individual factor, nor identify the underlying mechanism driving this rejuvenating phenotype.

The exact role of each reprogramming factor even in the derivation of induced pluripotent stem cells remains largely unknown (Plath and Lowry, 2011). The field's consensus is that proliferation is the first step to complete reprogramming. It is hypothesized that Myc acts first, causing changes in cell

energy metabolism, forcing the cell back into the cell cycle. In a hallmark study in which each reprogramming factor is individually over-expressed in somatic cells and then CHIP-sequenced for each respective factor, the authors found that Sox2, Nanog, and Klf4 act in concert, binding the promoter regions of largely the same ES cell specific pluripotency genes (Sridharan et al., 2009). Myc, however, binds to the promoter sequences of cell cycle genes, and of energy metabolism genes. The authors further demonstrate that Myc is the first affecting transcription factor during the first steps of reprogramming and is largely dispensable once the cells are in the later stages of pluripotency. After 5 days of Myc expression, the other reprogramming factors begin to do their job—the total process of reprogramming taking 8-10 days.

In the previous study, OSKM expression was induced globally in a transgenic mouse with doxycycline for 2 days, followed by 5 days of doxycycline withdrawal (Ocampo et al., 2016b). Repeated rounds of treatment of doxycycline prolonged longevity. However, if previous reports are true that Myc is the dominant transcription factor acting upon chromatin in the first days of reprogramming, then the observed effects from this partial reprogramming study are likely attributable to the activation of Myc. Furthermore, the ageing field has long-viewed slowed cell cycle and loss of ATP production as the underpinnings of the ageing process (López-Otín et al., 2013). Myc alone can induce enhanced mitochondrial respiration and cell cycle, so it seems likely that Myc alone is the reprogramming factor responsible for the rejuvenation-effect seen in partial reprogramming. Future work must look at whether global, transient, Myc overexpression alone can recapitulate the results of this previous study.

Since the original derivation of iPS cells using OSKM (Takahashi et al., 2006), follow up work has found different combination of transcription factors and small molecules that can induce pluripotency (Huangfu et al., 2008; Yu et al., 2007). Myc expression itself has been shown to be dispensable, if replaced with two other transcription factors Nanog and Lin28a. Valproic acid, a histone deacytelase inhibitor, can significantly improve iPS cell generation. One study even found that all four original reprogramming factors can be replaced with antibodies that induce the expression of each reprogramming factor (Blanchard et al., 2017). Overexpression of OSKM remains the most robust method for generating iPS cells, yet the relevance of these pathways for iPS cell generation remains unknown for partial reprogramming. Recent work in our group has shown that the transient overexpression of many of the individual reprogramming factors not tested in this study have a surprising phenotype on adult OPCs. For instance, the overexpression of Lin28a seems to direct adult OPCs to an astrocytic fate. Future work will be to determine whether any of these additional factors can similarly rejuvenate

aged OPCs.

Myc, OPCs, and rejuvenation

While Myc activation can reactivate aged OPCs both *in vitro* and *in vivo,* the roles of Myc in the normal development and ageing of OPCs remain unknown. In this chapter, we found that the inhibition of Myc activity with a small molecule inhibits OPC proliferation and differentiation. While the loss of proliferation and differentiation is the phenotypic sign of OPC ageing, the Myc inhibited neonatal OPCs neither resembled aged OPCs transcriptomically nor in terms of their DNA damage. One possible explanation for this is our reliance on a small molecule to inhibit Myc in neonatal OPCs; the small molecule could have sub-toxic effects on cells, impacting cell behaviour in ways other than just by inhibiting Myc. If this is the case, then the treatment of neonatal OPCs with the Myc inhibitor is an inappropriate method for depleting Myc activity in neonatal OPCs. A better strategy than the one presented in this chapter would be to genetically knock-down Myc expression with either a siRNA or with CRISPR. With this approach, we could determine whether the effects of neonatal OPC Myc depletion are a biological phenomenon or simply a side effect of the small molecule's toxicity.

A major limitation to the work presented in this chapter is our lack of understanding of the role of Myc in normal CNS development and homeostasis. It is possible that the effects of the overexpression of Myc in aged OPCs are epiphenomenological and that Myc has no role in normal OPC biology or in OPC ageing; rather, Myc overexpression simply activates other secondary genes that do have a role in OPC function. This would also explain why the inhibition of Myc in neonatal OPCs does not drive an aged-like transcriptomic profile. If Myc has no role in normal developmental OPC function, then Myc inhibition would not cause ageing. Future work must further characterise the role of Myc in OPC development, homeostasis, and regeneration by re-analysing Myc expression patterns in existing transcriptomics databases. Another strategy in development is to repurpose the Nested CRISPR system to knock out Myc in neonatal OPCs and in young adults with lesions in vivo. If neonatal OPCs lose their proliferative capacity or if young adults have less efficient remyelination, then we could determine whether Myc has a role in regulating OPC function. Neonatal OPCs depleted of Myc both *in vitro* and *in vivo* using RNAi/CRISPR could then be sequenced to determine if they possess aged-like transcriptomes. If Myc depletion does not affect OPCs in development or in regeneration, then likely the loss of Myc is not what underlies the ageing process and Myc has no role in the biology of OPCs. If that is the case, then the re-introduction of Myc in aged OPCs has no biological precedent and the observed

phenotype is pure epiphenomena.

In this chapter, I show that transient Myc overexpression causes aged OPCs to regain their proliferation capacity. Conversely, I show that transient inhibition of Myc with a small molecule causes neonatal OPCs to stop proliferating. However, a major limitation to this work in this chapter is that I do not address whether these two phenotypes are stable after the short 5 day experimental time-course. Do aged OPCs transfected with Myc continue proliferating after the exogenously supplied Myc mRNA is depleted? Do neonatal OPCs lose their proliferative capacity even after the Myci small molecule has been removed from the media? If our hypothesis is correct and transient Myc overexpression causes cellular rejuvenation in aged OPCs, then I would expect that, long term, these OPCs would continue to proliferate in growth factor media, as neonatal OPCs do. If this phenotype is not stable, then transient Myc over-expression does not cause true rejuvenation; rather, it causes a transient burst in cellular activity that cannot be maintained long term. These longer term experiments are currently ongoing in our group and are crucial to understanding the capacity of Myc to fully rejuvenate aged OPCs.

With the *in vivo* CRISPR system, we found that transient overexpression of Myc enhances the regenerative capacity of OPCs *in vivo* in an aged lesion environment. However, the implications of this study are limited due to the short time course and limited readout of the experiment. The reasons for our experimental approach are largely due to the limited number of aged animals that we have available. This is because aged animals are expensive to house and require regular and time-consuming maintenance. With limited aged animals, I had to compromise on the experimental approach. I settled on looking only at 14 days post lesion as it was a time point I would expect the lesion to have both proliferating OPCs and newly differentiating oligodendrocytes. I could therefore quantify both the number of proliferating OPCs and differentiating oligodendrocytes. However, the study does not look at the long-term remyelination of the lesion and it remains unknown whether the Myc-activated OPCs continued to proliferate, even after the lesioned area has remyelinated. If this is the case, then likely we have transformed a fraction of the OPCs to become cancerous. These long-term remyelination studies are necessary for us to understand whether Myc should be considered as a therapeutic target for remyelination.

Activity, ageing, and Myc

Myc is a canonical oncogene (Schwab et al., 1983; Seeger et al., 1985). Constitutive and long-term

overexpression of Myc leads to the formation of tumors across the body. Myc even has a established role in the formation of glioblastoma (Trent et al., 1986). Yet, overexpression of Myc *in vivo* transiently causes a lower incidence of tumor formation and prolonged longevity. Similarly, we describe here the role of Myc in regeneration, not in tumour formation. The exact difference between cancer formation and stem cell regeneration/rejuvenation remains an area of active investigation. Moreover, this dual role of Myc as tumor-driver and as the underpinning factor required in regeneration poses fundamental questions for the field of regeneration.

There has been increased interest in investigating the relationship between pluripotency and cancer. One study investigated the gene networks as somatic cells attain pluripotency and compared them to various primary cancers (Kim et al., 2010). The authors identified a group of Myc-associated genes as the underlying commonality between these groups of cells. The authors hypothesize that cancer cells resemble partially reprogrammed somatic cells in the sense that they are undifferentiated, do not commit to a particular lineage, and they maintain the capacity to self-renew. These findings bolster the hypothesis that there is a cancer stem cell, a sub-population of hyper-proliferative and dedifferentiated cells that drive the expansion of a tumour (Wong et al., 2008).

If stem cell gene networks and cancer gene networks share many similarities, then it remains unclear how adult stem cells maintain multi-potency without causing tumor formation. A recent hallmark paper identified shared transcriptional networks between cancer and adult activated stem cells following the wounding of the skin epithelia (Ge et al., 2017). The initiation of tumour formation transcriptomically matches the initiation of wound repair; both groups of cells experience the upregulation of proliferation genes that are involved in cell proliferation and growth. The authors identify that the divergent moment between cancer formation and the return of the stem cell to quiescence following wound healing, is the capacity for adult stem cells to appropriately epigenetically silence the pro-growth genes. An additional paper from the same group found that repeat wounding of the same epithelial region leads to the progressive epigenetic opening of the pro-growth domains, a process that could eventually lead to cancer formation (Naik et al., 2017). Together these papers put forward the hypothesis that tumor formation is caused by repeat stress of the same stem cell population, causing the opening of epigenetic domains around oncogenes, and the inability for the stem cell to become quiescent.

Despite this, repeat albeit transient OSKM overexpression does not drive tumorigenesis (Ocampo et al., 2016a). Moreover, iPS cells, which are effectively immortalized cell lines, can integrate into a

blastocyst, forming all three germ layers without tumor formation. Taken together, these papers highlight the importance of gene dosage, environment, and gene-expression timing on cell behavior. Low level 'micro-dosing' of Myc prolongs lifespan while transient bursts of stem cell activation progress towards cancer, as shown in the repeat wound healing experiments. Moreover, hyper-activation of reprogramming cells and their removal from their native niche allows for a complete developmental reset without tumorigenesis. Future work must continue to study the relationship between stem cell activation, rejuvenation, and cancer. If rejuvenation therapies are ever to enter the clinic, it will be important to fully characterize a safe non-tumorigenic amount of stem cell activity.

In vivo CRISPR and rejuvenation

In Chapter 5 of this thesis, I showed the capacity for AAVs combined with NHEJ to create cell-type specific gene knockouts. Here, I re-purpose the same underlying principles to create a cell-type specific gene over-expression system. We use this *in vivo* CRISPR technology to directly determine the effect of overexpressing a specific gene in a given adult stem cell population in the context of tissue homeostasis and injury. Currently, graduate students in our group are re-purposing this system and are building vectors with each of the reprogramming factors to determine whether additional factors can enhance remyelination in the aged CNS. In other instances, I am helping researchers in our group to knock-in additional genes into the Olig2 locus to determine the transcription factors necessary to drive trans-differentiation of OPCs into peripheral nervous system Schwann cells. These are just some of the ways that this OPC-specific overexpression system can help researchers rapidly dissect the role of individual genes/reprogramming factors in OPC biology.

Chapter 7

Final remarks and conclusions

Cell-cycle first, then differentiate

Remyelination is the process by which OPCs of the CNS replace lost oligodendrocytes following a demyelinating insult. However, with ageing, remyelination fails, and this has been attributed to the inability of OPCs to differentiate (Kuhlmann et al., 2008). To understand the mechanisms underlying OPC differentiation and its failure, primary neonatal stem cells or iPS-cell derived tissue-specific stem cells are often used as a proxy for understanding adult stem cell biology (Barres et al., 1994; Huang et al., 2011; Hubler et al., 2018). This is because primary neonatal and iPS cells readily expand, so researchers have more cell material with which they can experiment. However, there is an increasing body of work highlighting key differences between adult stem cells and neonatal or iPS-cell derived stem cells. In previous unrelated work with others, I have shown that pluripotency derived differentiation protocols often create cells that more closely resemble foetal cells than they do adult cells (Pagliuca et al., 2014). Moreover, in this thesis, I have shown that neonatal and aged OPCs have vastly different transcription profiles.

One obvious distinction between foetal and neonatal OPCs from aged OPCs is cell cycle. While the younger OPCs are actively engaged in cell cycle, aged OPCs slow their cell cycle time longer than 100 days (Young et al., 2013). As these younger stem cell populations are already activated, most previously reported OPC studies focus solely on describing the pathways that differentiate these activated cells into oligodendrocytes. While these signalling pathways are likely relevant for the aged OPC, they are alone unlikely to be sufficient drivers of remyelination in the aged CNS. In this thesis, isolated aged OPCs neither readily undergo cell cycle nor differentiate into oligodendrocytes even in response to well-established neonatal OPC proliferation and differentiation protocols (Barres et al., 1994). In other quiescent adult stem cell populations, such as muscle, the stem cell must first activate and undergo cell-cycle prior to differentiating (Gurevich et al., 2016). The same may be true for the OPC; in homeostatic adult CNS, there is some evidence that OPCs first undergo either symmetric or

asymmetric division before differentiating into oligodendrocytes (Zhu et al., 2011).

A conflicting study reports that adult mice OPCs differentiate without proliferation (Hughes et al., 2013). In this study, the authors use a Ng2 reporter mouse and *in vivo* imaging to show that cells can lose Ng2 expression without first proliferating. This work is done in 2-3 month-old animals, tracking individual Ng2 cells for 40 days. If other reports are correct, however, then 100% of Pdgfra expressing OPCs at this age in this region of the brain cycle within a 40 day window (Young et al., 2013). This work confounds the findings from Hughes et al., 2013, and bolsters an alternative hypothesis: that the tracked Ng2 cells simply come from a recently divided OPC. I hypothesize that OPCs must divide before differentiation. If OPCs cannot spontaneously differentiate without first undergoing cell cycle, then quiescent non-cycling aged OPCs will likely be unresponsive to differentiation signals. I argue that one must first activate the mechanisms that drive aged OPC proliferation in order to cause OPC differentiation.

Using this as a paradigm for adult OPC stem cell biology, I have looked for signals that drive OPC proliferation. Throughout this thesis, I find methods that enhance OPC proliferation, also enhance OPC differentiation. The clearest example of this is that the overexpression of Myc—a canonical oncogene—in aged OPCs both *in vivo* and *in vitro,* leads to a significant increase in OPC differentiation. These results show that, while aged OPCs do not efficiently differentiate into oligodendrocytes, aged OPCs that have been forced back into cell cycle with Myc do. Future work must further dissect the signals that cause proliferation in adult and aged OPCs. Doing so will identify novel therapies to promote remyelination in the aged brain.

A convergence of pathways

Throughout this thesis, I have examined methods for re-activating adult and aged OPCs. I have discussed three parallel pathways that can activate the adult OPC: Wnt-agonising proteins, mechanical signalling mediated via Piezo1 signalling, and the activity of the oncogene Myc. There is increasing evidence that these disparate signalling pathways converge, wherein stiffness regulates beta-catenin localisation, which in turn regulates Myc activity (Benham-Pyle et al., 2015; Mouw et al., 2014). Of the two studies highlighting this interconnected pathway, both were performed on immortalised cell lines, and both found that stiff materials causing mechanical strain drive the localisation of nuclear

beta-catenin which, in turn, upregulates Myc. These findings are in contrast to our results in the brain that a soft environment drives OPC proliferation and differentiation. As Wnt signalling and Myc drive proliferation, then a stiff environment—not a soft environment—would drive OPC proliferation.

Despite this, our hypothesis that a soft environment confers stem cell plasticity is not out-of-step with the broader stem cell field. Rather, a number of papers have similarly shown that a soft environment supports self-renewal in embryonic stem cells, iPS cell formation, and in muscle stem cells (Caiazzo et al., 2016; Chowdhury et al., 2010; Gilbert et al., 2010). The reports that Wnt and Myc are necessary for embryonic stem cell self-renewal *in vitro* further challenge these mechanics findings (Scognamiglio et al., 2016). In our sequencing work and unpublished work from collaborators, we find that embryonic stem cells and OPCs cultured on soft hydrogels have an increase in Myc-family genes. These findings complicate the prevailing view from cancer mechano-biologists that stiff environments drive cell self-renewal programmes.

There are a number of explanations that could account for these conflicting findings which link niche mechanics to canonical signalling pathways and cell activation-state. One possible hypothesis is that all cells are different, and that matrix mechanics differentially affect cells in the CNS and in embryonic stem cells versus immortalised cell lines. The finding that all cells exhibit different responses to niche mechanics is well-established (Engler et al., 2006). In this study, mesenchymal cells cultured on different stiffness hydrogels preferentially differentiate into either neurons, muscle, or bone. Mammals have multiple organs, each of differing mechanical environments (Swift et al., 2013). If all cells respond to niche mechanics differently, then future work must attempt to understand the mechanisms by which each cell population responds to their respective niche mechanical environments.

The gated ion channel Piezo1 could be the mechanism underlying these diverging cellular responses to niche mechanics. A well-established mechano-sensor (Coste et al., 2010), Piezo1 is inactive in a soft environment but activates in stiff environments, causing an increase in intracellular Calcium cations. These secondary ion messengers relay to the cell the surrounding environmental mechanics. Calcium signalling is a highly versatile signal that can regulate many cellular processes such as cell contractility and proliferation (Berridge et al., 2003). As such, depending on the intracellular calcium-dependent proteins, calcium signalling could drive diverse cellular events. The diversity in cell activity following intracellular calcium flux would reconcile the different and conflicting reports highlighting the role of Piezo1. In some cell-types, Piezo1 activity directly inhibits oncongenic Ras signalling (McHugh et

al., 2010). In the skin epithelium, however, Piezo1 activity drives cell proliferation following injury (Gudipaty et al., 2017). As each cell population contains its own set of calcium-dependent proteins, there will likely be many roles for Piezo1 across the many different cell populations. Mechano-sensors such as Piezo1 that convey niche mechanics via broadly-acting ion currents, may well explain the capacity for individual cell-types to respond differently to niche mechanics.

While it is plausible that each organismic niche retains its own unique mechano-response mechanism, it could also prove true that embryonic and adult stem cells behave differently from other differentiated cell types. As mentioned, a large body of evidence suggests that soft niche environments promote stem cell activation/self-renewal. However, most mechanistic work of mechano-biology has studied either the effects of niche mechanics on directed differentiation or on immortalised cancer cell lines. If a soft environment is indeed unique to stem cells, then perhaps stem cells contain an undescribed mechanism for activation in response to 'softness'. Future work must explore how stem cells are activated in a soft environment and must better understand the evolutionary reasons why stem cells prefer softer environments for self-renewal.

A niche theory for cellular ageing

In this thesis, I explore whether the ageing process is fixed or if cells can be coaxed to rejuvenate. We find that with niche environment, mechanics, or with the over-expression of Myc, we are able to force the aged cell back into cell cycle and rejuvenate it. Taken together, these results pose a new set of hypotheses for the ageing process: cells themselves do not immutably age; rather, the organism and the cellular niche ages which, in turn, activates the intracellular ageing pathways. This hypothesis emphasises that both cell-non-autonomous and cell-autonomous ageing processes are fundamentally linked and one cannot be understood without the other.

Finally, I propose that the ageing process begins once the mammalian organism switches from a pro-growth developmental programme to a steady-state homeostasis programme. Once the brain reaches maximal size, negative feedback from the niche confers to the adult stem cell in order to slow cell growth and temper its activity. I hypothesise that this process results from a loss of circulating hormones, niche growth factors, and the capacity of stem cells to sense maximal niche cell-density via mechano-sensors such as Piezo1. Once the CNS stem cells slow their cell cycle, tissue turn-over and re-modelling slows, thus beginning the ageing process. This process feeds forward, wherein prolonged

stem cell inactivity leads to canonical intracellular ageing pathways, impairing regeneration in the context of CNS injury or disease. Again, when these cells are removed from their niche, adult CNS stem cells can functionally rejuvenate, suggesting a largely niche mediated ageing process.

In this thesis, I show the effects of the overexpression of Myc in an *in vivo* environment using CRISPR/Cas9. We show that Myc overexpression in the context of a re-myelinating lesion accelerates OPC proliferation and differentiation. In follow-up work not presented in this thesis, I have found that Myc overexpression in OPCs did not lead to an increase in OPC proliferation in homeostatic tissues, as indicated by the low levels of EdU incorporation. I hypothesise that, despite oncogene activity, a healthy non-cancerous OPC will not re-enter cell cycle in its native niche environment. This is because environmental negative-feedback-acting ion channels such as Piezo1 limit cell growth. Future work will be to explore the intersection of pro-growth pathways such as Myc and stiffness-sensing pathways such as Piezo1. For instance, I hope to explore whether Myc overexpression in a Piezo1 null OPC is sufficient to drive proliferation in un-lesioned homeostatic cortex.

Recent work indicates that the OPC is the underlying cell-type in the formation of cancerous gliomas in the CNS (Filbin et al., 2018). As oncogenic activity alone appears to have minimal effect in the homeostatic CNS, I hypothesise that additional OPC mutations are required for the formation of glioma. Using publically available sequencing databases, I will look at environmental-sensing machinery to understand how gliomas maintain growth capacity in a growth-adverse adult/aged CNS and whether or not OPC-derived gliomas have a modified environment stiffness-sensing programme. Doing so, I hope to harness certain aspects of glioma formation (e.g. the capacity to self-renew in the stiff aged CNS) with the goal of promoting healthy OPC activation in the diseased adult CNS.

Gene therapy for age-related disease

In this thesis, I have shown novel genome engineering methods for the adult and aged rodent CNS. Using adeno-associated viruses (AAVs) and CRISPR/Cas9 technology, I describe a nested CRISPR system by which a single intravenous injection can lead to OPC-specific modifications, widespread across the CNS. Using multiple gRNAs and synthetic nested gRNA cut sequences, I show that this system can be multiplexed, allowing for sequential DNA-editing events depending on gene expression. Together, these findings present a tool for neuroscientists by allowing for the rapid testing of single-genes in specific-cell types.

Recent work has shown a base-editing 'Camera' system in which a modified Cas9 creates single nucleotide changes to a known region of the genome (Tang and Liu, 2018). Driven by a pathway-specific promoter sequence, this base-editing Cas9 records in a known region of the genome whether or not a given pathway is expressed. The system can be multiplexed with multiple gRNAs under multiple promoters, allowing for the record of sequential steps within a signalling pathway. While the CRISPR 'camera' allows for the authors to efficiently record epistatic events within the canonical Wnt signalling pathway, the applicability of the system is limited by its reliance on known promoter sequences. Moreover, the system is limited to *in vitro* studies under a controlled environment. The nested CRISPR system, however, is not limited by promoter sequences; rather, using successive rounds of knock-in gRNAs that can be expressed in the 3' UTR of any gene, the nested CRISPR system could be used *in vivo* to do epistatic analysis on previously un-described cellular events. As shown in this thesis, the successive use of stop codons, ribozymes, and poly-A sequences allows for the sequence of cellular events to be recorded. For instance, in this thesis I show that, for every Pdgfra-expessing cell, if the cell subsequently expresses Piezo1, the cell will express GFP. As such, the nested CRISPR system could be used to record previously-undescribed cellular events in specific-cells *in vivo*.

While the applicability of the nested CRISPR system could be broad for neuroscientists studying rodents, there is not likely a therapeutic application for this CRISPR approach. The targeted, highly-accurate gene editing of specific-cell types within the human body would be an advance in medicine with broad implications. However, the CRISPR system can make mistakes that could lead to large scale genome vandalism (Kosicki et al., 2018). Moreover, the reliance on non-homologous end joining machinery to knock-in the gRNA DNA fragments means that non-specific DNA insertions are possible (Suzuki et al., 2016). To overcome the limitations of the CRISPR system, the Cas9 enzyme has been modified with point mutations and its nuclease activity deleted (Konermann et al., 2015). This nuclease-null Cas9 can be fused to transcriptional activation or repressive elements to drive endogenous gene expression. Complexing with a gRNA, this Cas9 system can be used to transiently drive/repress gene expression anywhere in the genome, without irreparably changing the DNA itself. For many age-related diseases for which gene dosage needs correcting, this CRISPR technology could prove truly revolutionary. This modified Cas9, however, is bulky and well exceeds the size constraints of an AAV. Future work will need to find methods for shrinking the size of the Cas9 protein itself, such as removing unneeded nuclease elements in order to package this CRISPR activation/repression machinery into a single AAV system. Combined with a tissue-specific promoter, such a system would allow

for transient, cell-type specific gene expression manipulations across the CNS.

Conclusions

This thesis investigates four questions in the field of OPC biology: What is the niche of the OPC? How does this niche change and affect OPCs with ageing? Is OPC rejuvenation different from forced stem cell re-activation? Can these age-related pathways be therapeutically targeted in OPCs in an *in vivo* environment? Using light-sheet microscopy, I have shown that OPCs live on the blood vessels of the adult CNS, while their progeny, the oligodendrocyte, reside in the parenchyma. These OPCs express the stem cell marker Lgr5 and agonising Lgr5 *in vitro* allows for efficient OPC proliferation and differentiation. I have found that, with ageing, CNS tissue progressively stiffens by 2-3 fold. OPCs, perhaps in their vascular niche, sense this stiffening via the mechano-sensing ion-channel Piezo1 and thereby exit cell cycle. Attenuating Piezo1 activity alone is sufficient to re-activate adult and aged OPCs, allowing for increased proliferation and more efficient CNS repair following injury. As increased OPC activity underlies enhanced regeneration, I found that transient overexpression of the oncogene Myc can alone functionally rejuvenate aged OPCs. Finally, I have created a novel dual-AAV CRISPR system which efficiently targets and genome engineers OPCs in the adult and aged mouse. Doing so, I have been able to rapidly study the effects of single genes, such as Myc and Piezo1, in aged OPCs *in vivo*. By adapting principles of adult stem cell biology from other better-understood tissue niches, I have identified novel pathways that govern adult and aged OPC activation. More importantly, with genome engineering I have developed a set of tools that may help to rapidly expand our understanding of ageing OPC biology.

References

Albert, M., Antel, J., Brück, W., and Stadelmann, C. (2007). Extensive cortical remyelination in patients with chronic multiple sclerosis. Brain Pathol. 17, 129–138.

Alilain, W.J., Horn, K.P., Hu, H., Dick, T.E., and Silver, J. (2011). Functional regeneration of respiratory pathways after spinal cord injury. Nature 475, 196–200.

Andersen, O., Lygner, P.-E., Bergstr m, T., Andersson, M., and Vablne, A. (1993). Viral infections trigger multiple sclerosis relapses: a prospective seroepidemiological study. Journal of Neurology 240, 417–422.

Armstrong, R.C., Le, T.Q., Frost, E.E., Borke, R.C., and Vana, A.C. (2002). Absence of fibroblast growth factor 2 promotes oligodendroglial repopulation of demyelinated white matter. J. Neurosci. 22, 8574–8585.

Arnett, H.A. (2004). bHLH Transcription Factor Olig1 Is Required to Repair Demyelinated Lesions in the CNS. Science 306, 2111–2115.

Bacon, C., Lakics, V., Machesky, L., and Rumsby, M. (2007). N-WASP regulates extension of filopodia and processes by oligodendrocyte progenitors, oligodendrocytes, and Schwann cells-implications for axon ensheathment at myelination. Glia 55, 844–858.

Baer, A.S., Syed, Y.A., Kang, S.U., Mitteregger, D., Vig, R., ffrench-Constant, C., Franklin, R.J.M., Altmann, F., Lubec, G., and Kotter, M.R. (2009). Myelin-mediated inhibition of oligodendrocyte precursor differentiation can be overcome by pharmacological modulation of Fyn-RhoA and protein kinase C signalling. Brain 132, 465–481.

Baker, D.J., Wijshake, T., Tchkonia, T., LeBrasseur, N.K., Childs, B.G., van de Sluis, B., Kirkland, J.L., and van Deursen, J.M. (2011). Clearance of p16Ink4a-positive senescent cells delays ageing-associated disorders. Nature 479, 232–236.

Barres, B.A., Hart, I.K., Coles, H.S., Burne, J.F., Voyvodic, J.T., Richardson, W.D., and Raff, M.C. (1992). Cell death and control of cell survival in the oligodendrocyte lineage. Cell 70, 31–46.

Barres, B.A., Koroshetz, W.J., Swartz, K.J., Chun, L.L., and Corey, D.P. (1990). Ion channel expression by white matter glia: the O-2A glial progenitor cell. Neuron 4, 507–524.

Barres, B.A., Lazar, M.A., and Raff, M.C. (1994). A novel role for thyroid hormone, glucocorticoids and retinoic acid in timing oligodendrocyte development. Development 120, 1097–1108.

Benham-Pyle, B.W., Pruitt, B.L., and Nelson, W.J. (2015). Cell adhesion. Mechanical strain induces E-cadherin-dependent Yap1 and β-catenin activation to drive cell cycle entry. Science 348, 1024–1027.

Bergles, D.E., Roberts, J.D., Somogyi, P., and Jahr, C.E. (2000). Glutamatergic synapses on oligodendrocyte precursor cells in the hippocampus. Nature 405, 187–191.

Bernitz, J.M., Kim, H.S., MacArthur, B., Sieburg, H., and Moore, K. (2016). Hematopoietic Stem Cells Count and Remember Self-Renewal Divisions. Cell 167, 1296–1309.e10.

Berridge, M.J., Bootman, M.D., and Roderick, H.L. (2003). Calcium signalling: dynamics, homeostasis and remodelling. Nature Reviews Molecular Cell Biology 4, 517–529.

Bhutani, N., Brady, J.J., Damian, M., Sacco, A., Corbel, S.Y., and Blau, H.M. (2010). Reprogramming towards pluripotency requires AID-dependent DNA demethylation. Nature 463, 1042–1047.

Bjerknes, M., and Cheng, H. (1999). Clonal analysis of mouse intestinal epithelial progenitors. Gastroenterology 116, 7–14.

Bjornson, C.R.R., Cheung, T.H., Liu, L., Tripathi, P.V., Steeper, K.M., and Rando, T.A. (2012). Notch Signaling Is Necessary to Maintain Quiescence in Adult Muscle Stem Cells. Stem Cells 30, 232–242.

Blakemore, W.F. (1974). Pattern of remyelination in the CNS. Nature 249, 577–578.

Blakemore, W.F., and Franklin, R.J.M. (2008). Remyelination in experimental models of toxin-induced demyelination. Curr. Top. Microbiol. Immunol. 318, 193–212.

Blakemore, W.F., Eames, R.A., Smith, K.J., and McDonald, W.I. (1977). Remyelination in the spinal cord of the cat following intraspinal injections of lysolecithin. J. Neurol. Sci. 33, 31–43.

Blanchard, J.W., Xie, J., El-Mecharrafie, N., Gross, S., Lee, S., Lerner, R.A., and Baldwin, K.K. (2017). Replacing reprogramming factors with antibodies selected from combinatorial antibody libraries. Nat. Biotechnol. 35, 960–968.

Boudou, T., Ohayon, J., Arntz, Y., Finet, G., Picart, C., and Tracqui, P. (2006). An extended modeling of the micropipette aspiration experiment for the characterization of the Young“s modulus and Poisson”s ratio of adherent thin biological samples: Numerical and experimental studies. Journal of Biomechanics 39, 1677–1685.

Bradbury, E.J., Moon, L.D.F., Popat, R.J., King, V.R., Bennett, G.S., Patel, P.N., Fawcett, J.W., and McMahon, S.B. (2002). Chondroitinase ABC promotes functional recovery after spinal cord injury. Nature 416, 636–640.

Bribián, A., Barallobre, M.J., Soussi-Yanicostas, N., and de Castro, F. (2006). Anosmin-1 modulates the FGF-2-dependent migration of oligodendrocyte precursors in the developing optic nerve. Mol. Cell. Neurosci. 33, 2–14.

Brinkman, E.K., Chen, T., Amendola, M., and van Steensel, B. (2014). Easy quantitative assessment of genome editing by sequence trace decomposition. Nucleic Acids Res. 42, e168–e168.

Brunet, T., and King, N. (2017). The Origin of Animal Multicellularity and Cell Differentiation. Dev. Cell 43, 124–140.

Buczacki, S.J.A., Zecchini, H.I., Nicholson, A.M., Russell, R., Vermeulen, L., Kemp, R., and Winton, D.J. (2013). Intestinal label-retaining cells are secretory precursors expressing Lgr5. Nature 495, 65–69.

Bujalka, H., Koenning, M., Jackson, S., Perreau, V.M., Pope, B., Hay, C.M., Mitew, S., Hill, A.F., Lu, Q.R., Wegner, M., et al. (2013). MYRF is a membrane-associated transcription factor that autoproteolytically cleaves to directly activate myelin genes. PLoS Biol. 11, e1001625.

Butcher, D.T., Alliston, T., and Weaver, V.M. (2009). A tense situation: forcing tumour progression. Nat. Rev. Cancer 9, 108–122.

Cai, J., Qi, Y., Hu, X., Tan, M., Liu, Z., Zhang, J., Li, Q., Sander, M., and Qiu, M. (2005). Generation of oligodendrocyte precursor cells from mouse dorsal spinal cord independent of Nkx6 regulation and Shh signaling. Neuron 45, 41–53.

Caiazzo, M., Okawa, Y., Ranga, A., Piersigilli, A., Tabata, Y., and Lutolf, M.P. (2016). Defined three-dimensional microenvironments boost induction of pluripotency. Nat Mater 15, 344–352.

Camargo, F.D., Gokhale, S., Johnnidis, J.B., Fu, D., Bell, G.W., Jaenisch, R., and Brummelkamp, T.R. (2007). YAP1 increases organ size and expands undifferentiated progenitor cells. Curr. Biol. 17, 2054–2060.

Cantó, C., Jiang, L.Q., Deshmukh, A.S., Mataki, C., Coste, A., Lagouge, M., Zierath, J.R., and Auwerx, J. (2010). Interdependence of AMPK and SIRT1 for metabolic adaptation to fasting and exercise in skeletal muscle. Cell Metab. 11, 213–219.

Capecchi, M. (1989). Altering the genome by homologous recombination. Science 244, 1288–1292.

Carrano, A.C., Liu, Z., Dillin, A., and Hunter, T. (2009). A conserved ubiquitination pathway determines longevity in response to diet restriction. Nature 460, 396–399.

Challis, R.C., Kumar, S.R., Chan, K.Y., Challis, C., Jang, M.J., Rajendran, P.S., Tompkins, J.D., Shivkumar, K., Deverman, B.E., and Gradinaru, V. (2018). Widespread and targeted gene expression by systemic AAV vectors: Production, purification, and administration. bioRxiv 246405.

Chapouton, P., Skupien, P., Hesl, B., Coolen, M., Moore, J.C., Madelaine, R., Kremmer, E., Faus-Kessler, T., Blader, P., Lawson, N.D., et al. (2010). Notch Activity Levels Control the Balance between Quiescence and Recruitment of Adult Neural Stem Cells. Journal of Neuroscience 30, 7961–7974.

Cheung, T.H., and Rando, T.A. (2013). Molecular regulation of stem cell quiescence. Nature Reviews Molecular Cell Biology 14, 329–340.

Cho, Y.M., Kwon, S., Pak, Y.K., Seol, H.W., Choi, Y.M., Park, D.J., Park, K.S., and Lee, H.K. (2006). Dynamic changes in mitochondrial biogenesis and antioxidant enzymes during the spontaneous differentiation of human embryonic stem cells. Biochemical and Biophysical Research Communications 348, 1472–1478.

Chowdhury, F., Li, Y., Poh, Y.-C., Yokohama-Tamaki, T., Wang, N., and Tanaka, T.S. (2010). Soft substrates promote homogeneous self-renewal of embryonic stem cells via downregulating cell-matrix tractions. Plos One 5, e15655.

Christ, A.F., Franze, K., Gautier, H., Moshayedi, P., Fawcett, J., Franklin, R.J.M., Karadottir, R.T., and Guck, J. (2010). Mechanical difference between white and gray matter in the rat cerebellum measured by scanning force microscopy. Journal of Biomechanics 43, 2986–2992.

Colman, R.J., Anderson, R.M., Johnson, S.C., Kastman, E.K., Kosmatka, K.J., Beasley, T.M., Allison, D.B., Cruzen, C., Simmons, H.A., Kemnitz, J.W., et al. (2009). Caloric Restriction Delays Disease Onset and Mortality in Rhesus Monkeys. Science 325, 201–204.

Compston, A., and Coles, A. (2002). Multiple sclerosis. The Lancet 359, 1221–1231.

Conboy, I.M., Conboy, M.J., Wagers, A.J., Girma, E.R., Weissman, I.L., and Rando, T.A. (2005). Rejuvenation of aged progenitor cells by exposure to a young systemic environment. Nature 433, 760–764.

Confavreux, C., and Vukusic, S. (2006). Age at disability milestones in multiple sclerosis. Brain 129, 595–605.

Cong, L., Ran, F.A., Cox, D., Lin, S., Barretto, R., Habib, N., Hsu, P.D., Wu, X., Jiang, W., Marraffini, L.A., et al. (2013). Multiplex genome engineering using CRISPR/Cas systems. Science 339, 819–823.

Coste, B., Mathur, J., Schmidt, M., Earley, T.J., Ranade, S., Petrus, M.J., Dubin, A.E., and Patapoutian, A. (2010). Piezo1 and Piezo2 Are Essential Components of Distinct Mechanically Activated Cation Channels. Science 330, 55–60.

Dawson, M.R.L., Polito, A., Levine, J.M., and Reynolds, R. (2003). NG2-expressing glial progenitor cells: an abundant and widespread population of cycling cells in the adult rat CNS. Mol. Cell. Neurosci. 24, 476–488.

Day, K., Waite, L.L., Thalacker-Mercer, A., West, A., Bamman, M.M., Brooks, J.D., Myers,

R.M., and Absher, D. (2013). Differential DNA methylation with age displays both common and dynamic features across human tissues that are influenced by CpG landscape. Genome Biol 14, R102.

de Lau, W., Barker, N., Low, T.Y., Koo, B.-K., Li, V.S.W., Teunissen, H., Kujala, P., Haegebarth, A., Peters, P.J., van de Wetering, M., et al. (2011). Lgr5 homologues associate with Wnt receptors and mediate R-spondin signalling. Nature 476, 293–297.

De Waele, J., Reekmans, K., Daans, J., Goossens, H., Berneman, Z., and Ponsaerts, P. (2015). 3D culture of murine neural stem cells on decellularized mouse brain sections. Biomaterials 41, 122–131.

Deng, W., Aimone, J.B., and Gage, F.H. (2010). New neurons and new memories: how does adult hippocampal neurogenesis affect learning and memory? Nat. Rev. Neurosci. 11, 339–350.

Ding, Q., Lee, Y.-K., Schaefer, E.A.K., Peters, D.T., Veres, A., Kim, K., Kuperwasser, N., Motola, D.L., Meissner, T.B., Hendriks, W.T., et al. (2013). A TALEN genome-editing system for generating human stem cell-based disease models. Cell Stem Cell 12, 238–251.

Dixon, J.R., Selvaraj, S., Yue, F., Kim, A., Li, Y., Shen, Y., Hu, M., Liu, J.S., and Ren, B. (2012). Topological domains in mammalian genomes identified by analysis of chromatin interactions. Nature 485, 376–380.

Doetsch, F., Caillé, I., Lim, D.A., García-Verdugo, J.M., and Alvarez-Buylla, A. (1999). Subventricular Zone Astrocytes Are Neural Stem Cells in the Adult Mammalian Brain. Cell 97, 703–716.

Doudna, J.A., and Charpentier, E. (2014). Genome editing. The new frontier of genome engineering with CRISPR-Cas9. Science 346, 1258096–1258096.

Dupont, S., Zacchigna, L., Cordenonsi, M., Soligo, S., Adorno, M., Rugge, M., and Piccolo, S. (2005). Germ-layer specification and control of cell growth by Ectodermin, a Smad4 ubiquitin ligase. Cell 121, 87–99.

Dziedzic, T., Metz, I., Dallenga, T., König, F.B., Müller, S., Stadelmann, C., and Brück, W. (2010). Wallerian degeneration: a major component of early axonal pathology in multiple sclerosis. Brain Pathol. 20, 976–985.

Ebers, G.C. (1998). Randomised double-blind placebo-controlled study of interferon β-1a in relapsing/remitting multiple sclerosis. The Lancet 352, 1498–1504.

Economos, A.C., and Lints, F.A. (1985). Growth rate and life span in Drosophila V. The effect of prolongation of the period of growth on the total duration of life (J.H. Northrop, 1917)--revisited.

Eisenhoffer, G.T., Loftus, P.D., Yoshigi, M., Otsuna, H., Chien, C.-B., Morcos, P.A., and Rosenblatt, J. (2012). Crowding induces live cell extrusion to maintain homeostatic cell numbers in

epithelia. Nature 484, 546–549.

Elkin, B.S., Ilankovan, A., and Morrison, B. (2010). Age-dependent regional mechanical properties of the rat hippocampus and cortex. J Biomech Eng 132, 011010.

Emery, B., Agalliu, D., Cahoy, J.D., Watkins, T.A., Dugas, J.C., Mulinyawe, S.B., Ibrahim, A., Ligon, K.L., Rowitch, D.H., and Barres, B.A. (2009). Myelin gene regulatory factor is a critical transcriptional regulator required for CNS myelination. Cell 138, 172–185.

Engler, A.J., Sen, S., Sweeney, H.L., and Discher, D.E. (2006). Matrix elasticity directs stem cell lineage specification. Cell 126, 677–689.

Fancy, S.P.J., Zhao, C., and Franklin, R.J.M. (2004). Increased expression of Nkx2.2 and Olig2 identifies reactive oligodendrocyte progenitor cells responding to demyelination in the adult CNS. Molecular and Cellular Neuroscience 27, 247–254.

Farina, C., Weber, M.S., Meinl, E., Wekerle, H., and Hohlfeld, R. (2005). Glatiramer acetate in multiple sclerosis: update on potential mechanisms of action. Lancet Neurol 4, 567–575.

Filbin, M.G., Tirosh, I., Hovestadt, V., Shaw, M.L., Escalante, L.E., Mathewson, N.D., Neftel, C., Frank, N., Pelton, K., Hebert, C.M., et al. (2018). Developmental and oncogenic programs in H3K27M gliomas dissected by single-cell RNA-seq. Science 360, 331–335.

Finzsch, M., Stolt, C.C., Lommes, P., and Wegner, M. (2008). Sox9 and Sox10 influence survival and migration of oligodendrocyte precursors in the spinal cord by regulating PDGF receptor alpha expression. Development 135, 637–646.

Florea, M. (2017). Aging and immortality in unicellular species. Mech. Ageing Dev. 167, 5–15.

Folmes, C.D.L., Dzeja, P.P., Nelson, T.J., and Terzic, A. (2012). Metabolic plasticity in stem cell homeostasis and differentiation. Cell Stem Cell 11, 596–606.

Foran, D.R., and Peterson, A.C. (1992). Myelin acquisition in the central nervous system of the mouse revealed by an MBP-Lac Z transgene. Journal of Neuroscience 12, 4890–4897.

Franklin, R.J.M., and Goldman, S.A. (2015). Glia Disease and Repair-Remyelination. Cold Spring Harb Perspect Biol 7, a020594.

Franze, K., Francke, M., Günter, K., Christ, A.F., Körber, N., Reichenbach, A., and Guck, J. (2011). Spatial mapping of the mechanical properties of the living retina using scanning force microscopy. Soft Matter 7, 3147–3154.

Frühbeis, C., Fröhlich, D., Kuo, W.P., Amphornrat, J., Thilemann, S., Saab, A.S., Kirchhoff, F., Möbius, W., Goebbels, S., Nave, K.-A., et al. (2013). Neurotransmitter-triggered transfer of exosomes mediates oligodendrocyte-neuron communication. PLoS Biol. 11, e1001604.

Fünfschilling, U., Supplie, L.M., Mahad, D., Boretius, S., Saab, A.S., Edgar, J., Brinkmann,

B.G., Kassmann, C.M., Tzvetanova, I.D., Möbius, W., et al. (2012). Glycolytic oligodendrocytes maintain myelin and long-term axonal integrity. Nature 485, 517–521.

Garbern, J., Cambi, F., Shy, M., and Kamholz, J. (1999). The Molecular Pathogenesis of Pelizaeus-Merzbacher Disease. Archives of Neurology 56, 1210.

Ge, Y., Gomez, N.C., Adam, R.C., Nikolova, M., Yang, H., Verma, A., Lu, C.P.-J., Polak, L., Yuan, S., Elemento, O., et al. (2017). Stem Cell Lineage Infidelity Drives Wound Repair and Cancer. Cell 169, 636–650.e14.

Gems, D., Sutton, A.J., Sundermeyer, M.L., Albert, P.S., King, K.V., Edgley, M.L., Larsen, P.L., and Riddle, D.L. (1998). Two pleiotropic classes of daf-2 mutation affect larval arrest, adult behavior, reproduction and longevity in Caenorhabditis elegans. Genetics 150, 129–155.

Gibson, E.M., Purger, D., Mount, C.W., Goldstein, A.K., Lin, G.L., Wood, L.S., Inema, I., Miller, S.E., Bieri, G., Zuchero, J.B., et al. (2014). Neuronal activity promotes oligodendrogenesis and adaptive myelination in the mammalian brain. Science 344, 1252304–1252304.

Gilbert, P.M., Havenstrite, K.L., Magnusson, K.E.G., Sacco, A., Leonardi, N.A., Kraft, P., Nguyen, N.K., Thrun, S., Lutolf, M.P., and Blau, H.M. (2010). Substrate Elasticity Regulates Skeletal Muscle Stem Cell Self-Renewal in Culture. Science 329, 1078–1081.

Glass, B. (1988). Hydra and the Birth of Experimental Biology 1744. Abraham Trembley's Memoirs Concerning the Polyps. Book I: Some Reflections on Abraham Trembley and His Memoires. Book II: A Translation from the French of Memoires, pour servir a L'histoire d" un genre de polypes d"eau douce, a bras en forme de cornes.Sylvia G. Lenhoff , Howard M. Lenhoff. The Quarterly Review of Biology 63, 62–63.

Goldschmidt, T., Antel, J., König, F.B., Bruck, W., and Kuhlmann, T. (2009). Remyelination capacity of the MS brain decreases with disease chronicity. Neurology 72, 1914–1921.

Goodell, M.A., and Rando, T.A. (2015). Stem cells and healthy aging. Science 350, 1199–1204.

Gopinath, S.D., and Rando, T.A. (2008). Stem Cell Review Series: Aging of the skeletal muscle stem cell niche. Aging Cell 7, 590–598.

Griffiths, I., Klugmann, M., Anderson, T., Yool, D., Thomson, C., Schwab, M.H., Schneider, A., Zimmermann, F., McCulloch, M., Nadon, N., et al. (1998). Axonal swellings and degeneration in mice lacking the major proteolipid of myelin. Science 280, 1610–1613.

Gudipaty, S.A., Lindblom, J., Loftus, P.D., Redd, M.J., and Edes, K. (2017). Mechanical stretch triggers rapid epithelial cell division through Piezo1. Nature.

Guelen, L., Pagie, L., Brasset, E., Meuleman, W., Faza, M.B., Talhout, W., Eussen, B.H., de Klein, A., Wessels, L., de Laat, W., et al. (2008). Domain organization of human chromosomes revealed by mapping of nuclear lamina interactions. Nature 453, 948–951.

Gurevich, D.B., Nguyen, P.D., Siegel, A.L., Ehrlich, O.V., Sonntag, C., Phan, J.M.N., Berger, S., Ratnayake, D., Hersey, L., Berger, J., et al. (2016). Asymmetric division of clonal muscle stem cells coordinates muscle regeneration *in vivo*. Science 353, aad9969–aad9969.

Hallas, B.H., Das, G.D., and Das, K.G. (1980). Transplantation of brain tissue in the brain of rat. II. Growth characteristics of neocortical transplants in hosts of different ages. American Journal of Anatomy 158, 147–159.

Hamilton, T.G., Klinghoffer, R.A., Corrin, P.D., and Soriano, P. (2003). Evolutionary divergence of platelet-derived growth factor alpha receptor signaling mechanisms. Mol. Cell. Biol. 23, 4013–4025.

Hao, E., Tyrberg, B., Itkin-Ansari, P., Lakey, J.R.T., Geron, I., Monosov, E.Z., Barcova, M., Mercola, M., and Levine, F. (2006). Beta-cell differentiation from nonendocrine epithelial cells of the adult human pancreas. Nature Medicine 12, 310–316.

Hao, H.-X., Xie, Y., Zhang, Y., Charlat, O., Oster, E., Avello, M., Lei, H., Mickanin, C., Liu, D., Ruffner, H., et al. (2012). ZNRF3 promotes Wnt receptor turnover in an R-spondin-sensitive manner. Nature 485, 195–200.

Harman, D. (1956). Aging: A Theory Based on Free Radical and Radiation Chemistry. Journal of Gerontology 11, 298–300.

Harrison, D.E., Strong, R., Sharp, Z.D., Nelson, J.F., Astle, C.M., Flurkey, K., Nadon, N.L., Wilkinson, J.E., Frenkel, K., Carter, C.S., et al. (2009). Rapamycin fed late in life extends lifespan in genetically heterogeneous mice. Nature 460, 392–395.

Hauser, S.L., and Oksenberg, J.R. (2006). The neurobiology of multiple sclerosis: genes, inflammation, and neurodegeneration. Neuron 52, 61–76.

He, L., Si, G., Huang, J., Samuel, A.D.T., and Perrimon, N. (2018). Mechanical regulation of stem-cell differentiation by the stretch-activated Piezo channel. Nature 555, 103–106.

Hertz, H. (1882). Über die Berührung fester elastischer Körper. (Journal für die reine und angewandte Mathematik).

Hill, R.A., Li, A.M., and Grutzendler, J. (2018). Lifelong cortical myelin plasticity and age-related degeneration in the live mammalian brain. Nature Neuroscience 21, 683–695.

Hinks, G.L., and Franklin, R.J. (2000). Delayed changes in growth factor gene expression during slow remyelination in the CNS of aged rats. Mol. Cell. Neurosci. 16, 542–556.

Holstein, T.W., Hobmayer, E., and David, C.N. (1991). Pattern of epithelial cell cycling in hydra. Developmental Biology 148, 602–611.

Holzenberger, M., Dupont, J., Ducos, B., Leneuve, P., Géloën, A., Even, P.C., Cervera, P., and Le Bouc, Y. (2003). IGF-1 receptor regulates lifespan and resistance to oxidative stress in mice.

Nature 421, 182–187.

Hornig, J., Fröb, F., Vogl, M.R., Hermans-Borgmeyer, I., Tamm, E.R., and Wegner, M. (2013). The transcription factors Sox10 and Myrf define an essential regulatory network module in differentiating oligodendrocytes. PLoS Genet. 9, e1003907.

Hsu, Y.-C., Pasolli, H.A., and Fuchs, E. (2011). Dynamics between stem cells, niche, and progeny in the hair follicle. Cell 144, 92–105.

Hu, Q.-D., Ang, B.-T., Karsak, M., Hu, W.-P., Cui, X.-Y., Duka, T., Takeda, Y., Chia, W., Sankar, N., Ng, Y.-K., et al. (2003). F3/Contactin Acts as a Functional Ligand for Notch during Oligodendrocyte Maturation. Cell 115, 163–175.

Huang, J.K., Jarjour, A.A., Oumesmar, B.N., Kerninon, C., Williams, A., Krezel, W., Kagechika, H., Bauer, J., Zhao, C., Baron-Van Evercooren, A., et al. (2011). Retinoid X receptor gamma signaling accelerates CNS remyelination. Nature Neuroscience 14, 45–53.

Huangfu, D., Maehr, R., Guo, W., Eijkelenboom, A., Snitow, M., Chen, A.E., and Melton, D.A. (2008). Induction of pluripotent stem cells by defined factors is greatly improved by small-molecule compounds. Nat. Biotechnol. 26, 795–797.

Hubler, Z., Allimuthu, D., Bederman, I., Elitt, M.S., Madhavan, M., Allan, K.C., Shick, H.E., Garrison, E., T Karl, M., Factor, D.C., et al. (2018). Accumulation of 8,9-unsaturated sterols drives oligodendrocyte formation and remyelination. Nature 338, 491.

Huch, M., Dorrell, C., Boj, S.F., van Es, J.H., Li, V.S.W., van de Wetering, M., Sato, T., Hamer, K., Sasaki, N., Finegold, M.J., et al. (2013). In vitro expansion of single Lgr5+ liver stem cells induced by Wnt-driven regeneration. Nature 494, 247–250.

Hughes, E.G., Kang, S.H., Fukaya, M., and Bergles, D.E. (2013). Oligodendrocyte progenitors balance growth with self-repulsion to achieve homeostasis in the adult brain. Nature Neuroscience 16, 668–676.

Hughes, E.G., Orthmann-Murphy, J.L., Langseth, A.J., and Bergles, D.E. (2018). Myelin remodeling through experience-dependent oligodendrogenesis in the adult somatosensory cortex. Nature Neuroscience 468, 244.

Jagielska, A., Norman, A.L., Whyte, G., Van Vliet, K.J., Guck, J., and Franklin, R.J.M. (2012). Mechanical Environment Modulates Biological Properties of Oligodendrocyte Progenitor Cells. Http://Dx.Doi.org/10.1089/Scd.2012.0189 21, 2905–2914.

Jaks, V., Barker, N., Kasper, M., van Es, J.H., Snippert, H.J., Clevers, H., and Toftgård, R. (2008). Lgr5 marks cycling, yet long-lived, hair follicle stem cells. Nature Genetics 40, 1291–1299.

Jaskelioff, M., Muller, F.L., Paik, J.-H., Thomas, E., Jiang, S., Adams, A.C., Sahin, E., Kost-Alimova, M., Protopopov, A., Cadiñanos, J., et al. (2011). Telomerase reactivation reverses tissue

degeneration in aged telomerase-deficient mice. Nature 469, 102–106.

Jeune, B. (2013). Living longer — but better? Aging Clinical and Experimental Research 14, 72–93.

Jung, P., Sato, T., Merlos-Suárez, A., Barriga, F.M., Iglesias, M., Rossell, D., Auer, H., Gallardo, M., Blasco, M.A., Sancho, E., et al. (2011). Isolation and *in vitro* expansion of human colonic stem cells. Nature Medicine 17, 1225–1227.

Kanfi, Y., Naiman, S., Amir, G., Peshti, V., Zinman, G., Nahum, L., Bar-Joseph, Z., and Cohen, H.Y. (2012). The sirtuin SIRT6 regulates lifespan in male mice. Nature 483, 218–221.

Katajisto, P., Döhla, J., Chaffer, C.L., Pentinmikko, N., Marjanovic, N., Iqbal, S., Zoncu, R., Chen, W., Weinberg, R.A., and Sabatini, D.M. (2015). Stem cells. Asymmetric apportioning of aged mitochondria between daughter cells is required for stemness. Science 348, 340–343.

Katsimpardi, L., Litterman, N.K., Schein, P.A., Miller, C.M., Loffredo, F.S., Wojtkiewicz, G.R., Chen, J.W., Lee, R.T., Wagers, A.J., and Rubin, L.L. (2014). Vascular and neurogenic rejuvenation of the aging mouse brain by young systemic factors. Science 344, 630–634.

Kay, M.A., He, C.-Y., and Chen, Z.-Y. (2010). A robust system for production of minicircle DNA vectors. Nat. Biotechnol. 28, 1287–1289.

Kenyon, C., Chang, J., Gensch, E., Rudner, A., and Tabtiang, R. (1993). A C. elegans mutant that lives twice as long as wild type. Nature 366, 461–464.

Keough, M.B., Rogers, J.A., Zhang, P., Jensen, S.K., Stephenson, E.L., Chen, T., Hurlbert, M.G., Lau, L.W., Rawji, K.S., Plemel, J.R., et al. (2016). An inhibitor of chondroitin sulfate proteoglycan synthesis promotes central nervous system remyelination. Nat Commun 7, 11312.

Kessaris, N., Fogarty, M., Iannarelli, P., Grist, M., Wegner, M., and Richardson, W.D. (2005). Competing waves of oligodendrocytes in the forebrain and postnatal elimination of an embryonic lineage. Nature Neuroscience 9, 173–179.

Khazipov, R., Zaynutdinova, D., Ogievetsky, E., Valeeva, G., Mitrukhina, O., Manent, J.-B., and Represa, A. (2015). Atlas of the Postnatal Rat Brain in Stereotaxic Coordinates. Front Neuroanat 9, 161.

Kim, E., Koo, T., Park, S.W., Kim, D., Kim, K., Cho, H.-Y., Song, D.W., Lee, K.J., Jung, M.H., Kim, S., et al. (2017). *In vivo* genome editing with a small Cas9 orthologue derived from Campylobacter jejuni. Nat Commun 8, 14500.

Kim, J., Sturgill, D., Tran, A.D., Sinclair, D.A., and Oberdoerffer, P. (2016). Controlled DNA double-strand break induction in mice reveals post-damage transcriptome stability. Nucleic Acids Res. 44, e64–e64.

Kim, J., Woo, A.J., Chu, J., Snow, J.W., Fujiwara, Y., Kim, C.G., Cantor, A.B., and Orkin, S.H.

(2010). A Myc network accounts for similarities between embryonic stem and cancer cell transcription programs. Cell 143, 313–324.

Kleinsmith, l.j., and pierce, g.b. (1964). Multipotentiality of single embryonal carcinoma cells. Cancer Res. 24, 1544–1551.

Kleinstiver, B.P., Prew, M.S., Tsai, S.Q., Topkar, V.V., Nguyen, N.T., Zheng, Z., Gonzales, A.P.W., Li, Z., Peterson, R.T., Yeh, J.-R.J., et al. (2015). Engineered CRISPR-Cas9 nucleases with altered PAM specificities. Nature 523, 481–485.

Komatsu, M., Waguri, S., Chiba, T., Murata, S., Iwata, J.-I., Tanida, I., Ueno, T., Koike, M., Uchiyama, Y., Kominami, E., et al. (2006). Loss of autophagy in the central nervous system causes neurodegeneration in mice. Nature 441, 880–884.

Konermann, S., Brigham, M.D., Trevino, A.E., Joung, J., Abudayyeh, O.O., Barcena, C., Hsu, P.D., Habib, N., Gootenberg, J.S., Nishimasu, H., et al. (2015). Genome-scale transcriptional activation by an engineered CRISPR-Cas9 complex. Nature 517, 583–588.

Kornek, B., Storch, M.K., Weissert, R., Wallstroem, E., Stefferl, A., Olsson, T., Linington, C., Schmidbauer, M., and Lassmann, H. (2000). Multiple sclerosis and chronic autoimmune encephalomyelitis: a comparative quantitative study of axonal injury in active, inactive, and remyelinated lesions. Am. J. Pathol. 157, 267–276.

Koser, D.E., Moeendarbary, E., Hanne, J., Kuerten, S., and Franze, K. (2015). CNS Cell Distribution and Axon Orientation Determine Local Spinal Cord Mechanical Properties. Biophysical Journal 108, 2137–2147.

Koser, D.E., Thompson, A.J., Foster, S.K., Dwivedy, A., Pillai, E.K., Sheridan, G.K., Svoboda, H., Viana, M., Costa, L.D.F., Guck, J., et al. (2016). Mechanosensing is critical for axon growth in the developing brain. Nature Neuroscience 19, 1592–1598.

Kosicki, M., Tomberg, K., and Bradley, A. (2018). Repair of double-strand breaks induced by CRISPR-Cas9 leads to large deletions and complex rearrangements. Nat. Biotechnol. 36, 765–771.

Kotter, M.R., Li, W.-W., Zhao, C., and Franklin, R.J.M. (2006). Myelin impairs CNS remyelination by inhibiting oligodendrocyte precursor cell differentiation. J. Neurosci. 26, 328–332.

Kroon, E., Martinson, L.A., Kadoya, K., Bang, A.G., Kelly, O.G., Eliazer, S., Young, H., Richardson, M., Smart, N.G., Cunningham, J., et al. (2008). Pancreatic endoderm derived from human embryonic stem cells generates glucose-responsive insulin-secreting cells *in vivo*. Nat. Biotechnol. 26, 443–452.

Kuhlmann, T., Miron, V., Cuo, Q., Wegner, C., Antel, J., and Bruck, W. (2008). Differentiation block of oligodendroglial progenitor cells as a cause for remyelination failure in chronic multiple sclerosis. Brain 131, 1749–1758.

Kujoth, G.C., Hiona, A., Pugh, T.D., Someya, S., Panzer, K., Wohlgemuth, S.E., Hofer, T., Seo, A.Y., Sullivan, R., Jobling, W.A., et al. (2005). Mitochondrial DNA mutations, oxidative stress, and apoptosis in mammalian aging. Science 309, 481–484.

Kurosu, H., Yamamoto, M., Clark, J.D., Pastor, J.V., Nandi, A., Gurnani, P., McGuinness, O.P., Chikuda, H., Yamaguchi, M., Kawaguchi, H., et al. (2005). Suppression of aging in mice by the hormone Klotho. Science 309, 1829–1833.

Küspert, M., Hammer, A., Bösl, M.R., and Wegner, M. (2011). Olig2 regulates Sox10 expression in oligodendrocyte precursors through an evolutionary conserved distal enhancer. Nucleic Acids Res. 39, 1280–1293.

Kwok, J.C.F., Dick, G., Wang, D., and Fawcett, J.W. (2011). Extracellular matrix and perineuronal nets in CNS repair. Dev Neurobiol 71, 1073–1089.

Lacraz, G., Rouleau, A.-J., Couture, V., Söllrald, T., Drouin, G., Veillette, N., Grandbois, M., and Grenier, G. (2015). Increased Stiffness in Aged Skeletal Muscle Impairs Muscle Progenitor Cell Proliferative Activity. Plos One 10, e0136217.

Lake, B.B., Chen, S., Sos, B.C., Fan, J., Kaeser, G.E., Yung, Y.C., Duong, T.E., Gao, D., Chun, J., Kharchenko, P.V., et al. (2018). Integrative single-cell analysis of transcriptional and epigenetic states in the human adult brain. Nat. Biotechnol. 36, 70–80.

Lang, B.T., Cregg, J.M., DePaul, M.A., Tran, A.P., Xu, K., Dyck, S.M., Madalena, K.M., Brown, B.P., Weng, Y.-L., Li, S., et al. (2015). Modulation of the proteoglycan receptor PTPσ promotes recovery after spinal cord injury. Nature 518, 404–408.

Lappe-Siefke, C., Goebbels, S., Gravel, M., Nicksch, E., Lee, J., Braun, P.E., Griffiths, I.R., and Nave, K.-A. (2003). Disruption of Cnp1 uncouples oligodendroglial functions in axonal support and myelination. Nature Genetics 33, 366–374.

Lazarini, F., and Lledo, P.-M. (2011). Is adult neurogenesis essential for olfaction? Trends Neurosci. 34, 20–30.

Lee, H., and Kim, J.-S. (2018). Unexpected CRISPR on-target effects. Nat. Biotechnol. 36, 703–704.

Lee, V.W., de Kretser, D.M., Hudson, B., and Wang, C. (1975). Variations in serum FSH, LH and testosterone levels in male rats from birth to sexual maturity. J. Reprod. Fertil. 42, 121–126.

Lee, Y., Morrison, B.M., Li, Y., Lengacher, S., Farah, M.H., Hoffman, P.N., Liu, Y., Tsingalia, A., Jin, L., Zhang, P.-W., et al. (2012). Oligodendroglia metabolically support axons and contribute to neurodegeneration. Nature 487, 443–448.

Leeman, D.S., Hebestreit, K., Ruetz, T., Webb, A.E., McKay, A., Pollina, E.A., Dulken, B.W., Zhao, X., Yeo, R.W., Ho, T.T., et al. (2018). Lysosome activation clears aggregates and enhances quiescent neural stem cell activation during aging. Science 359, 1277–1283.

Li, J., Hou, B., Tumova, S., Muraki, K., Bruns, A., Ludlow, M.J., Sedo, A., Hyman, A.J., McKeown, L., Young, R.S., et al. (2014). Piezo1 integration of vascular architecture with physiological force. Nature 515, 279–282.

Li, L., and Clevers, H. (2010). Coexistence of quiescent and active adult stem cells in mammals. Science 327, 542–545.

Lin, M.-J., Tang, L.-Y., Reddy, M.N., and Shen, C.-K.J. (2005). DNA methyltransferase gene dDnmt2 and longevity of Drosophila. J. Biol. Chem. 280, 861–864.

Lin, S.-C., and Bergles, D.E. (2004). Synaptic signaling between GABAergic interneurons and oligodendrocyte precursor cells in the hippocampus. Nature Neuroscience 7, 24–32.

Liu, L., Cheung, T.H., Charville, G.W., Hurgo, B.M.C., Leavitt, T., Shih, J., Brunet, A., and Rando, T.A. (2013). Chromatin modifications as determinants of muscle stem cell quiescence and chronological aging. Cell Rep 4, 189–204.

Livet, J., Weissman, T.A., Kang, H., Draft, R.W., Lu, J., Bennis, R.A., Sanes, J.R., and Lichtman, J.W. (2007). Transgenic strategies for combinatorial expression of fluorescent proteins in the nervous system. Nature 450, 56–62.

Loffredo, F.S., Steinhauser, M.L., Jay, S.M., Gannon, J., Pancoast, J.R., Yalamanchi, P., Sinha, M., Dall'Osso, C., Khong, D., Shadrach, J.L., et al. (2013). Growth Differentiation Factor 11 Is a Circulating Factor that Reverses Age-Related Cardiac Hypertrophy. Cell 153, 828–839.

López-Otín, C., Blasco, M.A., Partridge, L., Serrano, M., and Kroemer, G. (2013). The Hallmarks of Aging. Cell 153, 1194–1217.

Lu, Q.R., Yuk, D., Alberta, J.A., Zhu, Z., Pawlitzky, I., Chan, J., McMahon, A.P., Stiles, C.D., and Rowitch, D.H. (2000). Sonic hedgehog--regulated oligodendrocyte lineage genes encoding bHLH proteins in the mammalian central nervous system. Neuron 25, 317–329.

Lu, Q.R., Sun, T., Zhu, Z., Ma, N., Garcia, M., Stiles, C.D., and Rowitch, D.H. (2002). Common developmental requirement for Olig function indicates a motor neuron/oligodendrocyte connection. Cell 109, 75–86.

Lukjanenko, L., Jung, M.J., Hegde, N., Perruisseau-Carrier, C., Migliavacca, E., Rozo, M., Karaz, S., Jacot, G., Schmidt, M., Li, L., et al. (2016). Loss of fibronectin from the aged stem cell niche affects the regenerative capacity of skeletal muscle in mice. Nature Medicine 22, 897–905.

Mahishale, V. (2015). Ageing world: Health care challenges. Journal of the Scientific Society 42, 138.

Makinodan, M., Rosen, K.M., Ito, S., and Corfas, G. (2012). A critical period for social experience-dependent oligodendrocyte maturation and myelination. Science 337, 1357–1360.

Mali, P., Yang, L., Esvelt, K.M., Aach, J., Guell, M., DiCarlo, J.E., Norville, J.E., and Church, G.M. (2013). RNA-guided human genome engineering via Cas9. Science 339, 823–826.

Marión, R.M., Strati, K., Li, H., Tejera, A., Schoeftner, S., Ortega, S., Serrano, M., and Blasco, M.A. (2009). Telomeres acquire embryonic stem cell characteristics in induced pluripotent stem cells. Cell Stem Cell 4, 141–154.

Marta, C.B., Adamo, A.M., Soto, E.F., and Pasquini, J.M. (1998). Sustained neonatal hyperthyroidism in the rat affects myelination in the central nervous system. Journal of Neuroscience Research 53, 251–259.

Martin-Montalvo, A., Mercken, E.M., Mitchell, S.J., Palacios, H.H., Mote, P.L., Scheibye-Knudsen, M., Gomes, A.P., Ward, T.M., Minor, R.K., Blouin, M.-J., et al. (2013). Metformin improves healthspan and lifespan in mice. Nat Commun 4, 2192.

Maruyama, T., Dougan, S.K., Truttmann, M.C., Bilate, A.M., Ingram, J.R., and Ploegh, H.L. (2015). Increasing the efficiency of precise genome editing with CRISPR-Cas9 by inhibition of nonhomologous end joining. Nat. Biotechnol. 33, 538–542.

Matsumura, H., Mohri, Y., Binh, N.T., Morinaga, H., Fukuda, M., Ito, M., Kurata, S., Hoeijmakers, J., and Nishimura, E.K. (2016). Hair follicle aging is driven by transepidermal elimination of stem cells via COL17A1 proteolysis. Science 351, 4395–4395.

Matsuoka, T., Ahlberg, P.E., Kessaris, N., Iannarelli, P., Dennehy, U., Richardson, W.D., McMahon, A.P., and Koentges, G. (2005). Neural crest origins of the neck and shoulder. Nature 436, 347–355.

Matsushima, G.K., and Morell, P. (2001). The neurotoxicant, cuprizone, as a model to study demyelination and remyelination in the central nervous system. Brain Pathol. 11, 107–116.

McCord, R.P., Nazario-Toole, A., Zhang, H., Chines, P.S., Zhan, Y., Erdos, M.R., Collins, F.S., Dekker, J., and Cao, K. (2013). Correlated alterations in genome organization, histone methylation, and DNA-lamin A/C interactions in Hutchinson-Gilford progeria syndrome. Genome Research 23, 260–269.

McHugh, B.J., Buttery, R., Lad, Y., Banks, S., Haslett, C., and Sethi, T. (2010). Integrin activation by Fam38A uses a novel mechanism of R-Ras targeting to the endoplasmic reticulum. J. Cell. Sci. 123, 51–61.

McKenzie, I.A., Ohayon, D., Li, H., de Faria, J.P., Emery, B., Tohyama, K., and Richardson, W.D. (2014). Motor skill learning requires active central myelination. Science 346, 318–322.

McKinnon, R.D., Matsui, T., Dubois-Dalcq, M., and Aaronson, S.A. (1990). FGF modulates the PDGF-driven pathway of oligodendrocyte development. Neuron 5, 603–614.

McRae, P.A., Rocco, M.M., Kelly, G., Brumberg, J.C., and Matthews, R.T. (2007). Sensory deprivation alters aggrecan and perineuronal net expression in the mouse barrel cortex. J. Neu-

rosci. 27, 5405–5413.

Menn, B., García-Verdugo, J.M., Yaschine, C., Gonzalez-Perez, O., Rowitch, D., and Alvarez-Buylla, A. (2006). Origin of oligodendrocytes in the subventricular zone of the adult brain. J. Neurosci. 26, 7907–7918.

Mertens, J., Paquola, A.C.M., Ku, M., Hatch, E., Böhnke, L., Ladjevardi, S., McGrath, S., Campbell, B., Lee, H., Herdy, J.R., et al. (2015). Directly Reprogrammed Human Neurons Retain Aging-Associated Transcriptomic Signatures and Reveal Age-Related Nucleocytoplasmic Defects. Cell Stem Cell 17, 705–718.

Michailov, G.V., Sereda, M.W., Brinkmann, B.G., Fischer, T.M., Haug, B., Birchmeier, C., Role, L., Lai, C., Schwab, M.H., and Nave, K.-A. (2004). Axonal neuregulin-1 regulates myelin sheath thickness. Science 304, 700–703.

Michishita, E., McCord, R.A., Berber, E., Kioi, M., Padilla-Nash, H., Damian, M., Cheung, P., Kusumoto, R., Kawahara, T.L.A., Barrett, J.C., et al. (2008). SIRT6 is a histone H3 lysine 9 deacetylase that modulates telomeric chromatin. Nature 452, 492–496.

Mihaylova, M.M., and Shaw, R.J. (2011). The AMPK signalling pathway coordinates cell growth, autophagy and metabolism. Nat Cell Biol 13, 1016–1023.

Miller, J.D., Ganat, Y.M., Kishinevsky, S., Bowman, R.L., Liu, B., Tu, E.Y., Mandal, P.K., Vera, E., Shim, J.-W., Kriks, S., et al. (2013). Human iPSC-based modeling of late-onset disease via progerin-induced aging. Cell Stem Cell 13, 691–705.

Miller, T.E., Wang, J., Sukhdeo, K., Horbinski, C., Tesar, P.J., Wechsler-Reya, R.J., and Rich, J.N. (2014). Lgr5 Marks Post-Mitotic, Lineage Restricted Cerebellar Granule Neurons during Postnatal Development. Plos One 9, e114433.

Miron, V.E., Boyd, A., Zhao, J.-W., Yuen, T.J., Ruckh, J.M., Shadrach, J.L., van Wijngaarden, P., Wagers, A.J., Williams, A., Franklin, R.J.M., et al. (2013). M2 microglia and macrophages drive oligodendrocyte differentiation during CNS remyelination. Nature Neuroscience 16, 1211–1218.

Mitra, S.K., Hanson, D.A., and Schlaepfer, D.D. (2005). Focal adhesion kinase: in command and control of cell motility. Nature Reviews Molecular Cell Biology 6, 56–68.

Morgan, T.H. (1901). Growth and regeneration in Planaria lugubris. Archiv Für Entwickelungsmechanik Der Organismen 13, 179–212.

Moshayedi, P., da F Costa, L., Christ, A., Lacour, S.P., Fawcett, J., Guck, J., and Franze, K. (2010). Mechanosensitivity of astrocytes on optimized polyacrylamide gels analyzed by quantitative morphometry. Journal of Physics: Condensed Matter 22, 194114.

Moskalev, A.A., Shaposhnikov, M.V., Plyusnina, E.N., Zhavoronkov, A., Budovsky, A., Yanai, H., and Fraifeld, V.E. (2013). The role of DNA damage and repair in aging through the prism of

Koch-like criteria. Ageing Res. Rev. 12, 661–684.

Mosteiro, L., Pantoja, C., Alcazar, N., Marión, R.M., Chondronasiou, D., Rovira, M., Fernandez-Marcos, P.J., Muñoz-Martin, M., Blanco-Aparicio, C., Pastor, J., et al. (2016). Tissue damage and senescence provide critical signals for cellular reprogramming *in vivo*. Science 354, aaf4445–aaf4445.

Mostoslavsky, R., Chua, K.F., Lombard, D.B., Pang, W.W., Fischer, M.R., Gellon, L., Liu, P., Mostoslavsky, G., Franco, S., Murphy, M.M., et al. (2006). Genomic instability and aging-like phenotype in the absence of mammalian SIRT6. Cell 124, 315–329.

Mouw, J.K., Yui, Y., Damiano, L., Bainer, R.O., Lakins, J.N., Acerbi, I., Ou, G., Wijekoon, A.C., Levental, K.R., Gilbert, P.M., et al. (2014). Tissue mechanics modulate microRNA-dependent PTEN expression to regulate malignant progression. Nature Medicine 20, 360–367.

Moyon, S., Dubessy, A.L., Aigrot, M.S., Trotter, M., Huang, J.K., Dauphinot, L., Potier, M.C., Kerninon, C., Melik Parsadaniantz, S., Franklin, R.J.M., et al. (2015). Demyelination causes adult CNS progenitors to revert to an immature state and express immune cues that support their migration. J. Neurosci. 35, 4–20.

Naik, S., Larsen, S.B., Gomez, N.C., Alaverdyan, K., Sendoel, A., Yuan, S., Polak, L., Kulukian, A., Chai, S., and Fuchs, E. (2017). Inflammatory memory sensitizes skin epithelial stem cells to tissue damage. Nature 550, 475–480.

Nakata, S., Campos, B., Bageritz, J., Bermejo, J.L., Becker, N., Engel, F., Acker, T., Momma, S., Herold-Mende, C., Lichter, P., et al. (2013). LGR5 is a marker of poor prognosis in glioblastoma and is required for survival of brain cancer stem-like cells. Brain Pathol. 23, 60–72.

Nisoli, E., Tonello, C., Cardile, A., Cozzi, V., Bracale, R., Tedesco, L., Falcone, S., Valerio, A., Cantoni, O., Clementi, E., et al. (2005). Calorie restriction promotes mitochondrial biogenesis by inducing the expression of eNOS. Science 310, 314–317.

Nissim, L., Perli, S.D., Fridkin, A., Perez-Pinera, P., and Lu, T.K. (2014). Multiplexed and programmable regulation of gene networks with an integrated RNA and CRISPR/Cas toolkit in human cells. Mol. Cell 54, 698–710.

Niu, J., Mei, F., Wang, L., Liu, S., Tian, Y., Mo, W., Li, H., Lu, Q.R., and Xiao, L. (2012). Phosphorylated olig1 localizes to the cytosol of oligodendrocytes and promotes membrane expansion and maturation. Glia 60, 1427–1436.

Obri, A., Khrimian, L., Karsenty, G., and Oury, F. (2018). Osteocalcin in the brain: from embryonic development to age-related decline in cognition. Nat Rev Endocrinol 14, 174–182.

Ocampo, A., Reddy, P., Martinez-Redondo, P., Platero-Luengo, A., Hatanaka, F., Hishida, T., Li, M., Lam, D., Kurita, M., Beyret, E., et al. (2016). In Vivo Amelioration of Age-Associated Hallmarks by Partial Reprogramming. Cell 167, 1719–1733.e12.

Oh, J., Lee, Y.D., and Wagers, A.J. (2014). Stem cell aging: mechanisms, regulators and therapeutic opportunities. Nature Medicine 20, 870–880.

Okita, K., Ichisaka, T., and Yamanaka, S. (2007). Generation of germline-competent induced pluripotent stem cells. Nature 448, 313–317.

Osborne, T.B., Mendel, L.B., and Ferry, E.L. (1917). The effect of retardation of growth upon the breeding period and duration of life of rats. Science 45, 294–295.

Oury, F., Khrimian, L., Denny, C.A., Gardin, A., Chamouni, A., Goeden, N., Huang, Y.-Y., Lee, H., Srinivas, P., Gao, X.-B., et al. (2013). Maternal and offspring pools of osteocalcin influence brain development and functions. Cell 155, 228–241.

Pagliuca, F.W., Millman, J.R., Gürtler, M., Segel, M., Van Dervort, A., Ryu, J.H., Peterson, Q.P., Greiner, D., and Melton, D.A. (2014). Generation of functional human pancreatic β cells *in vitro*. Cell 159, 428–439.

Panciera, T., Azzolin, L., Fujimura, A., Di Biagio, D., Frasson, C., Bresolin, S., Soligo, S., Basso, G., Bicciato, S., Rosato, A., et al. (2016). Induction of Expandable Tissue-Specific Stem/Progenitor Cells through Transient Expression of YAP/TAZ. Cell Stem Cell 19, 725–737.

Papastefanaki, F., and Matsas, R. (2015). From demyelination to remyelination: the road toward therapies for spinal cord injury. Glia 63, 1101–1125.

Patel, A., Malinovska, L., Saha, S., Wang, J., Alberti, S., Krishnan, Y., and Hyman, A.A. (2017). ATP as a biological hydrotrope. Science 356, 753–756.

Pelvig, D.P., Pakkenberg, H., Stark, A.K., and Pakkenberg, B. (2008). Neocortical glial cell numbers in human brains. Neurobiol. Aging 29, 1754–1762.

Peric-Hupkes, D., Meuleman, W., Pagie, L., Bruggeman, S.W.M., Solovei, I., Brugman, W., Gräf, S., Flicek, P., Kerkhoven, R.M., van Lohuizen, M., et al. (2010). Molecular maps of the reorganization of genome-nuclear lamina interactions during differentiation. Mol. Cell 38, 603–613.

Pertea, M., Kim, D., Pertea, G.M., Leek, J.T., and Salzberg, S.L. (2016). Transcript-level expression analysis of RNA-seq experiments with HISAT, StringTie and Ballgown. Nature Protocols 11, 1650–1667.

Petersen, M.A., Ryu, J.K., Chang, K.-J., Etxeberria, A., Bardehle, S., Mendiola, A.S., Kamau-Devers, W., Fancy, S.P.J., Thor, A., Bushong, E.A., et al. (2017). Fibrinogen Activates BMP Signaling in Oligodendrocyte Progenitor Cells and Inhibits Remyelination after Vascular Damage. Neuron 96, 1003–1012.e1007.

Pfeiffer, S.E., Warrington, A.E., and Bansal, R. (1993). The oligodendrocyte and its many cellular processes. Trends in Cell Biology 3, 191–197.

Piaton, G., Aigrot, M.S., Williams, A., Moyon, S., Tepavcevic, V., Moutkine, I., Gras, J., Matho, K.S., Schmitt, A., Soellner, H., et al. (2011). Class 3 semaphorins influence oligodendrocyte precursor recruitment and remyelination in adult central nervous system. Brain 134, 1156–1167.

Plath, K., and Lowry, W.E. (2011). Progress in understanding reprogramming to the induced pluripotent state. Nat. Rev. Genet. 12, 253–265.

Pohl, H.B.F., Porcheri, C., Mueggler, T., Bachmann, L.C., Martino, G., Riethmacher, D., Franklin, R.J.M., Rudin, M., and Suter, U. (2011). Genetically Induced Adult Oligodendrocyte Cell Death Is Associated with Poor Myelin Clearance, Reduced Remyelination, and Axonal Damage. Journal of Neuroscience 31, 1069–1080.

Porrello, E.R., Mahmoud, A.I., Simpson, E., Hill, J.A., Richardson, J.A., Olson, E.N., and Sadek, H.A. (2011). Transient regenerative potential of the neonatal mouse heart. Science 331, 1078–1080.

Prager-Khoutorsky, M., Lichtenstein, A., Krishnan, R., Rajendran, K., Mayo, A., Kam, Z., Geiger, B., and Bershadsky, A.D. (2011). Fibroblast polarization is a matrix-rigidity-dependent process controlled by focal adhesion mechanosensing. Nat Cell Biol 13, 1457–1465.

Prigione, A., Hossini, A.M., Lichtner, B., Serin, A., Fauler, B., Megges, M., Lurz, R., Lehrach, H., Makrantonaki, E., Zouboulis, C.C., et al. (2011). Mitochondrial-associated cell death mechanisms are reset to an embryonic-like state in aged donor-derived iPS cells harboring chromosomal aberrations. Plos One 6, e27352.

Pringle, N.P., Mudhar, H.S., Collarini, E.J., and Richardson, W.D. (1992). PDGF receptors in the rat CNS: during late neurogenesis, PDGF alpha-receptor expression appears to be restricted to glial cells of the oligodendrocyte lineage. Development 115, 535–551.

Psachoulia, K., Jamen, F., Young, K.M., and Richardson, W.D. (2009). Cell cycle dynamics of NG2 cells in the postnatal and ageing brain. Neuron Glia Biol. 5, 57–67.

Pyka, M., Wetzel, C., Aguado, A., Geissler, M., Hatt, H., and Faissner, A. (2011). Chondroitin sulfate proteoglycans regulate astrocyte-dependent synaptogenesis and modulate synaptic activity in primary embryonic hippocampal neurons. European Journal of Neuroscience 33, 2187–2202.

Qi, Y., Tan, M., Hui, C.-C., and Qiu, M. (2003). Gli2 is required for normal Shh signaling and oligodendrocyte development in the spinal cord. Molecular and Cellular Neuroscience 23, 440–450.

Quarta, M., Brett, J.O., DiMarco, R., De Morree, A., Boutet, S.C., Chacon, R., Gibbons, M.C., Garcia, V.A., Su, J., Shrager, J.B., et al. (2016). An artificial niche preserves the quiescence of muscle stem cells and enhances their therapeutic efficacy. Nat. Biotechnol. 34, 752–759.

Ran, F.A., Hsu, P.D., Lin, C.-Y., Gootenberg, J.S., Konermann, S., Trevino, A.E., Scott, D.A., Inoue, A., Matoba, S., Zhang, Y., et al. (2013). Double nicking by RNA-guided CRISPR Cas9

for enhanced genome editing specificity. Cell 154, 1380–1389.

Rando, T.A. (2006). Stem cells, ageing and the quest for immortality. Nature 441, 1080–1086.

Ransohoff, R.M. (2012). Animal models of multiple sclerosis: the good, the bad and the bottom line. Nature Neuroscience 15, 1074–1077.

Redmond, S.A., Mei, F., Eshed-Eisenbach, Y., Osso, L.A., Leshkowitz, D., Shen, Y.-A.A., Kay, J.N., Aurrand-Lions, M., Lyons, D.A., Peles, E., et al. (2016). Somatodendritic Expression of JAM2 Inhibits Oligodendrocyte Myelination. Neuron 91, 824–836.

Richardson, W.D., Pringle, N., Mosley, M.J., Westermark, B., and Dubois-Dalcq, M. (1988). A role for platelet-derived growth factor in normal gliogenesis in the central nervous system. Cell 53, 309–319.

Rivers, L.E., Young, K.M., Rizzi, M., Jamen, F., Psachoulia, K., Wade, A., Kessaris, N., and Richardson, W.D. (2008). PDGFRA/NG2 glia generate myelinating oligodendrocytes and piriform projection neurons in adult mice. Nature Neuroscience 11, 1392–1401.

Rosenbloom, K.R., Sloan, C.A., Malladi, V.S., Dreszer, T.R., Learned, K., Kirkup, V.M., Wong, M.C., Maddren, M., Fang, R., Heitner, S.G., et al. (2012). ENCODE Data in the UCSC Genome Browser: year 5 update. Nucleic Acids Res. 41, D56–D63.

Rossi, L., Salvetti, A., Batistoni, R., Deri, P., and Gremigni, V. (2008). Planarians, a tale of stem cells. Cell. Mol. Life Sci. 65, 16–23.

Ruckh, J.M., Zhao, J.-W., Shadrach, J.L., van Wijngaarden, P., Rao, T.N., Wagers, A.J., and Franklin, R.J.M. (2012). Rejuvenation of Regeneration in the Aging Central Nervous System. Cell Stem Cell 10, 96–103.

Rudolph, K.L., Chang, S., Lee, H.W., Blasco, M., Gottlieb, G.J., Greider, C., and DePinho, R.A. (1999). Longevity, stress response, and cancer in aging telomerase-deficient mice. Cell 96, 701–712.

Russell, R.C., Fang, C., and Guan, K.-L. (2011). An emerging role for TOR signaling in mammalian tissue and stem cell physiology. Development 138, 3343–3356.

Sanai, N., Tramontin, A.D., Quiñones-Hinojosa, A., Barbaro, N.M., Gupta, N., Kunwar, S., Lawton, M.T., McDermott, M.W., Parsa, A.T., Manuel-García Verdugo, J., et al. (2004). Unique astrocyte ribbon in adult human brain contains neural stem cells but lacks chain migration. Nature 427, 740–744.

Sato, T., van Es, J.H., Snippert, H.J., Stange, D.E., Vries, R.G., van den Born, M., Barker, N., Shroyer, N.F., van de Wetering, M., and Clevers, H. (2011). Paneth cells constitute the niche for Lgr5 stem cells in intestinal crypts. Nature 469, 415–418.

Satoh, A., Brace, C.S., Rensing, N., Cliften, P., Wozniak, D.F., Herzog, E.D., Yamada, K.A.,

and Imai, S.-I. (2013). Sirt1 extends life span and delays aging in mice through the regulation of Nk2 homeobox 1 in the DMH and LH. Cell Metab. 18, 416–430.

Schaefer, K.A., Wu, W.-H., Colgan, D.F., Tsang, S.H., Bassuk, A.G., and Mahajan, V.B. (2017). Unexpected mutations after CRISPR-Cas9 editing *in vivo*. Nat. Methods 14, 547–548.

Schwab, M., Alitalo, K., Klempnauer, K.H., Varmus, H.E., Bishop, J.M., Gilbert, F., Brodeur, G., Goldstein, M., and Trent, J. (1983). Amplified DNA with limited homology to myc cellular oncogene is shared by human neuroblastoma cell lines and a neuroblastoma tumour. Nature 305, 245–248.

Scognamiglio, R., Cabezas-Wallscheid, N., Thier, M.C., Altamura, S., Reyes, A., Prendergast, Á.M., Baumgärtner, D., Carnevalli, L.S., Atzberger, A., Haas, S., et al. (2016). Myc Depletion Induces a Pluripotent Dormant State Mimicking Diapause. Cell 164, 668–680.

Seeger, R.C., Brodeur, G.M., Sather, H., Dalton, A., Siegel, S.E., Wong, K.Y., and Hammond, D. (1985). Association of Multiple Copies of the N- mycOncogene with Rapid Progression of Neuroblastomas. New England Journal of Medicine 313, 1111–1116.

Shen, Q., Wang, Y., Kokovay, E., Lin, G., Chuang, S.-M., Goderie, S.K., Roysam, B., and Temple, S. (2008a). Adult SVZ stem cells lie in a vascular niche: a quantitative analysis of niche cell-cell interactions. Cell Stem Cell 3, 289–300.

Shen, S., Sandoval, J., Swiss, V.A., Li, J., Dupree, J., Franklin, R.J.M., and Casaccia-Bonnefil, P. (2008b). Age-dependent epigenetic control of differentiation inhibitors is critical for remyelination efficiency. Nature Neuroscience 11, 1024–1034.

Shields, S.A., Gilson, J.M., Blakemore, W.F., and Franklin, R.J.M. (1999). Remyelination occurs as extensively but more slowly in old rats compared to young rats following gliotoxin-induced CNS demyelination. Glia 28, 77–83.

Shimi, T., Butin-Israeli, V., Adam, S.A., Hamanaka, R.B., Goldman, A.E., Lucas, C.A., Shumaker, D.K., Kosak, S.T., Chandel, N.S., and Goldman, R.D. (2011). The role of nuclear lamin B1 in cell proliferation and senescence. Genes & Development 25, 2579–2593.

Shin, J.-W., Spinler, K.R., Swift, J., Chasis, J.A., Mohandas, N., and Discher, D.E. (2013). Lamins regulate cell trafficking and lineage maturation of adult human hematopoietic cells. Proc. Natl. Acad. Sci. U.S.a. 110, 18892–18897.

Short, K.R., Bigelow, M.L., Kahl, J., Singh, R., Coenen-Schimke, J., Raghavakaimal, S., and Nair, K.S. (2005). Decline in skeletal muscle mitochondrial function with aging in humans. Proceedings of the National Academy of Sciences 102, 5618–5623.

Shytikov, D., Balva, O., Debonneuil, E., Glukhovskiy, P., and Pishel, I. (2014). Aged mice repeatedly injected with plasma from young mice: a survival study. Biores Open Access 3, 226–232.

Sim, F.J., Zhao, C., Penderis, J., and Franklin, R.J.M. (2002). The age-related decrease in CNS remyelination efficiency is attributable to an impairment of both oligodendrocyte progenitor recruitment and differentiation. J. Neurosci. 22, 2451–2459.

Simonsen, A., Cumming, R.C., Brech, A., Isakson, P., Schubert, D.R., and Finley, K.D. (2014). Promoting basal levels of autophagy in the nervous system enhances longevity and oxidant resistance in adult Drosophila. Autophagy 4, 176–184.

Sinha, M., Jang, Y.C., Oh, J., Khong, D., Wu, E.Y., Manohar, R., Miller, C., Regalado, S.G., Loffredo, F.S., Pancoast, J.R., et al. (2014). Restoring systemic GDF11 levels reverses age-related dysfunction in mouse skeletal muscle. Science 344, 649–652.

Sjöbeck, M., Haglund, M., and Englund, E. (2005). Decreasing myelin density reflected increasing white matter pathology in Alzheimer's disease—a neuropathological study. International Journal of Geriatric Psychiatry 20, 919–926.

Smith, J.M. (1958). Prolongation of the Life of Drosophila subobscura by a Brief Exposure of Adults to a High Temperature. Nature 181, 496–497.

Smith, K.J., Blakemore, W.F., and McDonald, W.I. (1979). Central remyelination restores secure conduction. Nature 280, 395–396.

Snaidero, N., Möbius, W., Czopka, T., Hekking, L.H.P., Mathisen, C., Verkleij, D., Goebbels, S., Edgar, J., Merkler, D., Lyons, D.A., et al. (2014). Myelin membrane wrapping of CNS axons by PI(3,4,5)P3-dependent polarized growth at the inner tongue. Cell 156, 277–290.

Snippert, H.J., van der Flier, L.G., Sato, T., van Es, J.H., van den Born, M., Kroon-Veenboer, C., Barker, N., Klein, A.M., van Rheenen, J., Simons, B.D., et al. (2010). Intestinal crypt homeostasis results from neutral competition between symmetrically dividing Lgr5 stem cells. Cell 143, 134–144.

Soattin, L., Fiore, M., Gavazzo, P., Viti, F., Facci, P., Raiteri, R., Difato, F., Pusch, M., and Vassalli, M. (2016). The biophysics of piezo1 and piezo2 mechanosensitive channels. Biophysical Chemistry 208, 26–33.

Song, H.-J., Stevens, C.F., and Gage, F.H. (2002). Neural stem cells from adult hippocampus develop essential properties of functional CNS neurons. Nature Neuroscience 5, 438–445.

Spalding, K.L., Bergmann, O., Alkass, K., Bernard, S., Salehpour, M., Huttner, H.B., Boström, E., Westerlund, I., Vial, C., Buchholz, B.A., et al. (2013). Dynamics of hippocampal neurogenesis in adult humans. Cell 153, 1219–1227.

Spangrude, G., Heimfeld, S., and Weissman, I. (1988). Purification and characterization of mouse hematopoietic stem cells. Science 241, 58–62.

Spradling, A.C., Nystul, T., Lighthouse, D., Morris, L., Fox, D., Cox, R., Tootle, T., Frederick, R., and Skora, A. (2008). Stem cells and their niches: integrated units that maintain Drosophila

tissues. Cold Spring Harb. Symp. Quant. Biol. 73, 49–57.

Sridharan, R., Tchieu, J., Mason, M.J., Yachechko, R., Kuoy, E., Horvath, S., Zhou, Q., and Plath, K. (2009). Role of the Murine Reprogramming Factors in the Induction of Pluripotency. Cell 136, 364–377.

Stidworthy, M.F., Genoud, S., Li, W.-W., Leone, D.P., Mantei, N., Suter, U., and Franklin, R.J.M. (2004). Notch1 and Jagged1 are expressed after CNS demyelination, but are not a major rate-determining factor during remyelination. Brain 127, 1928–1941.

Stocum, D.L. (1979). Stages of forelimb regeneration inAmbystoma maculatum. Journal of Experimental Zoology 209, 395–416.

Suda, T., Takubo, K., and Semenza, G.L. (2011). Metabolic Regulation of Hematopoietic Stem Cells in the Hypoxic Niche. Cell Stem Cell 9, 298–310.

Susaki, E.A., Tainaka, K., Perrin, D., Yukinaga, H., Kuno, A., and Ueda, H.R. (2015). Advanced CUBIC protocols for whole-brain and whole-body clearing and imaging. Nature Protocols 10, 1709–1727.

Suzuki, K., Tsunekawa, Y., Hernandez-Benitez, R., Wu, J., Zhu, J., Kim, E.J., Hatanaka, F., Yamamoto, M., Araoka, T., Li, Z., et al. (2016). *In vivo* genome editing via CRISPR/Cas9 mediated homology-independent targeted integration. Nature 540, 144–149.

Swift, J., Ivanovska, I.L., Buxboim, A., Harada, T., Dingal, P.C.D.P., Pinter, J., Pajerowski, J.D., Spinler, K.R., Shin, J.-W., Tewari, M., et al. (2013). Nuclear Lamin-A Scales with Tissue Stiffness and Enhances Matrix-Directed Differentiation. Science 341, 1240104–1240104.

Szilard, L. (1959). On the nature of the aging process. Proceedings of the National Academy of Sciences 45, 30–45.

Tabebordbar, M., Zhu, K., Cheng, J.K.W., Chew, W.L., Widrick, J.J., Yan, W.X., Maesner, C., Wu, E.Y., Xiao, R., Ran, F.A., et al. (2016). *In vivo* gene editing in dystrophic mouse muscle and muscle stem cells. Science 351, 407–411.

Takahashi, K., Tanabe, K., Ohnuki, M., Narita, M., Ichisaka, T., Tomoda, K., and Yamanaka, S. (2007). Induction of pluripotent stem cells from adult human fibroblasts by defined factors. Cell 131, 861–872.

Tang, D.G., Tokumoto, Y.M., Apperly, J.A., Lloyd, A.C., and Raff, M.C. (2001). Lack of replicative senescence in cultured rat oligodendrocyte precursor cells. Science 291, 868–871.

Tang, W., and Liu, D.R. (2018). Rewritable multi-event analog recording in bacterial and mammalian cells. Science 360, eaap8992.

Thomson, J.A. (1998). Embryonic Stem Cell Lines Derived from Human Blastocysts. Science 282, 1145–1147.

Trent, J., Meltzer, P., Rosenblum, M., Harsh, G., Kinzler, K., Mashal, R., Feinberg, A., and Vogelstein, B. (1986). Evidence for rearrangement, amplification, and expression of Myc in a human glioblastoma. Proceedings of the National Academy of Sciences 83, 470–473.

Tripathi, R.B., Jackiewicz, M., McKenzie, I.A., Kougioumtzidou, E., Grist, M., and Richardson, W.D. (2017). Remarkable Stability of Myelinating Oligodendrocytes in Mice. Cell Rep 21, 316–323.

Tsai, H.-H., Niu, J., Munji, R., Davalos, D., Chang, J., Zhang, H., Tien, A.-C., Kuo, C.J., Chan, J.R., Daneman, R., et al. (2016). Oligodendrocyte precursors migrate along vasculature in the developing nervous system. Science 351, 379–384.

Urbanski, M.M., Kingsbury, L., Moussouros, D., Kassim, I., Mehjabeen, S., Paknejad, N., and Melendez Vasquez, C.V. (2016). Myelinating glia differentiation is regulated by extracellular matrix elasticity. Sci Rep 6, 33751.

van Es, J.H., Jay, P., Gregorieff, A., van Gijn, M.E., Jonkheer, S., Hatzis, P., Thiele, A., van den Born, M., Begthel, H., Brabletz, T., et al. (2005). Wnt signalling induces maturation of Paneth cells in intestinal crypts. Nat Cell Biol 7, 381–386.

Vanlandewijck, M., He, L., Mäe, M.A., Andrae, J., Ando, K., Del Gaudio, F., Nahar, K., Lebouvier, T., Laviña, B., Gouveia, L., et al. (2018). A molecular atlas of cell types and zonation in the brain vasculature. Nature 554, 475–480.

Végh, M.J., Rausell, A., Loos, M., Heldring, C.M., Jurkowski, W., van Nierop, P., Paliukhovich, I., Li, K.W., del Sol, A., Smit, A.B., et al. (2014). Hippocampal extracellular matrix levels and stochasticity in synaptic protein expression increase with age and are associated with age-dependent cognitive decline. Mol Cell Proteomics 13, 2975–2985.

Wagers, A.J., and Weissman, I.L. (2004). Plasticity of adult stem cells. Cell 116, 639–648.

Wang, H., Rusielewicz, T., Tewari, A., Leitman, E.M., Einheber, S., and Melendez Vasquez, C.V. (2012). Myosin II is a negative regulator of oligodendrocyte morphological differentiation. Journal of Neuroscience Research 90, 1547–1556.

Wang, S., Sdrulla, A.D., diSibio, G., Bush, G., Nofziger, D., Hicks, C., Weinmaster, G., and Barres, B.A. (1998). Notch receptor activation inhibits oligodendrocyte differentiation. Neuron 21, 63–75.

Watanabe, H., Hoang, V.T., Mättner, R., and Holstein, T.W. (2009). Immortality and the base of multicellular life: Lessons from cnidarian stem cells. Semin. Cell Dev. Biol. 20, 1114–1125.

Waxman, S.G. (1977). Conduction in Myelinated, Unmyelinated, and Demyelinated Fibers. Archives of Neurology 34, 585–589.

Wilmut, I., Schnieke, A.E., McWhir, J., Kind, A.J., and Campbell, K.H. (1997). Viable offspring derived from fetal and adult mammalian cells. Nature 385, 810–813.

Wilson, P.A., and Hemmati-Brivanlou, A. (1995). Induction of epidermis and inhibition of neural fate by Bmp-4. Nature 376, 331–333.

Wilson, V.L., and Jones, P.A. (1983). DNA methylation decreases in aging but not in immortal cells. Science 220, 1055–1057.

Wilusz, J.E., JnBaptiste, C.K., Lu, L.Y., Kuhn, C.D., Joshua-Tor, L., and Sharp, P.A. (2012). A triple helix stabilizes the 3' ends of long noncoding RNAs that lack poly(A) tails. Genes & Development 26, 2392–2407.

Windrem, M.S., Nunes, M.C., Rashbaum, W.K., Schwartz, T.H., Goodman, R.A., McKhann, G., Roy, N.S., and Goldman, S.A. (2004). Fetal and adult human oligodendrocyte progenitor cell isolates myelinate the congenitally dysmyelinated brain. Nature Medicine 10, 93–97.

Windrem, M.S., Osipovitch, M., Liu, Z., Bates, J., Chandler-Militello, D., Zou, L., Munir, J., Schanz, S., McCoy, K., Miller, R.H., et al. (2017). Human iPSC Glial Mouse Chimeras Reveal Glial Contributions to Schizophrenia. Cell Stem Cell 21, 195–208.e196.

Wong, D.J., Liu, H., Ridky, T.W., Cassarino, D., Segal, E., and Chang, H.Y. (2008). Module map of stem cell genes guides creation of epithelial cancer stem cells. Cell Stem Cell 2, 333–344.

Woodruff, R.H., and Franklin, R.J.M. (1999). Demyelination and remyelination of the caudal cerebellar peduncle of adult rats following stereotaxic injections of lysolecithin, ethidium bromide, and complement/anti-galactocerebroside: A comparative study. Glia 25, 216–228.

Woodruff, R.H., Fruttiger, M., Richardson, W.D., and Franklin, R.J.M. (2004). Platelet-derived growth factor regulates oligodendrocyte progenitor numbers in adult CNS and their response following CNS demyelination. Mol. Cell. Neurosci. 25, 252–262.

Yang, Y., Wang, L., Bell, P., McMenamin, D., He, Z., White, J., Yu, H., Xu, C., Morizono, H., Musunuru, K., et al. (2016). A dual AAV system enables the Cas9-mediated correction of a metabolic liver disease in newborn mice. Nat. Biotechnol. 34, 334–338.

Yasuda, T., Tsumita, T., Nagai, Y., Mitsuzawa, E., and Ohtani, S. (1975). Experimental allergic encephalomyelitis (EAE) in mice. I. Induction of EAE with mouse spinal cord homogenate and myelin basic protein. Jpn. J. Exp. Med. 45, 423–427.

Yau, S.Y., Lau, B.W.M., Zhang, E.D., Lee, J.C.D., Li, A., Lee, T.M.C., Ching, Y.P., Xu, A.M., and So, K.F. (2012). Effects of voluntary running on plasma levels of neurotrophins, hippocampal cell proliferation and learning and memory in stressed rats. Neuroscience 222, 289–301.

Yeung, M.S.Y., Zdunek, S., Bergmann, O., Bernard, S., Salehpour, M., Alkass, K., Perl, S., Tisdale, J., Possnert, G., Brundin, L., et al. (2014). Dynamics of oligodendrocyte generation and myelination in the human brain. Cell 159, 766–774.

Yoshioka, S., Fujii, W., Ogawa, T., Sugiura, K., and Naito, K. (2015). Development of a mono-promoter-driven CRISPR/Cas9 system in mammalian cells. Sci Rep 5, 18341.

Young, K.M., Psachoulia, K., Tripathi, R.B., Dunn, S.-J., Cossell, L., Attwell, D., Tohyama, K., and Richardson, W.D. (2013). Oligodendrocyte dynamics in the healthy adult CNS: evidence for myelin remodeling. Neuron 77, 873–885.

Yu, J., Vodyanik, M.A., Smuga-Otto, K., Antosiewicz-Bourget, J., Frane, J.L., Tian, S., Nie, J., Jonsdottir, G.A., Ruotti, V., Stewart, R., et al. (2007). Induced pluripotent stem cell lines derived from human somatic cells. Science 318, 1917–1920.

Zawadzka, M., Rivers, L.E., Fancy, S.P.J., Zhao, C., Tripathi, R., Jamen, F., Young, K., Goncharevich, A., Pohl, H., Rizzi, M., et al. (2010). CNS-Resident Glial Progenitor/Stem Cells Produce Schwann Cells as well as Oligodendrocytes during Repair of CNS Demyelination. Cell Stem Cell 6, 578–590.

Zeisel, A., Munoz-Manchado, A.B., Codeluppi, S., Lonnerberg, P., La Manno, G., Jureus, A., Marques, S., Munguba, H., He, L., Betsholtz, C., et al. (2015). Cell types in the mouse cortex and hippocampus revealed by single-cell RNA-seq. Science 347, 1138–1142.

Zhang, H., Vutskits, L., Calaora, V., Durbec, P., and Kiss, J.Z. (2004). A role for the polysialic acid-neural cell adhesion molecule in PDGF-induced chemotaxis of oligodendrocyte precursor cells. J. Cell. Sci. 117, 93–103.

Zhang, H., Ryu, D., Wu, Y., Gariani, K., Wang, X., Luan, P., D'Amico, D., Ropelle, E.R., Lutolf, M.P., Aebersold, R., et al. (2016). NAD repletion improves mitochondrial and stem cell function and enhances life span in mice. Science 352, 1436–1443.

Zhang, W., Li, J., Suzuki, K., Qu, J., Wang, P., Zhou, J., Liu, X., Ren, R., Xu, X., Ocampo, A., et al. (2015). A Werner syndrome stem cell model unveils heterochromatin alterations as a driver of human aging. Science 348, 1160–1163.

Zhu, X., Bergles, D.E., and Nishiyama, A. (2008). NG2 cells generate both oligodendrocytes and gray matter astrocytes. Development 135, 145–157.

Zhu, X., Hill, R.A., Dietrich, D., Komitova, M., Suzuki, R., and Nishiyama, A. (2011). Age-dependent fate and lineage restriction of single NG2 cells. Development 138, 745–753.

Zirath, H., Frenzel, A., Oliynyk, G., Segerström, L., Westermark, U.K., Larsson, K., Munksgaard Persson, M., Hultenby, K., Lehtiö, J., Einvik, C., et al. (2013). MYC inhibition induces metabolic changes leading to accumulation of lipid droplets in tumor cells. Proc. Natl. Acad. Sci. U.S.a. 110, 10258–10263.